SANDIA REPORT

SAND2004-6329
Unlimited Release
Printed December 2004

Geologic Investigation of Playa Lakes, Tonopah Test Range, Nevada: Data Report

Christopher A. Rautman

Prepared by
Sandia National Laboratories
Albuquerque, New Mexico 87185 and Livermore, California 94550

Sandia is a multiprogram laboratory operated by Sandia Corporation,
a Lockheed Martin Company, for the United States Department of Energy
under Contract DE-AC04-94AL85000.

Issued by Sandia National Laboratories, operated for the United States Department of Energy by Sandia Corporation.

Available to DOE and DOE contractors from

U.S. Department of Energy
Office of Scientific and Technical Information
P.O. Box 62
Oak Ridge, TN 37831

Telephone:(865)576-8401
Facsimile:(865)576-5728
E-Mail:reports@adonis.osti.gov
Online ordering: http://www.doe.gov/bridge

Available to the public from

U.S. Department of Commerce
National Technical Information Service
5285 Port Royal Rd
Springfield, VA 22161

Telephone:(800)553-6847
Facsimile:(703)605-6900
E-Mail:orders@ntis.fedworld.gov
Online order: http://www.ntis.gov/help/ordermethods.asp?loc=7-4-0#online

SAND2004-6329

Unlimited Release
Printed December 2004

Geologic Investigation of Playa Lakes, Tonopah Test Range, Nevada: Data Report

Christopher A. Rautman
Underground Storage Technology Department
Sandia National Laboratories
Albuquerque, New Mexico 87185-0706

ABSTRACT

Subsurface geological investigations have been conducted at two large playa lakes at the Tonopah Test Range in central Nevada. These characterization activities were intended to provide basic stratigraphic-framework information regarding the lateral distribution of "hard" and "soft" sedimentary materials for use in defining suitable target regions for penetration testing. Both downhole geophysical measurements and macroscopic lithologic descriptions were used as a surrogate for quantitative mechanical-strength properties, although some quantitative laboratory strength measurements were obtained as well.

Both rotary (71) and core (19) holes on a systematic grid were drilled in the southern half of the Main Lake; drill hole spacings are 300 ft north-south and 500-ft east-west. The drilled region overlaps a previous cone-penetrometer survey that also addressed the distribution of hard and soft material. Holes were drilled to a depth of 40 ft and logged using both geologic examination and down-hole geophysical surveying. The data identify a large complex of very coarse-grained sediment (clasts up to 8 mm) with interbedded finer-grained sands, silts and clays, underlying a fairly uniform layer of silty clay 6 to 12 ft thick. Geophysical densities of the coarse-grained materials exceed 2.0 g/cm^3, and this petrophysical value appears to be a valid discriminator of hard vs. soft sediments in the subsurface.

Thirty-four holes, including both core and rotary drilling, were drilled on a portion of the much larger Antelope Lake. A set of pre-drilling geophysical surveys, including time-domain electromagnetic methods, galvanic resistivity soundings, and terrain-conductivity surveying, was used to identify the gross distribution of conductive and resistive facies with respect to the present lake outline. Conductive areas were postulated to represent softer, clay-rich sediments with larger amounts of contained conductive ground water. Initial drilling, consisting of cored drill holes to 100-ft (33-m) depth, confirmed both the specific surface geophysical measurements and the more general geophysical model of the subsurface lake facies. Good agreement of conductive regions with drill holes containing little to no coarse-grained sediments was observed, and vice-versa. A second phase of grid drilling on approximately 300-ft (100-m) centers was targeted at delineating a region of sufficient size containing essentially no coarse-grained "hard" material. Such a region was identified in the southwestern portion of Antelope Lake.

ACKNOWLEDGMENTS

The work described in this data report involved the active participation of and collaboration with a large number of individuals and organizations. The overall investigation of these playa lakes would have been impossible without their input.

I particularly wish to acknowledge the contributions of Stewart Sandberg and Noel Rogers, with Geophysical Solutions, Inc. of Albuquerque, New Mexico for the conduct and data reduction of the surface geophysical surveys. The drilling programs were conducted in several stages by different drillers and helpers under contract from Layne Environmental Services, of Phoenix, with main offices in Phoenix, Arizona. Downhole geophysical logging was performed by Damien Stewart and Alex Desselle, under contract with Century Geophysical Corporation, Tulsa, Oklahoma.

Ron Graichen, geological consultant, Winlock, Washington, logged most of the cored holes and provided invaluable geological expertise throughout the drilling effort. David Bronowski and Moo Lee measured rock material properties on core specimens in the Geomechanics Department rock laboratory at Sandia National Laboratories.

Finally, I wish to acknowledge the superb logistical and other field support provided by the staff of Westinghouse and Sandia National Laboratories located at the Tonopah Test Range, outside of Tonopah, Nevada. None of the several field surveys or work programs would have been possible without their support.

This work was supported by the U.S. Department of Energy, Stockpile Stewardship Program.

Sandia is a multiprogram laboratory operated by Sandia Corporation, a Lockheed-Martin Company, for the United States Department of Energy under contract DE-AC04-94AL85000.

Contents

Figures

Tables

INTRODUCTION

A group of playas, or dry lake beds, at Tonopah Test Range (TTR) in Nye County, central Nevada, have been used for several decades as targets and impact locations for a wide variety of developmental and testing programs for air-delivered weapon systems. In more recent years, increased emphasis on penetrating weapons has led to the utilization of the subsurface geology of these lakes, in addition to simply the open real estate and airspace of this remote region. However, use of the subsurface part of these playas has placed these penetrator testing programs at the mercy of internal heterogeneity of the sediments beneath the flat and relatively featureless topographic surfaces.

That the internal geology of these lakes is not featureless was demonstrated when a flight test of a penetrator assembly encountered earth materials that produced anomalous results in the on-board instrumentation. The program of geologic characterization described in this report was undertaken with the initial objective of determining the cause of this unexpected response. After the degree of heterogeneity became apparent from early investigations, the objectives of the study were expanded to include the description and understanding of the geometry of the various layered units encountered and to include the delineation of target area(s) that could be used for testing with some assurance that the subsurface materials would meet specifications.

This report is intended to serve as an archive of relevant descriptive information. Much raw data is included in essentially unreduced form, particularly in the appendices and on the CD-R that is included in the back pocket. Additionally, we interpret some of these data with respect to their implications for understanding the geology of these playa lakes, using commonly accepted geologic principles and the integration of the various types of geologic data obtained.

BACKGROUND

Tonopah Test Range (TTR) is located in central Nevada (fig. 1), some 25–30 miles southeast of the old-time mining town of Tonopah. The test range is located within the Basin and Range geological province, a continental-scale swath of extensional tectonism and significant volcanic activity over the past 60 million years or so. The test range is more specifically located near the northern limit of the Southwestern Nevada Volcanic Field, where voluminous sheets of rhyolitic tuff and associated volcanic rocks lap onto Paleozoic carbonate rocks (both limestones and dolomites) of much greater age. The structural style of the Basin and Range Province is one of fault-block mountains separated by depositional basins that contain mostly unconsolidated sediments of late Tertiary to Quaternary age. The relationship of the volcanic rocks to crustal extension is complex and overlapping in time and space, with the result that the volcanics may be found both in the faulted ranges and in the intervening basinal areas.

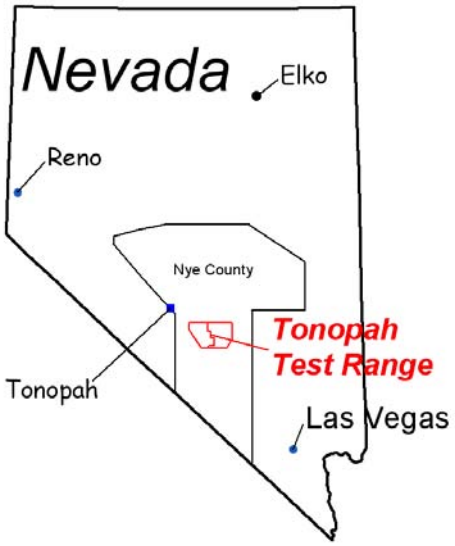

Figure 1. Index map showing location of the Tonopah Test Range in Nye County, Nevada.

Within the Tonopah Test Range itself, the playa lakes of Main Lake (also identified as "Mud Lake" in some reports) and Antelope Lake, as well as a number of other, significantly smaller playas, are located between the Cactus Range to the west and the Kawitch Range to the east (fig. 2). The Cactus Range (summarized from Ekren and others, 1971) comprises widespread rhyolitic extrusive and shallow-intrusive rocks that range in age from Oligocene through Miocene, overlying sparse exposures of much older Paleozoic sediments and one small outcrop of Mesozoic granite. Two probable calderas, one related to the tuff of Antelope Springs and one to the younger tuff of White Bloch Spring, appear to be present within the range, although these eruptive centers seem to have been disrupted significantly by severe post-eruption faulting. The core of the Cactus Range is flanked by later Miocene to Pliocene volcanic and sedimentary rocks. A northwest-trending Basin-and-Range normal fault of large displacement bounds the range to the east.

The Kawitch Range (fig. 2; discussion again summarized from Ekren and others, 1971) is a complex uplift, comprising three major, en echelon segments. The southern seg-

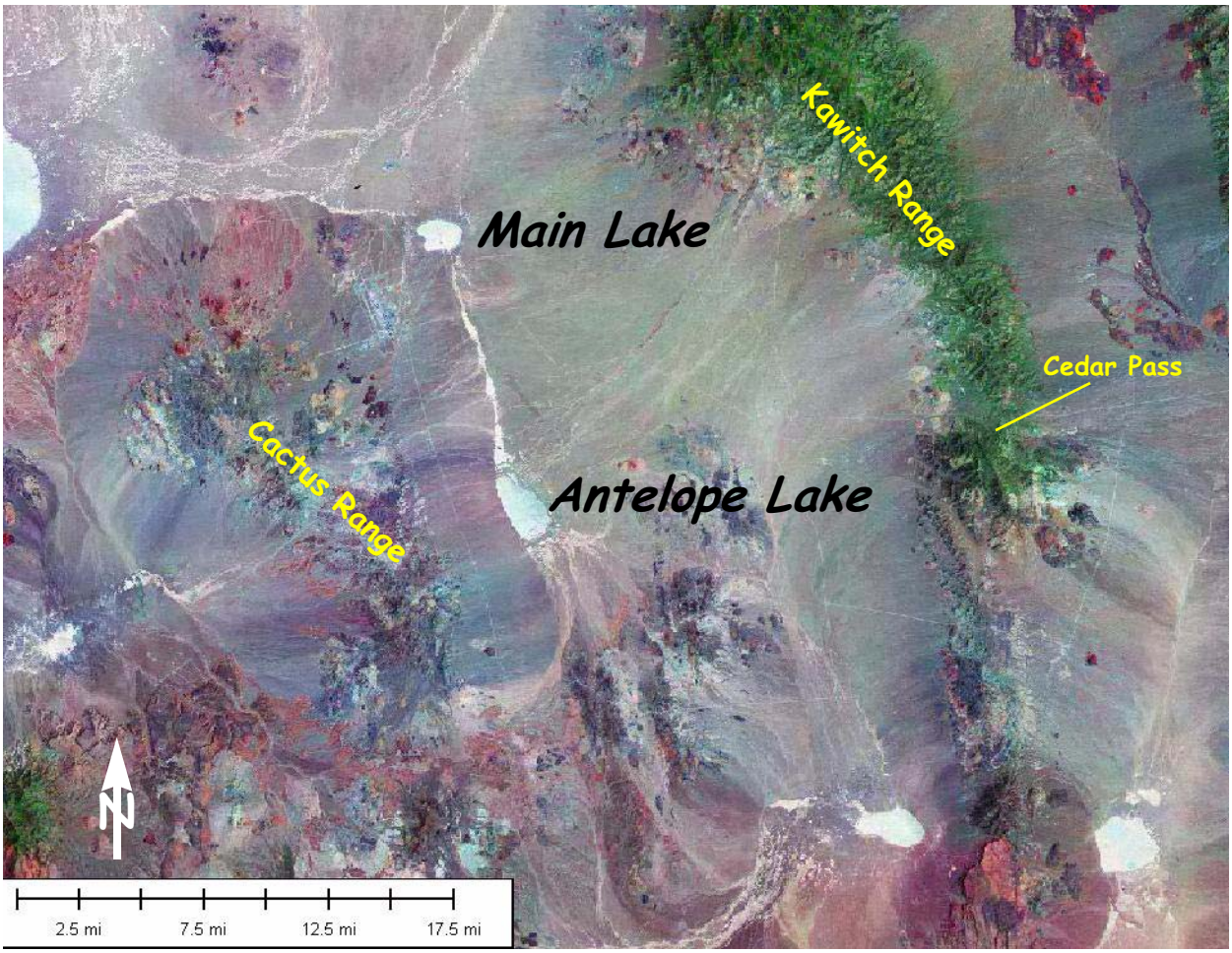

Figure 2. Landsat imagery for part of the Tonopah Test Range and vicinity showing Main Lake, Antelope Lake, the Cactus Range to the west and the Kawitch Range to the east (in green shades). Playa lakes are white.

ment, which is located farther south than the playa lakes of interest, comprises dominantly quartzose sedimentary rocks of Precambrian and Cambrian age. The central segment, which lies immediately south of Cedar Pass and roughly parallel in latitude with Antelope Lake, is entirely volcanic in origin. Almost the entire segment consists of intra-caldera Fraction Tuff of Miocene age; thicknesses of the Fraction Tuff are known to exceed 7000 ft. The northern segment, located to the north of Cedar Pass and probably a source area for some of the sediments underlying the modern playas, comprises a variety of generally pre-Fraction-Tuff Tertiary volcanic materials. A few small outcrops of Lower Paleozoic carbonate and quartzose sedimentary rocks, possible landslide blocks, are exposed in several locations. The entire Kawitch Range appears largely to be a composite horst block, bounded on both the east and west sides by poorly exposed north- and northwest-trending normal faults.

Elevations are distinctly higher in the Kawitch Range (to 8500 ft) than elsewhere on Tonopah Test Range (generally 5300–5500 ft). As indicated in figure 2, Main Lake and Antelope Lake are located markedly closer to the Cactus Range (maximum elevation ~7000 ft) than to the Kawitch Range. This relative positioning is believed to determine — in part — the source(s) of the sediments that now fill the lake basins.

Previous Characterization Studies of TTR Playa Lakes

There appear to have been two principal previous investigations of playa lakes at Tonopah Test Range. Some 70-plus shallow drive-cores were obtained by a contracted geotechnical consulting firm in the 1963-1964 time frame from the entire Main Lake area (Woodward-Clyde-Sherrad, 1964). Varying vertical distributions of silty clay, silty sand, and sand were encountered, mostly unlithified. A few holes contained material described as "slightly cemented," and one deep hole encountered "very hard sand conglomerate" at approximately 70 ft depth. The report concluded that units could not be correlated between holes, given the wide hole spacing. A second investigation in 1996 used a truck-mounted cone penetrometer to push a hydraulically driven instrumented probe into the lake sediments at 95 locations, recording the depth of refusal and a continuous record of resistance to penetration at each site (Hansen and Patterson, 1996). Unlike the earlier survey, the cone penetrometer locations covered Antelope Lake (13 locations), Browns and Pedro Lakes (3 locations each), as well as the TTR Main Lake (75 locations).

The results of the cone-penetrometer survey on the Main Lake are shown in figure 3, in both map (top) view and perspective view from the northwest. In parts (a) and (b) of the illustration, the emphasis is on the modeled depth-to-refusal of the hydraulically driven penetrometer probe. The depths are indicated by the color coding in the legend bar. In parts (c) and (d), the same depths-to-refusal are shown; however, these illustrations also show the overall extent of the cone-penetrometer survey with respect to the present-day topographic lake margin.

The depth of refusal, which essentially correlates with what was commonly known regarding the depth to the "top of the hard layer" prior to the present study, increases consistently toward the north, away from the shoreline. Depths increase from immediately below the surface of the lake bed to a maximum observed value of approximately 10 ft. A number of more-or-less north-south ridges and valleys are present on the top of the hard layer, but toward the northern limit of the surveyed area, the depth of refusal is fairly consistent at approximately 8–10 ft. Note, however, that no information regarding the thickness of the hard layer underlying the refusal depth was

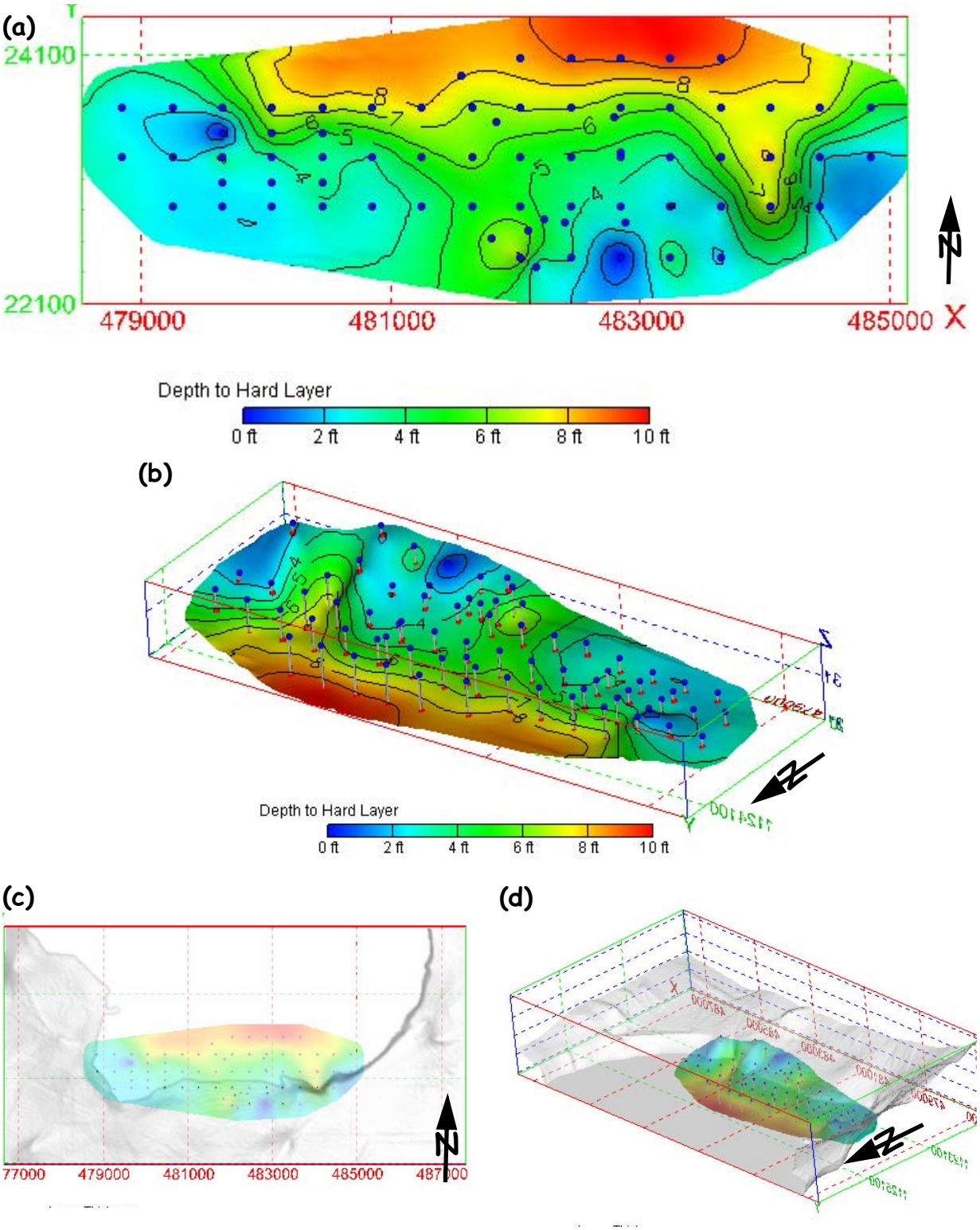

Figure 3. Results of the cone-penetrometer survey on the southern margin of the Main Lake. (a) Color-coded depths to refusal (the “hard layer”) in feet. (b) Perspective view of (a). (c) Depths to the hard layer showing the extent of the cone-penetrometer survey with respect to the lake margin (topographic). (d) Perspective view of (c). Vertical exaggeration in (b) and (d): 50x.

obtained by the cone penetrometer examination.

OBJECTIVES

The intent of the current investigations was to define the basic subsurface geology of the two major playa lakes at Tonopah Test Range: the Main Lake and Antelope Lake (fig. 2). Both lakes have been used for past penetrator testing, but most major testing activities have been carried out on the Main Lake. In particular, most interest has been focused on the presence or absence of one or more so-called *hard layers;* viz. the cone-penetrometer study. Sediments that behave in a "hard" manner when penetrated during a weapon drop can generate deceleration forces in excess of certification levels and may potentially damage critical weapon components.

A Note on Coordinate Systems

Most large-scale topographic maps, such as the 1:24,000 7.5-minute series published by the U.S. Geological Survey, historically have been based upon the local state plane-coordinate system. At TTR, this is the Nevada state plane coordinate system, central zone, referenced to the North American Datum of 1927 (NAD-27). State plane coordinates are typically given in feet. With the rise of Global Positioning Satellite systems for determining spatial coordinates in real time in the field, the World Geodetic System of 1984 (WGS-84) has become the primary reference, in that the underlying electronic measurements are determined within this system. Because the same nominal coordinates (geographic: latitude and longitude; UTM, etc.) referenced to different datums can differ in physical position by up to a hundred meters or more, it has become increasingly important to ensure that the projection system (UTM, state plane) and the datum of reference (NAD-27, NAD-83, WGS-84) is identified properly.

The characterization activities at Main Lake, which were conducted first under this effort, used the Nevada state plane coordinate system, NAD-27, in feet, for consistency with most historical maps and spatially located data. However, with the initiation of the surface-based geophysical studies of Antelope Lake, we began to use Universal Transverse Mercator (UTM) coordinates, zone 11, WGS-84, in meters. The reason for the change was principally logistical. Most modern geophysical measurements are measured, computed and displayed in SI units. The geophysical contractor therefore preferred to work in metric coordinates, and although these coordinates could have been UTM meters, NAD-27, we decided simply to use the native GPS coordinate system: WGS-84.

Most references to coordinates in this document retain their original values: Main Lake activities and models in NAD-27 state plane coordinates, in feet; Antelope Lake activities and models in WGS-84 UTM coordinates, in meters. However, locations of drill holes — which provide the permanent hard data resulting from these studies — are given in both systems in Appendices B and F. Numerous computer programs now exist that can perform conversions among coordinate systems and datums quickly and conveniently (GeoComp Systems, 1999; U.S. Army Corps of Engineers, 2000).

GEOLOGICAL CHARACTERIZATION STUDIES OF MAIN LAKE

The subsurface geology of the TTR Main Lake was examined in the region generally used by recent penetrator testing activities, which is located in the southern portion of the modern lake bed (fig. 4). The current investigations were designed to overlap partially with the cone penetrometer survey (fig. 5; Hansen and Patterson, 1996), but to extend farther north toward the center of the lake. A concrete

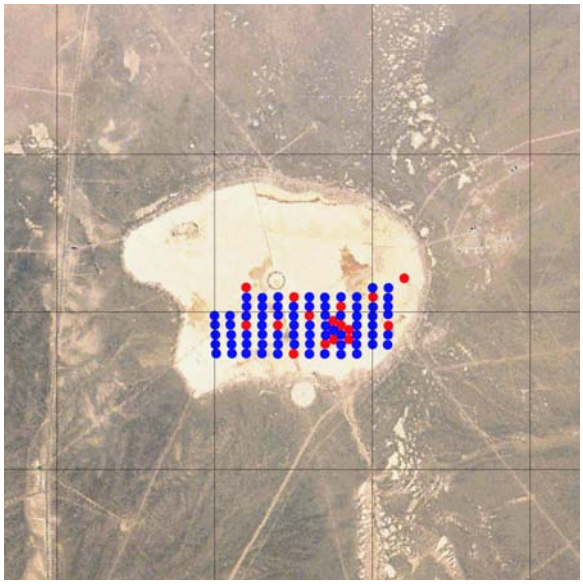

Figure 4. Aerial photograph overview of the TTR Main Lake showing the locations of holes drilled as part of this characterization effort. Red symbols indicate core holes; blue symbols indicate rotary holes. Width of image approximately 5 miles.

hard target used for some testing activities occupies a position near the southern shore of the modern lake (fig. 5).

METHODS

Core Drilling

Core samples were obtained using mining-industry-standard HX wireline equipment (fig. 6), using polymer mud, sometimes with minor bentonite addition, as the circulating medium. The use of mining-type equipment rather than an auger drill or more sophisticated equipment such as ultrasonic drilling was dictated in part by the need for rapid deployment of a first-pass characterization program. An idle mining-style rig was available immediately in central Nevada. Later, a more extensive drilling program was conducted using the same basic type of equipment because the initial drilling had yielded satisfactory results in a cost-effective manner.

Wireline coring equipment uses an *inner tube* within the outer *core barrel*, which — if properly adjusted — can significantly reduce contact of actively circulating drilling fluid with the core as it is drilled and thereby increase core recovery, even in weakly consolidated materials such as anticipated in a playa lake bed. The inner tube is what is retrieved via the *wireline hoist*, a winch system separate from that use to raise and lower the drilling pipe. This means of core retrieval allows large intervals of hole to be cored without the time-consuming need to remove all of the drill rods from the hole. Additionally, a *triple-wall core barrel* can be used, in which the core is recovered inside yet-another cylindrical tube within the inner tube; again exposure of the core to actively moving drilling fluids is reduced. This third tube is usually what is referred to as a *split tube*, meaning that the innermost tubing is split lengthwise during manufacture and is held together by adhesive tape and its snug fit within the normal inner tube. The core inside this split tube can be removed from the coring assembly simply by cutting the tape which holds the two halves of the barrel together, thus exposing the core without needing to extrude it from a solid assembly. Two examples of removing core from the inner tube (not a split tube) are shown in figure 7.

Cuttings are removed from the hole and the bit is cooled by a circulating fluid system. Addition of a synthetic polymer to water that produces needed viscosity while adding only minimal solids to the mud system was used for these holes. Minor amounts of bentonite clay were used in the mud system for a few of the early drill holes. Despite the relatively soft, non-cemented nature of the lake sediments, core recovery was generally excellent, and the drilling progressed sufficiently rapidly that the interior of the core was generally dry upon initial recovery, even though the outer portion of the core was wetted by the drilling fluid.

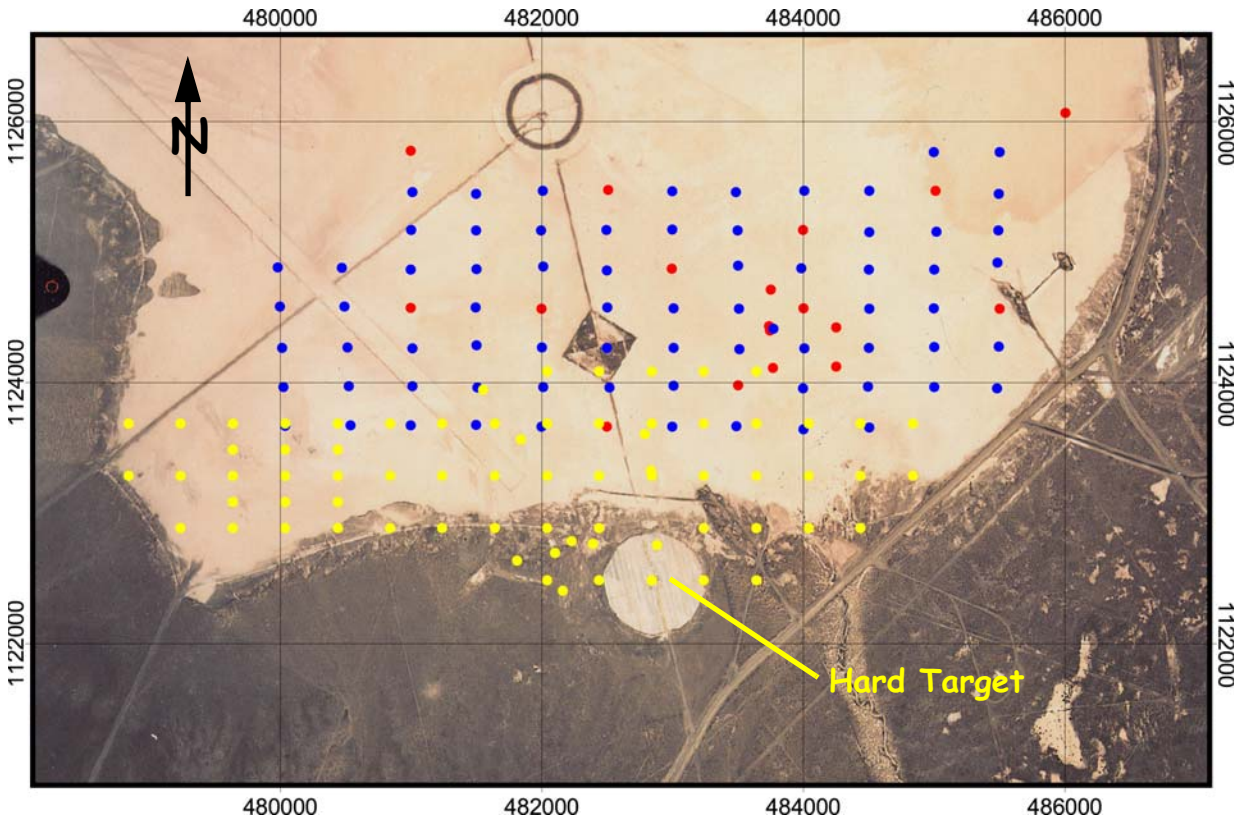

Figure 5. Detail of the southern Main Lake area showing several permanently marked targets, as well as the core holes (red) and rotary holes (blue) of this program compared with the positions of cone-penetrometer testing (yellow) reported by Hansen and Pattersen (1996). Grid is Nevada state plane coordinate system, NAD-27, in feet.

Rotary Drilling

Rotary drilling produces an open hole similar to that left after core drilling. However, intact core samples are not obtained, as a rotary bit simply crushes or otherwise disaggregates the penetrated rocks and the cuttings are circulated out of the hole by drilling mud. Rotary drilling at Main Lake was conducted using the same wireline-core rig, but using a tricone rotary bit instead of the usual core barrel assembly. Cuttings samples are frequently collected during rotary operations by screening (sieving) the mud returns. However, the soft lake sediments disaggregated so completely that no meaningful cuttings samples could be obtained.

Downhole Geophysical Logging

Geophysical logging surveys were conducted in the open hole remaining after drilling was completed, by lowering a cylindrical logging tool into the hole on the end of a cable, as illustrated in figure 8. Various physical properties are then measured as a function of depth as the probe is withdrawn from the hole. The result is a continuous recording of attributes that may be reduced to interpretable geologic data. Both core and rotary holes were logged in an identical manner.

The only logging tool used in all holes at the Main Lake was the so-called *density-resistivity* log. A radioactive cesium source on the bottom of the probe irradiates the adjacent material, and gamma rays from the source are

Figure 6. Photographs of core rig in operation of Main Lake. Note core rods and drilling mud.

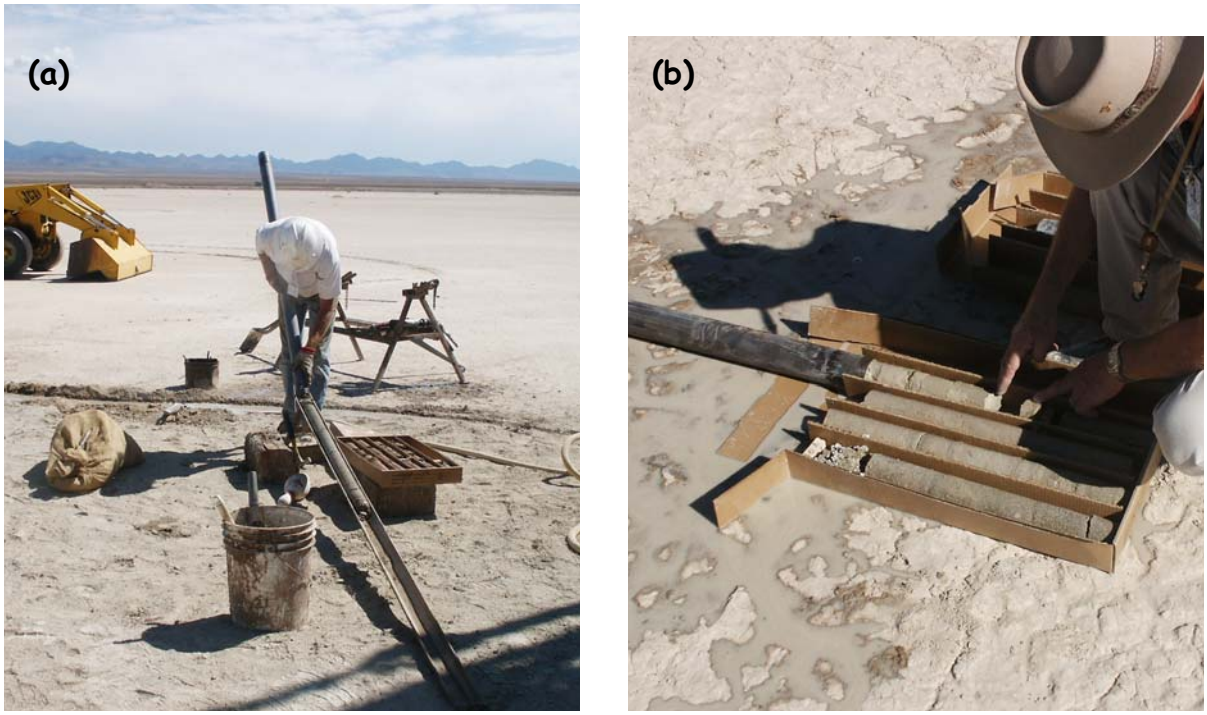

Figure 7. Photographs showing core handing at the rig. (a) Removing core from the inner tube onto a staging rack prior to marking and boxing. (b) Extruding core from the inner tube to avoid excessive disruption of soft or friable core. The inner tube is on the left-hand side of the photograph.

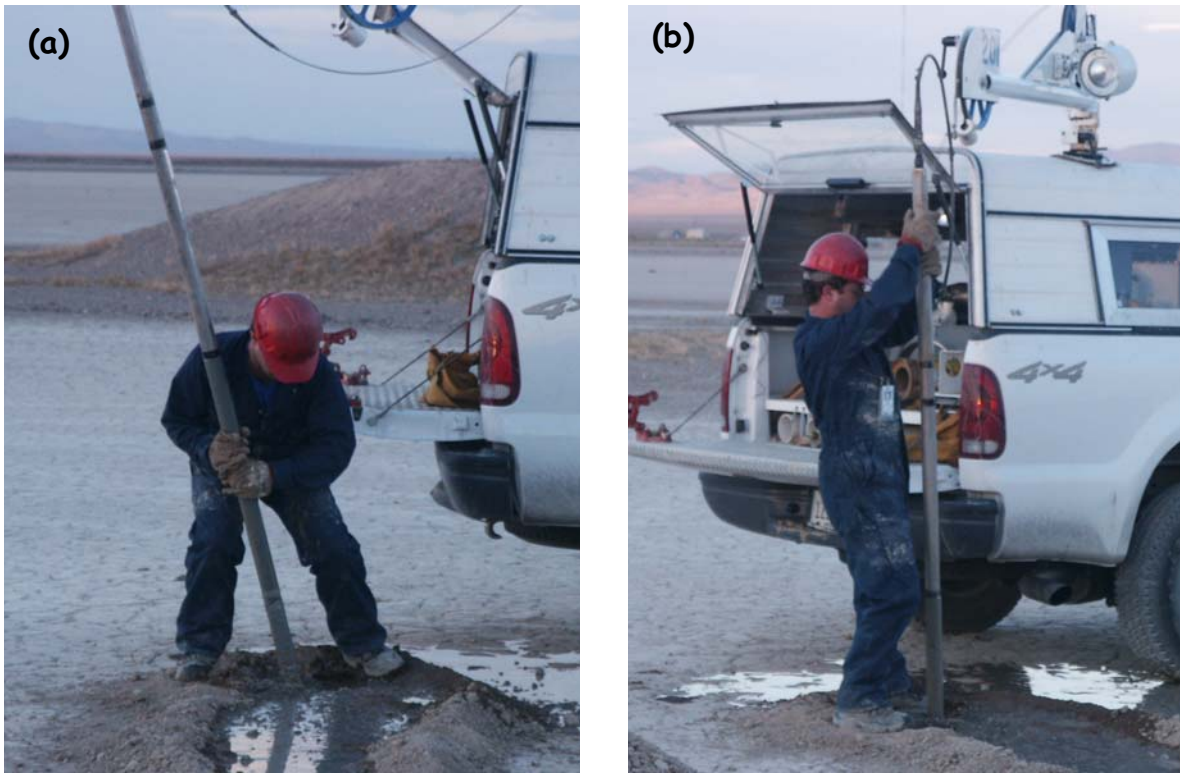

Figure 8. Photographs of inserting and lowering a geophysical logging sonde into a bore hole. In (a), note the black bands near the upper part of the probe that delineate one of the sensors, isolating it electrically from the remainder of the probe. In (b), note the wireline winch mounted on the truck and the cablehead attachment to the probe.

attenuated en route to a nearby detector in direct proportion to the density of the intervening rock. Following numerical processing, the result is a continuous record of density calibrated in g/cm^3. A caliper log measuring the hole diameter and calibrated in inches is recorded simultaneously by an extensible lever-arm that pushes the radioactive source and detector against the borehole wall as part of the density measurements. This produces a record of borehole diameter as a function of depth.

Two other measurements are part of the density-resistivity log. Electrical resistivity, in Ω-m, of the rock formations is measured between two electrodes on the downhole probe. Electrical resistivity to currents in earth materials (or by extension, its inverse: electrical conductivity) is largely a function of the moisture content in the rock, and the resistivity tool is frequently used to discriminate more coarse-grained materials from finer materials that typically contain more interstitial water because of capillarity. Finally, a passive detector measures the natural gamma activity of the rocks. This detector is located at the opposite end of the logging sonde from the gamma-based density-measuring equipment to reduce false signals from the attached radioactive source. The principal effect of this separation is that the natural gamma trace cannot be recorded to the total depth of the borehole, and the deepest measurements are located at the total depth minus the length of the tool (about 10 ft). Natural gamma activity in rocks is linked principally to potassium-40, a naturally occurring isotope of potassium found dominantly in feldspars and clays. Feldspars are

Figure 9. Slightly silty bentonitic clays at 4 ft depth in drill hole ML-3. Note dessication cracking characteristic of bentonitic materials. Width of core is ~2 inches.

particularly abundant in virtually all of the sediments in this region because the source terrane is composed largely of felsic volcanic rocks.

Results of Characterization at the Main Lake

Drilling and Geophysical Logging

Characterization of the Main Lake began initially with three core holes drilled immediately adjacent to the impact location of the test assembly that generated the need for the program. These three holes were drilled on a time-sensitive basis and they provided the first glimpses of the subsurface geology. Photographs of core recovered from these first three holes are presented in Appendix A.

The principal observation related to the purpose at hand was that below the known, approximately six-foot thick, surficial clay interval (fig. 9), there are alternating layers of clayey and silty sand among clayey "gravel" beds; this is indicated in figure 10 and figure 11 (a) and (b). Actually, the gravels are very coarse sandy granule conglomerates, as the dominant grain size of the coarser-than-silt fraction is about 1 to about 4–6 mm. The terms, *very fine pebbles* or *fine pebbles*, have also been used for this range of grain size (2–8 mm; AGI data sheet 29.1, 1989), but *granule* seems to convey better the small size of the clasts.

A matrix of clay and silt encloses the granules, but in figure 11(a), many of the large clasts appear to be in grain-to-grain contact and not "floating" in the matrix. Grain-on-grain contact will prove important in interpretation of the laboratory strength of these rocks and of the drop test results (see also page 29). Figure 11(b) shows granule-rich core in which the clasts may truly be floating in the matrix. However, note that the matrix portion of the sediment in this case was sufficiently hard that the diamond core bit abraded through the individual volcanic-rock fragments, rather than grinding away the matrix and leaving intact granules.

Photographs in jpeg format of most of the core collected from the Main Lake (holes ML-1 through ML-10) are contained on the CD-R in the rear of this report. Core was photographed by box (nominally 10 ft of core), and the filename contains both the drill hole identifier and the actual footage (multipled by 10 to eliminate decimal points) present in that photograph. For example, file ML-2_130-245.jpg shows the box containing core from drill hole ML-2, 13.0 ft to 24.5 ft. Additional photographs illustrate various aspects of the sediments; the file names of these files contain phrases describing the specific features.

In figure 10, note that although no downhole geophysical logging was conducted in any of drill holes ML-1, ML-2, or ML-3, a second-phase rotary drill , MLR-44, was drilled very close to ML-1. A simplified version of the three principal log traces from this borehole is shown associated with the core log for hole ML-1 (also see discussion on page 98).

The main phase of drilling on the Main Lake began with a series of core holes distributed widely over a 500-ft (east-west) by 300-ft

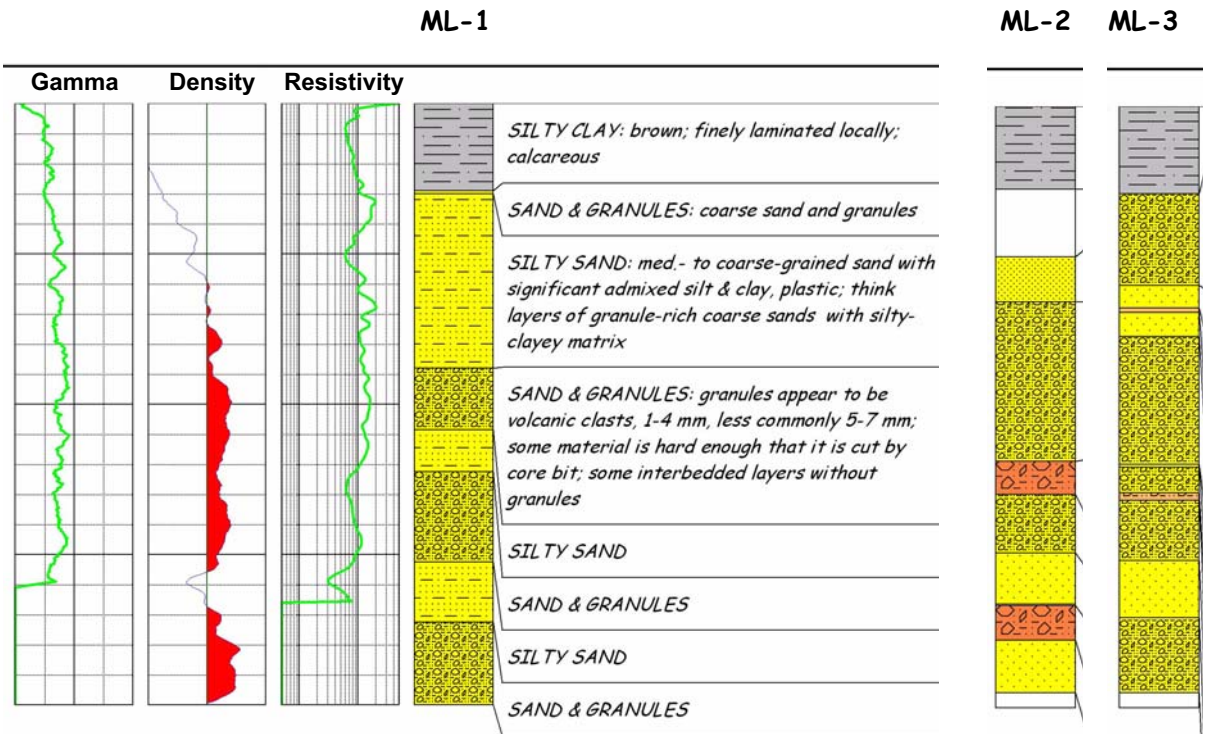

Figure 10. Core logs for drill holes ML-1, ML-2, and ML-3, together with geophysical logs from rotary hole MLR-44. Density values > 2.0 g/cm^3 shaded red. Total depth of each hole is 40 ft. All four holes are located within a radius of less than 20 ft.

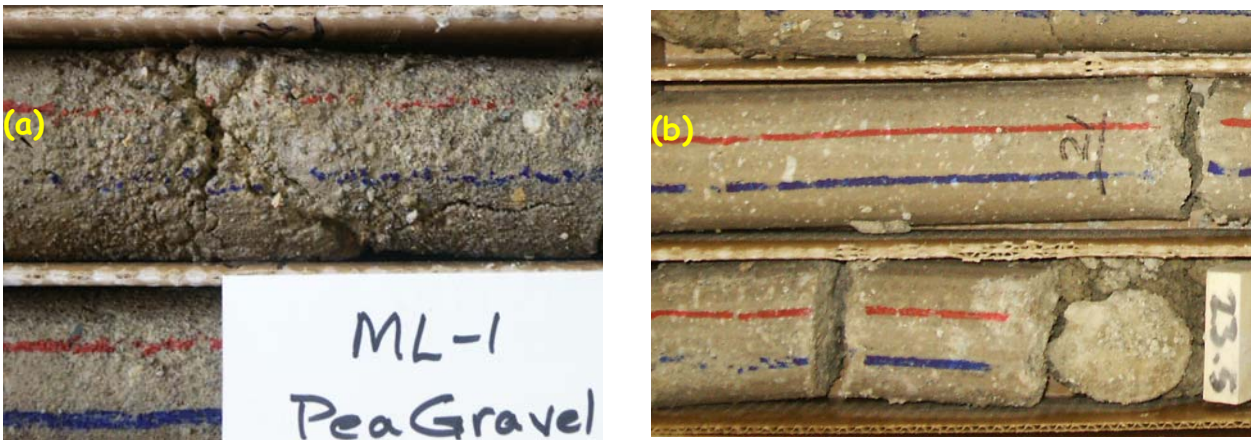

Figure 11. Photographs of fine to very fine gravel/granules in core samples: (a) at a depth of ~23 ft in drill hole ML-1; (b) at a depth of approximately 21 ft in drill hole ML-2. Note that granules in (b) have been cut through by the drillbit, despite their presence in a clay-rich matrix. Width of core tray in each image is approximately 2 inches.

(north-south) nominal grid to explore the overall distribution of the coarser layers. This exploratory phase consists of holes ML-4 though ML-11. Ultimately, however, rotary drilling was commenced to fill in the grid in a quasi-systematic manner. Several additional core holes were drilled, generally more focused in the vicinity of the initial holes ML-1 through ML-3. The final drilling pattern for both core and rotary drill holes on the Main Lake is shown in figure 12. Core holes are shown as red symbols, whereas rotary holes are shown by the blue symbols. There are a total of 90 boreholes, 19 core and 71 rotary. The collar coordinates for all holes drilled on the Main Lake are given in Appendix B, table B-1. Locations are given in latitude and longitude, UTM metric coordinates (both WGS-84), and in Nevada state plane coordinate systems (NAD-27) for convenience. Geologic and geophysical logs for the 90 drill holes are presented in Appendices C and D.

A complete discussion and interpretation of the results of drilling at the Main Lake is beyond the scope of this data report. However, a general sense of the subsurface geology is conveyed by figure 13, which shows density — perhaps *the* most useful geophysical parameter — as determined by the downhole geophysical logging. Correlation of the lithologic core logs from the early holes of the gridded main-phase of drilling with the geophysical data from the same holes indicated that density values of 2.0–2.1 g/cm^3 appeared to be a fair discriminator of sediments containing gravels and very coarse sands from finer grained materials.

In figure 13, each drill hole is shown as a vertical sequence of colored spheres, for which the color is proportional to the density on one-half-foot composite intervals, as indicated by the color scale at the bottom of the figure. The view in part (a) of the figure is from a southwesterly direction and from above, whereas the view in part (b) is from the northeast.

Although the sheer density of the drilling pattern makes it difficult to see "into" the more rearward portions of the illustrated volume, the overall trend of density changes (recall that high density is interpreted as hard sediment) is fairly obvious. Densities are greatest in the eastern and southeastern portion of the mapped volume. The thickness and number of dense (hard) layers diminishes toward the west, with some lesser decrease to the north.

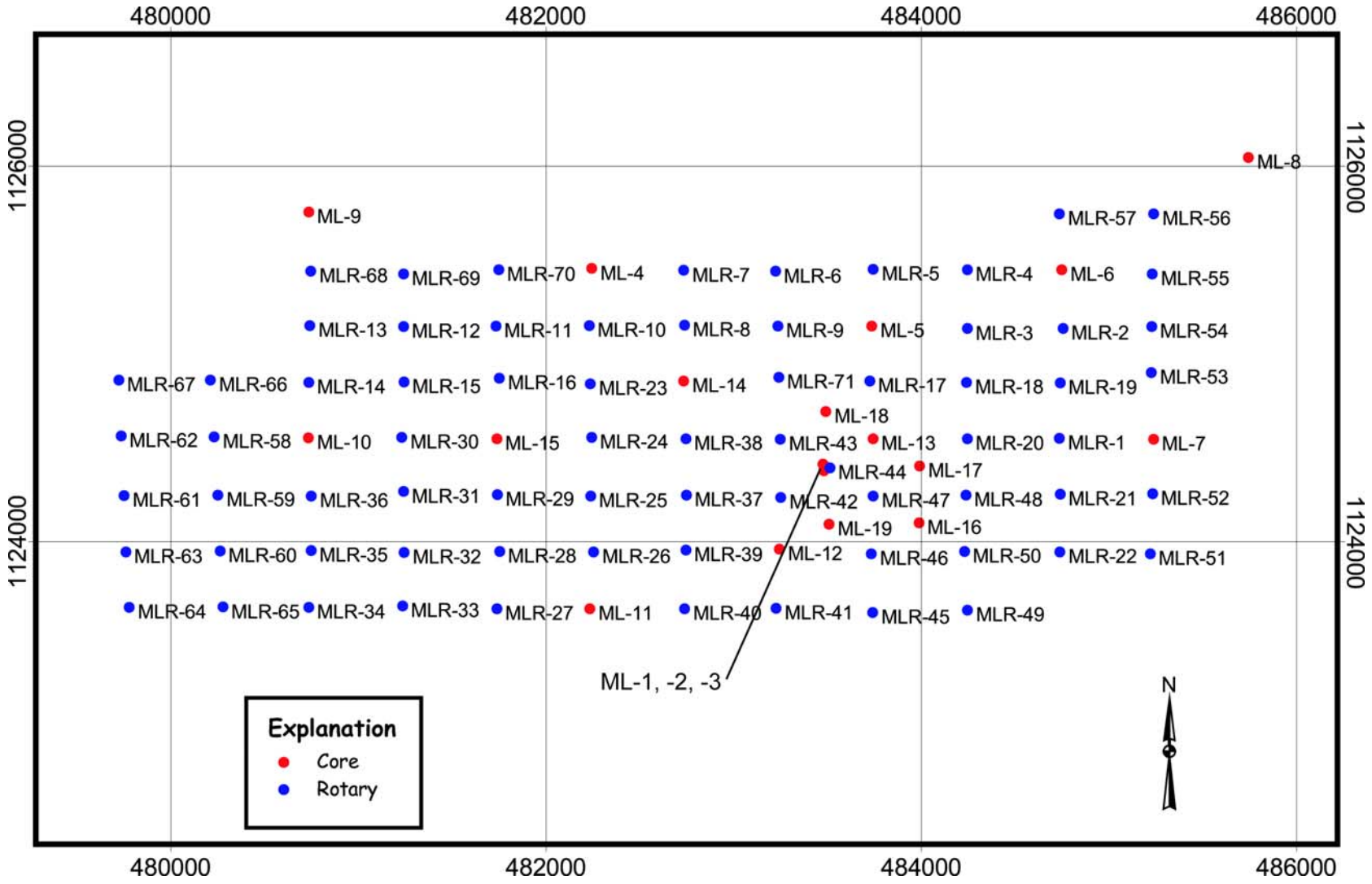

Figure 12. Map of the Main Lake showing locations of both rotary and cored holes. Grid is Nevada state plane coordinate system, central zone, in feet; NAD-27.

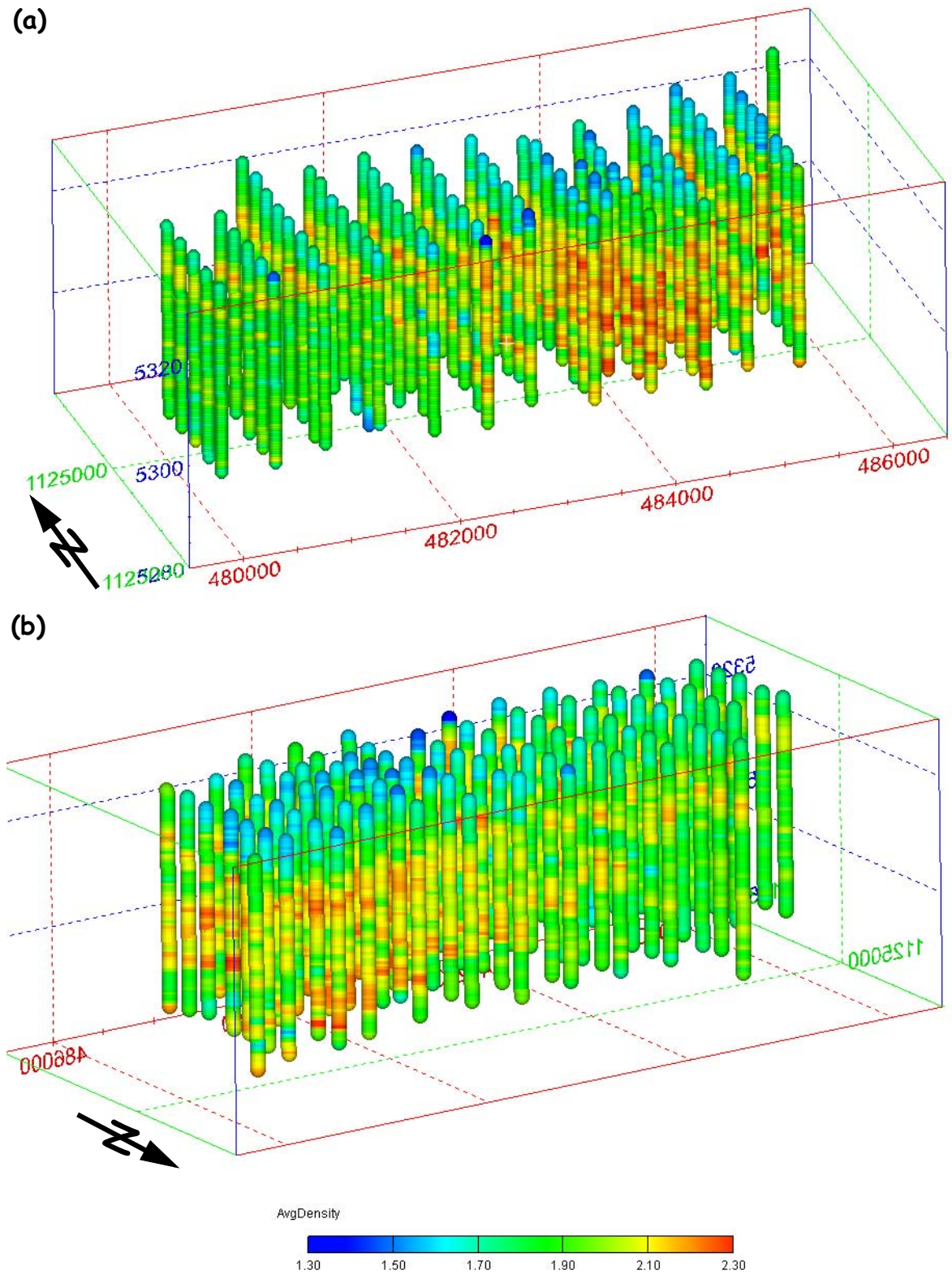

Figure 13. Drilling results for density at the Main Lake. (a) view from the southwest; (b) view from the northeast. One-half-foot averaged densities shown by color scale. Boreholes are all approximately 40 ft deep. Grid is Nevada state plane coordinate system, NAD-27, in feet.

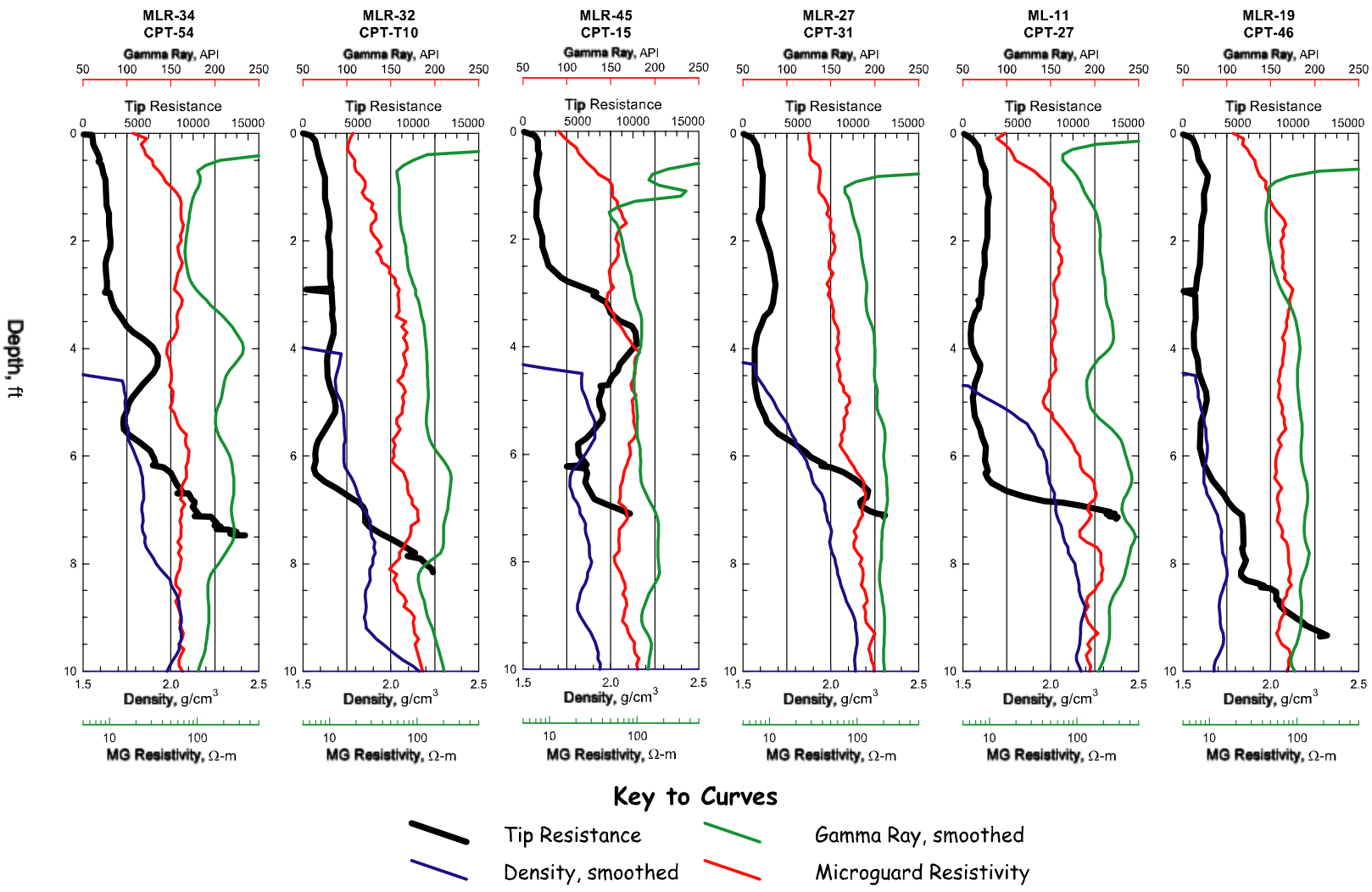

Figure 14. Comparison of the data from several cone penetrometer tests and geophysical logs from corresponding core or rotary drill holes. Degree of correlation between tip resistance and the various geophysical traces differs somewhat among pairs. Cone penetrometer data digitized from Hansen and Patterson (1996).

Additional insight into the utility of geophysical density as a surrogate for "hardness" (as distinct from "coarseness") of the sediment is gained from figure 14. This illustration presents a pair-wise comparison of tip-resistance data from several of the cone-penetrometer "pushes" (fig. 5) with the three principal geophysical traces from nearby rotary and cored holes. Recall that the cone-penetrometer values represent the relative resistance to penetration as the hydraulically driven penetrometer probe is pushed into the ground (page 15).

For each pair of tests in figure 14, the density trace appears to lose resolution and drift consistently toward unphysically low values in the upper four feet or so of the hole. This phenomenon is almost certainly related to emergence from the drill hole of the gamma detector on the mid part of the geophysical logging sonde.

As with the correlation of geophysical log information with the macroscopic lithologic character of the core, the correspondence of the geophysical data with resistance to penetration is not exact. However, unlike the core-to-geophysics correlation for which the data come from the same physical location, the penetrometer data are are from spatial positions separated by up to several tens of feet.

Nevertheless, most of the pair-wise comparisons indicate that there is approximate correspondence between inflection points in the tip-resistance trace and distinct changes in at least one of the three geophysical traces. Note in particular the correspondence between resistance and the gamma-ray log in pair MLR-34–Cpt-54 and between resistance and the Microguard resistivity as well as gamma-ray traces in pair MLR-32–Cpt-T10. In at least one example (ML-11–Cpt-27), the correspondence of abrupt changes in log character is quite pronounced, but the depth at which the changes occur is offset by approximately 1.5 ft. This is consistent with the recording of these data at two slightly separated positions.

Rock Mechanics Data for the Southern Main Lake Area

A fairly substantial number of specimens were taken from the core recovered from the first ten holes for material properties testing (Appendix E, table E-2). In general samples were selected to cover a variety of lithologic types and the entire geographic area of the drilling program. The shallower parts of the holes were emphasized over the deepest sections. Additionally, emphasis was placed on the general depth interval of the problem hard layer in the original flight test: approximately 15 to 25 ft. Only one or two specimens from the uppermost silty clay (soft) layer (fig. 10) were selected, as this unit was not of particular interest for this study.

In the end, however, only a minimal number of core specimens were actually tested. The results of laboratory properties testing on samples from the first three core holes, ML-1 through ML-3, are tabulated in table E-1. All of these samples are from the immediate vicinity of the drop test that initiated this study. It is not clear why the properties testing was limited to this small suite of specimens.

Of interest are the results of the confined compressive strength (triaxial) testing, the results of which are shown in the lower part of table E-1. The strength of the tested samples increases markedly — from less than 1 MPa for the unconfined condition (test TTR-UC01) to almost 700 MPa at a confining pressure of 400 MPa (test TTR-TA04). This increase is illustrated graphically in figure 15, using logarithmic scaling on both axes. Even though the lithostatic confining pressure on the materials anywhere within the depth range sampled by the drill holes on Main Lake is rather low, the effective confining pressure experienced by the rock mass during an impact event at many

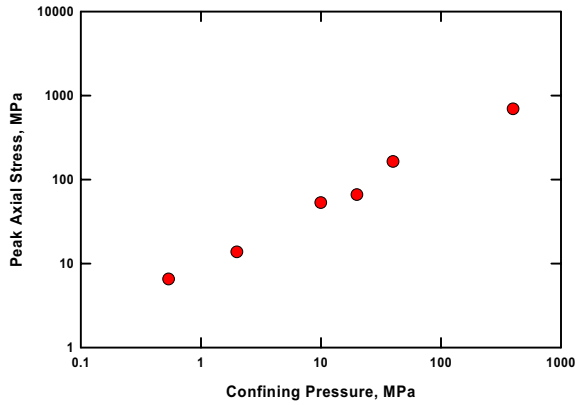

Figure 15. Increase in compressive strength with confining pressure of core specimens from the Main Lake. Data from table E-1; log-log scaling.

hundreds of feet per second is likely to be significantly greater than lithostatic. The lithostatic gradient is widely assumed to be roughly 1 psi (6.9kPa or 0.0069 MPa) per foot of burial. Thus, even materials at the 40-ft maximum depth of burial that were sampled by the drilling program only experience an in-situ confining pressure of about 0.25 MPa.

The strength of the rock mass under rapid loading conditions is probably greater than it might be otherwise because of the grain-on-grain nature of the clasts in several intervals. The large clasts are resistant pieces of siliceous volcanic rocks. Under confining pressure and shock-like loading, the fact that these hard fragments are in direct contact with one another (e.g., fig. 11) appears to cause the sediment mass to behave much like the parent volcanic rock. Were the granules and fine pebbles more dispersed ("floating") in the mud matrix, some early strain would be more easily accommodated by displacements of the larger clasts within the soft, fine-grained matrix. It is most likely this exponential increase in "apparent" compressive strength of the granule-bearing beds under impact loading conditions is the principal cause of the component failure that initiated this study.

Discussion of Main Lake Geology

A portion of the subsurface geology of the Tonopah Test Range Main Lake has been characterized in some detail. A near-surface unit of relatively recent, soft, clay-rich sediments from the "modern" lake is underlain at depths below about 6–10 ft by what appears to be a complex sequence of interfingered finer and coarser grained materials. Coarse-grained materials range in size up to fine gravel (up to 1–2 cm).

The dominance of clayey material, even within what are obviously quite coarse-grained units, suggests deposition as debris flows, in which the coarser clasts were transported suspended in a relatively high-viscosity mass of mixed particle sizes and water. Some degree of sorting within the local source terrane is evident, in that the range of coarser grain sizes is somewhat restricted to granules through fine gravel. Given the distance of the Main Lake to the adjoining highlands of the Kawitch or Cactus Ranges (fig. 2), in-transport sorting such as this is not unexpected in this geologic environment. Based upon the geometry of the main mass of coarse-grained material encountered in the subsurface of the Main Lake (e.g., fig. 13), and the observed decrease in the quantities of coarser and more dense units toward the west, it is most likely that these debris-flow-like deposits came to rest as a delta-like mass near the eastern margin of the paleo-Main Lake. Clearly, however, there was only minimal reworking of the deposited sediments, as the granule-bearing beds remain clay rich.

A geophysical density threshold value of 2.0–2.1 g/cm^3 seems to perform well as a discriminator between coarse grained, frequently granule-bearing intervals and finer grained sediments . This correlation is observed (e.g., Appendices C and D) in virtually every core hole that encountered coarse-grained materials. The match of density-defined "hard" intervals with the logged extent of the coarse-

grained units is not one-to-one. However, it is not always easy to identify the presence of smaller quantities of coarse clasts in these muddy, clay-rich sediments. Additionally, uncertainties in the depth positioning of the logged core segments within intervals of poor core recovery may be responsible for some of the lack of detailed correlation.

There are some additional observations and features that may bear on the origin of the relatively well-sorted coarse sediments encountered by the Main Lake (and Antelope Lake; see below) drilling. Parts of the margins of the modern Main Lake, the margins of Antelope Lake, and local areas elsewhere on Antelope Lake, are covered by well-sorted granules to fine pebbles of the same siliceous volcanic fragments that compose the subsurface clayey gravel units. The overall appearance of the marginal gravel deposits is shown in figure 16(a); a close-up view of the clasts is in figure 16(b). The granule and pebble deposits are generally elevated very slightly above the remainder of the lakebed (less than a few centimeters).

The mechanism of the sorting observed in these bank deposits is not entirely clear. Potentially, the fine and very fine gravel clasts may be lag deposits from which the finer silt- and sand-sized fractions have been removed by the wind. Wind speeds on the lake beds (indeed, at TTR in general) can be quite high at certain times, and the otherwise flat lake beds contain nothing to break the wind. The areas immediately to the east and northeast of both the Main Lake and Antelope Lake are covered by extensive dune deposits up to several meters thick. The dunes are composed of silt and sand-sized materials, so it would not be unlikely that

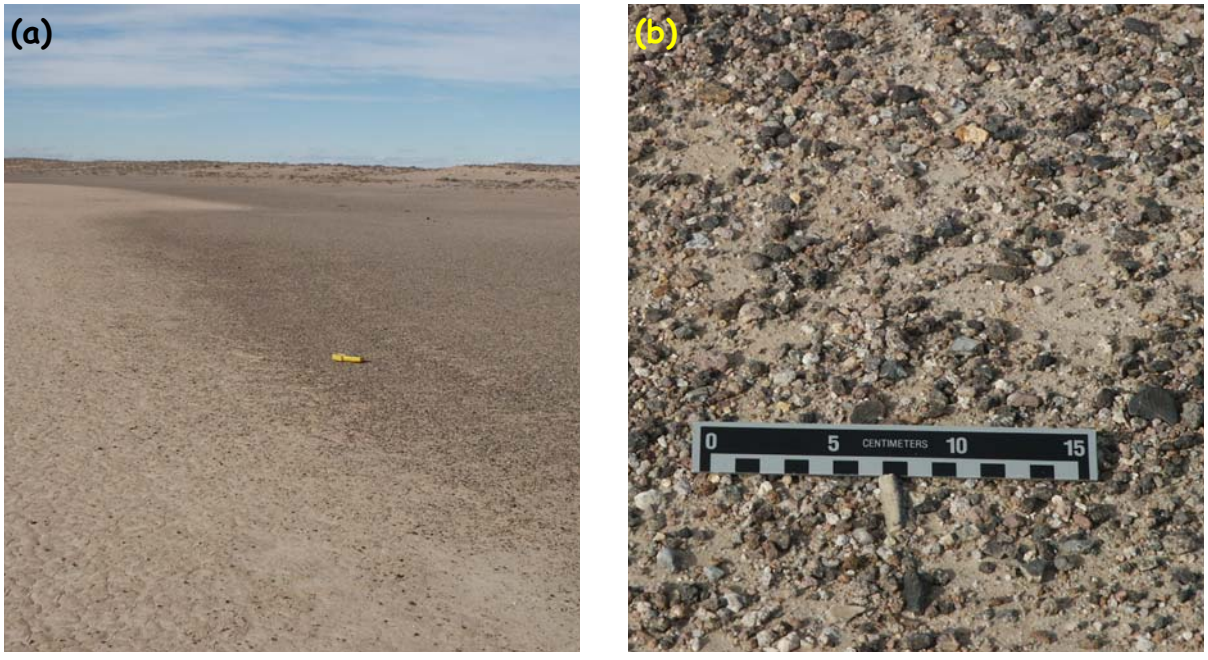

Figure 16. Overview (a) and close-up (b) of relatively well-sorted granules and fine pebbles (dark) found around the margins of Main and Antelope Lakes. The background in (a) shows dune deposits just outside the modern lakebed. The yellow GPS datalogger in (a) is approximately 20 centimeters long. Scale bar in (b) is in centimeters.

coarser clasts available in the source region(s) might remain behind as lag deposits.

Examples have been observed on the Main Lake of places where isolated pebble-sized clasts appear to have sunk into the clays of the lake surface; see figure 17. The surrounding clays have been depressed slightly surrounding the central crater, as would be expected if the clast had subsided under gravity into a soft, plastic material. The lake beds have been observed to remain quite hard, even under an inch or so of standing water accumulated after larger rainfall or snowfall events. However after several days, the very top few millimeters of the lake clays does become soft and slippery. It would be easy to envision that the top several centimeters to possibly a meter or so might conceivably become soft and plastic during extended wet periods, such as unquestionably occured during Pleistocene pluvial periods. Under such conditions, entire lake-margin gravel deposits, such as that in figure 16(a) could become clast-supported clayey conglomerates identical to those encountered in the drill holes (for example, fig. 11).

Although some lateral correlation between drill holes appears possible, it is not entirely clear that individual beds can be so correlated. In other words, the drill hole spacing, even at 300 by 500 ft, may be too wide to capture the detail of individual channel deposits. However, for the purpose at-hand of identifying suitable target regions for penetrating tests, the overall dominance of high-density, likely coarse-grained material in the subsurface of Main Lake, for example as shown in figure 13, suggests that coarse, hard layers are widespread across the southeastern and southern portion of the lake.

The display of figure 13 also makes it quite clear that the more dense (= harder) materials decrease markedly to the west; for example, west of 482,000 ft East, Nevada state plane coordinates. If target regions are desired on the Main Lake for penetration events reaching below about 10–12 ft, it may be possible to find suitable regions west of this easting value. Refer also to figures 4 and 5 for the positioning of the Main Lake drill holes relative to the modern lake margins. Note that the degree of

Figure 17. Photographs of individual pebble-sized clasts that appear to have sunk into soft clayey sediment on the surface of the Main Lake. (a) Close-up veiw; note possible trail (arrow). (b) Multiple clasts (arrows) with likely second-generation mud cracks

encroachment of coarse-grained materials from the western shoreline is not known, as the westernmost "column" of drill holes shows no evidence of a wedge of coarser clastics in this area.

Geologic Characterization of Antelope Lake

Antelope Lake, located approximately 10–12 miles south of the Main Lake (fig. 2), had not been characterized previously in any significant detail prior to this study. Thirteen of the cone penetrometer holes reported by Hansen and Patterson (1996) were drilled in a profile trending roughly north-northwest across the long dimension of Antelope Lake, but the maximum depth interrogated by this technique was 10 feet. A number of recovery pits for various air-dropped test assemblies have been excavated over the years, but no systematic geologic data appear to have been recorded at these sites. Indeed, even the locations of those excavations appear not to have been recorded.

The lack of definitive, spatially located subsurface information led to a two-stage investigation of Antelope Lake. Initially, a surface-based geophysical investigation was designed to provide some basic information on the stratigraphic framework of the lake bed and the likely distribution of gross lithologic types. This investigation consisted of time-domain electromagnetic (TEM) soundings on relatively close spacings coupled with more sparse Schlumberger-array resistivity soundings. Later a drilling program was targeted (a) to confirm some of the geophysical interpretations and (b) to identify a suitable target region and aim point for future testing.

The overall positioning of the geophysical survey within the large areal expanse of Antelope Lake itself (roughly 1.5 by 3 miles) was controlled by inferences based on the tectonic and topographic setting of the lake. Figure 2 indicates that the depositional basin, of which Antelope Lake is the deepest current portion, is asymmetric, with steeper slopes to the west formed by the Cactus Range at a distance of roughly 5–6 miles. In contrast, the terrain to the east of Antelope Lake is of markedly less relief, with the distance to sediment-source terrane comparable to the Cactus Range in excess of 20 miles. This general topographic positioning, combined with the presence of numerous feeder channels and arroyos leading into Antelope Lake from the Cactus Range, suggested that the west side of the lake might reasonably contain more coarse debris ("harder" material) than the eastern side. Accordingly, the layout of the geophysical survey positions was biased toward the eastern portion of the lake.

The second stage of characterization was based upon drilling constrained by the results of the surface geophysics. The drilling approach was essentially identical to that described for the Main Lake, except that an expanded suite of downhole geophysical logs was acquired and the holes were completed to a greater total depth. Both rotary and cored holes were drilled. The expanded suite of geophysical logs plus experience gained from the surface geophysical investigations allowed greater reliance on less-expensive rotary drilling methods.

The drilling itself was conducted in two successive phases. First, the initial core holes were targeted at confirming interpretations from the surface geophysics. Thus the first four holes were drilled in areas characterized by markedly different surface-geophysical measurements (principally the TEM results). After that, drilling was guided partially by the surface geophysical interpretation generally and more specifically by the previous drilling results in seeking an area free of identifiable coarse-grained/"hard" sedimentary layers.

METHODS

Time-Domain Electromagnetic Profiling

Electromagnetic (EM) soundings are frequently performed using *transient*, or *time-domain* (TEM), methods. The most typical configuration for these soundings uses a central-loop configuration, illustrated in figure 18. Figure 19 shows two views of an actual field TEM measurement in progress, giving a better idea of the scale involved.

In the central-loop geometry, a current is passed through the larger, external-loop transmitter for a sufficiently long time that a steady-state magnetic field is generated in the Earth. This current is terminated abruptly, which causes the induced magnetic field to decay, inducing secondary electrical currents to flow in the ground. These subsurface currents propagate downward and outward giving rise to a secondary magnetic field, which decays in par-

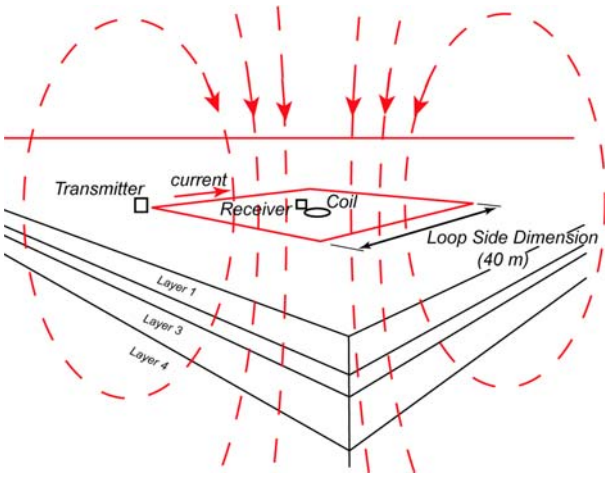

Figure 18. Schematic representation of the geometry and physics of time-domain electromagnetic measurements.

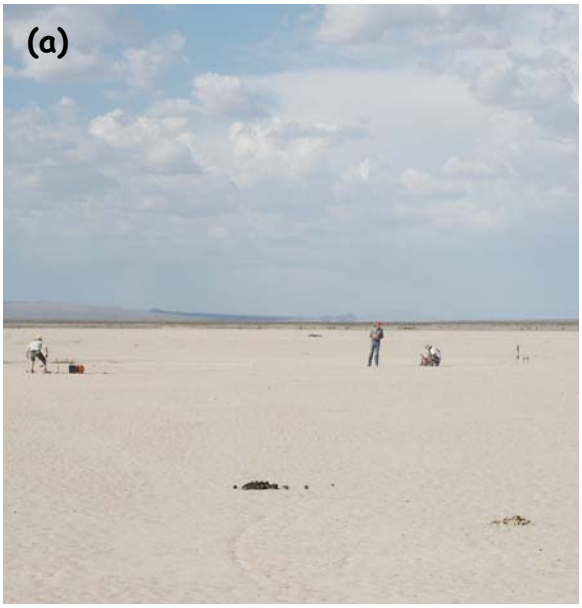

Figure 19. Field TEM measurements. (a) One-half (approximately) of a TEM loop. The transmitter assembly and wire spool are on the left and the central loop system is on the right. (b) Detail of a TEM central-loop layout. The receiver coil is slightly elevated above the lake surface on the right and the recording equipment is inside the orange box on the left.

allel with the original induced field, but with some time lag. The smaller, central loop of the sounding set-up detects the secondary magnetic field, as this decaying field in turn induces electrical currents in the central loop. The induced electrical currents in the central-loop receiver are sampled as a function of time. Early-time voltages correlate with shallow currents flowing near the transmitter wire (the external loop), whereas late-time samples correlate with deeper-penetrating currents.

Multiple TEM soundings may be collected adjacent to one another along a linear traverse, forming a profile that may be modeled, analytically or numerically, using a layered-earth model of resistivity. Such a resistivity profile may, in combination with other information, be used to infer the lithologic variation with depth, and potentially laterally as well.

The TEM survey at Antelope Lake (fig. 19) utilized 40-m TEM loops separated by 40-m spaces along three traverses, as shown in figure 20. Additional details of the specific instrumentation and data processing for the TEM survey are presented in Appendix J. All TEM data were reduced to apparent resistivity values for presentation.

Galvanic Resistivity (Schlumberger) Soundings

Direct-current (or galvanic) resistivity soundings were acquired at Antelope Lake using the classical *Schlumberger-array* electrode configuration. This geometry consists of a sequence of progressively larger spacings for a collinear, four-electrode array. Current electrodes are on the outside, and electrodes measuring the potential (voltage) are on the inside. The classical Schlumberger-array geometry is shown schematically in figure 21 and in the field in figure 22.

An electrical current is transmitted between positions A and B in figure 21, and the resulting voltage is recorded at positions M and N. The A-B distance is increased, holding M-N constant, the current is transmitted again and the corresponding voltage recorded. This process of increasing the distance between the current electrodes (and ultimately of the potential electrodes as well) is repeated multiple times, constituting a vertical sounding in which larger A-B distances correspond to sampling the electrical properties of progressively deeper earth materials.

Data from a Schlumberger sounding are reduced analytically to apparent resistivity, the resistivity of a homogeneous isotropic half-space. Apparent resistivity is then plotted as a function of the distance AB/2 to obtain a vertical profile. Additional details of the instrumentation and data processing for the resistivity surveys are presented in Appendix J. The positions of the Schlumberger resistivity soundings on Antelope Lake are shown in figure 20, in conjunction with the TEM transmitter locations

Frequency-Domain Electromagnetic Surveys

A second type of electromagnetic survey, using what is known in the geophysical industry as *EM-31* or a *terrain conductivity* meter, was conducted across part of Antelope Lake, partially as an experiment, because the technique is relatively inexpensive and a survey can be executed very quickly. Unlike the time-domain EM described previously, this survey methodology is conducted in the frequency domain, meaning simply that the initiating signal is transmitted continuously and the received signal, as modified by its passage through earth materials, is recorded continuously as well.

These electromagnetic data are typically taken in what is described as a *Slingram* configuration, illustrated schematically in figure 23. A sinusoidal current is generated in the transmitter coil and a voltage is monitored in a coplanar receiver coil some distance away hor-

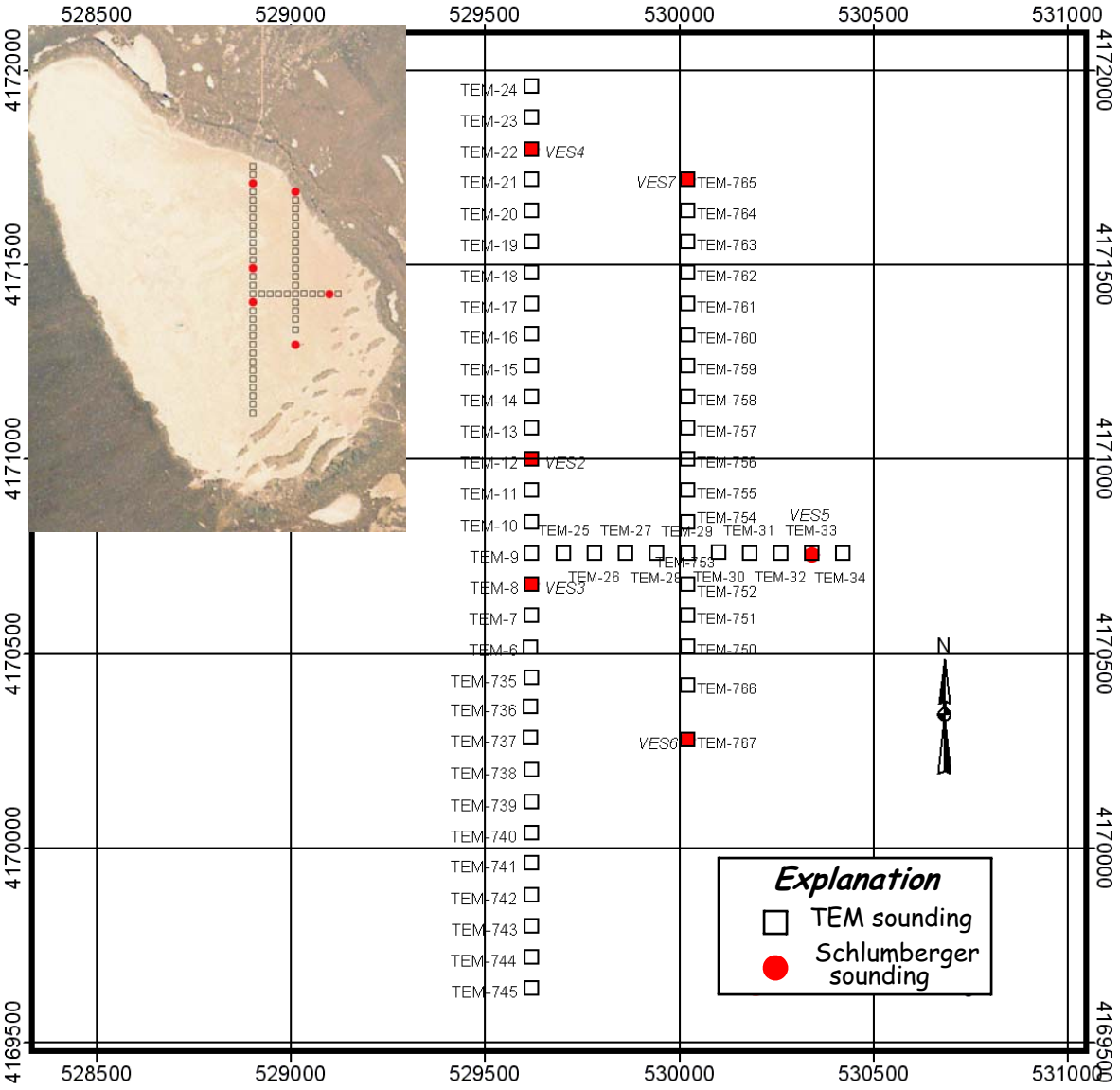

Figure 20. Locations of time-domain electromagnetic measurements and Schlumberger resistivity soundings on Antelope Lake. The square TEM symbols and intervening gaps are *approximately* to scale. Inset aerial photograph shows positioning of TEM surveys with respect to the overall lake. UTM grid, zone 11, in meters, WGS-84.

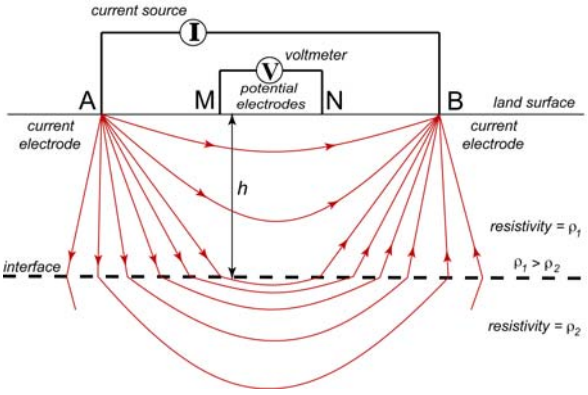

Figure 21. Schematic representation of the geometry and physics of a Schlumberger galvanic resistivity sounding.

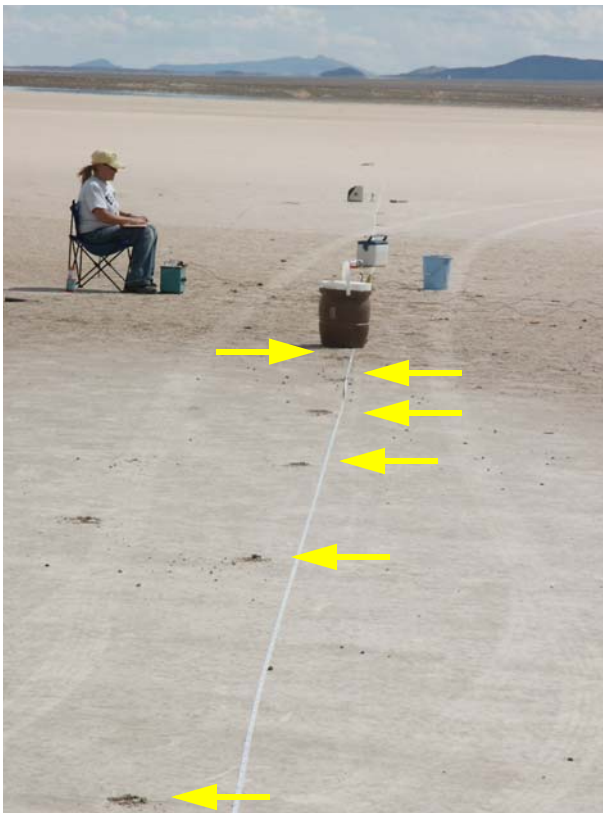

Figure 22. Layout of a Schlumberger vertical-electric sounding in the field on Antelope Lake. A number of progressively larger spacing (empty) electrode holes are visible to the left of the survey tape (narrow white stripe); a similar sequence of expanding electrode holes is on the other side of the water jug. The electronic equipment is in the small box at the foot of the technician.

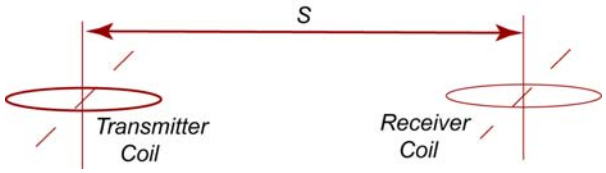

Figure 23. Schematic representation of the geometry of a Slingram-type horizontal-coplanar electromagnetic coil configuration. *S* is a fixed separation distance.

izontally. The time-varying primary magnetic field induced by the transmitter current induces eddy currents to flow in the earth. These eddy currents, in turn generate a secondary magnetic field, which together with a component of the transmitter magnetic field, are detected at the receiver coil as a voltage.

Because the geometry of the system and the specifics of the varying input current (frequency and intensity) are known, the received signal can be processed to remove the direct input contribution to the total receiver response. This leaves a residual signal that represents distortion of the input signal by the earth materials through which the signal has passed. It is this residual, modified signal that yields information regarding the geology and its subsurface physical properties. Furthermore, the residual secondary signal can be separated into *in-phase* and *quadrature* components, vis-a-vis the phase of the input sinusoidal current. These two components can be analyzed separately, potentially yielding additional geologic information.

The EM-31 system employed at Antelope Lake (fig. 24) produces a direct readout of the quadrature component as the apparent conductivity of the subsurface in millisiemens per meter (mS/m). The reciprocal of this value (times 1000) is apparent resistivity in ohm-

Figure 24. Bicycle-towed EM-31 equipment. Horizontal white cylinder is the Slingram-configured EM transmitter and receiver assembly. Vertical device is GPS receiver. Electronics equipment is inside the cart.

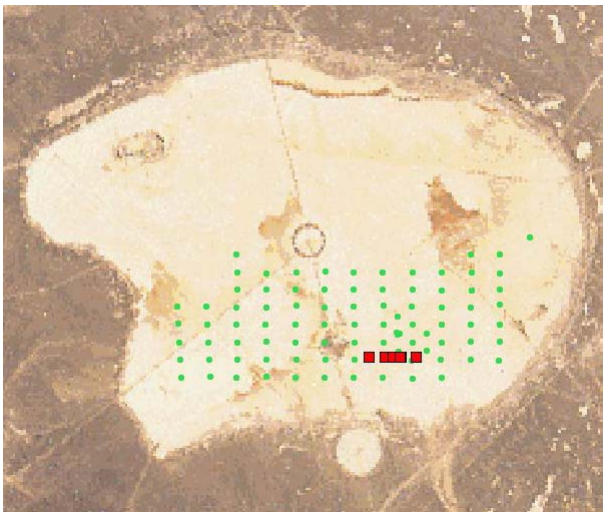

Figure 25. Locations of TEM loops (red squares), Schlumberger sounding (collocated with one of the TEM loops), and pre-existing drill holes (green dots) for the geophysical calibration surveys on Main Lake.

meters (Ω-m), and may be more-or-less directly compared to the apparent resistivity values produced by the time-domain electromagnetic method. The in-phase measurement can also be interpreted, particularly with respect to detecting buried metal conductors. Additional details regarding the frequency-domain EM method and information regarding data-reduction formulae are presented in Appendix J.

Calibration of Surface Geophysical Methods

A brief set of surveys using the different geophysical methods was conducted on the Main Lake prior to their use on Antelope Lake. The intent was to "calibrate," to the extent possible, the geophysical measurements in an area for which there was abundant information from a similar geologic environment. Because principal interest at Antelope Lake was to be focused on identifying and avoiding coarse-grained (hard) sediments, the test locations on Main Lake were selected to be in a general region of known coarse material. Furthermore, the calibration measurements were located in an area containing both rotary and core drill holes.

Figure 25 shows the position of the calibration study on the Main Lake. The study consisted of six 40-m TEM loops, one vertical electrical (Schlumberger) sounding, and three traverses of EM-31 measurements. The measurements were aligned east-west, and the six TEM loops were centered on core hole ML-12. Rotary holes MLR-39 and -46 are located at either end of the TEM transect. Geologic and geophysical logs of these drill holes are presented in Appendices C and D, figures C-9, C-55, C-61, and D-12.

Figure 26 shows the results of the EM-31 calibration survey on the Main Lake. The terrain conductivity values are in part (a), whereas the in-phase data are presented in part (b). The tracks of the bicycle-towed EM-31 equipment are shown on both figures as the irregular east-west lines. Only three EM-31 profiles were collected and these are nominally 20 m apart.

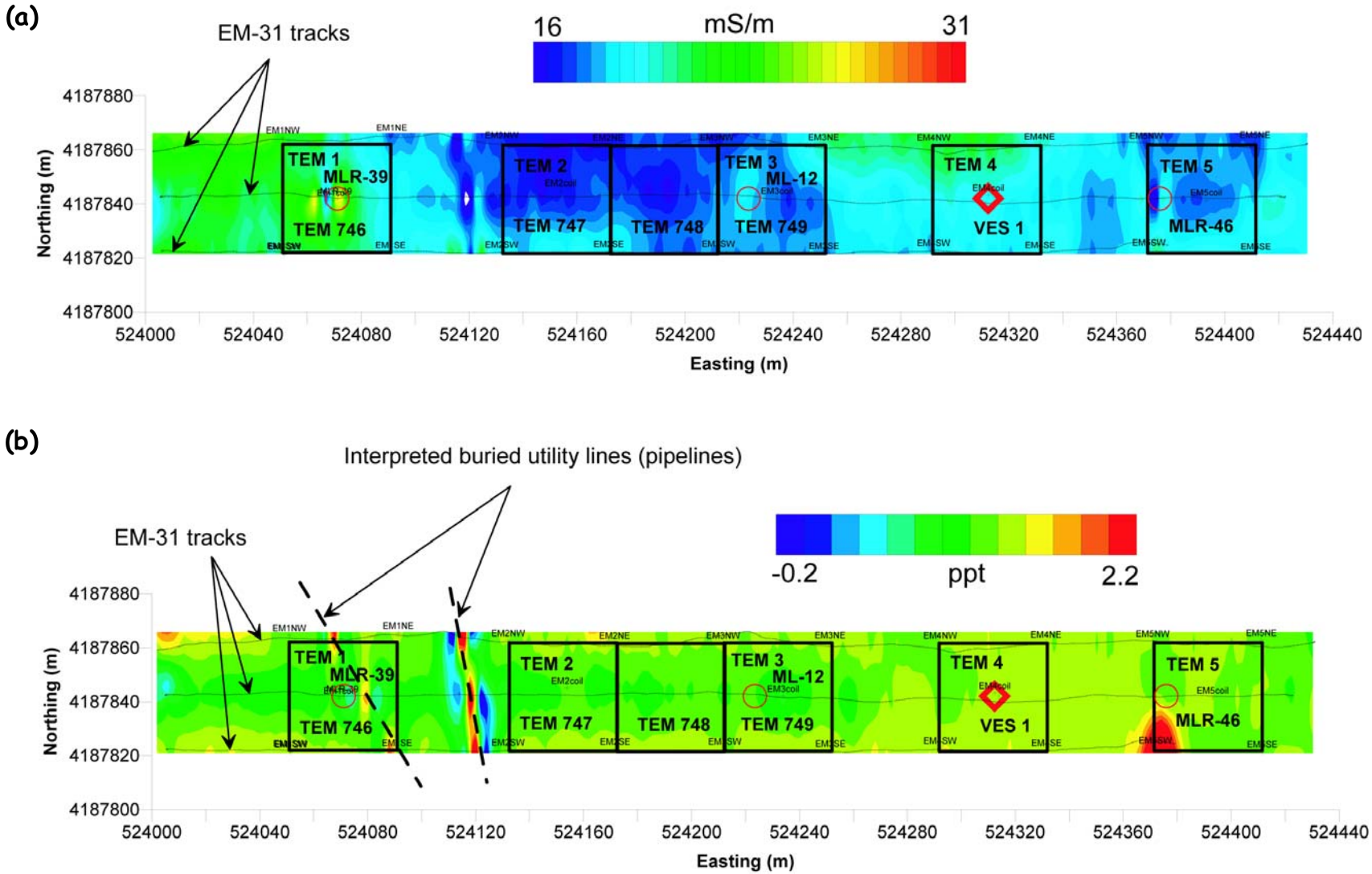

Figure 26. Maps showing results of EM-31 calibration survey on the Main Lake. (a) Terrain conductivity (quadrature) values. (b) In-phase values. Locations are also shown for the TEM and VES profiles. UTM coordinates in meters, WGS-84.

Both the in-phase and quadrature data are interesting, though for different reasons. The contoured in-phase data, shown in figure 26(b), clearly indicate the presence of buried conductors in the near-surface. As indicated by the annotation on the map, each traverse line encountered two very narrow, highly conductive regions that can be connected as inferred linear metallic objects. The more north-south trends of the color contours is related to the fact that the data were contoured using a north-south/east-west gridding algorithm

The map of interpolated terrain conductivity values, fig. 26(a), indicates a substantial degree of heterogeneity on a scale *smaller* than the drill hole spacing. Aliasing of information by the drilling pattern may potentially be an issue. However, at the scale of the overall problem — identifying suitable target areas — the conclusions presented in the section on the *Results of Characterization at the Main Lake* most likely are unaffected.

Figure 27 presents the results of the TEM calibration measurements. Two of the TEM loops produced measurements that were unusable. As indicated in figure 26, the indications are that these positions are underlain by buried conductors of some type, probably pipelines or electrical cabling. Only data from the eastern-most four TEM loops have been contoured and modeled. The resistivity contours indicate a fairly resistive section of likely coarse grained material down to a depth of 10–20 m (30–60 ft). This interval is underlain by a much more conductive interval which extends to at least a depth of 40 m (100 ft+). The layered-earth model resulting from the joint inversion of the TEM and Schlumberger data indicates a highly resistive near-surface interval from 0 to slightly less than 10 m (30 ft) and that the resistivities are markedly less below this depth.

Because the drilling at the Main lake went only to a depth of 40 ft, the sampled interval

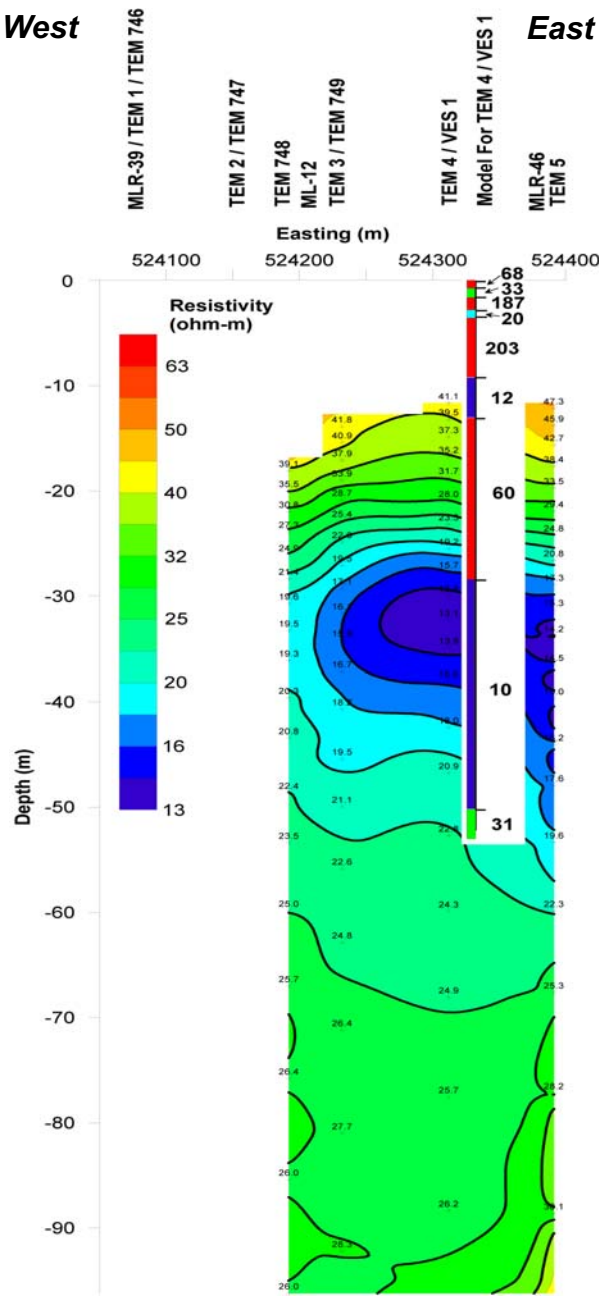

Figure 27. TEM resistivity profile for the calibration measurements on the Main Lake. The jointly modeled resistivity profile is also shown. Note that data from the westernmost TEM loops were unusable. Vertical exaggeration 10x.

represented by the drill holes was almost exclusively in the resistive portion of the stratigraphic section. Rotary hole MLR-46 (fig. C-61), on the east side of figure 27, encountered at least two major intervals of materials with densities exceeding 2.0 g/cm^3 (inferred coarse clayey granule beds), one from 14–18 ft and one from 20–32 ft. Core hole ML-12, located near the center of the original TEM profile and at the western end of the contoured region in figure 27, encountered granule-bearing clays at a depth of 4 ft, and went into coarse sand, sand with granules, and actual gravel below about 6 ft. The geophysical log for hole ML-12 (figs. C-9 and D-9) indicates that the entire hole is resistive and contains material above a density of 2.0 g/cm^3 from 10 ft to the bottom of the logged interval.

This interpretation is portrayed graphically in the stratigraphic cross section of figure 28. The figure presents the geophysical logs from the one core and two rotary holes, together with the layered-earth resistivity model derived from the joint inversion of the TEM data and the Schlumberger resistivity measurements. With the understanding that both the TEM and Sclumberger methods lose resolution with increasing depth, the correspondence between the three sets of geophysical logs, the core-lithology log, and the inferred electrical model is quite striking.

The very uppermost clays of the modern lake bed are moderately resistive, as might be expected for dry materials in the Nevada desert. This surficial layer is underlain by a

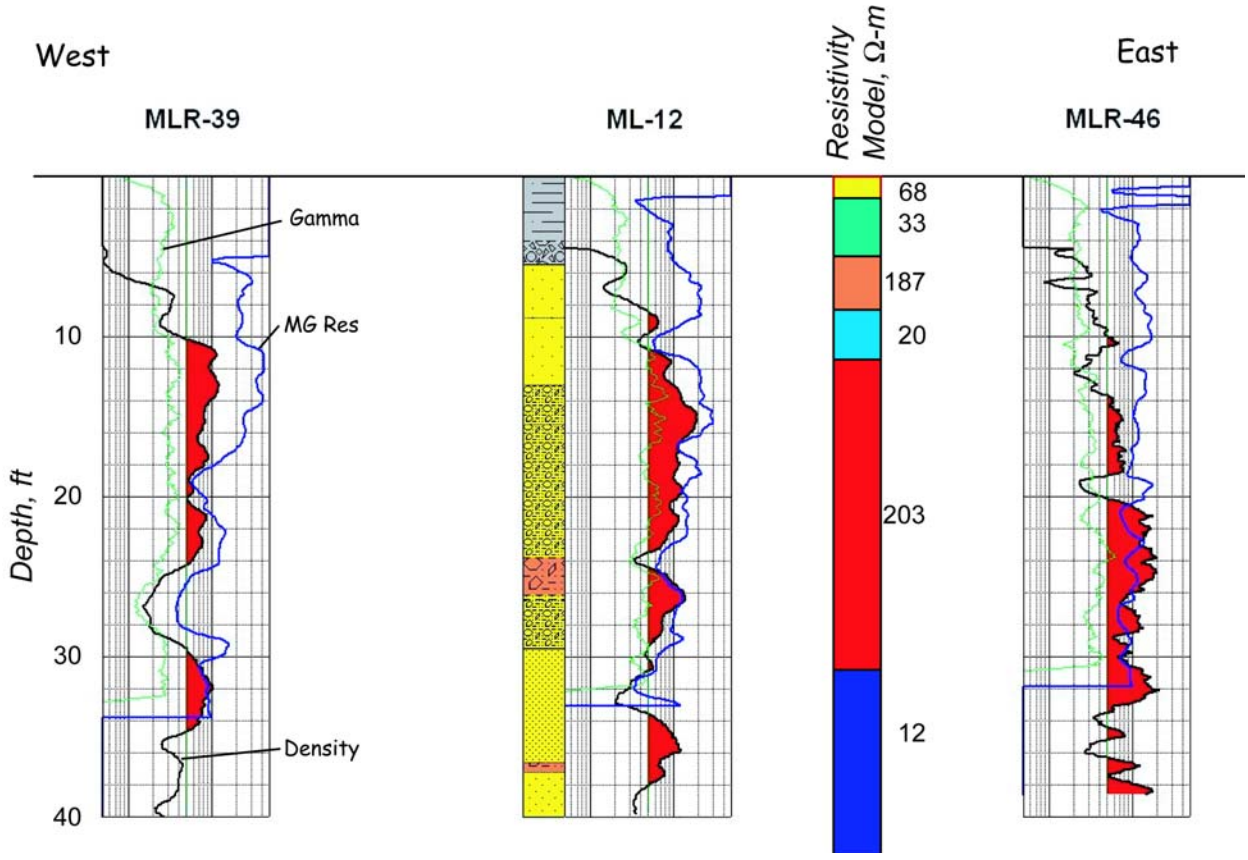

Figure 28. Stratigraphic cross section corresponding to the interpreted TEM profile on the Main Lake. Resistivity model is layered-earth resistivity profile resulting from joint inversion of TEM and Schlumberger resistivity data. Density values > 2.0 g/cm^3 shaded red on log profiles. Compare to figure 27.

relatively thicker layer of fairly low resistivity materials, presumably more-moist clays. A highly resistive layer underlies this conductive unit, but the resistive material is relatively thin. Because the density trace tends to lose its effectiveness close to the surface, it is unclear whether this thin resistive unit (187 Ω-m in fig. 28) represents the sands encountered in core hole ML-12 at about 5–10 ft, or whether it represents the clayey gravel interval immediately above the cleaner sandy unit. In any event, the major feature of this part of the lake is the very thick, highly resistive interval (203 Ω-m in fig. 28) that is present from approximately 10 to 30 ft in all three drill holes. Much of this interval in each hole is characterized by sediments with density values substantially in excess of 2.0 g/cm^3.

These geophysical data, their interpretation and modeling, plus the lithologic information obtained from two rotary holes and a core hole were taken as confirmation that the overall stratigraphic framework of the playa lake sediments at Tonopah Test Range could be deduced in no small part from surface-based geophysics. The calibration of the geophysical methods is based on a relatively small number of soundings, and regions of overall low resistivity (mostly soft materials) were not calibrated in a similar fashion. Nevertheless, the good correlations among the surface-based geophysics, the downhole geophysics, and the core descriptions were taken as strong evidence that the application of these surface-based geophysical methods at Antelope Lake would be successful in identifying the stratigraphic framework of the lake.

Drilling

The essentials of the drilling effort at Antelope Lake are identical to the program of core and rotary drilling at the TTR Main lake, described beginning on page 18. Two technique differences involved the design of the drilling bits used. Although inconsequential to the geological results, the differences profoundly affected drilling rates and consequently drilling costs. Therefore, these differences are described in the following paragraphs for historical purposes and potential use in future drilling activities in these playa lake sediments. A map showing the general layout of the drilling program is shown in figure 29.

Core Bits — The core-bits used in the Main Lake drilling activity were of a diamond-impregnated design intended for use in "moderately-hard" formations [fig. 30(a)]. No particular effort was made in selecting bits for the Main Lake drilling. In fact, the initial bit was a re-run bit from a previous drilling job and because it produced satisfactory results, use of this style bit was continued. However, early use of the same diamond-impregnated core bit at Antelope Lake resulted in extremely slow advance rates, presumably because of the presence of dominantly finer-grained and softer materials in the subsurface of Antelope Lake. As is relatively standard practice in the drilling industry when confronted with soft sediments, a core bit with surface-set, much larger individual diamonds in a stepped configuration was obtained [fig. 30(b)], and the drilling rate increased significantly.

The effectiveness of the impregnated core bits at Main Lake is attributed to the presence throughout much of the stratigraphic interval drilled of modestly coarse granule and fine-gravel rock fragments. Apparently, the rotary motion of the impregnated bit was sufficient to loosen these coarser clasts from the clayey and silty matrix, and the tumbling and grinding of the rock fragments themselves with bit rotation contributed to the "cutting" of the next increment of the formation. In contrast at Antelope Lake, a general absence of granule and fine-gravel size fractions in the sediment allowed the dominant clayey and silty materials to clog the spaces between the fine diamonds distrib-

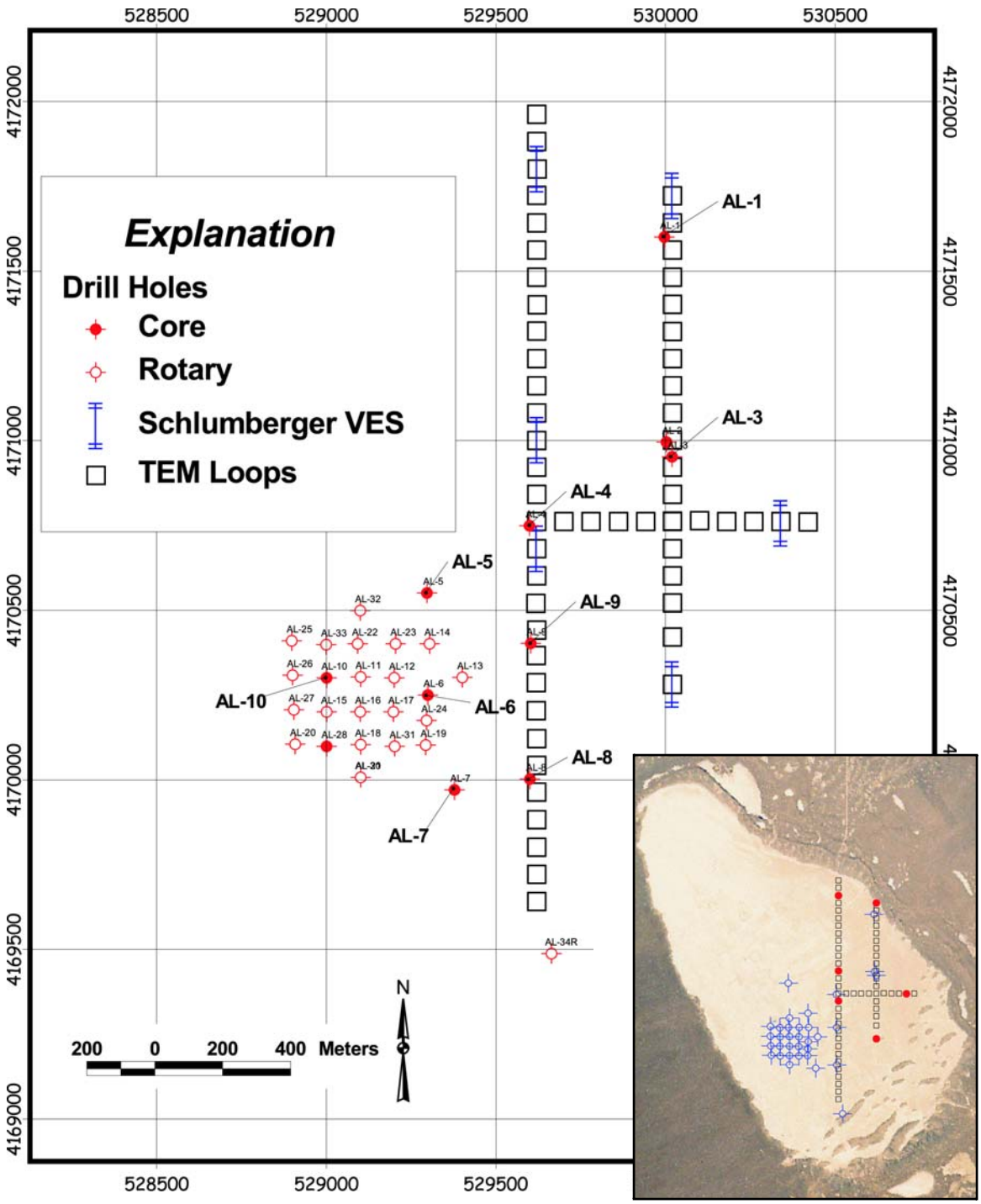

Figure 29. Locations of drill holes on Antelope Lake, shown with reference to the TEM profiles. Inset: aerial photograph of the larger Antelope Lake area. UTM grid, zone 11, in meters, WGS-84

uted throughout the bit face, leading to much more difficult removal of material at the cutting surface and slower advance rates. Substitution of the coarse, surface-set diamond bit provided a more aggressive, jagged cutting surface, presumably allowing gouging and removal of strips of fine-grained sediment by individual diamond points. The stepped arrangement of the set diamonds probably augmented this aggressive gouging action with drill string rotation.

Rotary Bits — The rotary bits used at Main Lake were of a standard toothed-tricone design [fig. 31(a)], with rotating toothed cones that are designed to crush a hard rock into fragments, which can then be flushed from the hole. The design is suitable for moderately hard and somehwhat soft formations. As with the coring experience at the Main Lake, the default bit produced acceptable results at Main Lake and no further thought was invested in drilling mechanics. Use of the same bit type at Antelope Lake produced advance rates that were inefficient. Drilling rates in the upper 50-60 ft of the lake were tolerable, but below these depths, the rate of penetration was completely unacceptable.

Examination of the tricone bit upon removal from the first two or three holes indicated that the formation near total depth was a very soft clay or only slightly silty clay and that this material was "gummy," potentially indicating that this interval is below the static water table and thus fully saturated. The teeth of the bit would be completely impacted by sediment, effectively preventing rotation of the teeth and "cutting" of the formation. The clay-plugged tricone mechanism was presenting essentially a smooth surface to the bottom of the hole.

We then switched to a completely different bit design, a design known in the industry as a *drag bit* [fig. 31(b)]. Here, elongate, rigid carbide-tipped teeth gouge into the soft material, scraping the bottom of the hole into potentially cohesive strips of clay that are then flushed from the hole. This design produced much improved penetration rates. However, the sediments near the 100 ft TD of the Antelope Lake

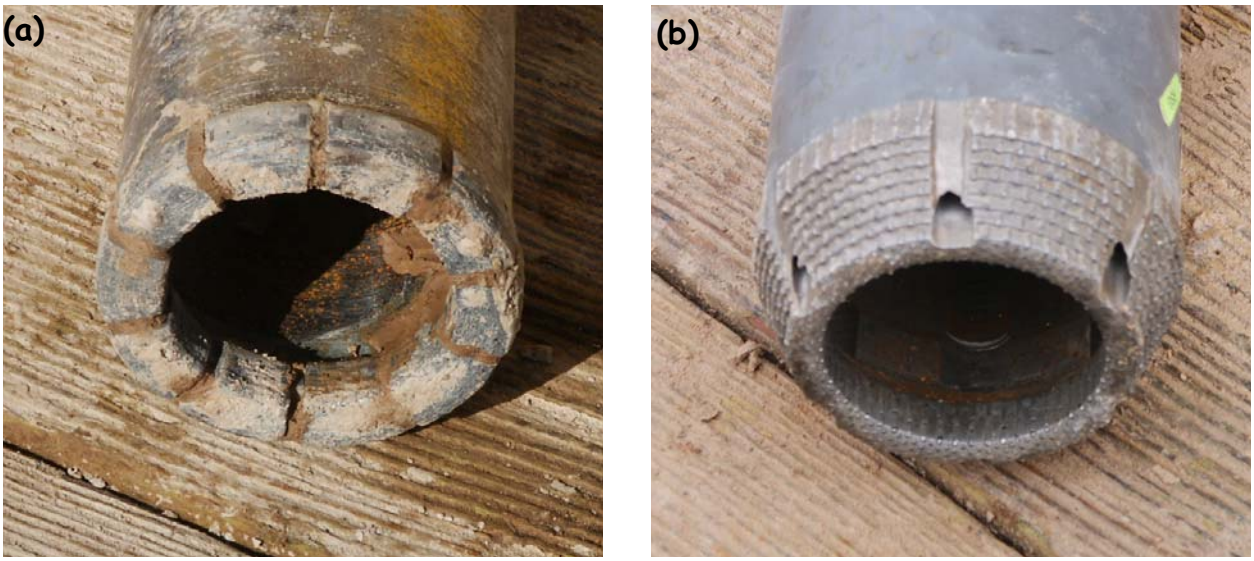

Figure 30. Photographs of different style core bits used during characterization drilling. (a) Diamond-impregnated bit; (b) surface-set diamond bit with stepped design. Overall HQ-size bit diameter is slightly larger than 3-½ inches.

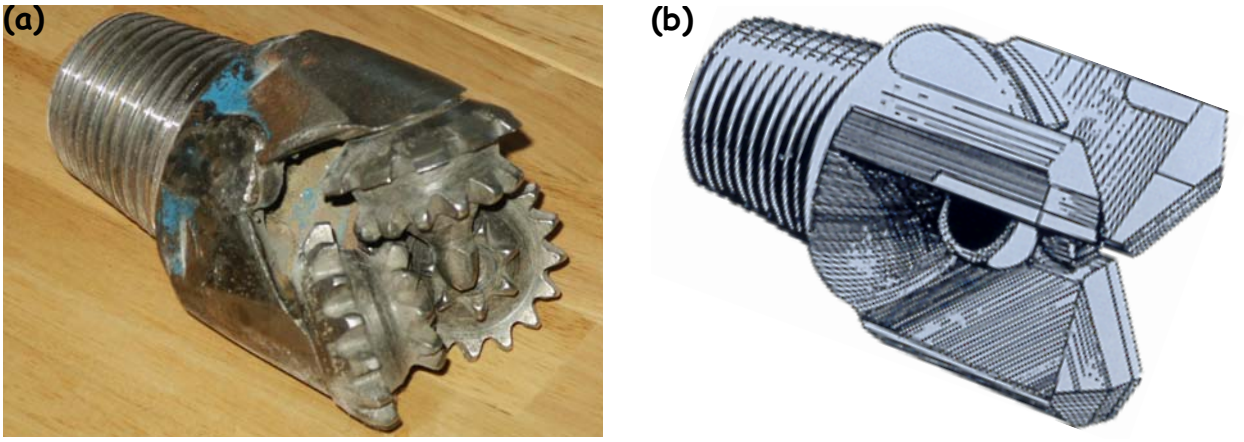

Figure 31. (a) Photograph of a standard tricone drilling bit for use in medium-hard formations; (b) illustration of a drag bit for use in soft and very soft formations.

holes are sufficiently soft that there was some tendency for even these drag teeth to become coated with soft gummy clay.

Downhole Geophysical Logging

Geophysical logging of completed open holes was similar to that described beginning on page 19 for the Main Lake drilling activities. The principal difference involves the acquisition of an expanded suite of logs. The density-resistivity tool, with natural gamma and caliper log employed at the Main Lake, was run in all Antelope Lake boreholes. Several other resistivity-type logs were also run, partly because of the extensive resistivity-based surface geophysical investigations that had already been conducted and partly because the tools were available from another job at no extra cost.

The so-called *resistivity* log consists of three separate resistivity measurements of the formation, a measurement of the resistivity of the fluid in the borehole, and the same natural-gamma measurement present on the density-resistivity tool. The several different resistivity traces are designed to examine the materials at different distances away from the borehole wall (see discussion in Appendix G on page 225). The natural gamma trace is commonly run on many different logging probes to provide a common basis for correlation among traces recorded on different logging runs. In addition, the "SP" trace (for *spontaneous potential* or *self-potential*) was recorded. This trace measures small currents generated in the borehole by the (potentially) contrasting salinity of the formation fluids and the drilling mud. A temperature sensor was present on this resistivity tool as well, although the useful information acquired by the temperature log in this geologic setting was minimal.

The so-called *induction* log was also run in several of the holes at Antelope Lake. The induction log merely measures resistivity as the inverse of the conductivity of the formation. The physics of the induction-based measurement is less sensitive to highly conductive earth materials, but the ultimate portrayal of the information is essentially the same. Not a great deal of usable information was generated solely by the induction traces.

Because it is possible to deduce certain information regarding mechanical properties of rock by means of the transmission of sound, a sonic logging tool was run in virtually all of the drill holes at Antelope Lake. The sonic tool

measures a number of quantities, including a recording of the full waveform of the sonic impulse recorded at two different positions along the downhole sonde. However, the basic quantities of interest included on presentations of the sonic log are the interval transit time (in microseconds per foot) and the ubiquitous natural-gamma correlation trace. The sonic logs did not always produce usable data as a result of cycle-skipping that produces unrealistic interval transit times

Results of Characterization at Antelope Lake

Surface-Based Geophysics

Several types of electrical geophysical methods were employed in the initial investigation. The two most useful techniques turned out to be time-domain electromagnetics (TEM) and Schlumberger electrical resistivity soundings (pages 33 and 34, respectively). Both methods provide estimates of the electrical properties of the subsurface as a function of depth. However, the resolution of the methods decreases with increasing depth below the ground surface, because the signals necessarily pass through overlying materials thus distorting the measurements of the actual properties at a specific depth. Essentially all of this distortion results from selective attenuation of the higher frequencies at greater depths. On the positive side, the final interpretation resulted from a relatively unique *joint* inversion of the data from both methods (Sandberg, 1995), thus reducing the "degrees of freedom" inherent in any geophysical interpretation.

Two north-south TEM profiles, shown in figure 32, were run from the interior portion of the lake toward and actually onto the northeastern shore of the lake. An east-west TEM profile, also represented in figure 32, connected these former profiles and again extended from the interior of the lake toward (but not reaching) the eastern shoreline. Vertical electrical resistivity soundings (Schlumberger soundings) were executed at a number of selected TEM positions based upon preliminary interpretation of the TEM data. These positions are also shown in figure 32 as the solid circles coincident with several of the TEM rectangles.

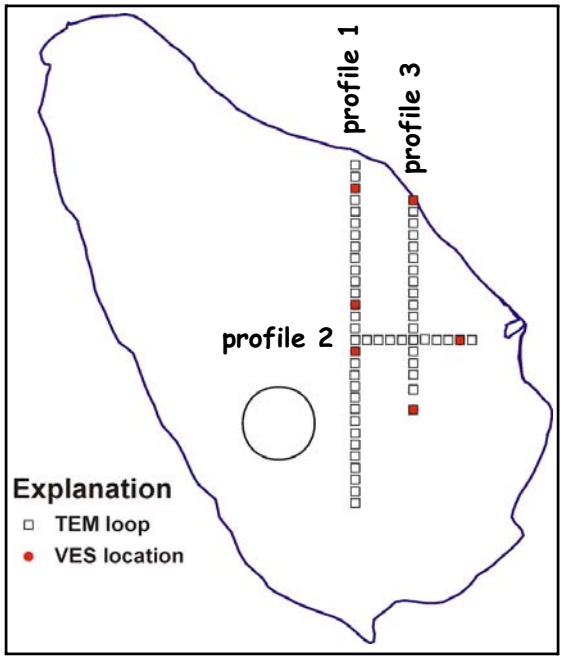

Figure 32. Locations of the TEM and Schlumberger (VES) geophysical soundings on Antelope Lake. Large open circle represents final target area selection based on the drilling results.

The final electrical resistivity interpretation of the TEM and Schlumberger data is shown in cross-sectional view in figures 33 through 35. The overall impression, discounting some major discontinuities, particularly obvious in figure 33 that are related to the presence of inferred faulting and deep percolation of saline (highly conductive) surface water to depth, is of shoreward thickening of more resistive materials. This effect is shown on all three profiles. Conversely, more conductive materials appear both to thicken and to climb stratigraphically to shallower depths toward the center of the lake.

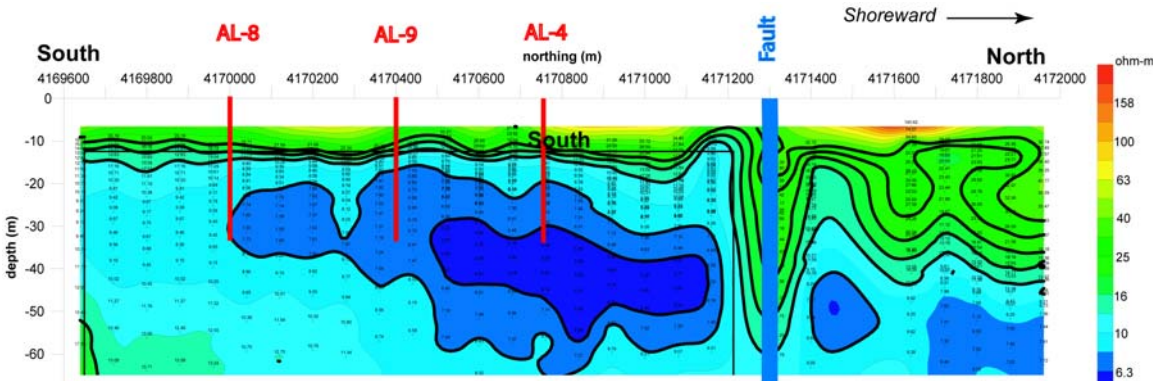

Figure 33. North-south TEM profile number 1 (west), showing modeled electrical resistivity. Drill holes approximately located in red. 10x vertical exaggeration.

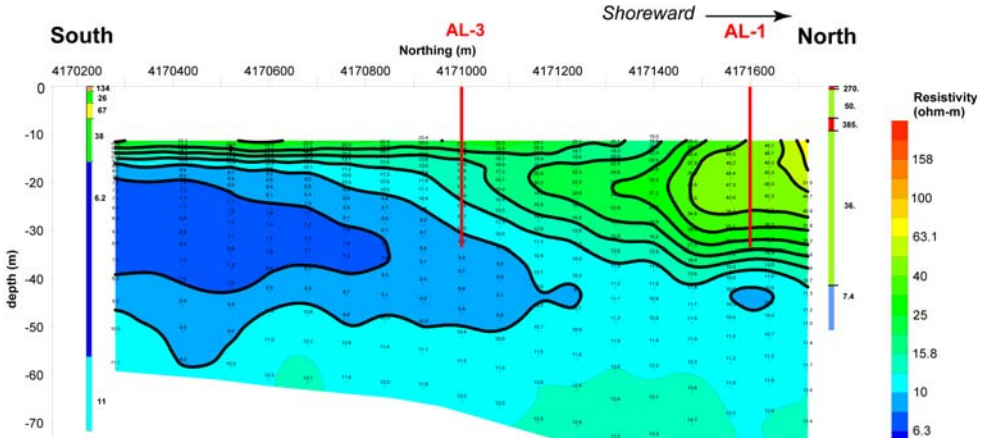

Figure 34. North-south TEM profile number 3 (east), showing modeled electrical resistivity. Drill holes approximately located in red. 10x vertical exaggeration.

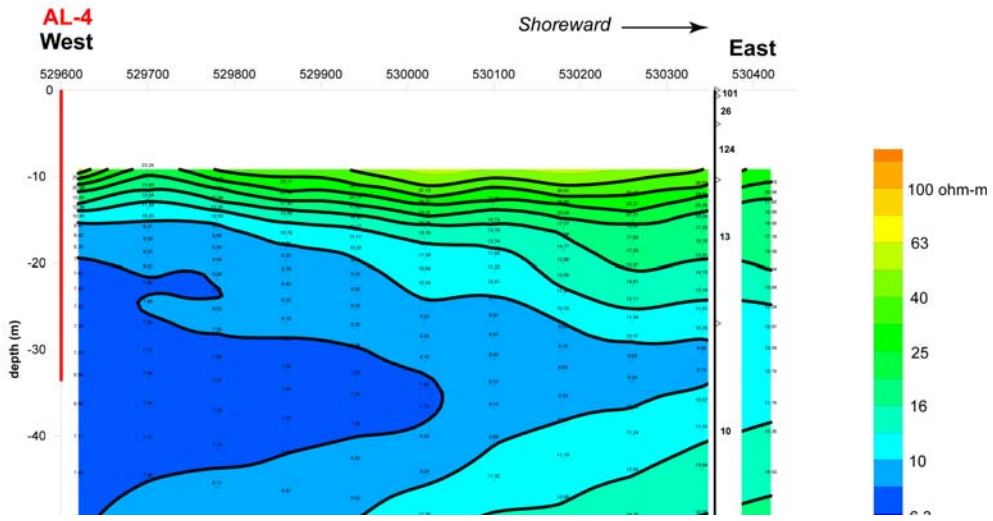

Figure 35. East-west TEM profile number 2, showing modeled electrical resistivity. Drill hole approximately located in red. 10x vertical exaggeration.

Under the paradigm that conductive materials contain more pore water than resistive materials (the electrical properties of the sedimentary particles themselves are generally considered nearly invariant across a wide variety of lithologies), the conductive materials in the center of the lake represent generally fine-grained sediments, whereas the resistive materials closer to the shoreline represent coarser materials. This is the intuitive distribution pattern expected for a depositional basin, but the geophysical surveys provide *actual spatial positions* where these transitions occur. This conceptual geophysical model, in conjunction with the surveyed locations of the TEM and Schlumberger soundings, provided the basis for the initial phase of the drilling program. The correlation of the quantity of contained pore water with grain size in an unsaturated geological medium, all else being equal, originates from the fact that capillary forces hold more water in the smaller spaces between small particles than can be held in the larger spaces between large grains. Additionally, the presence of large, impermeable and low porosity fragments of volcanic rock simply reduces the volume of empty space available to contain pore water. This latter mechanism also applies to sediments within the saturated zone below the static water table.

The EM-31 data, although of less importance than the TEM and Schlumberger resistivity data in terms of guiding the drilling efforts, are rather interesting geologically. The mapped and interpolated terrain conductivity data are shown in figure 36, together with the positions of the TEM-loop profiles for orientation and comparison with other figures. Because the use of the EM-31 equipment at Antelope Lake was a subsidiary, somewhat experimental effort, the extent of the terrain conductivity survey does not include the entire region of interest.

Two particular observations may be drawn from the admittedly limited areal extent of the EM-31 survey. First, and perhaps most prominent, there are five very-high-conductivity linear features trending from southwest to northeast across the mapped region. On the ground, these conductivity highs correspond precisely to very slightly irregular but prominently linear, shallow depressions (1-3 cm total relief) on the lake surface (fig. 37). The width of these depressions is quite variable [fig. 37(a)]. Subtle changes in color of the surficial clays and mud-crack patterns define the depressions much more effectively than actual topographic expression. However, the features are distinctly linear and GPS surveys along the centerlines of the depressions (fig. 38) coincide with the color bands shown in figure 36.

At the time of the geophysical survey (August 2003) and for some time thereafter (a period of several months), a number of sharply defined fractures in the lake surface were located more-or-less in the center of these depressed linear features. Examples of such fractures are shown in figure 39(a) and (b). In addition to the fractures, which measured up to 6 to 9 inches in depth, are sets of irregularly spaced sinkholes [fig 39(b)]. These sinkholes are generally circular in plan and conical in cross section; a small open hole, generally less than one inch in diameter, may be present in the center [fig. 39(f)]. Some sinkholes are clustered, and the upper portions of several individual sinks may be merged at the level of the overall ground surface.

The second, less obvious but perhaps more general observation relevant to the larger problem of delineating major facies changes in the subsurface, to be drawn from figure 36 involves the overall changes in terrain conductivity *excluding* the linear features. The mapped conductivity is lowest at the north end of TEM profile number 1 (see also fig. 32), and the conductivity values generally increase toward the south. Note that the strike of the pronounced change in conductivity from about 15–20 mS/m to 20–30 mS/m (dark blues to

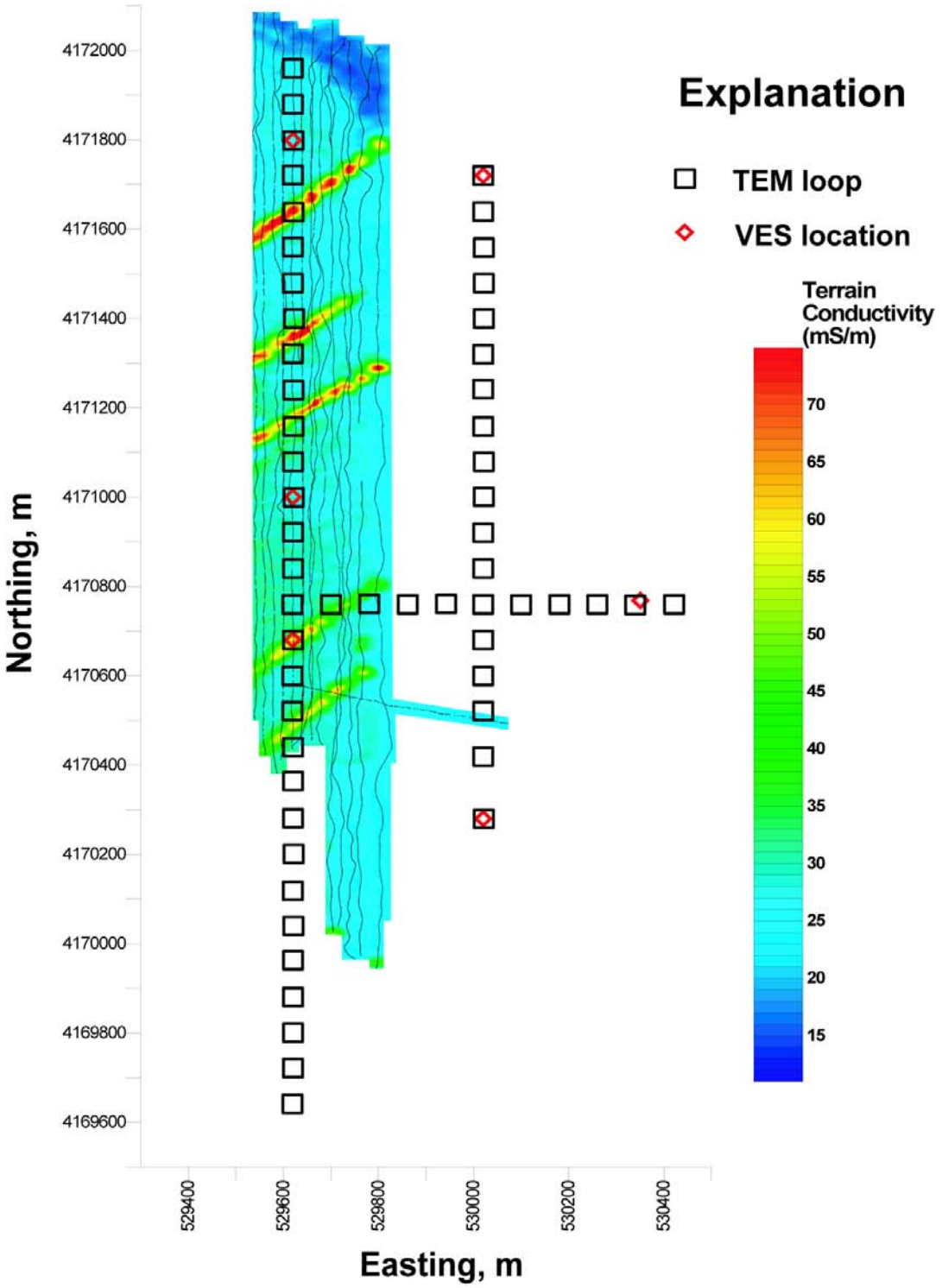

Figure 36. Map showing results of the bicycle-towed EM-31 terrain conductivity survey. TEM loop positions shown for reference. Irregular north-south lines represent data-acquisition tracks. Tick marks are UTM coordinates, zone 11, WGS-84, in meters.

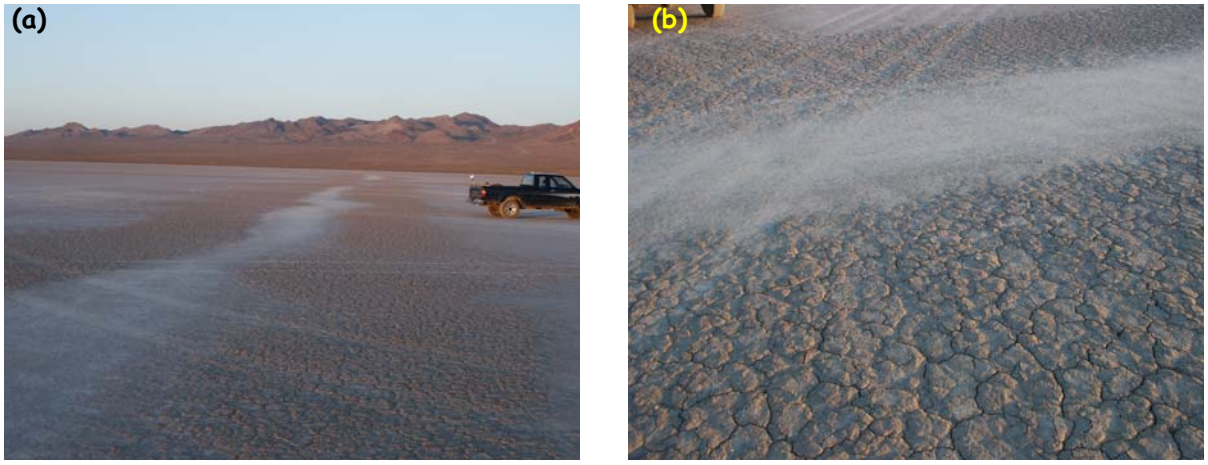

Figure 37. Linear rivulets on the surface of Antelope Lake (crossed by tire tracks) coincident with linear high-conductivity zones identified by EM-31 terrain conductivity surveying.

cyan) is essentially parallel to the shoreline of the lake at this position (fig. 32). A less marked but definite change in terrain conductivity values is present from east to west. This latter change is most evident at a northing of approximately 4,170,800 m. The values are on the order of 25 mS/m (cyan) on the eastern margin of the mapped area and about 35–40 mS/m (green) on the west. Taken in conjunction with the TEM profile results shown in figure 35, the impression is of southwestward and westward increasing conductivity (recall that resistivity is the inverse of conductivity) toward the center of the lake

Phase 1 Drilling and Geophysical Logging

The initial objective of the drilling was to confirm the geophysical interpretation. To do so, the first several holes were drilled in locations marked by distinct contrast of the geophysical character (figs. 34, 35), but as close to the TEM profiles as possible so that the materials being investigated would be essentially identical. All holes of the Phase 1 drilling were cored, allowing physical examination of the sediments, and logged using downhole geophysical tools (principally density and resistivity). Holes were drilled in numerical order (1, 2, 3, …), and the sequence is emphasized by the arrows in figure 40. Although the transition from Phase 1 drilling to Phase 2 is somewhat diffusely determined, core holes AL-1 through AL-4 were "purely" data-validation holes and holes AL-5 through AL-10 were located to test the implications of the validated conceptual geologic model.

Drill hole AL-1 (fig. 40) was located near the northern limit of the eastern north-south TEM profile number 3 in a region of generally highly resistive materials (figs. 34 and 36). The hole encountered almost continuous sands and "gravels" (sand plus granules) below a near-surface clayey interval roughly 12 ft thick. However, even this fine-grained surface unit is interrupted by a 2-ft granule-bearing horizon at a depth of 4–6 ft.

Drill hole AL-3 (hole AL-2 was abandoned for mechanical reasons) was drilled roughly 600 m to the south of AL-1 (fig. 40) along the same TEM profile number 3. The position was selected to be south of a major change in the TEM resistivities (fig. 34) that suggested a marked thinning of the resistive section (loss of coarse material). This expectation is precisely what was observed both in the core and geophysical logs. The very-near-surface coarse layer is absent, and the "surficial" silty clay

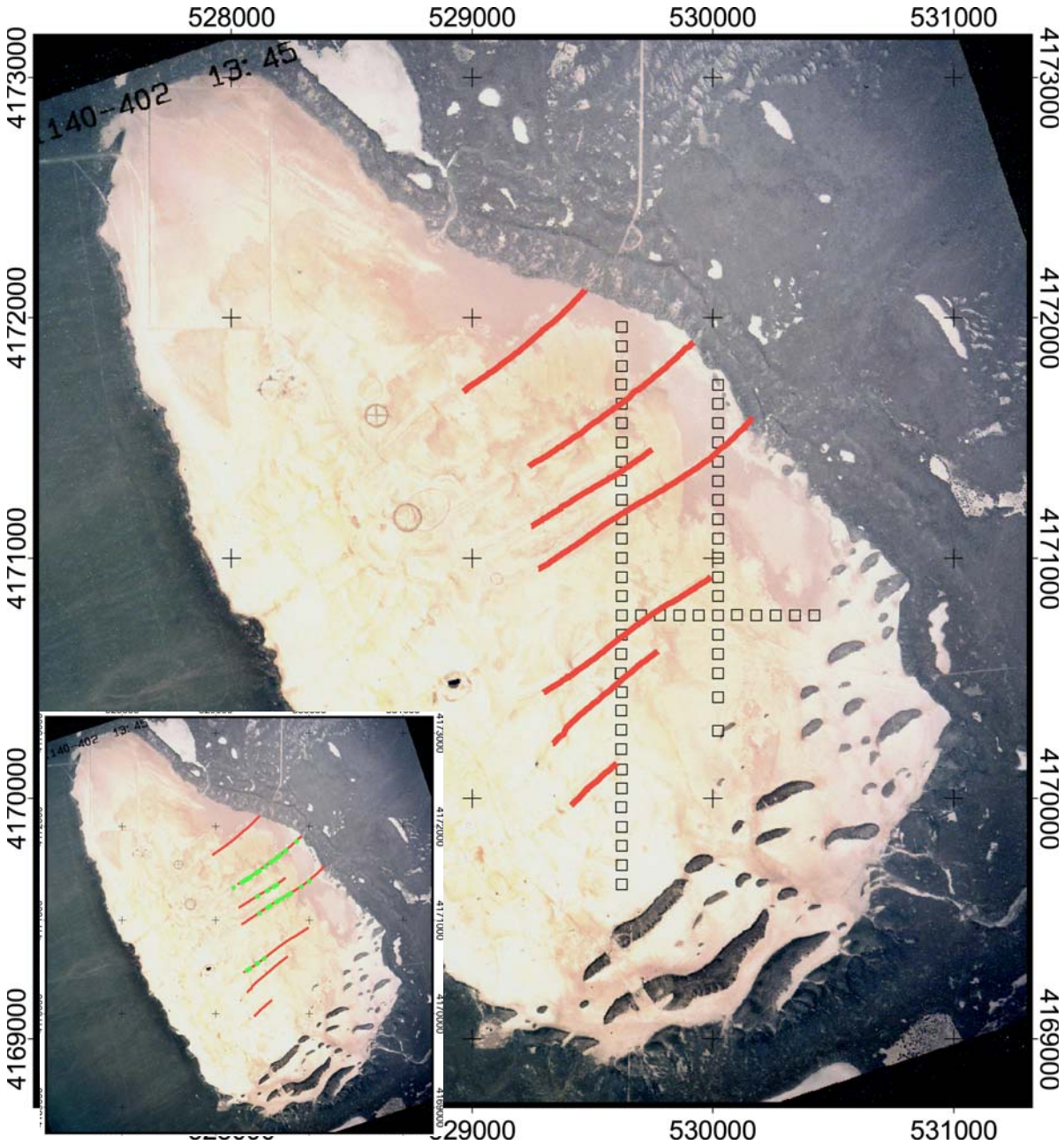

Figure 38. Locations of northeast-trending linear fractures surveyed by global positioning satellite receiver. Inset map shows positions of small sinkholes along rivulests/linear fractures. TEM locations shown for reference. UTM coordinates in meters, WGS-84.

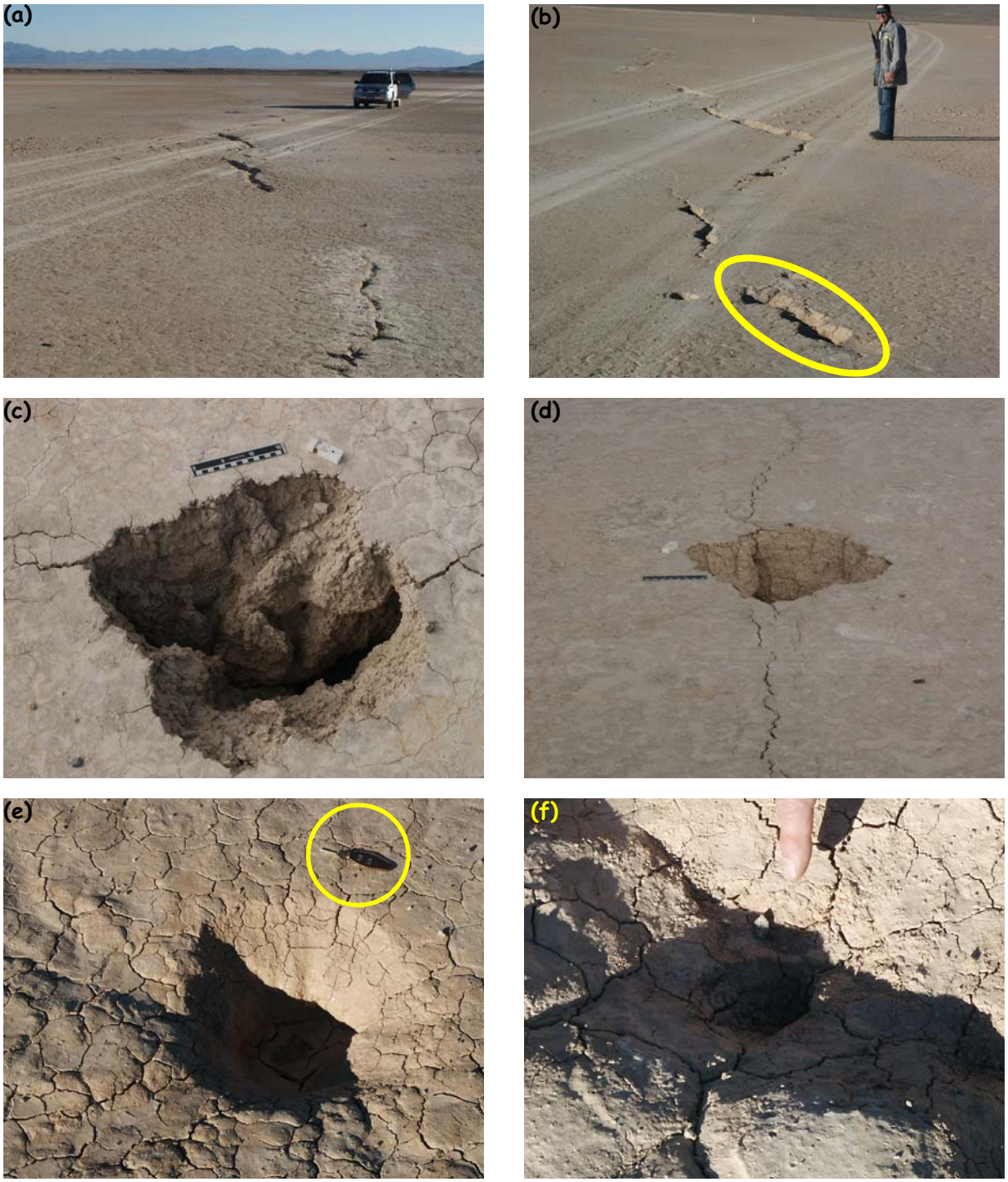

Figure 39. Photographs of cracks and sinkholes on the surface of Antelope Lake, located along linear shallow topographic depressions coincident with linear high conductivity zones identified by EM-31 terrain conductivity surveying. (a) and (b) Two examples of long fractures, exhibiting en-echelon patterns. Ellipse in (b) outlines a cluster of small sinkholes. (c) and (d) Collapse sink located along a linear fracture; note "fresh," recent appearance of sink margin and walls. Scale in cm. (e) and (f) Smooth-sided, conical sinks that probably served as drains for standing water. Sink in (d) has a (currently) closed bottom; sink in (e) leads to a 2–3-cm vertical hole of undetermined depth. Circled object in (e) is a hotel-type key for scale.

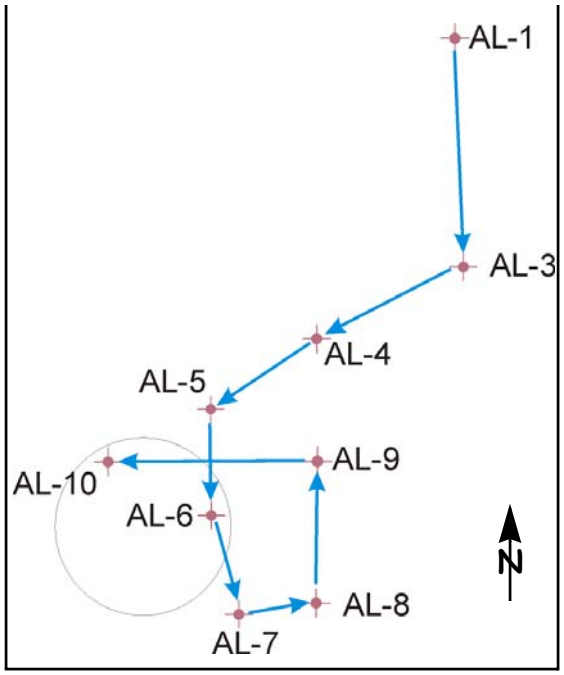

Figure 40. Location map of Phase 1 core holes AL-1 through AL-10. Succession of drilling to test first the geophysical data and then the geophysical interpretations is emphasized by the arrows. Circle indicates final target area selection. See figure 29 for relative spatial position on the lake.

unit extends to roughly 20 ft below ground level. A 20-ft-thick coarse-clastic layer is present from about 20 to 40 ft, whereafter the drill hole was in soft conductive clays and silty clays.

Drill hole AL-4 (fig. 40) was then drilled at the intersection of the western north-south TEM profile number 1 with the east-west profile number 2 (figs. 33 and 35). The geophysical interpretation (shown best in fig. 35) suggested that this hole should contain relatively little coarse-grained resistive materials. Indeed, the core indicated fine-grained silty clays to a depth of about 24 feet, underlain by a much thinner (~10 ft) coarse interval from 24 to 34 ft, and uniformly fine-grained materials thereafter.

We took the successful drilling of these three holes (discounting the abandoned AL-2) as validation of the geophysical data themselves. We then struck out to test the broader implications of the geophysically derived conceptual model that suggested that coarse materials should die out toward the west (and also to the south). AL-5 was boldly located about 300 m west and south of hole AL-3 in an effort to *disprove* this interpretation. However, the core from AL-5 indicated virtually no coarse grained material whatsoever. It should be noted that at approximately the time of drilling AL-4 and AL-5, the TTR site contractor was recovering an air-dropped test assembly from a location mostly west of and slightly north of core hole AL-4 (fig. 40). They had encountered sandy material at roughly the same depth as we did in AL-4, and thus our pre-drilling bias for AL-5 was to move southward rather than northward.

Drill holes AL-6 and AL-7 were stepped out nearly due south of AL-5 by about 300 m each. Neither of these holes contained core with coarse-grained sediment. Then, seeking to use the TEM data of figure 33, we stepped about 200 m to the east of AL-7 and drilled AL-8 with similar results: no coarse materials.

We then drilled core hole AL-9 some 400 m to the north of AL-8, attempting to begin outlining the desired 500-m-diameter target region. However, AL-9 contained a thin sandy unit from about 30-34 ft, enclosed within otherwise purely fine-grained sediments. This unit appeared to be identical in character to (but thinner than) the intervals observed in AL-4 and the unit-recovery pit. Note that drill holes AL-8 and -9 are also located along the western north-south TEM profile, as indicated on figure 29. However, by the time these two holes were drilled, we were no longer validating the geophysical data, strictly speaking.

Although we could have backed off toward AL-8 to locate the feather edge of this sandy unit, drilling costs were running higher than expected, and thus we observed that “west is

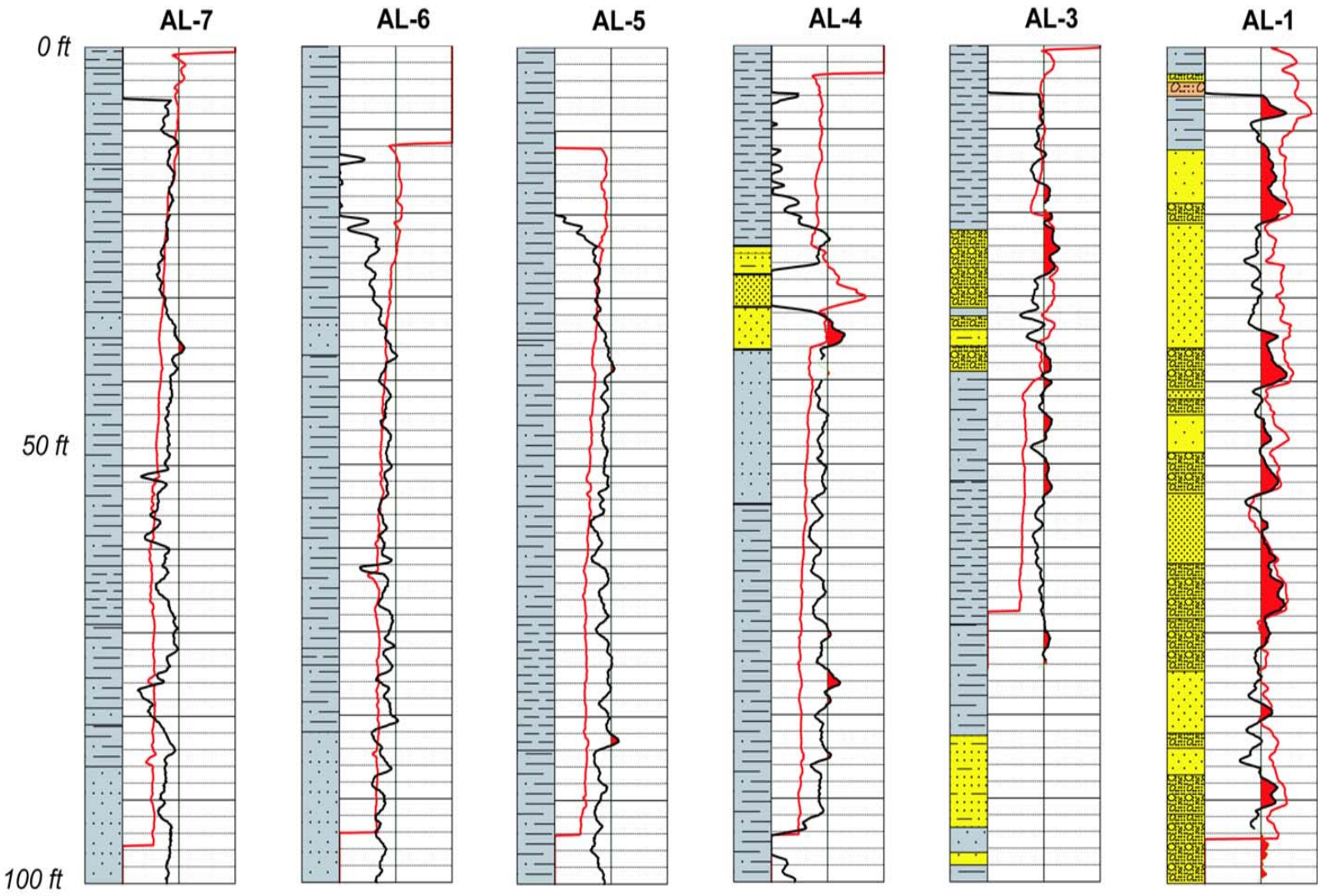

Figure 41. Stratigraphic cross section of initial core hole showing loss of coarse clastic materials ("hard") away from shoreline of Antelope Lake. Left-hand part of each log shows schematic representation of core; right-hand portion shows MG resistivity log in red and density log in black; densities greater than 2.0 g/cm^3 highlighted in red (center of graph is density = 2.00). Intervals of dominantly clay shown in grey; intervals of dominantly sand are shown in yellow; particularly coarse gravels shown in orange.

better" and stepped a similar 400 m to the west and drilled AL-10. This hole encountered no coarse materials, thus confirming the implications of the conceptual geologic model for Antelope Lake.

The results of this sequential exploration process are portrayed graphically using stratigraphic cross sections in figures 41 and 42. For each drill hole, the left-hand portion of the graphic presents a schematic representation of the core description, whereas the right-hand portion presents two of the geophysical logs using a constant measurement scale (though the scales are different for the two different curves). The overall changes in lithology as the drilling program progressed are quite obvious using this style of presentation.

Figure 41 presents the first six core holes (abandoned hole AL-2 excluded) and the geologic and geophysical logs displayed for each hole convey the same information described in the preceding paragraphs. Figure 42 is a similar stratigraphic cross section that captures the efforts to outline the target area and begin the grid-drilling part of the program. This section repeats drill hole AL-3 and then jumps to AL-9 and to AL-10 (fig. 40). Reencountering the thin sandy interval at ~30 ft in AL-9 and the absence of this sand in hole AL-10 is represented.

Sands and granule-bearing beds ("hard" materials) are depicted by yellow overprint, whereas intervals that are dominated by silt and clay are shown in grey. The grain size of the sediments are shown schematically by the stipple and "clast" patterns. Larger and/or more closely spaced symbols represent larger grains and smaller and/or more widely spaced symbols represent finer-grained sediments. The addition of short horizontal lines to an otherwise yellow pattern indicates the presence of silt-sized material. In a similar manner, patterns added to the grey intervals indicate admixtures of materials coarser than clay. The use of only horizontal lines indicates the presence of relatively "pure" clay. A dot-dash pattern indicates a silty clay, and a grey stipple pattern indicates a slightly sandy clay. An orange overprint indicates a particularly coarse granule bed or an actual "gravel," with clast sizes exceeding 4 mm.

The red geophysical log curve is the resistivity trace, plotted on a two-decade logarithmic scale from 3 to 300 Ω-m; resistivity increases from left to right. This increase typically corresponds to an increase in grain size. The black trace is the density log; it is plotted on a linear scale varying from 1.5 to 2.5 g/cm^3 from left to right. The center line of the graph represents a density of 2.0 g/cm^3, and intervals for which the density exceeds this value have been highlighted with red overprint. The log scales are identical across all logs, so that the relative positioning of the curves for different holes actually indicates more or less dense, or more or less resistive, intervals when comparing different drill holes.

Phase 2 Drilling and Geophysical Logging

Phase 2 drilling activities consisted simply of drilling a grid of holes, shown in figure 43, on 100-m centers in an effort to demonstrate than no coarse-grained layers exist within the bounds formed by successful core holes AL-6, AL-7, and AL-10. Some adjustments to the 100-m spacing were required by the presence of (successful) Phase-1 hole AL-6 off-grid and by a desire to ensure the coarse layer of (unsuccessful) Phase-1 hole AL-9 did not extend into the grid area. This latter test was accomplished via hole AL-13, which was successful in finding only fine-grained materials.

Because of budgetary considerations and actual costs associated with coring, almost all Phase 2 holes were drilled using rotary methods (no core). Geophysical logs from all Phase 2 holes are extremely "bland" by com-

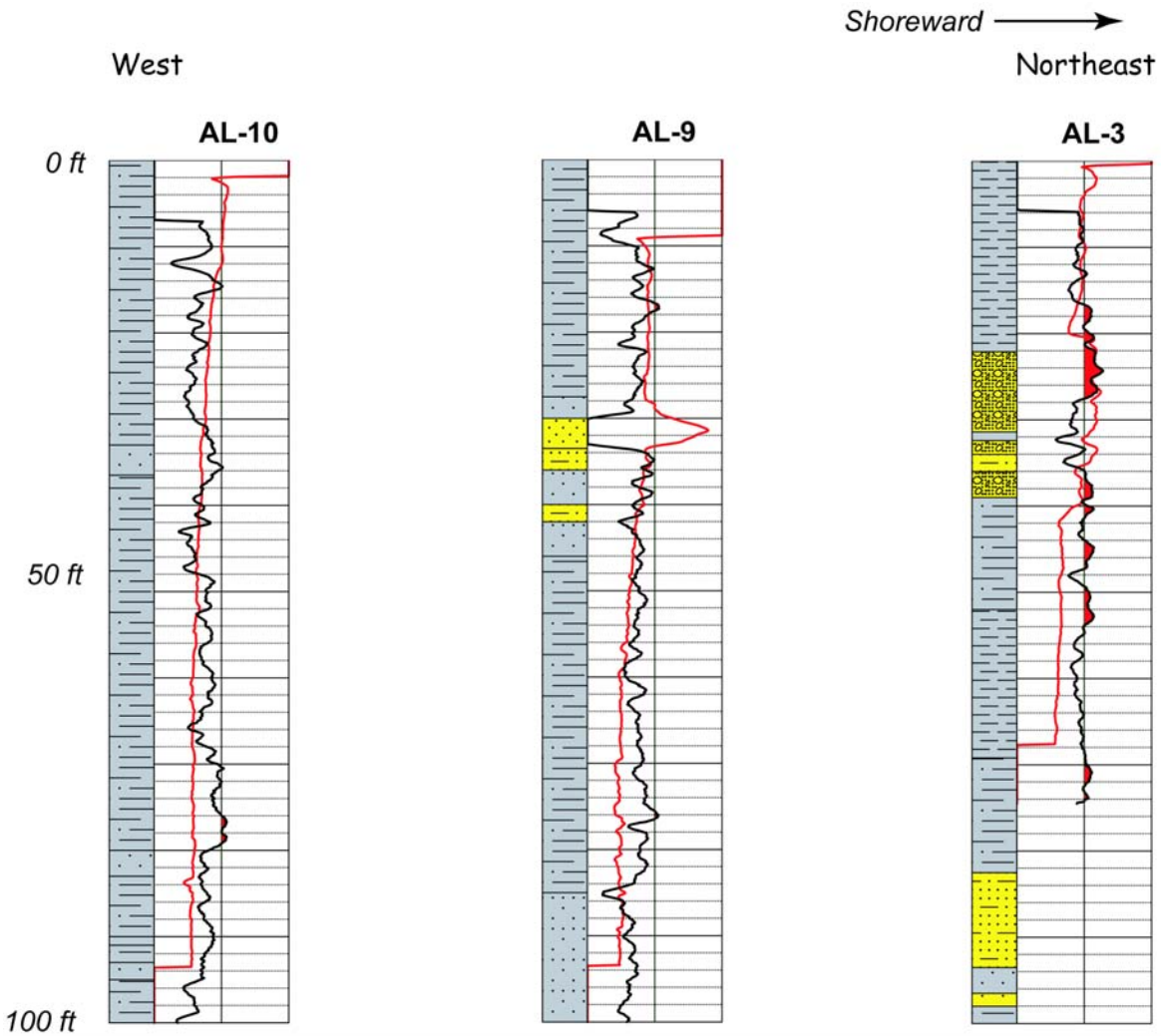

Figure 42. Stratigraphic cross section of initial core hole showing loss of coarse clastic materials (“hard”) away from shoreline of Antelope Lake.

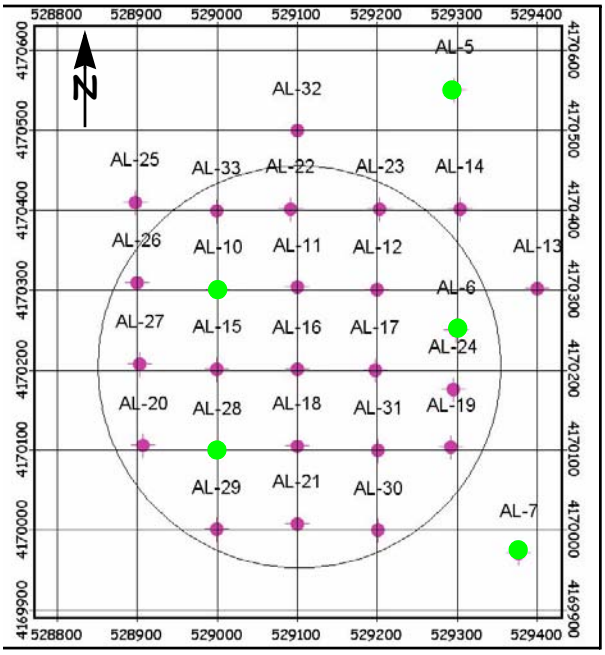

Figure 43. Location map of Phase 2 drill holes and complimentary Phase 1 drill holes constituting the confirmatory grid for the defined target area (circle = 500-m diameter). Slightly larger symbols in green represent core holes.

parison to those from the initial holes (AL-1 through AL-4/AL-5), suggesting relative homogeneity of conductive, low-density, "soft" sediments.

An exception to the rotary drilling decision was hole AL-28, which was partially cored, recovering material for laboratory testing from the uppermost part of the lake sediments. Coring and rotary drilling rates in this upper part of the lake section were generally quite acceptable. However, the lowermost 40 ft or so of each hole had been identified as extremely soft and gummy, and the clay-rich materials consistently clogged both the core bit and the rotary bit. Penetration rates dropped markedly in this deeper interval, and costs increased accordingly. Drill hole AL-28 was converted from core to rotary at a depth of approximately 66.5 ft. The positioning of AL-28 provided core material from the extreme southwestern part of the by-now well-defined 500-m target area.

The complete final drilling pattern is shown in figure 44. Note that drill hole AL-34 is located immediately adjacent to the impact location for the drop test known as *TD-2* (Togami , 2002).

Figures 45 and 46 portray the subsurface geology of the grid-drilling-cum-target region through east-west and north-south stratigraphic cross sections (respectively). These illustrations are quite similar to figures 41 and 42 in manner of presentation, only all but one of the drill holes are rotary. Thus, there is no core description for the majority of drill holes. Figure 45 presents the west-to-east profile, as that cross section contains core hole AL-6.

There are two principal observations to be drawn from figures 45 and 46. First, there is essentially no "hard" material that exceeds a density of 2.0 g/cm^3 within the selected target area. Second, the resistivity log from all drill holes is essentially featureless. A distinct increase in resistivity may be observed over the last five or so feet beneath the ground surface, but this would be expected as a result of drying of the very-near-surface sediments to the moisture content of the Nevada desert air.

The core hole included in the cross section of figure 45 clearly indicates that the lithologies associated with the featureless resistivity trace are exclusively clayey. There are some silty-clay (32–37 ft) and even sandy-clay (82 ft – TD) intervals indicated, but these are not sufficiently coarse that the resistivity ("moisture") profile is affected. Compare these resistivity traces, all of which are virtually identical, to the resistivity traces shown in figures 41 and 42, where the core samples indicate very significant coarse clastic ("hard") material. The density profiles, with the presence/absence of materials of density greater than 2.0 g/cm^3, reflect the same major differences in sediment type.

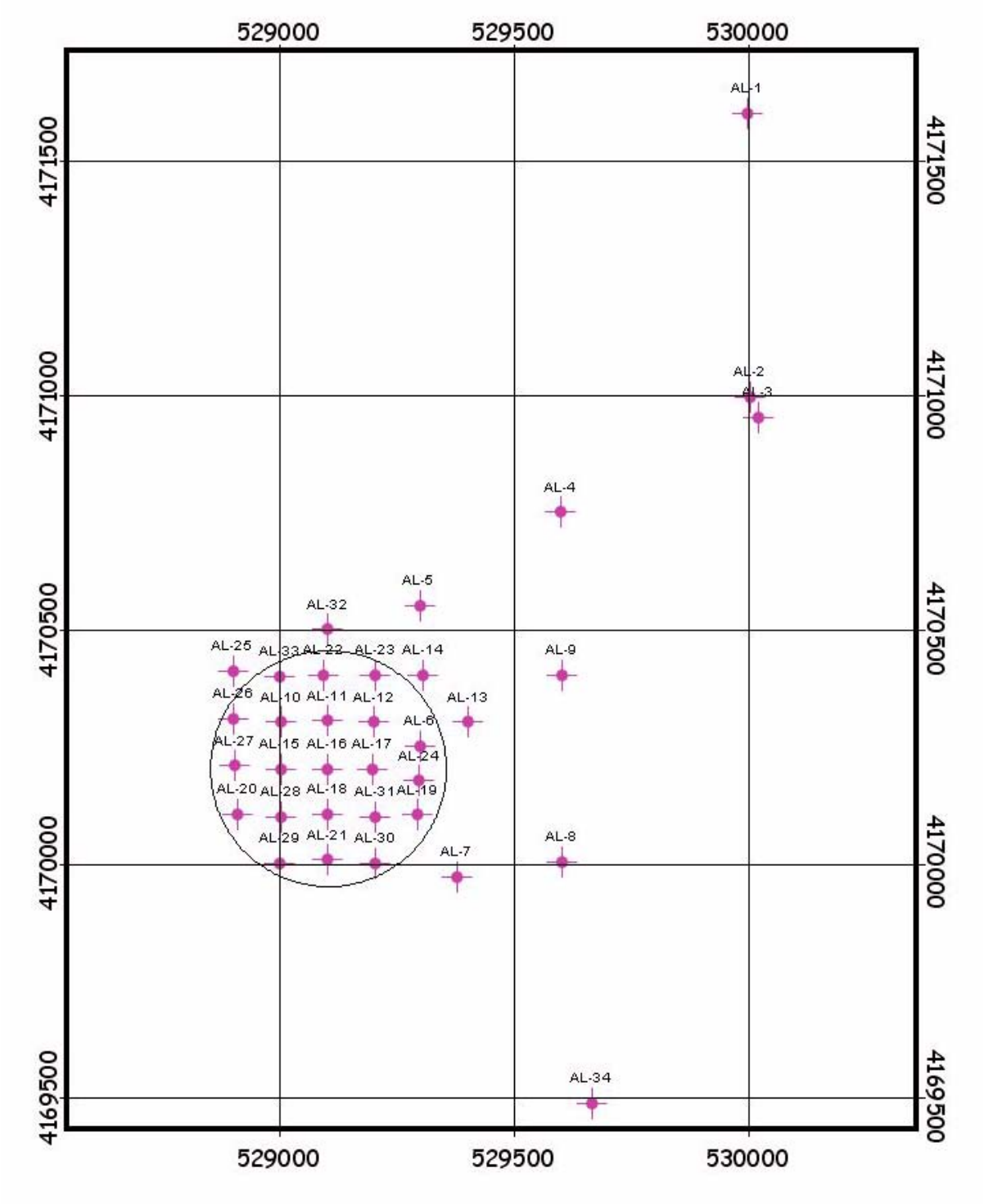

Figure 44. Location map showing all holes drilled on Antelope Lake. Grid represents UTM coordinates, zone 11 in meters, WGS-84.

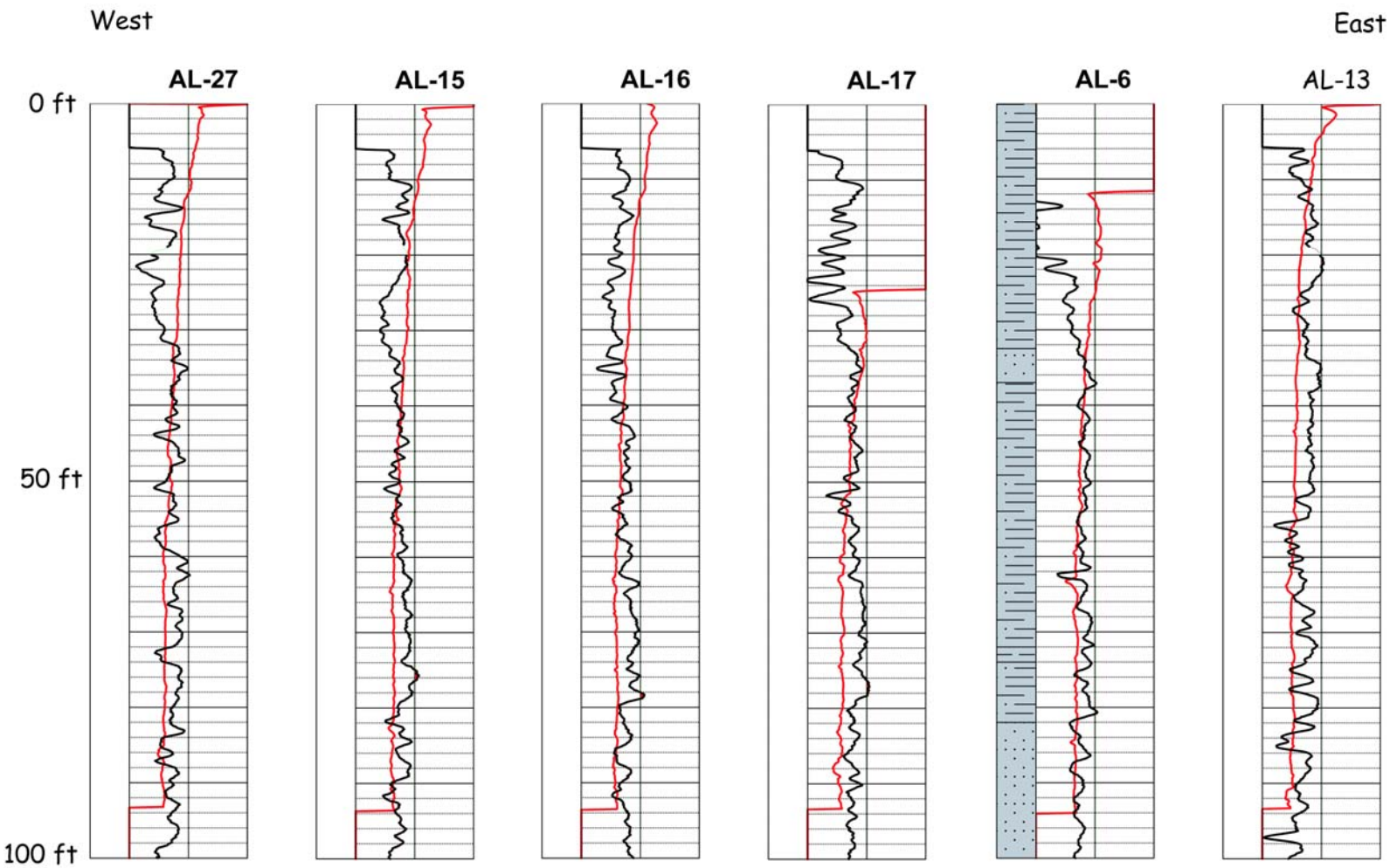

Figure 45. West-to-east stratigraphic cross section through the grid-drilling area showing subsurface geology of the final target area. Note that for drill hole AL-17, leakage of drilling fluid from the hole led to a lower fluid level (~24 ft) and air-filled borehole, and thus the resistivity trace should not be recorded for this shallow interval.

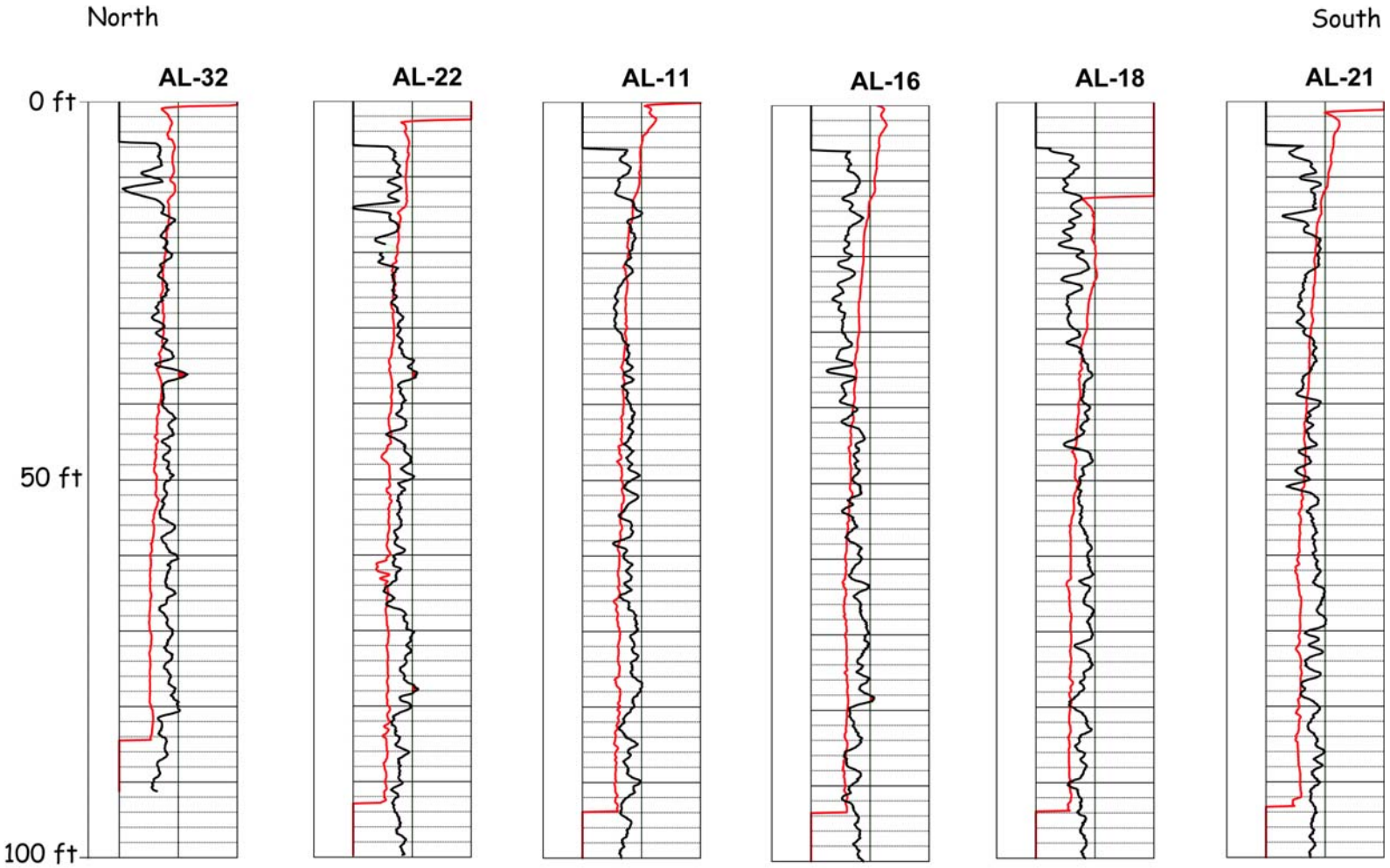

Figure 46. North-to-South stratigraphic cross section through the grid-drilling area showing subsurface geology of the final target area.

Rock Mechanics Data for the Antelope Lake Area

The use of rotary drilling for the majority of holes constituting the confirmatory grid limits the amount of core that is available for sampling and material-properties testing. However, the combination of confirmation of surface geophysics by the core and downhole geophysical logs and the confirmation of the downhole geophysics by the core across a broad spectrum of lithologies from very coarse to fine strongly suggested that the geophysical logs would be a sufficient indicator of suitable materials.

We sampled the available core with two objectives that were believed compatible with definition of a suitable test area and aim point. (1) We collected samples of the "hardest" material in each core hole within and adjacent to the 500-m-diameter test area. Typically, this was done using the most dense interval on the geophysical log, but physical hardness determined with a knife blade was also considered. (2) We also collected some samples of coarser-grained materials from holes farther away from the test region.

The object was to collect material that would both yield "worst-case" compressive strengths and provide a crude correlation between the geophysical-log signatures and lab-measured material properties. If the identifiably hardest/densest/coarsest materials from within the grid-defined test region did not pose a problem for penetration as determined by numerical calculations (e.g., cavity-expansion models; Longcope, 1990), then presumably the softer materials inferred elsewhere in the section via downhole geophysics should not either. Laboratory test results for the selected core specimens are reported in Appendix I. However, it should be noted that the average of the properties reported by the rock-mechanics laboratory *may overestimate* the *overall* strength of the bulk of the materials within the target region.

Discussion of Antelope Lake Geology

Antelope Lake represents a much larger area than the Main Lake, and the drilling intensity is significantly less (about half). Therefore, the geology of the subsurface of Antelope is in some ways much less well characterized than Main lake. However, to some extent, what is known about the subsurface geology of Antelope Lake suggests that the depositional system may be somewhat simpler, and that more meaningful geologic information is known than suggested only by the drilling statistics.

In distinct contrast to the lithologies encountered at the Main Lake, the bulk of the material sampled by the Antelope Lake drilling program is fine grained. With the exception of the coarse granule to fine-gravel deposits found in drill holes AL-1 and AL-3, virtually no truly coarse-grained sediments, equivalent to those from the Main Lake, were encountered; refer to the stratigraphic cross sections of figures 41 and 42. Admittedly thoug, we benefitted from the prior knowledge provided by the surface geophysical surveys, and thus we targeted the drill holes away from regions inferred to contain coarse grained sediments.

It is also noteworthy that the shallow portion of the sediments in Antelope Lake are disproportionately finer grained than the shallow portion of the sediments at Main Lake. Although fine-grained materials may be present at Main Lake at untested depths between 40 and 100 ft below the known coarse sediments (see fig. 27 on page 39), the shallow, 0- to 40-ft, interval at Antelope Lake is exceptionally fine grained as well. With the exception of hole AL-1, drilled almost at the shoreline of the lake, no sediments coarser than a silty or sandy clay were encountered

anywhere in the upper 20 ft of the lake bed. The proposed target region ultimately defined by the Antelope Lake drilling program appears to contain only fine grained sediments to the entire depth tested.

Although it is not particularly relevant to the selection of a target region on Antelope Lake, the large-scale fracturing observed on the surface of the lake — and in the surface geophysical data — is rather interesting. There is a very consistent northeast trend to the observed and mapped fractures (fig. 38). Additionally, these are not shallow features, as indicated by the high-conductivity expression of the one fracture/fault captured in the TEM profile of figure 33. The fact that numerous small sinkholes appear to have drained non-trivial quantities of fluid at some point during the recent history of these fracture features suggests a modestly deep-seated nature as well. The drainage of relatively saline water from the lake surface to depth is completely consistent with the conductive electromagnetic character of the fault in figure 33.

Another set of observations of the sediments forming Antelope Lake is interesting as well. During the drilling of a number of AL-series holes, fractures were observed to open up extending directly through the drill hole. Figure 47(a) presents a particularly spectacular example of one of these drilling-induced fractures. Figure 47(b) shows a similar fracture exhibiting en-echelon offset. Some of these drill-hole-related fractures extended many tens of feet; one was paced off as approximately 100 ft long, and it extended on both sides of the drill hole. In one case, a fracture intersected the mud pit adjacent to the drill rig and fluid flowed from the pit into the drill hole via the fracture.

These drilling-induced fractures cannot be shallow features either. The substantial lateral extent, and in particular, the tectonic-like en echelon offset patterns [fig. 47(b)] argue that these features represent some more deep-seated stress pattern present in the lake sediments. Additionally, many of the Antelope Lake drill holes lost substantial quantities of drilling mud during operations. This fluid must have gone "somewhere," and the ease and quantity of the losses suggests a large volume of non-matrix-porosity-related open space in the subsurface. Some of these holes may be

Figure 47. Fracture induced by drilling vibrations extending away from a drill hole on Antelope Lake. (a) Close-up view showing centimeter-scale width of fracture; (b) En-echelon fracture patterns of a drilling-induced fracture (centimeter scale is circled).

identified in the geophysical log profiles of Appendix G, as the logs for which the density and/or resistivity traces terminate some distance below the collar of the hole. These partial traces represent holes in which the fluid level, at the time of logging, was markedly below the ground surface. Other holes lost fluid as well, but the wellbores were refilled prior to or during logging. No significant fluid losses of any kind were encountered in the Main Lake drill holes.

SUMMARY AND CONCLUSIONS

Subsurface geological characterization activities have been conducted at two large playa lakes on the Tonopah Test Range in central Nevada. These characterization activities were intended to provide basic stratigraphic-framework information regarding the lateral distribution of "hard" and "soft" materials, using both geophysical-log information and macroscopic lithologic data as surrogates for mechanical strength properties. Some laboratory mechanical data have been obtained on specimens selected from continuous wireline core in a small number of holes.

Downhole geophysical logging was used successfully at both Antelope Lake and the Main Lake to interpret geology. Softer, finer-grained sediments exhibit low density and generally low resistivity characteristics. Conversely, harder, coarser-grained sediments tend to exhibit higher densities and higher resistivities. These are the interpretations of the surface-based geophysical measurements as well. The correlation is not perfect, but the recovery of core on which the correlations are based is not perfect either. Thus, some amount of disagreement between the logged core and the logged petrophysical properties may be attributable to core loss and resulting uncertainty regarding the true depth position of the recovered core.

Some 90 rotary and core holes were drilled across the southern half of the Main Lake, which is located near the northern boundary of the test range. Systematic grid drilling to a consistent depth of approximately 40 feet has identified a large complex of interbedded very coarse-grained sediment with finer grained sands, silts, and clays in the eastern portion of the investigated region. The hardest materials comprise clayey granule- (2–4 mm) and fine-pebble- (4–8 mm) bearing sediments, in which siliceous volcanic clasts are in grain-supported contact.

Densities of these coarser-grained materials below the surface of the Main Lake, as determined through downhole geophysical logging are invariably in excess of 2.0 g/cm^3, and frequently in excess of 2.1 g/cm^3. The correlation of density with lithology and "hardness" allows the use of non-cored rotary drilling for greater areal coverage. The dense, coarse-grained deposits of the Main Lake appear to be located more in the eastern part of the lake. The number and thickness of high-density intervals decreases toward the west and somewhat to the northwest.

A shallow unit of quite fine grained silty clays is present in the upper 6 to 10 ft of the Main Lake. This material appears relatively uniform throughout the investigated region, and it is probably related to the more recent history of the modern playa. Some thin, harder intervals have been identified by a previous cone-penetrometer survey close to the southern shoreline of the modern lake within this more shallow unit.

Antelope Lake, located approximately 10 miles to the south of Main Lake, has been investigated using a two-stage study. Initially, surface-based geophysical methods were used to identify the approximate overall distribution of major lithologic facies. Electrical methods were used to distinguish conductive regions (inferred to be clay rich and therefore "soft")

from resistive regions (inferred to be coarser grained and therefore "hard"). Joint inversion of time-domain electromagnetic profiles and galvanic resistivity soundings produced good results and provided the basis for an initial drilling effort. Frequency domain electromagnetic surveying (a terrain conductivity survey) was used on an experimental basis and provided corroborating information.

The initial phase of drilling on Antelope Lake was targeted to confirm specific geophysical interpretations at locations coincident with selected surface-based measurements. Following successful confirmation of local measurements, the initial phase of drilling was expanded to test the more general, geophysical-based, conceptual model of the lake. These drill holes led to preliminary selection of a region for delineation drilling in a second phase.

Delineation drilling was conducted on a grid and was targeted at defining a region, at least 500 m in diameter of more or less exclusively "soft" low-density, high-conductivity materials, that could be used as a target region for air-dropped penetrator events. The delineation drilling was successful, and the overall geophysical model of the lake is considered validated. The center of the 500-ft diameter area is located at approximately UTM coordinates 529,100 meters East, 4,170,200 meters North, WGS-84.

For both Main Lake and Antelope Lake, the eastern portions of the lake appear to contain more coarse-grained material. The coarser clasts are almost exclusively volcanic in origin. The westernmost margins of neither lake were sampled, but the extent of drilling toward the western shorelines of the modern lakes is sufficient to suggest that coarse-grained materials are much more restricted on this western side of the modern lakes. To some extent, this observation is consistent with a gross structural position of the modern playas on a major down-to-the west Basin-and-Range fault block.

REFERENCES

AGI, 1989, AGI data sheets: for geology in the field, laboratory and office, compiled by J.T. Dutro, Jr., R.V. Dietrich, and R.M. Foose, American Geological Institute, Alexandria, Va.

Akers, S.A., 1986, Mechanical properties of Antelope Lake soils, Final Report, November 1986, *prepared for* Sandia National Laboratories, Livermore, Calif., *by* Waterways Experiment Station, Department of the Army, Vicksburg, Miss.

Ekren, E.B., Anderson, R.E., Rogers, C.L., and Noble, D.C., 1971. Geology of Northern Nellis Air Force Base Bombing and Gunnery Range, Nye County, Nevada. U.S. Geological Survey Prof. Paper 651, 91 p.

GeoComp Systems, 1999, GeoCalc, ver. 4.20 for Windows, (Microsoft Windows™ software for converting coordinate systems and datums), GeoComp Systems, Inc., Blackburn, Victoria, Australia. http://www.geocomp.com.au.

Hansen, N.R., and Patterson, W.J., 1996, Mapping of a subsurface formation on the Main Lake at the Tonopah Test Range, Sandia Report SAND96-2361, Sandia National Laboratories, Albuquerque, N. Mex., 64 p. *Official Use Only.*

Longcope, Donald B. Jr., 1990, The Prediction of Loads on Penetrators into Rock via the Spherical Cavity Expansion Approximation, Sandia Report SAND87-0959, Sandia National Laboratories, Albuquerque, N.Mex.

Sandberg, S.K., 1995, Simultaneous modeling of TEM and resistivity-IP soundings to improve resolution in hydrogeological investigations. Ph.D. Dissertation, Rutgers University.

Togami, T., 2002, TD2 penetration data and recovery, Project Close-out Briefing Materials, November 2002, (a Microsoft PowerPoint® presentation stored on Sandia Fileshare System Dpnet2), Sandia National Laboratories, Albuquerque, N. Mex., 18 p. *Official Use Only/Export Controlled Information.*

U.S. Army Corps of Engineers, 2000 (date of last bug fix), Corpscon for Windows, ver. 5.11.08 (Microsoft Windows™ software for converting coordinate systems and datums), U.S. Army Corps of Engineers, Topographic Engineering Center, Alexandria, Va. GeoTrans Geographic Translator, ver. 2.2.3. U.S. Army Topographic Engineering Center, Geospatial Information Division & National Imagery and Mapping Agency, Exploitation Tools Division. http://crunch.tec.army.mil/software/corpscon/corpscon.html.

Woodward-Clyde-Sherrard and Associates, 1964, Boring and test data, Mud Lake, Tonopah Test Site, Report No. SC-DC-640888, Job No. 7733-6762, *prepared for* Sandia Corporation by Woodward-Clyde-Sherrad and Associates, Denver, Colo. Selected portions of this report are included as Appendix B in Hansen and Patterson (1996).

Appendix A: Geology in the Vicinity of Drill Hole ML-1

This page intentionally left blank.

INTRODUCTION

This appendix provides additional detailed information about the results of geological characterization from the initial investigations in the vicinity of the test assembly that triggered this overall project. This initial phase of characterization consisted of drilling core holes ML-1, ML-2, and ML-3. All core was logged geologically, but no geophysical logs were obtained (see also the note on page 22 and figure 10). We include photographs of all core from all three holes, as well as photographs and discussion of specific features observed in the core that are relevant to the issue of the "hard layer" that cause internal failure of the test unit.

The full-core photographs are presented in figures A-1 through A-12. In each figure, the core boxes contain a nominal 10 feet of core in five rows of 2 feet each. The physical length of core is generally less, as "natural" breaks in the core were used to divide the core into rows wherever possible. The core "reads like a book," from left to right and from top to bottom of the photograhs. The red and blue stripes indicate "up," as ***r**ed* is on the ***r**ight* when visualizing the core in its original vertical position in the ground. The labeled wooden core blocks mark the known depths of drilling breaks between core runs. Interpreted even-foot depths have been marked on the core wherever the physical condition of the core allowed.

Figures A-13 through A-18 illustrate specific features relevant to the identification of the so-called second hard layer. Figure A-13 presents images of material more-or-less typical of the upper, clay-rich portion of the Main Lake sedimentary section. The clays and silty clays are laminated locally [fig. A-13(b)], and the dessication cracking displayed in the photographs is typical of bentonitic muds. Bentonite is a generic term for any of a number of similar expandable-layer clays that adsorb into and release water molecules from within the layered clay-mineral structure.

Figure A-14 shows two examples of granule-bearing sediments from below the soft, clay-rich upper unit. This is the interval frequently termed the "first hard layer," and it probably corresponds to something close to the "depth of refusal" described in the cone-penetrometer study. Note that this material appears to have been sufficiently hard that the diamond core bit cut through the individual volcanic clasts (white objects) and that the core retains a relatively perfect cylindrical form. The photographs are from holes ML-1 and ML-3.

Photograhs of the so-called "second hard layer, the principal focus of this overall investigation, are presented in figure A-15. The general impression of the material type is nearly identical to that of the first hard layer from figure A-14. Coarse sand and small granules, in white or very light colors, are dispersed in a more brownish, silty and clay-rich matrix. The material in all three core holes is essentially identical.

Whereas it is somewhat difficult to determine macroscopically whether the volcanic clasts in the core shown in figures A-14 and A-15 are in grain-to-grain contact, thus forming a rigid framework, it is clear that the "pea gravels" shown in figure A-16 are in such contact. These latter photographs, which represent material present in all three core holes, clearly indicate the close-packed nature of the hard volcanic clasts. Part of this visibility is because the circulating drilling mud has washed away some of the silt and clay from the outside of the core in this interval at 25–26-ft depths, thus exposing the internal fabric of the core.

Figure A-17 is a photograph from a less-granule-rich and more sandy interval, in the general vicinity of the first hard layer. The core is from a depth of ~15 ft in core hole ML-10.

Although this material is not from the immediate ML-1–ML-3 location, the image is fairly typical of the "sands" encountered in the subsurface of the Main Lake. A photograph showing clearly the relatively uniform size distribution of the coarse volcanic granules is presented in figure A-18. In this image, the mud matrix of an interval, probably just slightly higher in the hole, has been washed away by the circulating drilling mud, allowing the heavier granules to be concentrated, here loose on the surface of the underlying core.

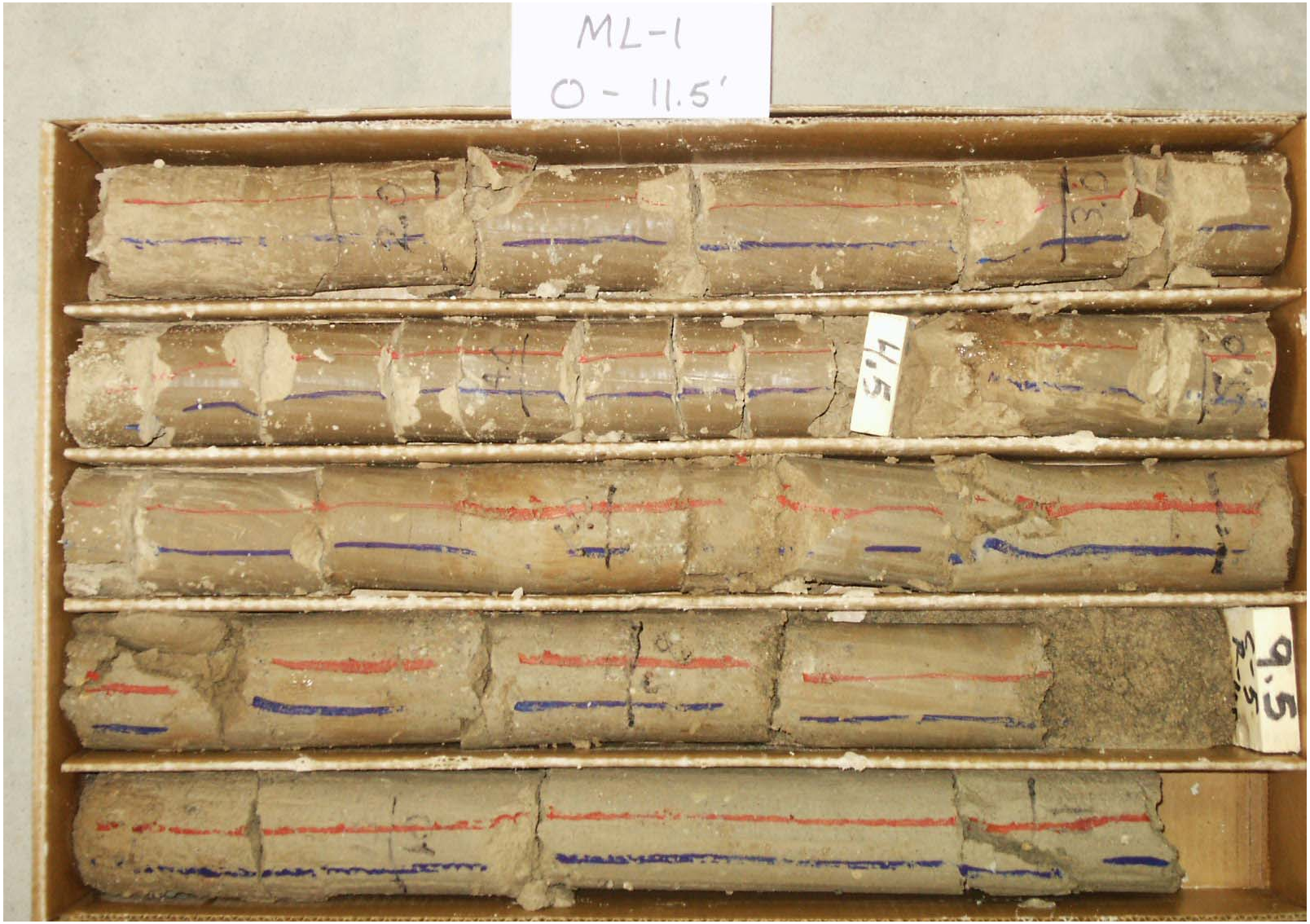

Figure A-1 Photograph of core from drill hole ML-1, 0 to 11.5 feet.

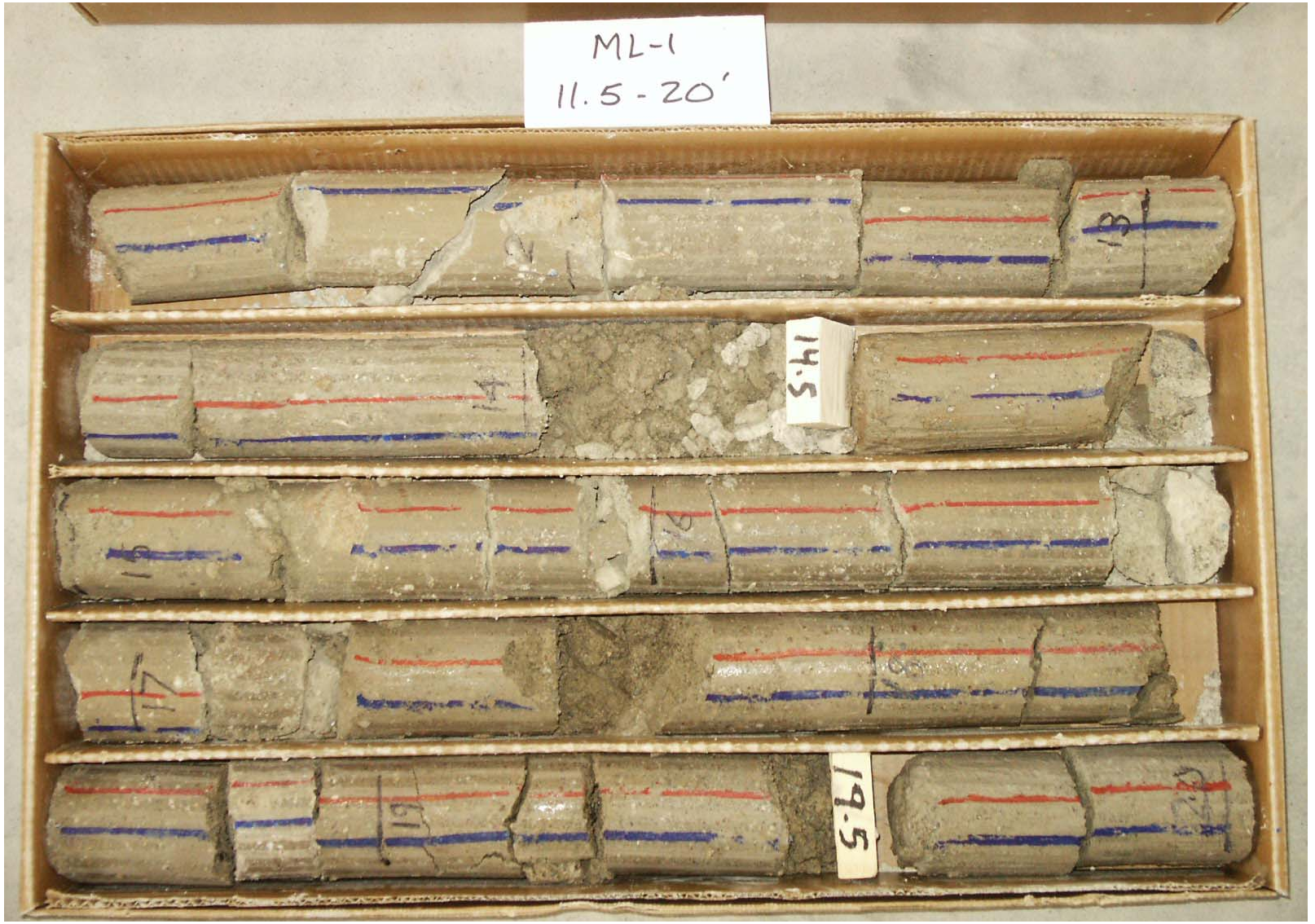

Figure A-2 Photograph of core from drill hole ML-1, 11.5 to 20.0 feet.

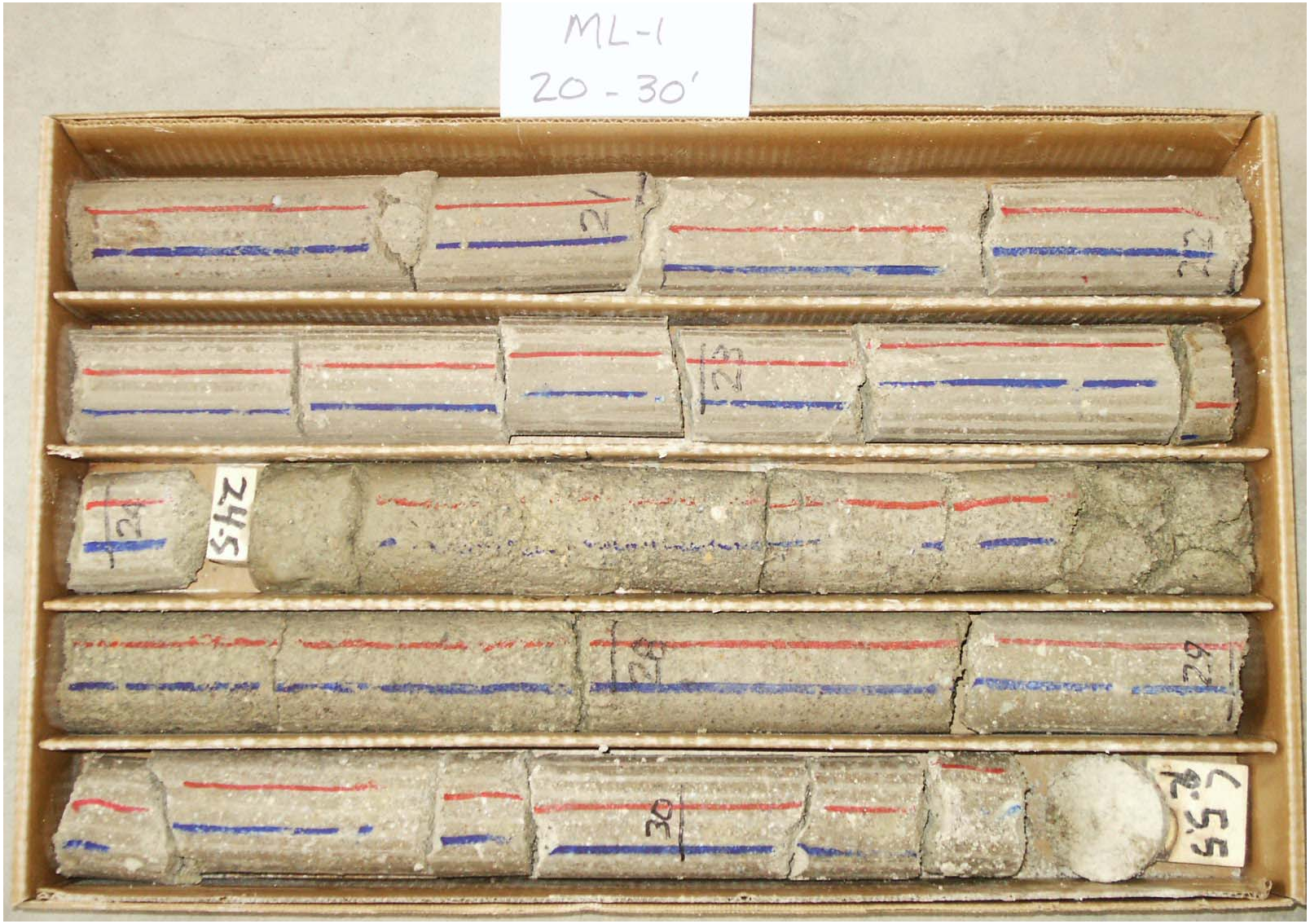

Figure A-3 Photograph of core from drill hole ML-1, 20.0 to 30.0 ft.

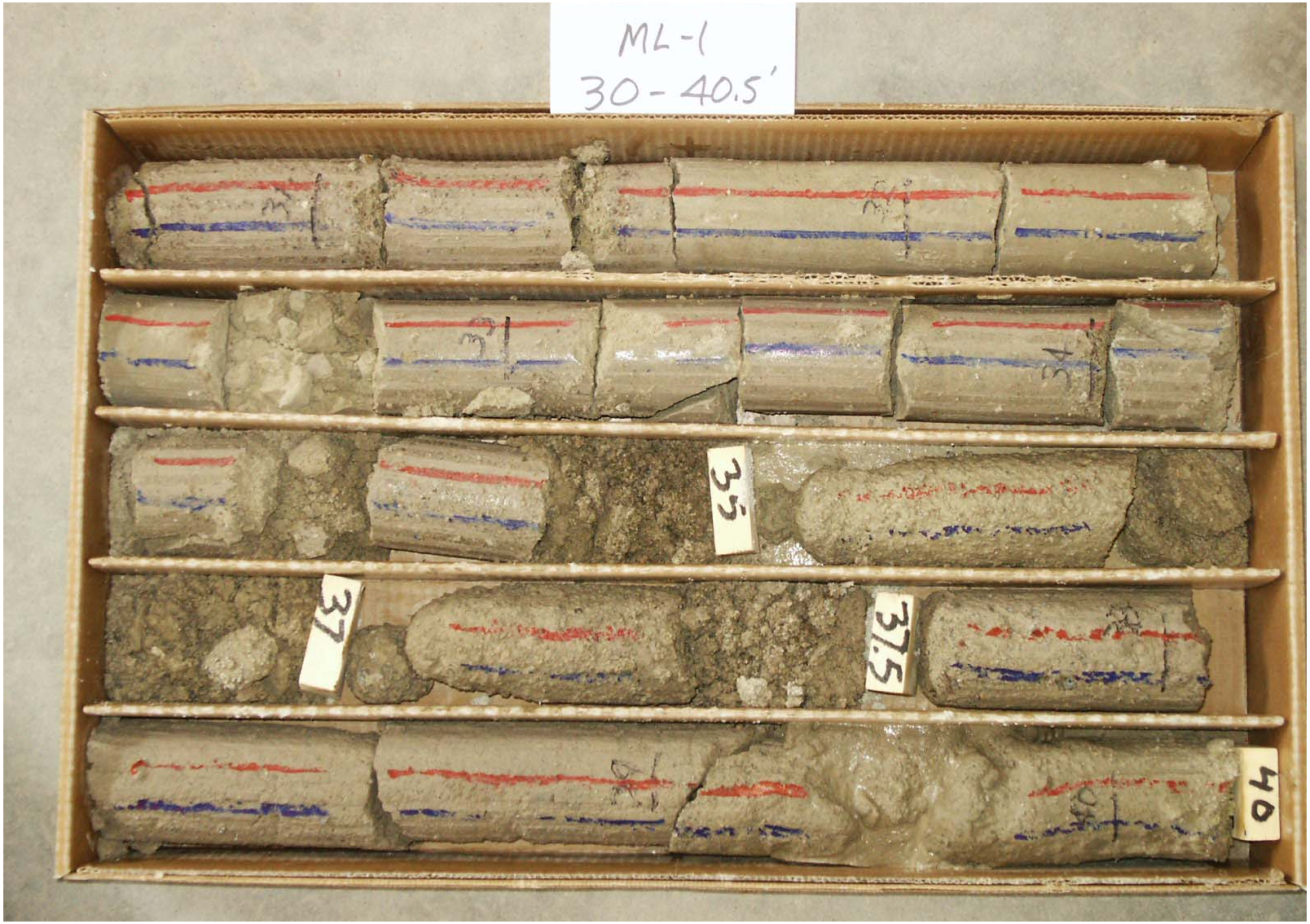

Figure A-4 Photograph of core from drill hole ML-1, 30.0 to 40.5 ft (TD).

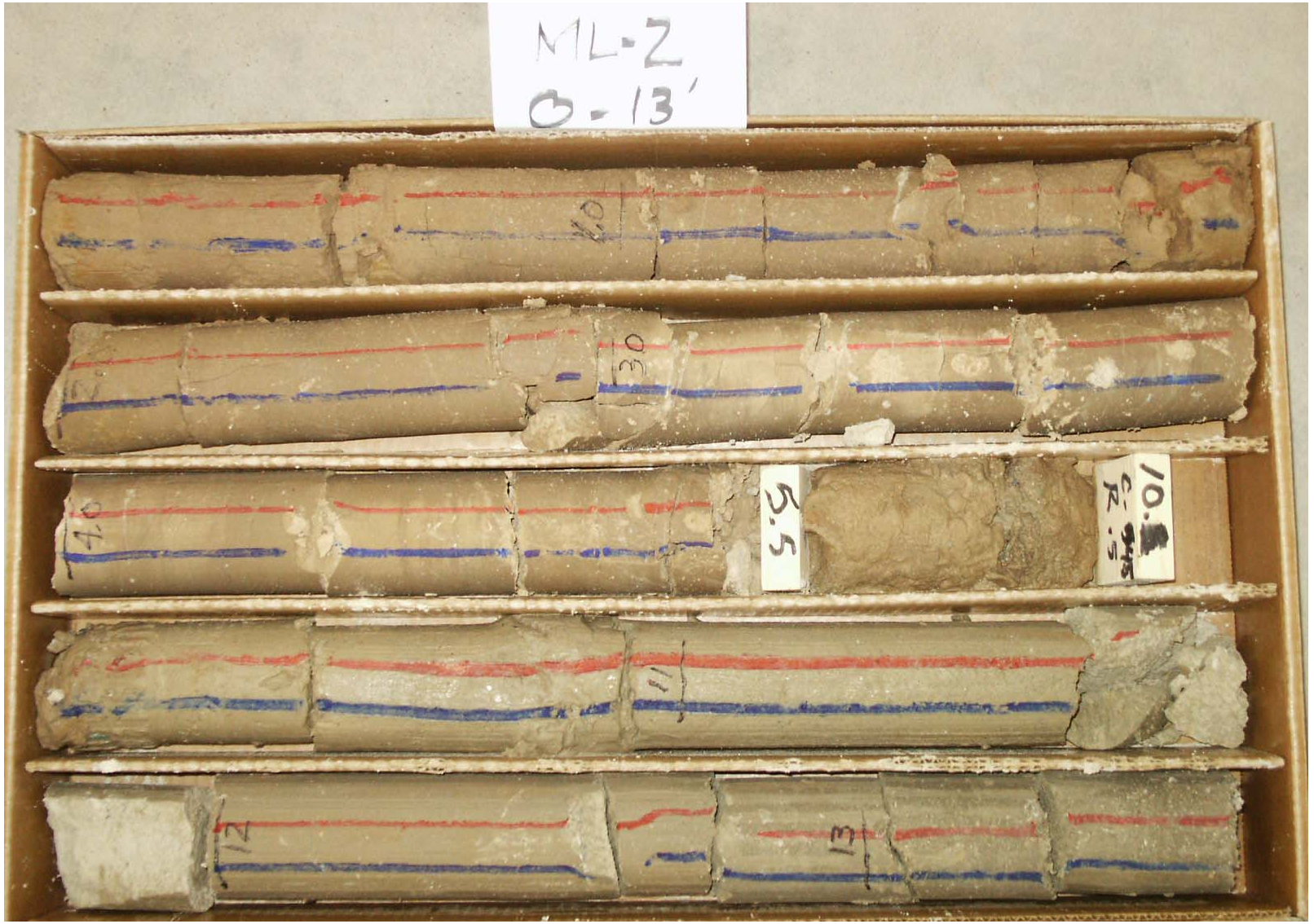

Figure A-5 Photograph of core from drill hole ML-2, 0 to 13.0 ft.

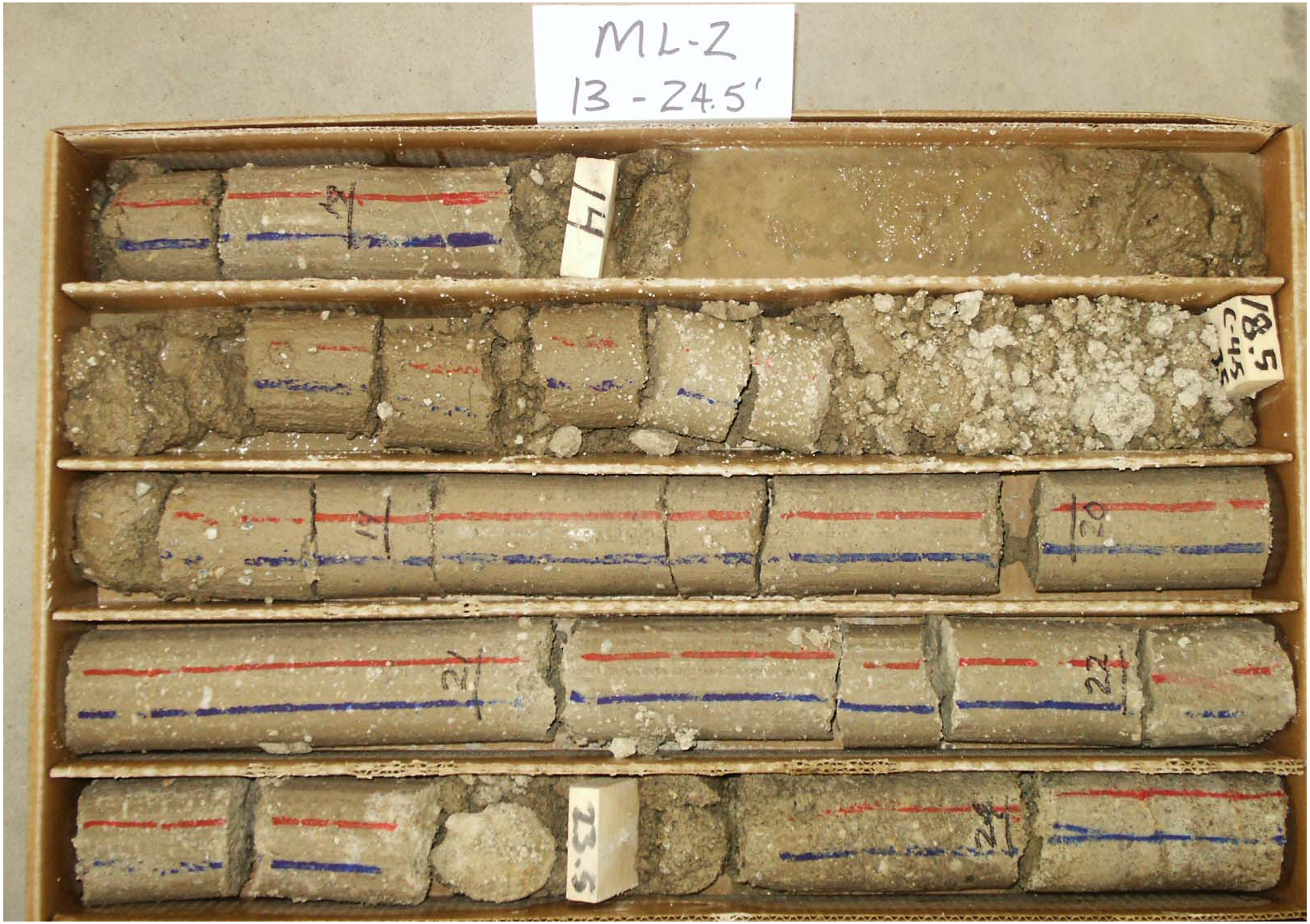

Figure A-6 Photograph of core from drill hole ML-2, 13.0 to 24.5 ft.

Figure A-7 Photograph of core from drill hole ML-2, 24.5 to 34.0 ft.

Figure A-8 Photograph of core from drill hole ML-2, 34.0 to 39.0 ft (TD).

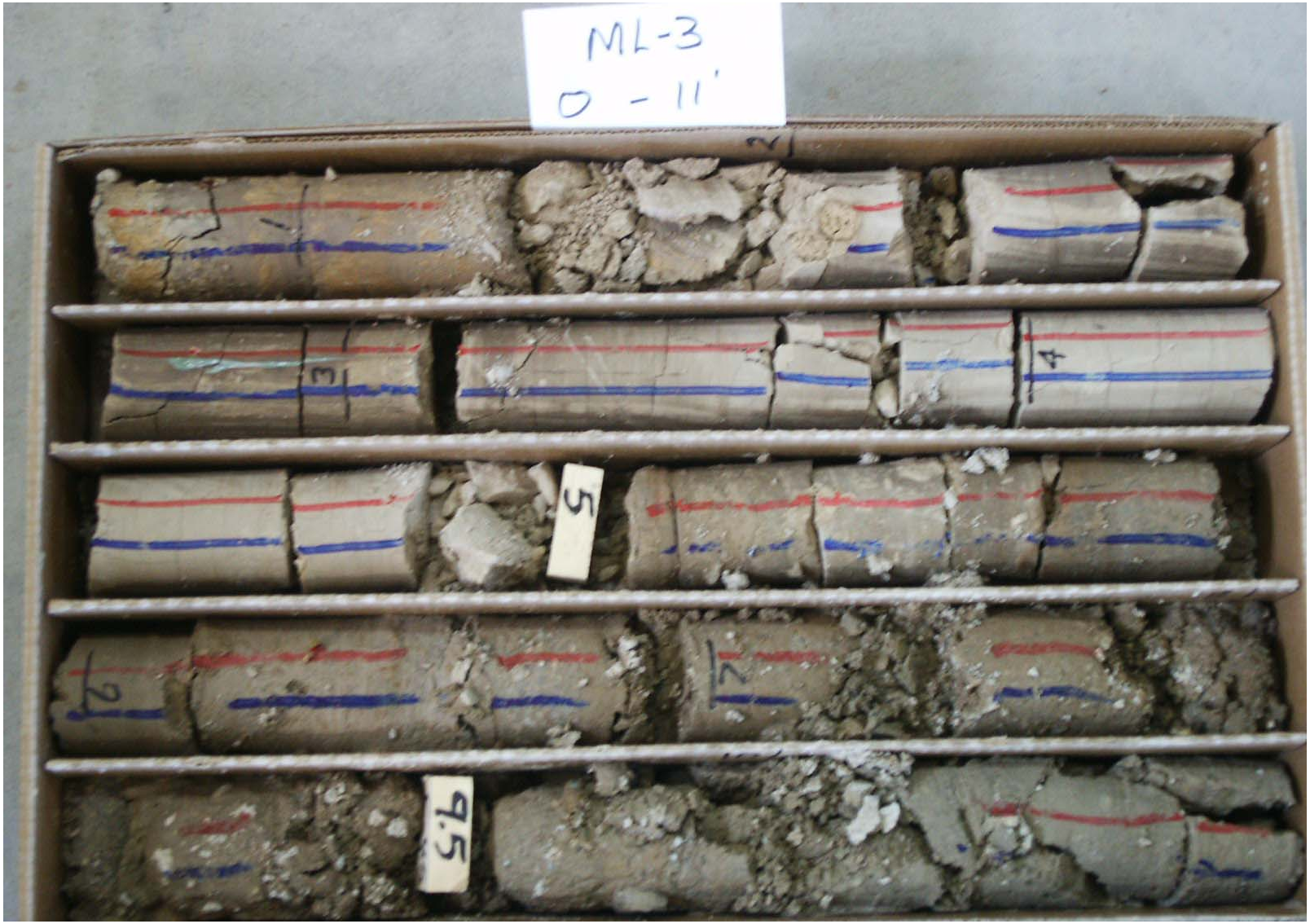

Figure A-9 Photograph of core from drill hole ML-3, 0 to 11.0 ft.

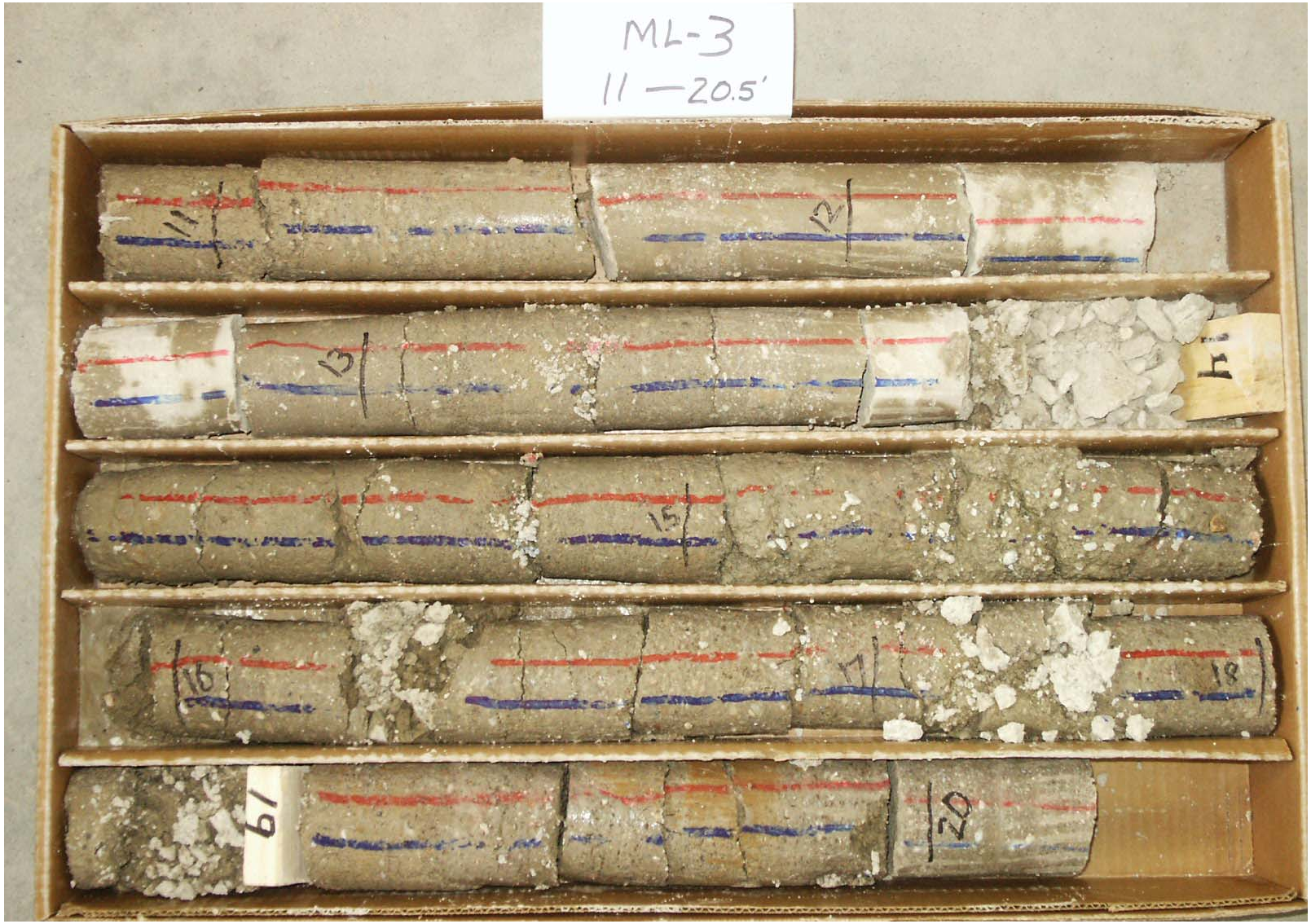

Figure A-10 Photograph of core from drill hole ML-3, 11.0 to 20.5 ft.

Figure A-11 Photograph of core from drillhole ML-3, 20.5 to 29.0 ft. The parallel striations from ~20–23 ft are from the core-catcher, the spring-like device that holds the core in the inner tube of the core barrel during retrieval

Figure A-12 Photograph of core from drill hole ML-3, 29.0 to 39.0 ft (TD).

Figure A-13 Photographs of core showing the "soft" upper, clay-rich portion of the lake sediments. Dessication cracking is typical of sediments containing bentonitic (expandable-layer) clays. (a) ML-1, ~3 ft; (b) ML-3, ~4 ft. Core trays are approximately 2 inches wide.

Figure A-14 Photographs of core from the so-called “first hard layer.” (a) Drill hole ML-1, ~13 ft; (b) drill hole ML-3, ~12 ft. Core trays are approximately 2 inches wide.

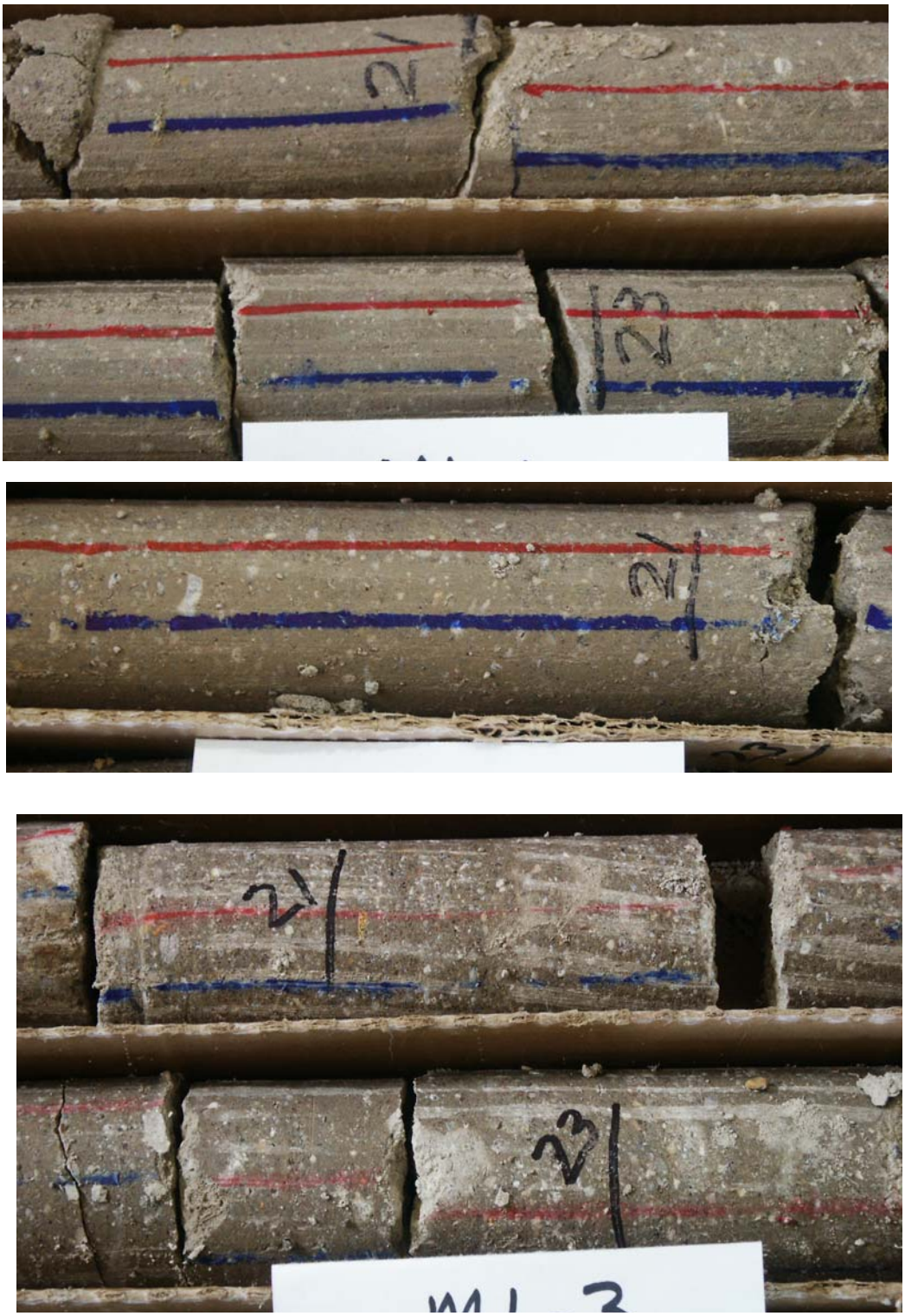

Figure A-15 Photographs of material characteristic of the so-called “second hard layer.” (a) ML-1, ~21–23 ft; (b) ML-2, ~21–23 ft; (c) ML-3, ~21–23 ft. Note that the mud-rich core is sufficiently hard that the volcanic clasts have been cut by the diamond core bit (compare to fig. A-16).

(a)

(b)

(c)

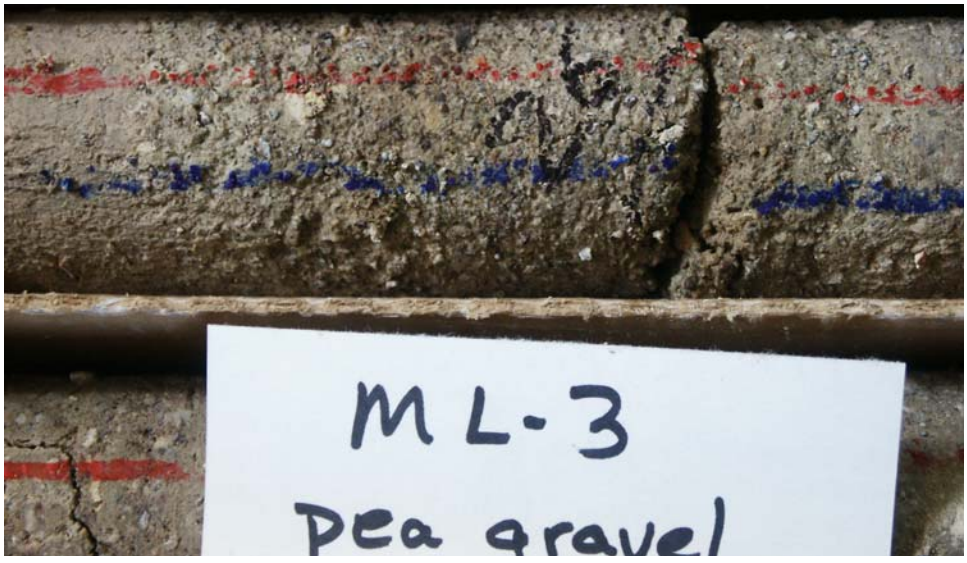

Figure A-16 Photographs of core showing the granule-rich, probably clast-supported “pea-gravel” layer. (a) ML-1, 25 ft; (b) ML-2, ~25 ft; (c) ML-3, ~26 ft. . Core trays are approximately 2 inches wide.

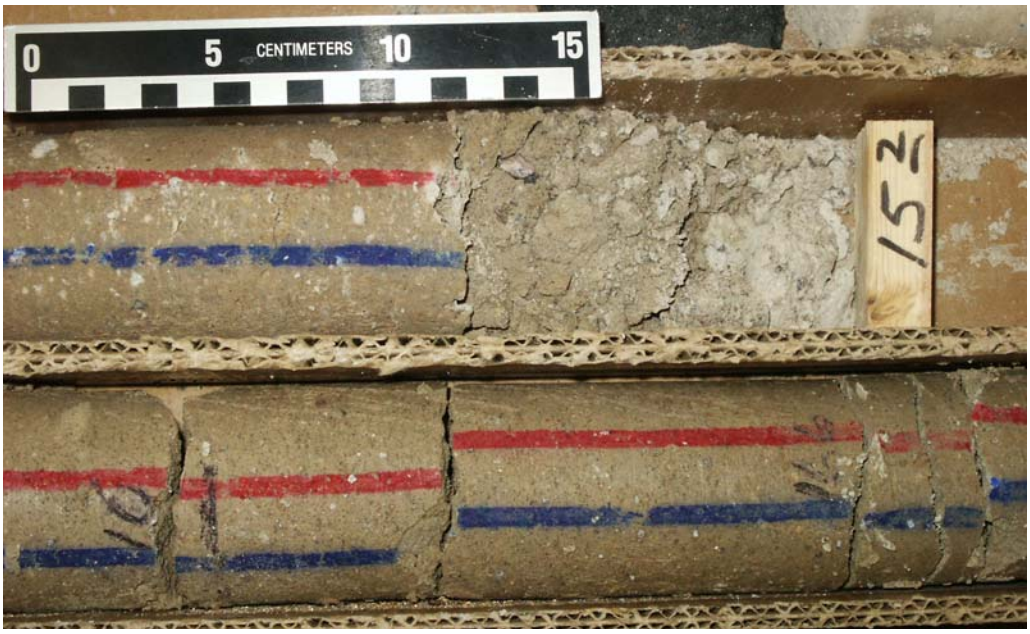

Figure A-17 Photograph of a more sand-rich portion of the “second hard layer” at ~16 ft in drill hole ML-10.

Figure A-18 Photograph showing loose volcanic-clast granules on the surface of an otherwise mud-rich interval of core from drill hole ML-3, ~37 ft.

This page intentionally left blank.

Appendix B: Coordinate Locations of Drill Holes on the Main Lake

This page intentionally left blank.

INTRODUCTION

This appendix contains the collar coordinates of all holes drilled on the Tonopah Test Range Main Lake. Locations are reported in latitude and longitude, UTM coordinates, and Nevada state plane coordinate system eastings and northings. Note that the geographic datum used for latitude/longitude and the UTM coordinates (WGS-84) is different than that for the Nevada state plane system (NAD-27). Use of coordinate values from one datum with reference to another datum can result in errors of up to several hundred feet.

The collar locations were surveyed using a Trimble Pro XRS global positioning satellite (GPS) receiver using real-time correction signals, either from the Wide-Area Augmentation System (WAAS) or beacon signals, probably transmitted by the military. WAAS corrections are generally considered of lower precision than beacon corrections, although the difference is most likely to be meaningless for purposes of drill hole location in the field. The GPS equipment records locations in native WGS-84 latitude and longitude, but can export the data in virtually any desired coordinate system.

Core holes on the Main Lake are identified by the prefix, *ML-*, whereas non-cored (rotary) holes are prefixed by *MLR-*. The two types of drill holes are tabulated separately in tables B-1 and B-2.

Table B-1: Drill hole locations for cored holes drilled on the Main Lake

[Geographic coordinates are WGS-84 values by Global Positioning Satellite. UTM coordinates are WGS-84, Zone 11. State Plane Coordinates are Nevada Coordinate System, Central Zone, NAD-27]

Hole Id	Depth	Latitude	Longitude	UTM East	UTM North	Horizontal Precision	GPS Elevation	Vertical Precision	State Plane East	State Plane North	Elevation
	(ft)	(degrees)	(degrees)	(m)	(m)	(m)	(m)	(m)	(ft)	(ft)	(ft)
ML-1	40.5	37.838900818	-116.723846162	4187976.9	524298.5	0.36	1626.4	0.51	1124421	483747	5336
ML-2	39.0	37.838935246	-116.723891924	4187980.7	524294.5	0.53	1625.4	0.84	1124433	483733	5333
ML-3	39.0	37.838840791	-116.723872593	4187970.2	524296.2	0.39	1626.5	0.51	1124399	483739	5337
ML-4	40.0	37.841795821	-116.728160427	4188297.0	523918.0	0.31	1626.0	0.52	1125476	482502	5335
ML-5	39.0	37.840960143	-116.722994069	4188205.6	524372.8	0.63	1624.5	0.70	1125170	483993	5330
ML-6	41.4	37.841783620	-116.719484988	4188297.9	524681.3	0.57	1626.4	0.90	1125470	485007	5336
ML-7	41.0	37.839307783	-116.717790406	4188023.6	524831.2	0.39	1625.6	0.60	1124568	485495	5333
ML-8	40.0	37.843427200	-116.716042356	4188481.2	524983.7	0.59	1626.5	1.41	1126068	486001	5336
ML-9	45.0	37.842623001	-116.733388528	4188387.4	523457.7	0.37	1624.4	0.67	1125778	480992	5330
ML-10	40.4	37.839317954	-116.733387317	4188020.7	523458.9	0.35	1625.2	0.50	1124574	480992	5332
ML-11	24.8	37.836821076	-116.728192540	4187745.0	523916.8	0.37	1624.2	0.55	1123664	482491	5329
ML-12	41.5	37.837692884	-116.724693711	4187842.7	524224.4	0.42	1625.2	0.68	1123981	483502	5332
ML-13	40.4	37.839310349	-116.722970704	4188022.6	524375.4	0.43	1624.9	0.69	1124570	484000	5331
ML-14	41.0	37.840149856	-116.726464722	4188114.8	524067.7	0.42	1624.8	0.68	1124876	482991	5331
ML-15	41.2	37.839303090	-116.729910776	4188020.0	523764.8	0.41	1624.5	0.65	1124568	481996	5330
ML-16	40.0	37.838082747	-116.722120047	4187886.6	524450.7	0.41	1625.0	0.61	1124123	484245	5331
ML-17	40.0	37.838909644	-116.722108820	4187978.3	524451.4	0.42	1626.7	0.62	1124424	484248	5337
ML-18	40.0	37.839708627	-116.723841509	4188066.5	524298.7	0.42	1626.4	0.64	1124715	483748	5336
ML-19	40.0	37.838059790	-116.723777191	4187883.6	524304.9	0.42	1626.7	0.65	1124114	483766	5337

Table B-2: Drill hole locations for rotary holes drilled on the Main Lake

[Geographic coordinates are WGS-84 values by Global Positioning Satellite. UTM coordinates are WGS-84, Zone 11. State Plane Coordinates are Nevada Coordinate System, Central Zone, NAD-27]

Hole Id	Depth	Latitude	Longitude	UTM East	UTM North	Horizontal Precision	GPS Elevation	Vertical Precision	State Plane East	State Plane North	Elevation
	(ft)	(degrees)	(degrees)	(m)	(m)	(m)	(m)	(m)	(ft)	(ft)	(ft)
MLR-1	40.6	37.839318647	-116.719527900	4188024.4	524678.4	0.32	1625.8	0.51	1124572	484994	5334
MLR-2	40.0	37.840922926	-116.719463794	4188202.4	524683.5	0.59	1626.8	0.66	1125156	485013	5338
MLR-3	40.0	37.840919987	-116.721228559	4188201.6	524528.2	0.60	1627.0	0.66	1125155	484503	5338
MLR-4	40.0	37.841784178	-116.721232669	4188297.5	524527.5	0.60	1624.4	0.66	1125470	484502	5330
MLR-5	40.0	37.841787052	-116.722965396	4188297.4	524375.1	0.61	1624.6	0.67	1125471	484002	5330
MLR-6	40.0	37.841756178	-116.724770814	4188293.5	524216.2	0.63	1626.2	0.70	1125461	483480	5336
MLR-7	40.0	37.841769103	-116.726462596	4188294.5	524067.4	0.62	1626.3	0.69	1125466	482992	5336
MLR-8	40.0	37.840969606	-116.726451014	4188205.8	524068.7	0.63	1625.4	0.72	1125174	482995	5333
MLR-9	40.0	37.840954793	-116.724727354	4188204.6	524220.3	0.63	1625.2	0.72	1125169	483493	5332
MLR-10	40.0	37.840960436	-116.728209078	4188204.3	523914.0	0.64	1626.6	0.73	1125171	482487	5337
MLR-11	40.0	37.840951090	-116.729931239	4188202.8	523762.5	0.60	1625.6	0.74	1125168	481990	5334
MLR-12	40.0	37.840947647	-116.731639048	4188202.0	523612.2	0.60	1625.2	0.74	1125167	481497	5332
MLR-13	40.0	37.840958406	-116.733363867	4188202.8	523460.4	0.60	1624.9	0.74	1125172	480999	5331
MLR-14	40.0	37.840125429	-116.733387090	4188110.3	523458.6	0.30	1624.6	0.48	1124868	480992	5330
MLR-15	40.0	37.840134986	-116.731629204	4188111.8	523613.3	0.30	1625.0	0.47	1124872	481500	5332
MLR-16	40.0	37.840189997	-116.729867178	4188118.4	523768.3	0.30	1623.7	0.46	1124891	482008	5327
MLR-17	40.0	37.840152025	-116.723030741	4188115.9	524369.9	0.37	1623.7	0.57	1124876	483982	5327
MLR-18	40.0	37.840131746	-116.721245043	4188114.1	524527.0	0.37	1624.7	0.56	1124868	484498	5331
MLR-19	40.0	37.840130568	-116.719517197	4188114.5	524679.0	0.35	1626.0	0.51	1124868	484997	5335
MLR-20	40.0	37.839308206	-116.721229352	4188022.8	524528.7	0.44	1625.5	0.74	1124569	484502	5333
MLR-21	40.0	37.838499514	-116.719513902	4187933.5	524679.9	0.39	1626.5	0.65	1124274	484998	5336
MLR-22	40.0	37.837654290	-116.719517225	4187839.7	524679.9	0.37	1626.5	0.66	1123966	484996	5337
MLR-23	40.0	37.840110562	-116.728186728	4188110.0	523916.2	0.39	1624.8	0.60	1124862	482494	5331
MLR-24	40.0	37.839324810	-116.728162302	4188022.8	523918.6	0.38	1624.7	0.59	1124576	482500	5331
MLR-25	40.0	37.838471507	-116.728181082	4187928.1	523917.2	0.47	1623.6	0.72	1124265	482495	5327

Table B-2: Drill hole locations for rotary holes drilled on the Main Lake (continued)

[Geographic coordinates are WGS-84 values by Global Positioning Satellite. UTM coordinates are WGS-84, Zone 11. State Plane Coordinates are Nevada Coordinate System, Central Zone, NAD-27]

Hole Id	Depth	Latitude	Longitude	UTM East	UTM North	Horizontal Precision	GPS Elevation	Vertical Precision	State Plane East	State Plane North	Elevation
	(ft)	(degrees)	(degrees)	(m)	(m)	(m)	(m)	(m)	(ft)	(ft)	(ft)
MLR-26	40.0	37.837650343	-116.728121773	4187837.1	523922.7	0.38	1624.6	0.57	1123966	482512	5330
MLR-27	40.0	37.836821781	-116.729911373	4187744.7	523765.5	0.37	1624.4	0.54	1123665	481995	5330
MLR-28	40.0	37.837656252	-116.729860142	4187837.3	523769.8	0.46	1624.6	0.65	1123969	482010	5330
MLR-29	40.0	37.838487797	-116.729902849	4187929.5	523765.7	0.45	1624.8	0.64	1124271	481998	5331
MLR-30	40.0	37.839326046	-116.731664441	4188022.1	523610.5	0.43	1625.3	0.60	1124577	481489	5332
MLR-31	40.0	37.838532451	-116.731633721	4187934.0	523613.4	0.43	1622.7	0.59	1124288	481498	5324
MLR-32	40.0	37.837645634	-116.731622980	4187835.6	523614.7	0.43	1625.9	0.59	1123965	481501	5335
MLR-33	40.0	37.836857787	-116.731648655	4187748.2	523612.7	0.42	1624.6	0.57	1123678	481493	5330
MLR-34	40.0	37.836841781	-116.733380470	4187746.0	523460.3	0.34	1624.8	0.50	1123673	480993	5331
MLR-35	40.0	37.837671594	-116.733338772	4187838.1	523463.7	0.34	1625.2	0.50	1123975	481005	5332
MLR-36	40.0	37.838469050	-116.733337413	4187926.6	523463.5	0.28	1625.5	0.44	1124265	481006	5333
MLR-37	40.0	37.838481741	-116.726413527	4187929.7	524072.8	0.32	1625.5	0.44	1124269	483005	5333
MLR-38	40.0	37.839306605	-116.726424507	4188021.3	524071.5	0.32	1625.5	0.44	1124569	483002	5333
MLR-39	40.0	37.837678860	-116.726423123	4187840.7	524072.2	0.32	1625.6	0.44	1123976	483002	5334
MLR-40	40.0	37.836824408	-116.726441704	4187745.8	524070.8	0.35	1627.2	0.51	1123665	482997	5339
MLR-41	40.0	37.836829703	-116.724755768	4187746.9	524219.2	0.42	1624.9	0.67	1123667	483484	5331
MLR-42	40.0	37.838453040	-116.724670489	4187927.0	524226.2	0.41	1623.4	0.65	1124258	483509	5326
MLR-43	40.0	37.839304628	-116.724681019	4188021.5	524224.9	0.40	1624.8	0.63	1124568	483506	5331
MLR-44	40.0	37.838885439	-116.723765986	4187975.2	524305.6	0.32	1625.1	0.45	1124415	483770	5332
MLR-45	40.0	37.836771728	-116.722973038	4187740.9	524376.1	0.34	1627.4	0.50	1123645	483998	5340
MLR-46	40.0	37.837629951	-116.722998079	4187836.1	524373.6	0.33	1626.0	0.47	1123958	483991	5335
MLR-47	40.0	37.838472308	-116.722965004	4187929.6	524376.2	0.34	1625.5	0.49	1124265	484001	5333
MLR-48	40.0	37.838484508	-116.721256463	4187931.4	524526.5	0.36	1625.2	0.51	1124269	484494	5332
MLR-49	40.0	37.836806854	-116.721224308	4187745.3	524529.9	0.40	1624.6	0.56	1123658	484503	5330

Table B-2: Drill hole locations for rotary holes drilled on the Main Lake (continued)

[Geographic coordinates are WGS-84 values by Global Positioning Satellite. UTM coordinates are WGS-84, Zone 11. State Plane Coordinates are Nevada Coordinate System, Central Zone, NAD-27]

Hole Id	Depth	Latitude	Longitude	UTM East	UTM North	Horizontal Precision	GPS Elevation	Vertical Precision	State Plane East	State Plane North	Elevation
	(ft)	(degrees)	(degrees)	(m)	(m)	(m)	(m)	(m)	(ft)	(ft)	(ft)
MLR-50	40.0	37.837662838	-116.721277980	4187840.2	524524.9	0.40	1624.7	0.55	1123970	484488	5331
MLR-51	40.0	37.837631259	-116.717851545	4187837.6	524826.4	0.36	1625.7	0.54	1123957	485477	5334
MLR-52	40.0	37.838505593	-116.717807714	4187934.6	524830.0	0.37	1625.5	0.56	1124276	485490	5333
MLR-53	40.0	37.840279166	-116.717831129	4188131.4	524827.3	0.36	1626.2	0.55	1124922	485484	5335
MLR-54	40.0	37.840954745	-116.717828719	4188206.4	524827.3	0.37	1624.1	0.56	1125168	485485	5329
MLR-55	40.0	37.841724207	-116.717816019	4188291.7	524828.2	0.37	1627.0	0.58	1125448	485488	5338
MLR-56	40.0	37.842599229	-116.717789028	4188388.8	524830.3	0.38	1625.0	0.59	1125766	485496	5332
MLR-57	40.0	37.842601328	-116.719530014	4188388.6	524677.1	0.41	1625.8	0.65	1125767	484994	5334
MLR-58	40.0	37.839329446	-116.735130978	4188021.6	523305.5	0.77	1626.8	1.62	1124579	480488	5337
MLR-59	40.0	37.838480549	-116.735059178	4187927.4	523312.0	0.34	1623.7	0.56	1124270	480509	5327
MLR-60	40.0	37.837664143	-116.735018615	4187836.8	523315.9	0.33	1624.1	0.55	1123973	480520	5329
MLR-61	40.0	37.838472625	-116.736791543	4187926.1	523159.6	0.31	1625.5	0.53	1124267	480008	5333
MLR-62	40.0	37.839345314	-116.736846617	4188022.9	523154.5	0.33	1624.1	0.52	1124585	479993	5329
MLR-63	40.0	37.837649718	-116.736758614	4187834.8	523162.8	0.32	1624.7	0.53	1123968	480018	5331
MLR-64	40.0	37.836835746	-116.736694953	4187744.5	523168.6	0.32	1624.1	0.54	1123671	480036	5329
MLR-65	40.0	37.836841736	-116.734964488	4187745.6	523320.9	0.33	1623.7	0.55	1123673	480536	5327
MLR-66	40.0	37.840160735	-116.735197650	4188113.8	523299.3	0.40	1624.4	0.70	1124882	480469	5329
MLR-67	40.0	37.840162447	-116.736893149	4188113.6	523150.1	0.36	1625.7	0.53	1124883	479980	5334
MLR-68	40.0	37.841756004	-116.733346561	4188291.3	523461.7	0.42	1622.8	0.78	1125462	481004	5324
MLR-69	40.0	37.841717114	-116.731639522	4188287.4	523611.9	0.50	1624.5	0.86	1125448	481497	5330
MLR-70	40.0	37.841777855	-116.729881731	4188294.6	523766.5	0.50	1624.7	0.84	1125469	482004	5331
MLR-71	40.0	37.840205727	-116.724709693	4188121.5	524222.1	0.49	1624.1	0.80	1124896	483498	5329

This page intentionally left blank.

Appendix C: Geophysical Logs for Drill Holes on the Main Lake

This page intentionally left blank.

INTRODUCTION

This appendix contains graphical presentations of the geophysical logs that were acquired from the Main Lake drill holes, both core and rotary. Both types of holes were logged in an identical fashion. The contractor for the geophysical logging was Century Geophysical Corporation of Tulsa Oklahoma, a well-known geophysical contractor with capabilities for logging "slim-hole" (vs. oil-well-sized) boreholes.

THE LOG DATA

The digital data were recorded in the field at 0.1-ft intervals, with depths measured in feet. The traces included in the displays are:

1. Density (g/cm^3)
2. Natural gamma (API units)
3. "MicroGuard" resistivity[1] (ohm-meters)
4. Caliper (inches)
5. Bit size (inches).

The digital data underlying these displays are contained on the CD-R in the pocket in the rear of this report in two formats. Modern logging data are recorded digitally and typically reported to the client company in *LAS* (log-ASCII standard) format. This format, which is in ASCII plain text (human readable), contains not only the curve measurements themselves, but also a number of informational fields containing data about the well itself, the location, and the specific types of logging tool(s) used in recording the log. A number of log-plotting software programs are capable of reading LAS-format files directly. The log data are also included in simple tabular form, again as ASCII text; these files are suitable for import and further manipulation in any of a number of spreadsheet-type programs such as Microsoft Excel®. Additional information regarding the LAS format and well logs in general may be found at http://www.spwla.org (the Society of Professional Well Log Analysts).

Data Processing

All of the displayed logs are presented in raw format on the figures that follow. However, two of the traces, natural gamma and density, were processed to smooth the curve and the processed data are also presented on the log figures. Smoothing can reduce both natural variability and some noise that may be present in the raw information, thereby improving the ability to represent the more geologically important features of the log.

In the case of the natural-gamma trace, the tool is measuring principally gamma rays from naturally occurring potassium-40 in certain feldspars and in clays. These levels are quite low, and because the size of the detector crystal that can fit in a slim-hole logging probe roughly 2 inches in diameter is fairly small, the counting statistics are less than optimal. The data are therefore inherently somewhat noisy. The density trace is also a nuclear tool subject to statistical counting variation. In this case, however, the radiation is an artificial field produced by a relatively intense source, and the counting variations are much reduced compared to those for the natural gamma curve. This relative variation is obvious on the various figures in the comparison of the raw and smoothed traces. In contrast, the electrical measurements, here the MicroGuard resistivity, are of a physical phenomenon that is ongoing and essentially steady-state in the borehole. These measurements are not subject to counting statistical variation.

1. *MicroGuard* appears to be a Century Geophysical Corporation name for their particular version of a focused resistivity tool. Focusing narrows the vertical extent of the resistivity investigation, providing better resolution of thin beds; see also page 225.

Both smoothed logs were generated by what is essentially a 9-point running average of the raw information. Presentation of both raw and smoothed curves on the figures allows the reader to examine the relationship and to draw conclusions as to whether important information may have been lost in the smoothing process.

DISCUSSION

The log data are shown in figures C-1 through C-86. Note that the right-hand column of each log is a repeat of the density data with density values greater than 2.00 g/cm^3 shaded red. Density values of 2.0 appear to be associated with much coarser materials — granules and pebbles of siliceous volcanic rock. Pure silica ("quartz") has a density of approximately 2.67 g/cm^3. It is these materials that appeared from initial work based on ML-1, ML-2, and ML-3 to correlate with the high-*g* loads encountered by the drop-test instrumentation that triggered this entire subsurface investigation (see page 13). For rotary holes from which there are no lithologic samples, a somewhat arbitrary threshold value density equal to 2.00 appeared to define "hard" layers that should be avoided in future air-dropped testing activities.

Data Quality

In general, the logs recorded at the Main Lake are of high quality. Borehole conditions were generally excellent and in-gauge, as indicated by the caliper log and the nominal borehole (bit) size. The density log, in particular is affected by rugose conditions in the borehole. Some downhole density tools are compensated for some degree of borehole rugosity via the caliper, but the tools employed in this survey did not have that capability. Therefore, it is essential to consider off-nominal borehole size in evaluating the density results. Note that the core holes and the rotary holes are of different diameters, as the core holes were not reamed to the larger hole size.

However, to a large extent, the density tool is more sensitive to *short-scale* variation in hole size than to broad changes over extended depths. This short-scale sensitivity is because wash-outs on a scale of a few inches to a few feet cause the radioactive source and/or the detector to separate from the borehole wall, thereby losing contact withe rock. This potentially allows gamma radiation to pass directly from the source to the detector and not to be attenuated by transit through the rock mass — the basis for the density determination. If the changes in borehole diameter are sufficiently gradual compared to the length of the logging tool (roughly 10 ft in this case), the logging sonde can accommodate itself to the enlarged diameter (up to the limits of the caliper arm that presses the sonde against the rock) and the measurements are not affected. In no case at the Main Lake were the drill holes sufficiently washed out that the caliper log exceeded its calibration.

Missing Data

No geophysical logs exist for core holes ML-1, ML-2, and ML-3. These holes were drilled on a very tight-turn-around basis to obtain geologic information regarding the cause of a specific flight-test failure. The remaining holes were part of a planned program that provided for the logistics necessary to have the geophysical contractor on-site. Rotary drill hole ML-44, however, was drilled as close as judged prudent to the location of ML-1 (about 25 ft). Therefore, we display the lithologic information from hole ML-1 on figure C-59 for reference.

Additionally, there is no geophysical log for rotary hole MLR-40. Either this hole was never logged in the crush of on-going field activities or the data have been lost. Data were

transferred from the logging contractor to Sandia in the field via 3-1/2 inch floppy disks at the end of most days. If only one hole were logged during the day, it might have been possible either not to transfer the data to a disk thinking to combine it with the next day's work (and then never doing that) or to have a single disk become lost physically at a later time.

Separately, all the geophysical logs contain some missing data, if for no other reason than that the data files contain the depth values for *all* recorded curves. Because different recording sensors are positioned physically at different locations on the sonde itself, the higher sensors are not capable of making measurements at greater or shallower depths in the hole than at which the they can be positioned. Additionally, the log-recording equipment may determine that some readings are un-physical as a result of the raw signals being processed, and thus may not output reduced data for that depth. Missing values are typically coded as –999.25 in LAS files and such values are typically "clipped" on the plots.

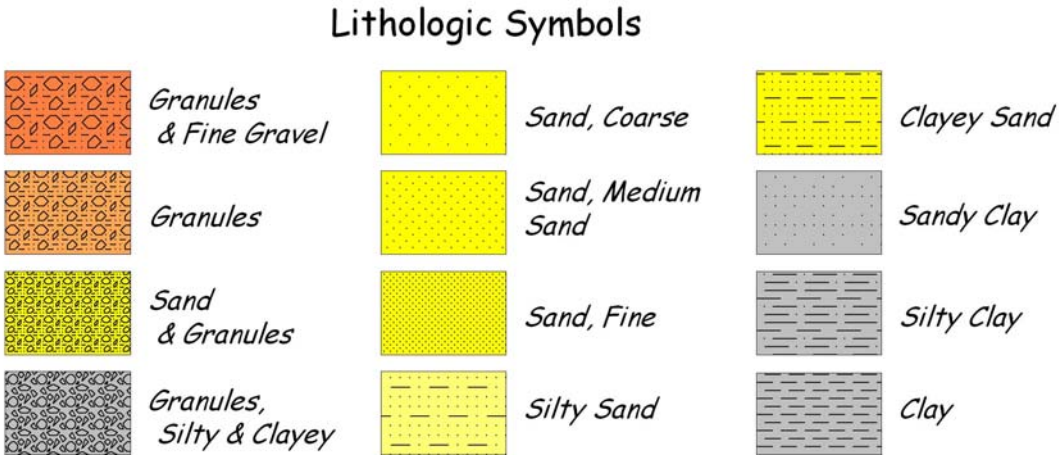

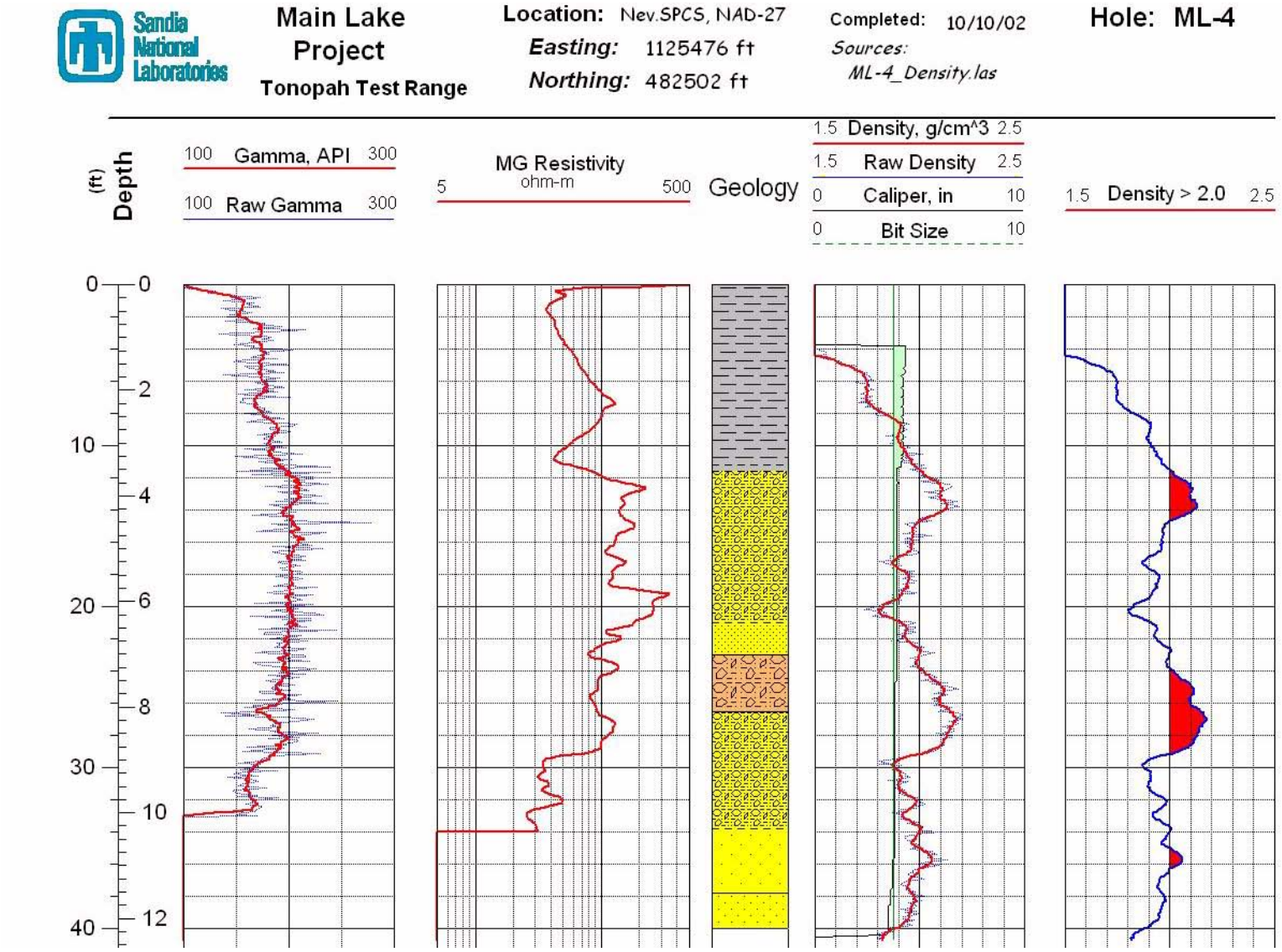

Figure C-1 Geophysical logs for drill hole ML-4

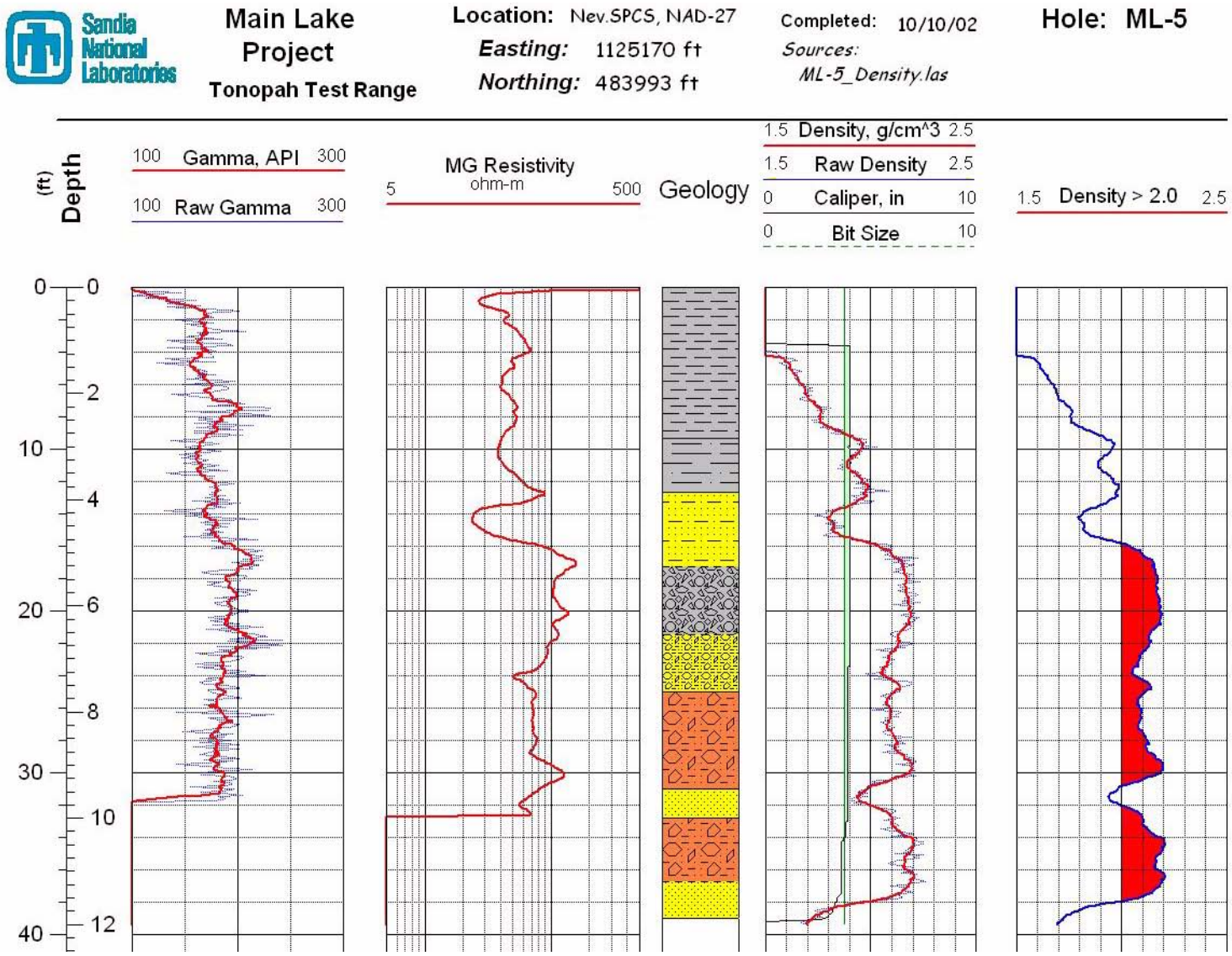

Figure C-2 Geophysical logs for drill hole ML-5

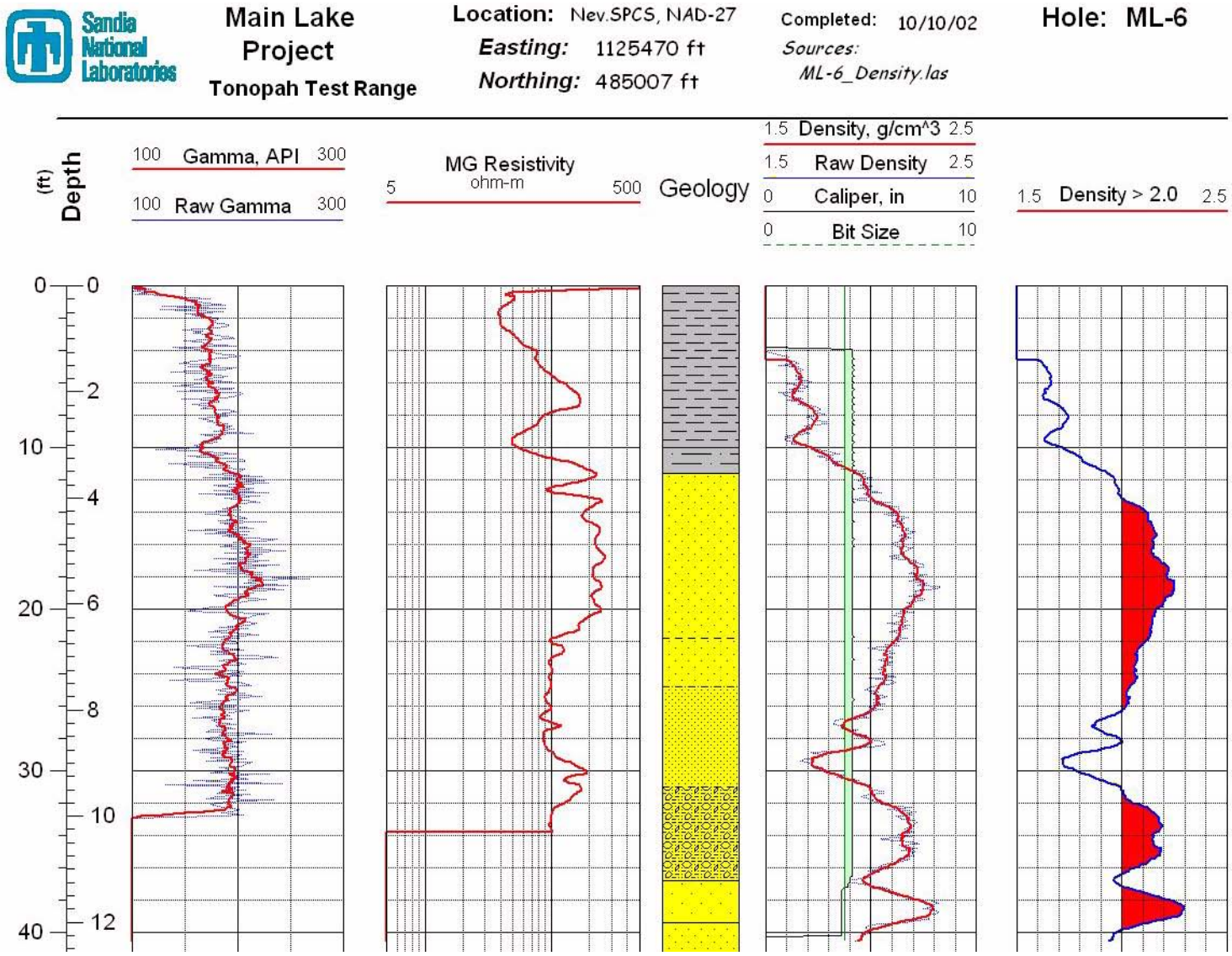

Figure C-3 Geophysical logs for drill hole ML-6

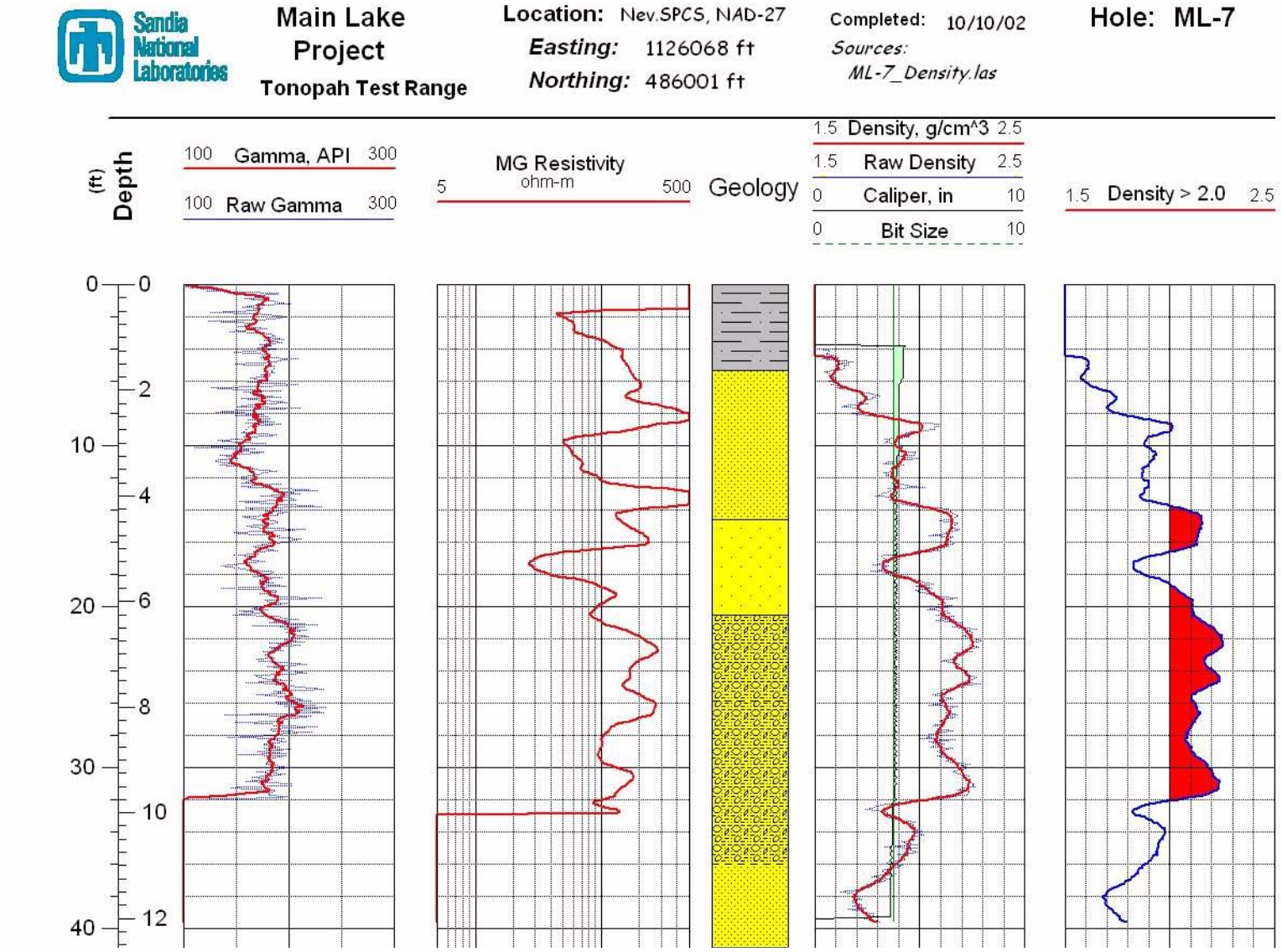

Figure C-4 Geophysical logs for drill hole ML-7

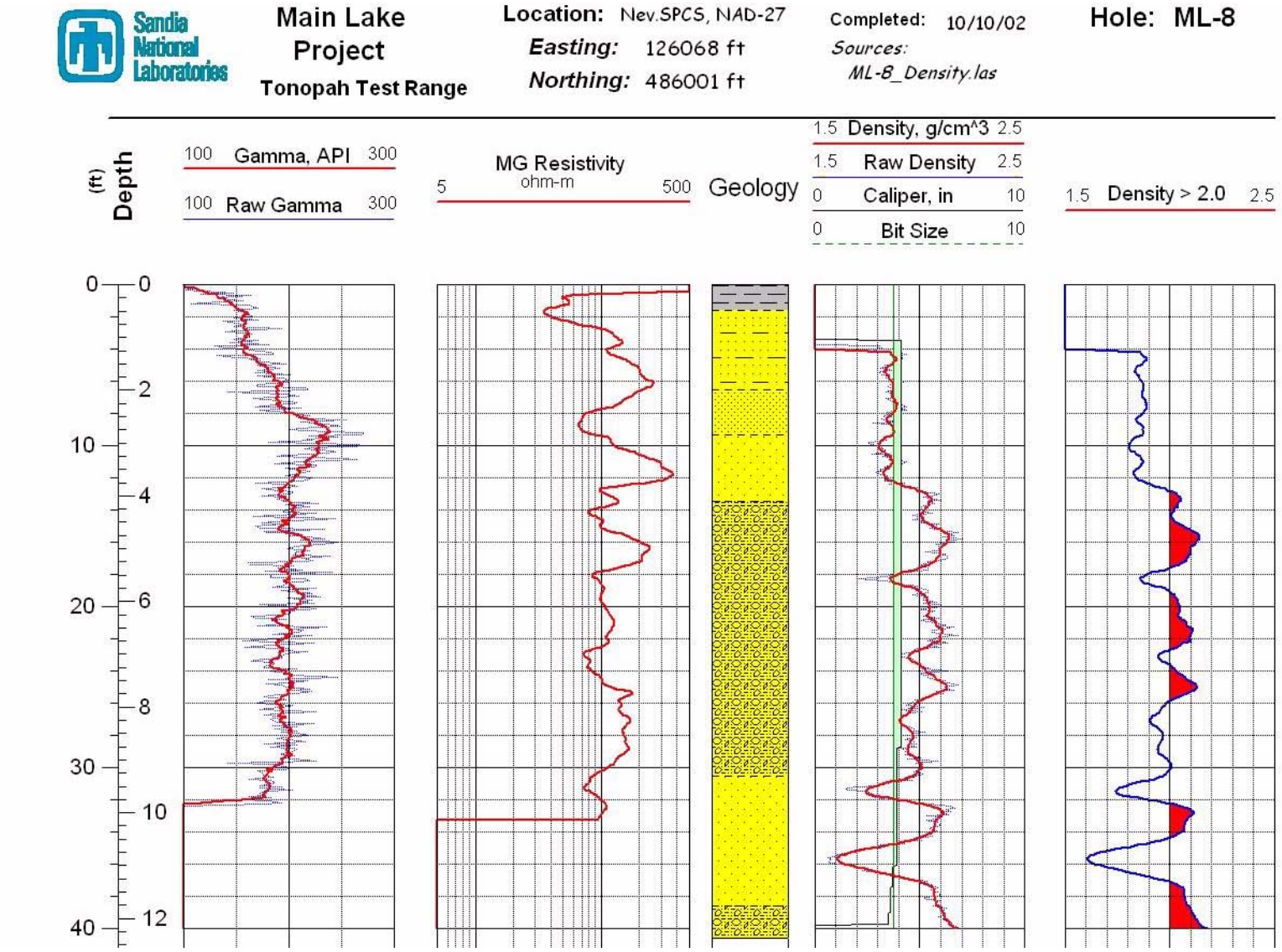

Figure C-5 Geophysical logs for drill hole ML-8

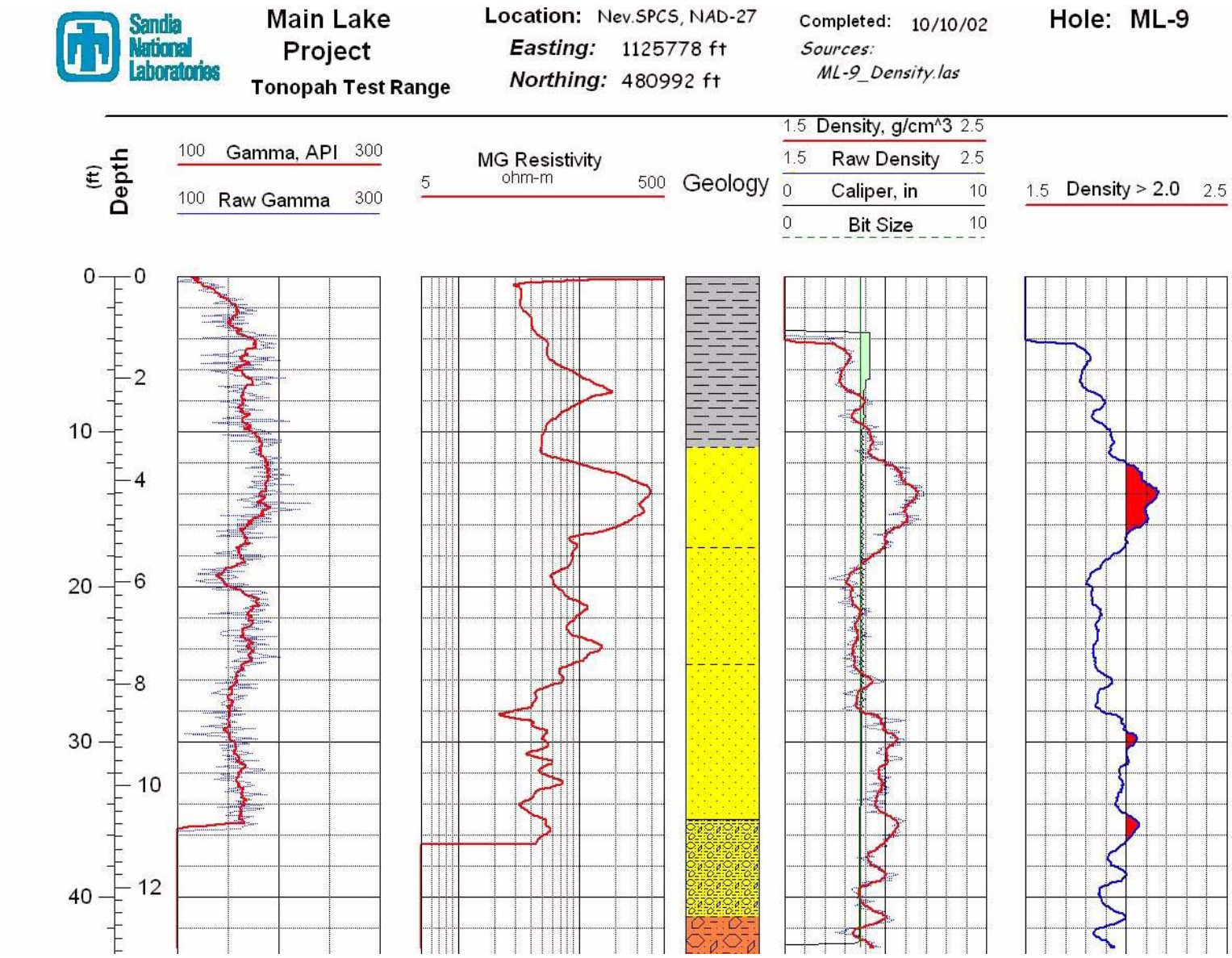

Figure C-6 Geophysical logs for drill hole ML-9

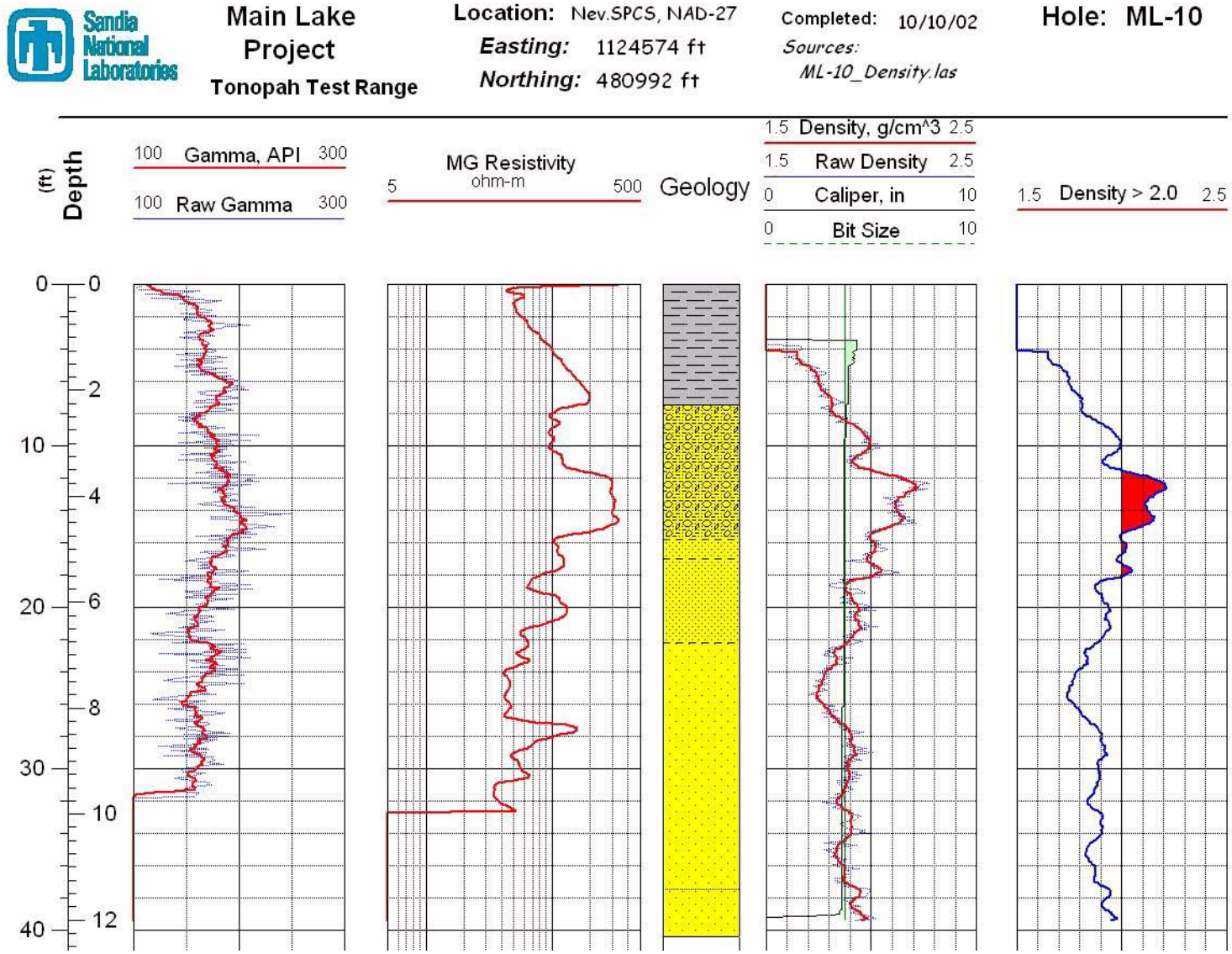

Figure C-7 Geophysical logs for drill hole ML-10

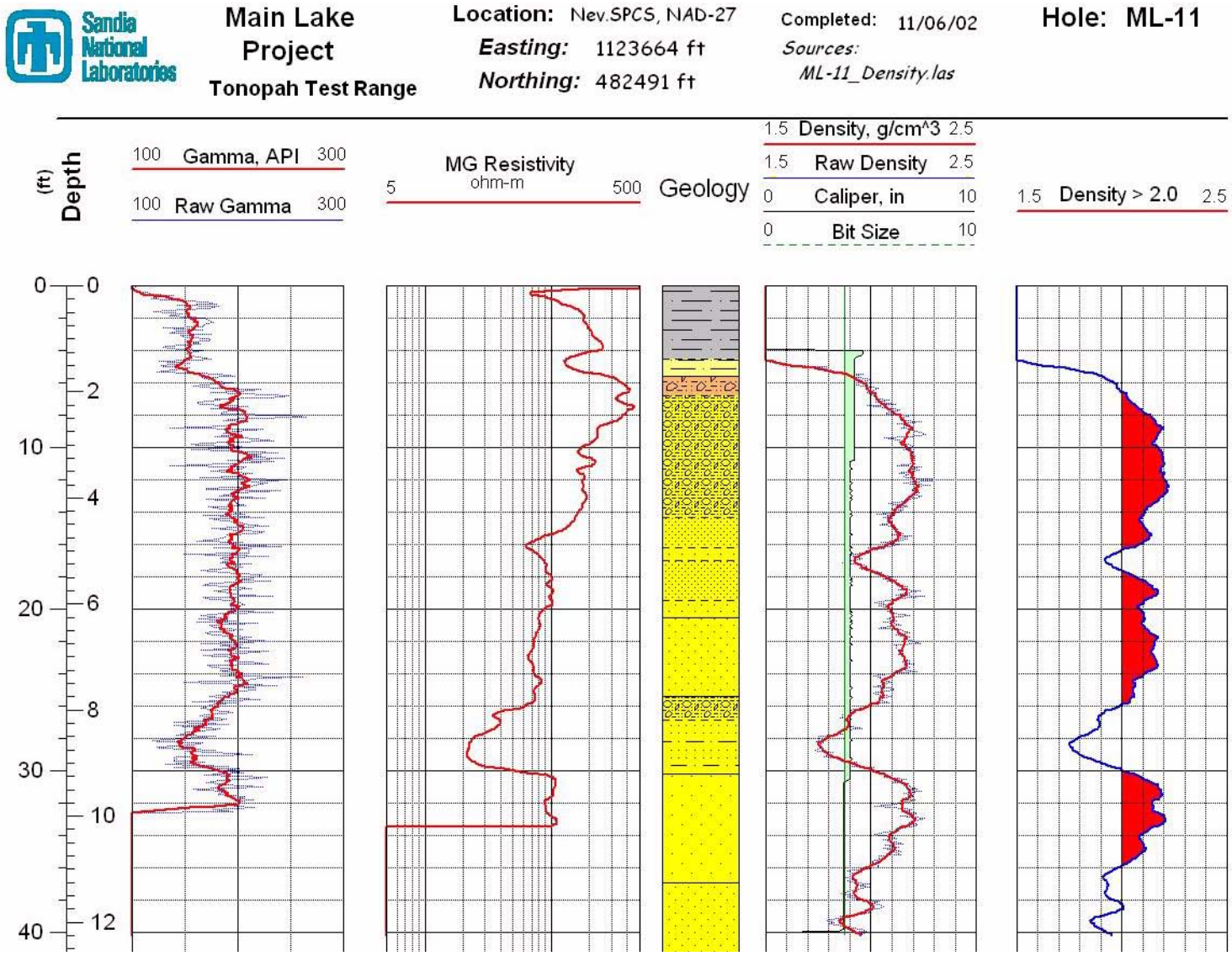

Figure C-8 Geophysical logs for drill hole ML-11

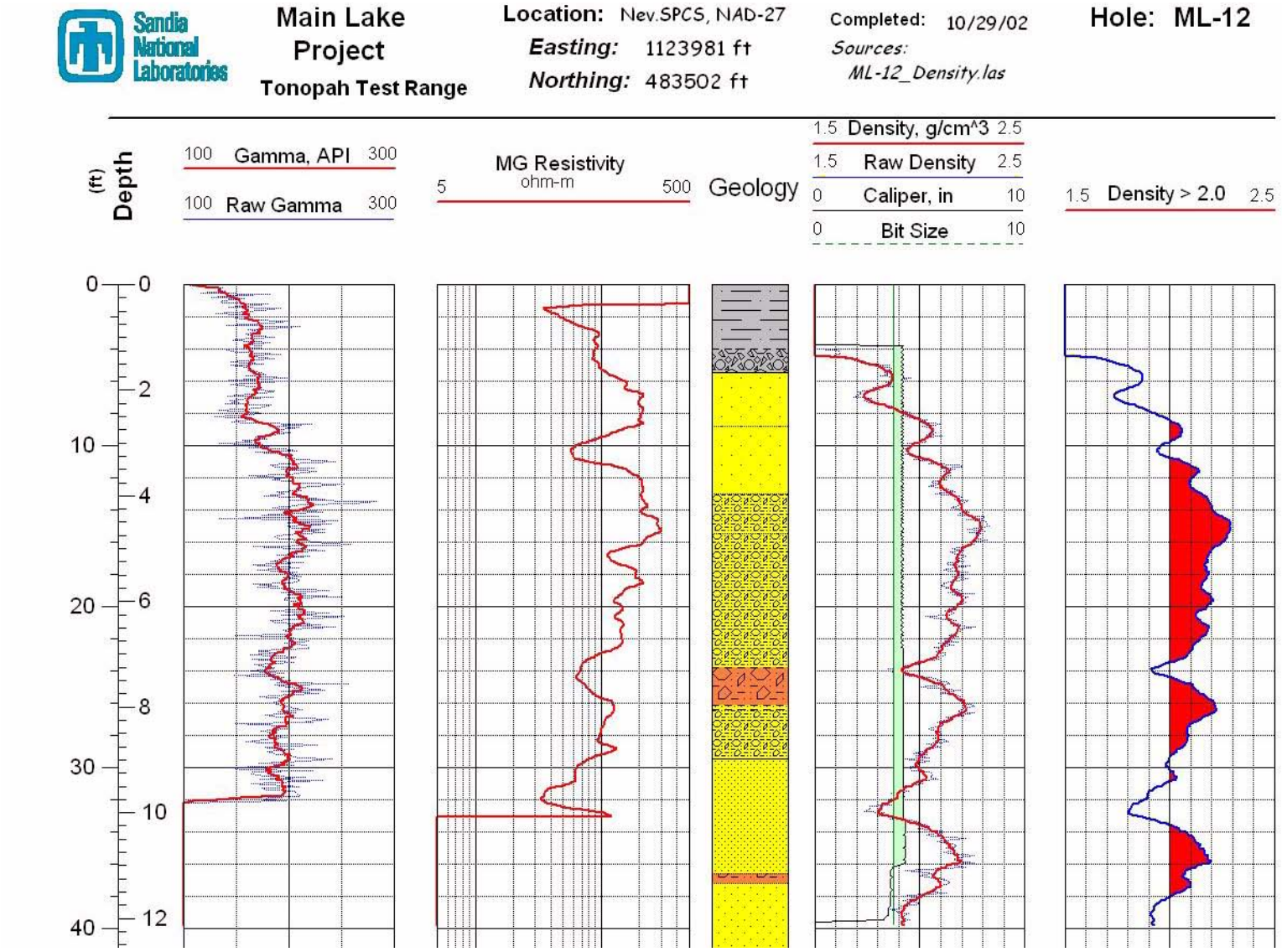

Figure C-9 Geophysical logs for drill hole ML-12

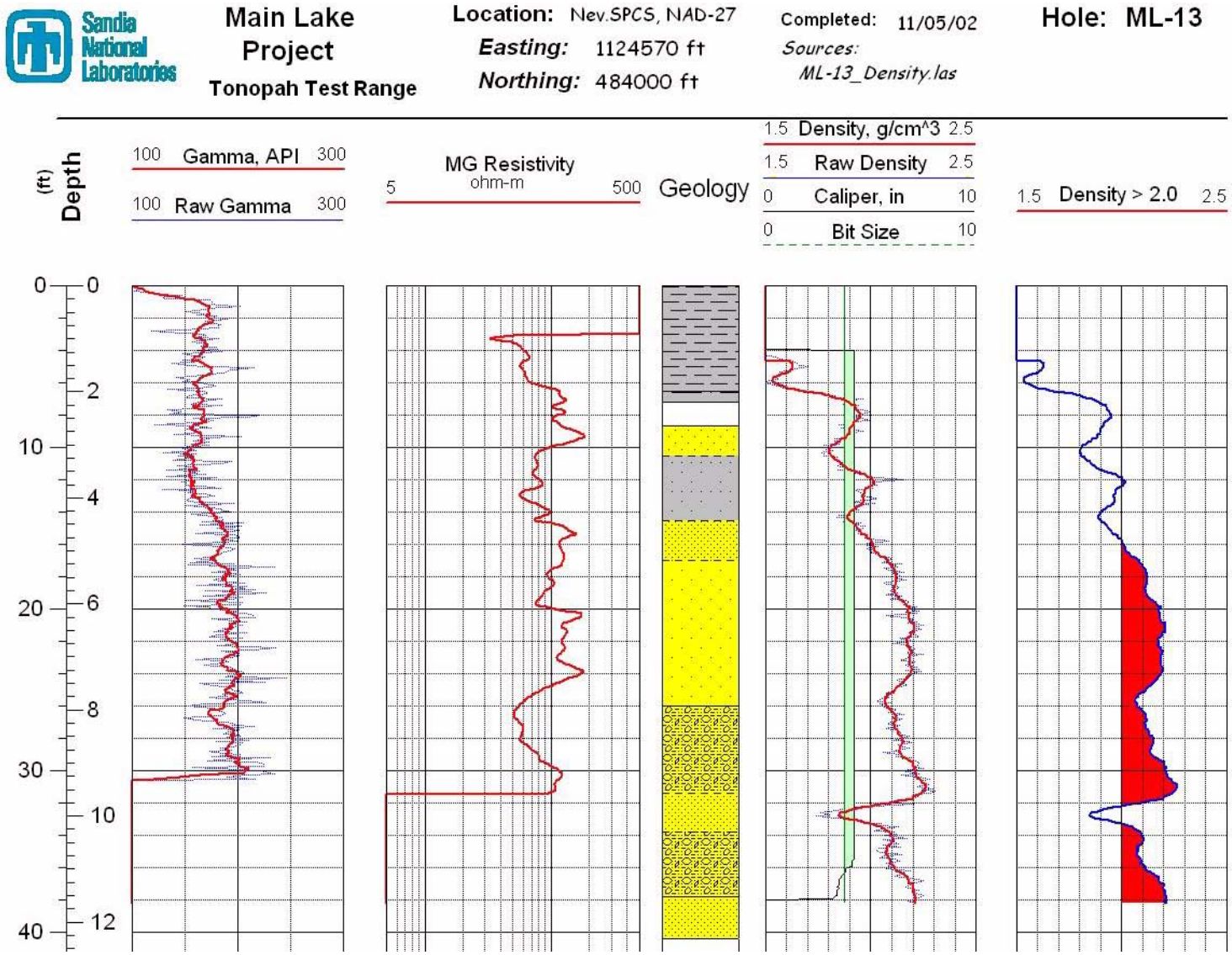

Figure C-10 Geophysical logs for drill hole ML-13

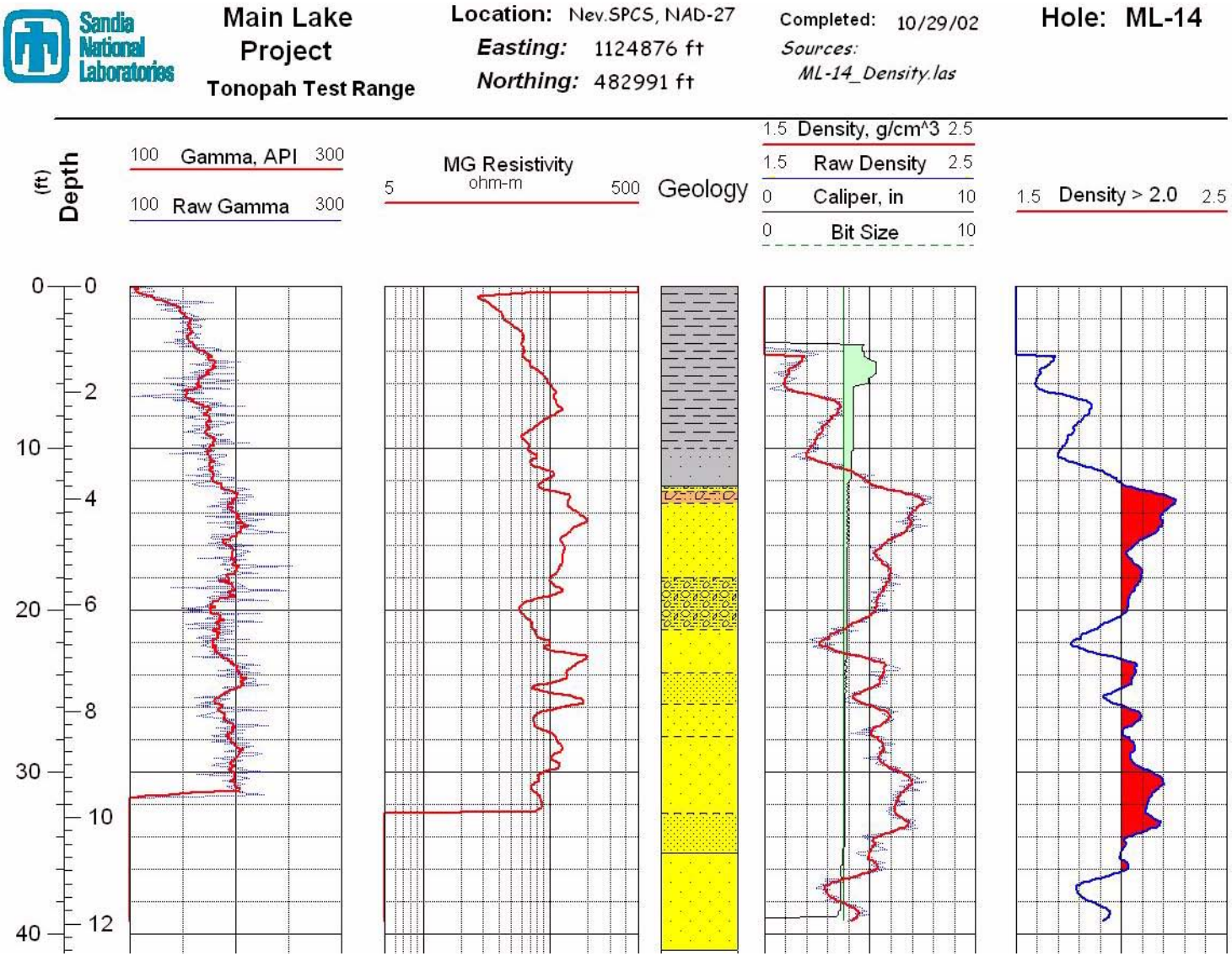

Figure C-11 Geophysical logs for drill hole ML-14

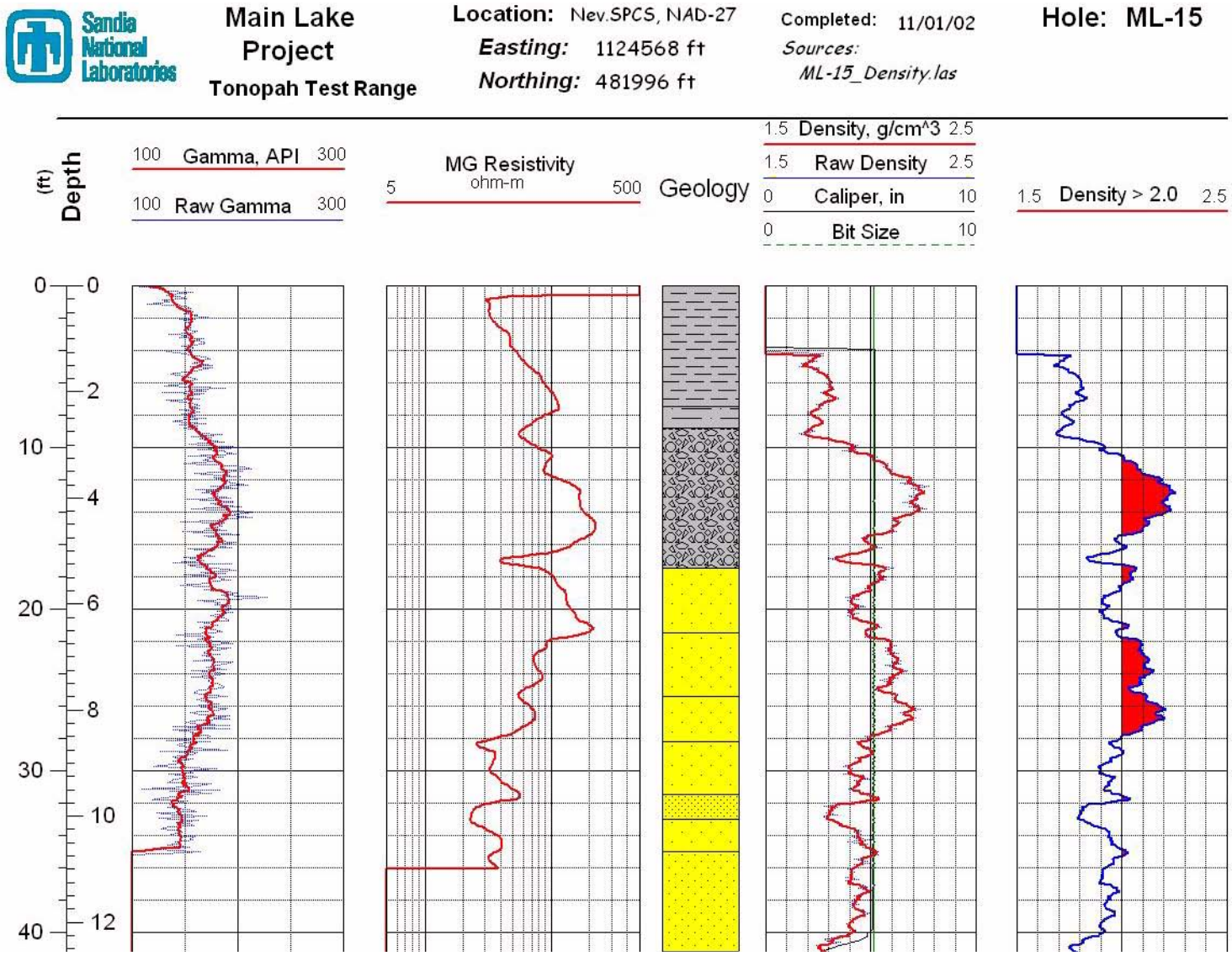

Figure C-12 Geophysical logs for drill hole ML-15

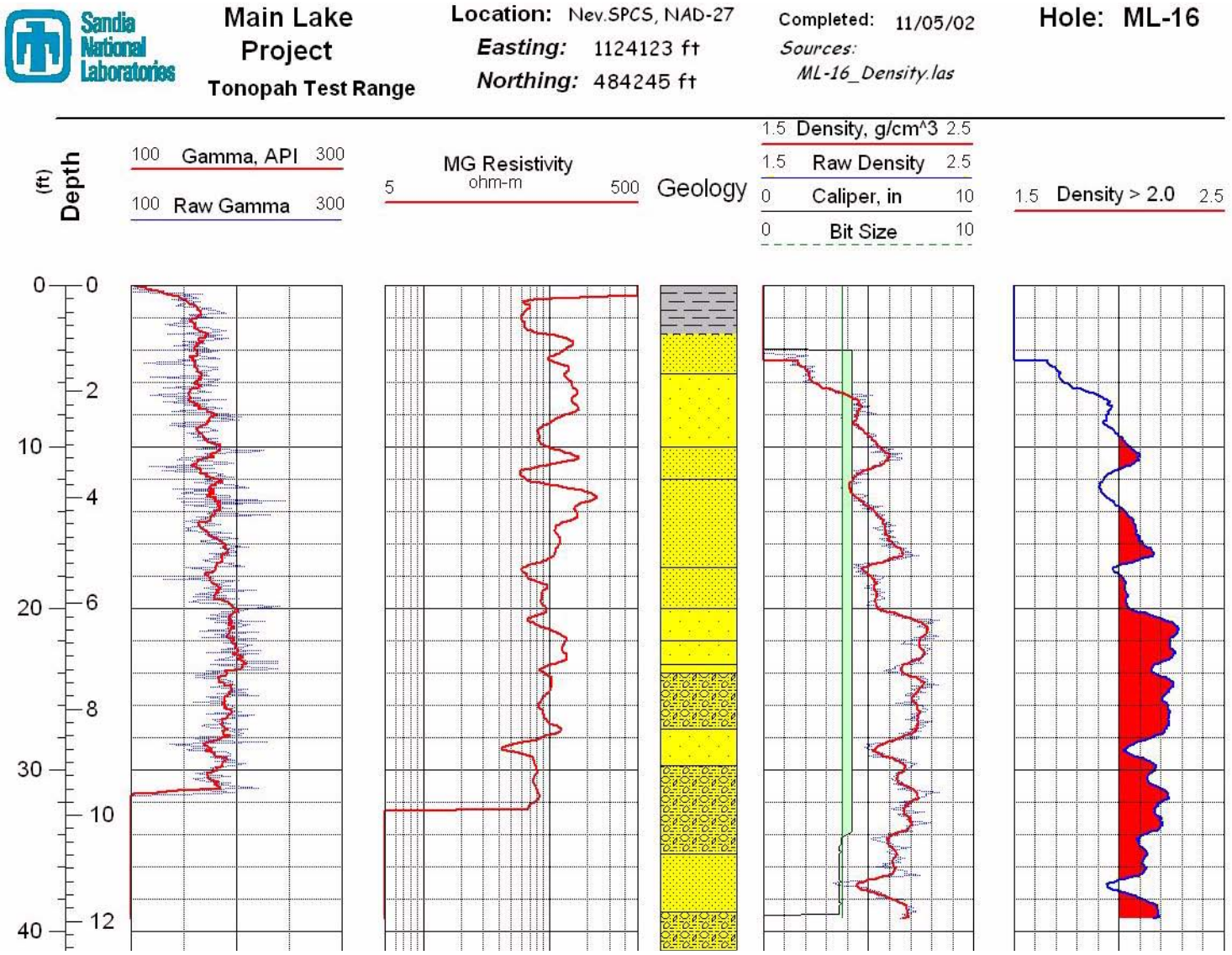

Figure C-13 Geophysical logs for drill hole ML-16

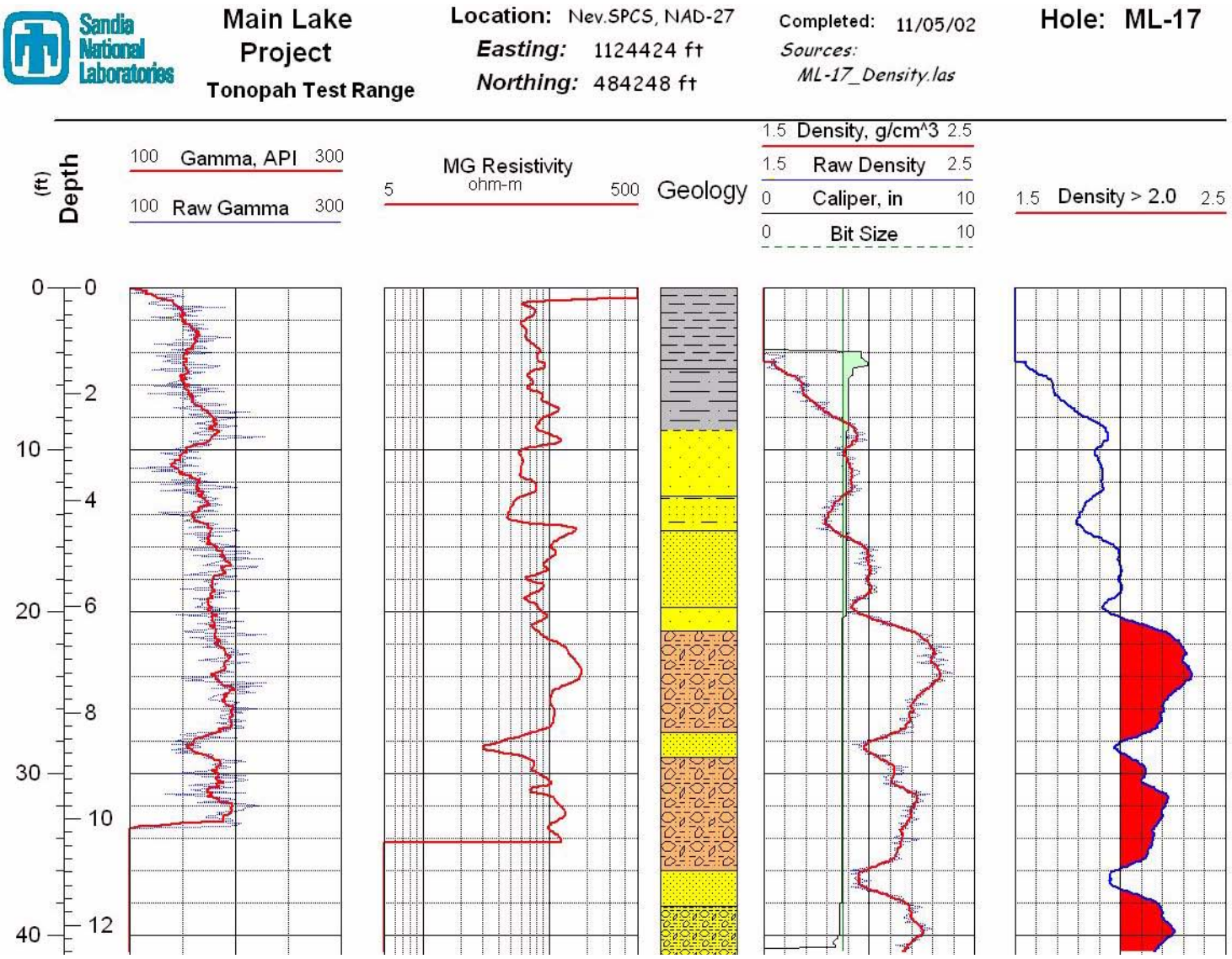

Figure C-14 Geophysical logs for drill hole ML-17

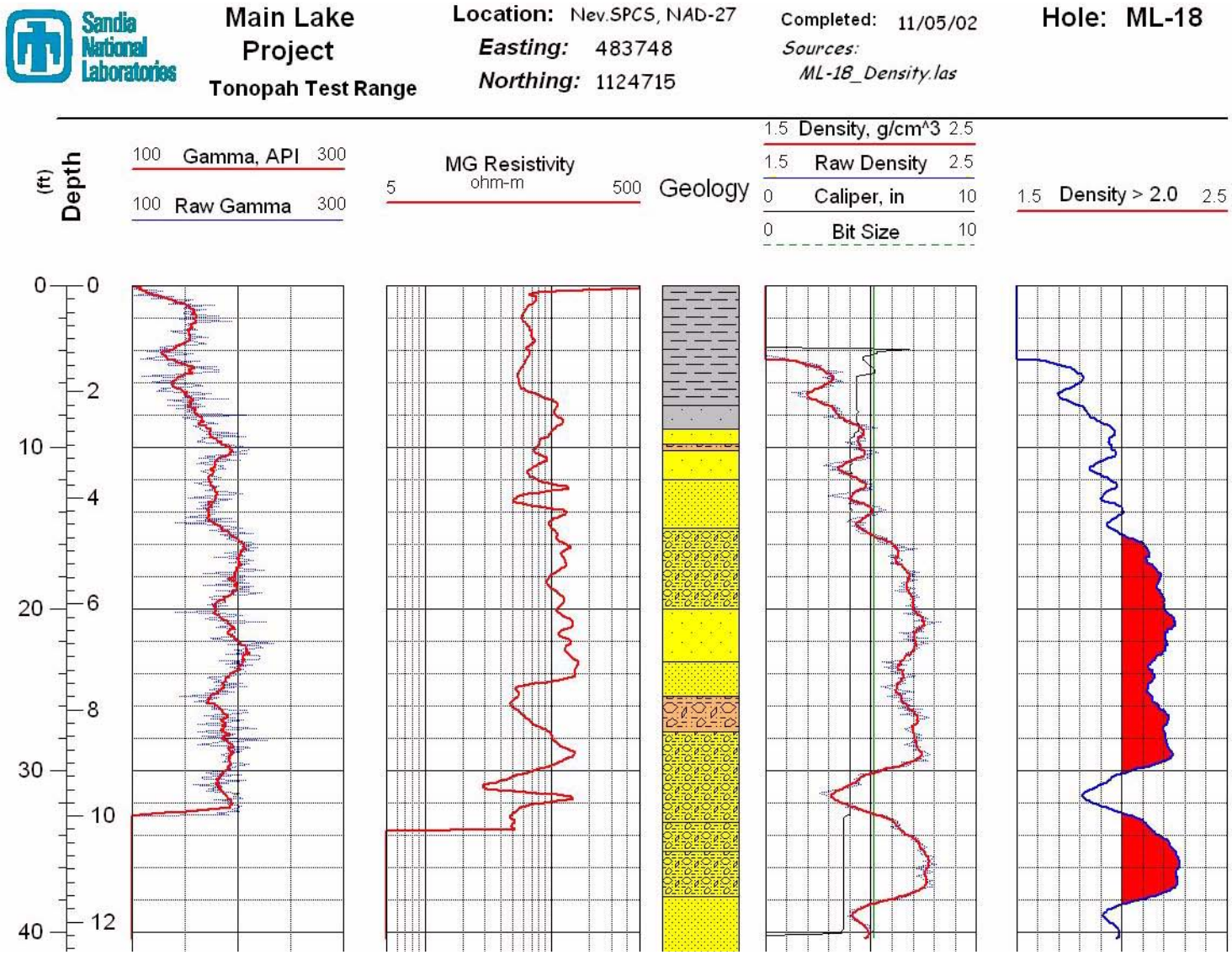

Figure C-15 Geophysical logs for drill hole ML-18

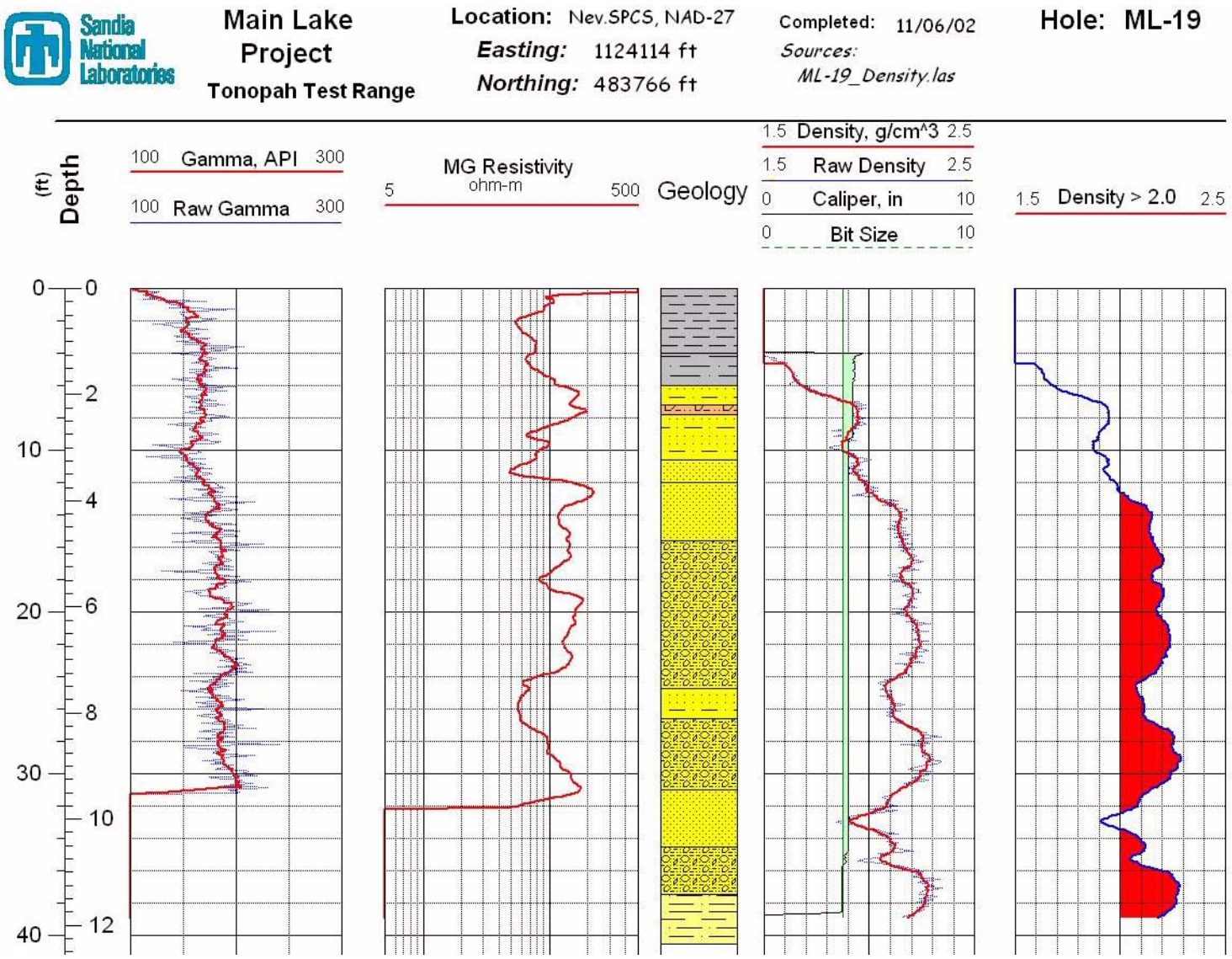

Figure C-16 Geophysical logs for drill hole ML-19

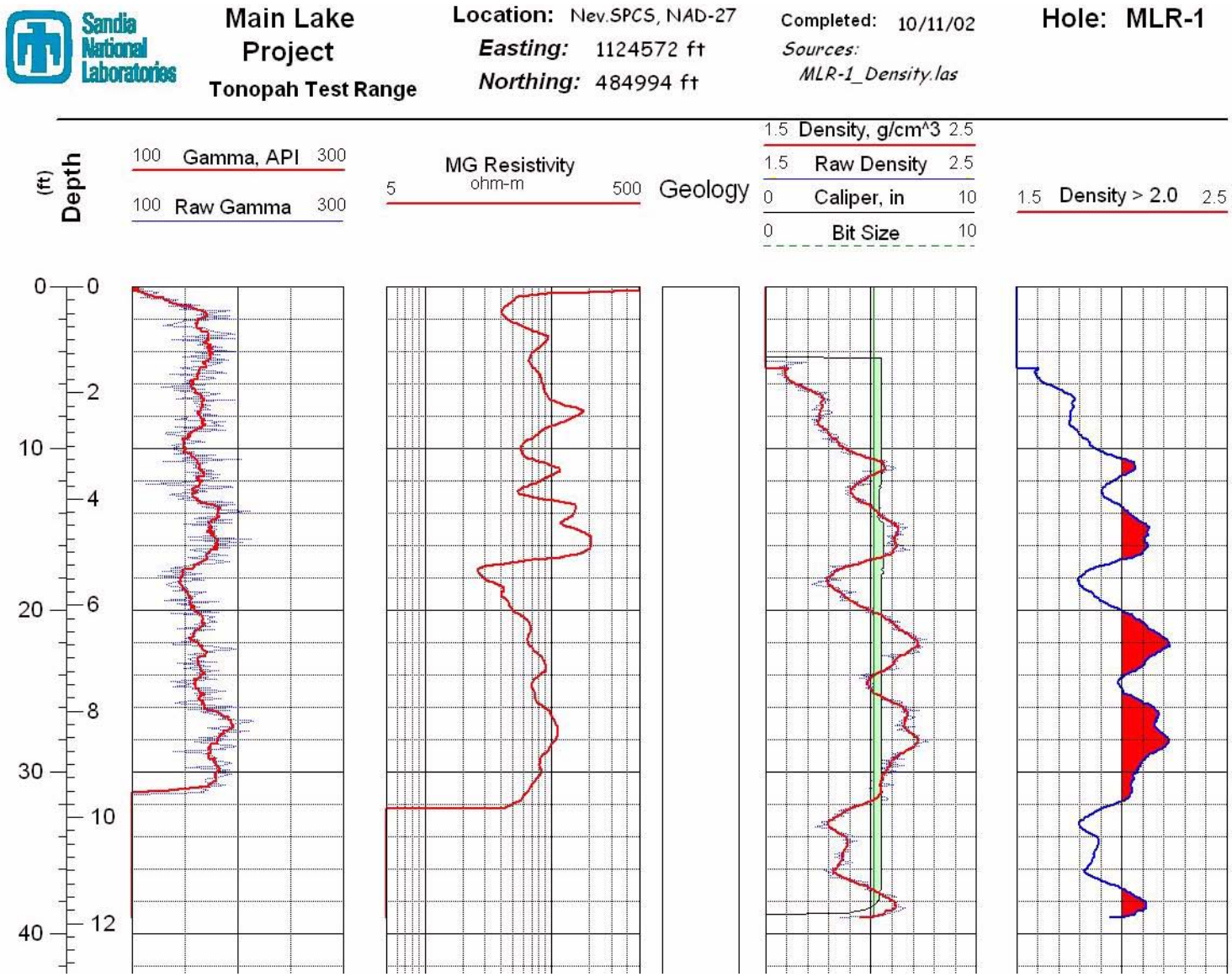

Figure C-17 Geophysical logs for drill hole MLR-1

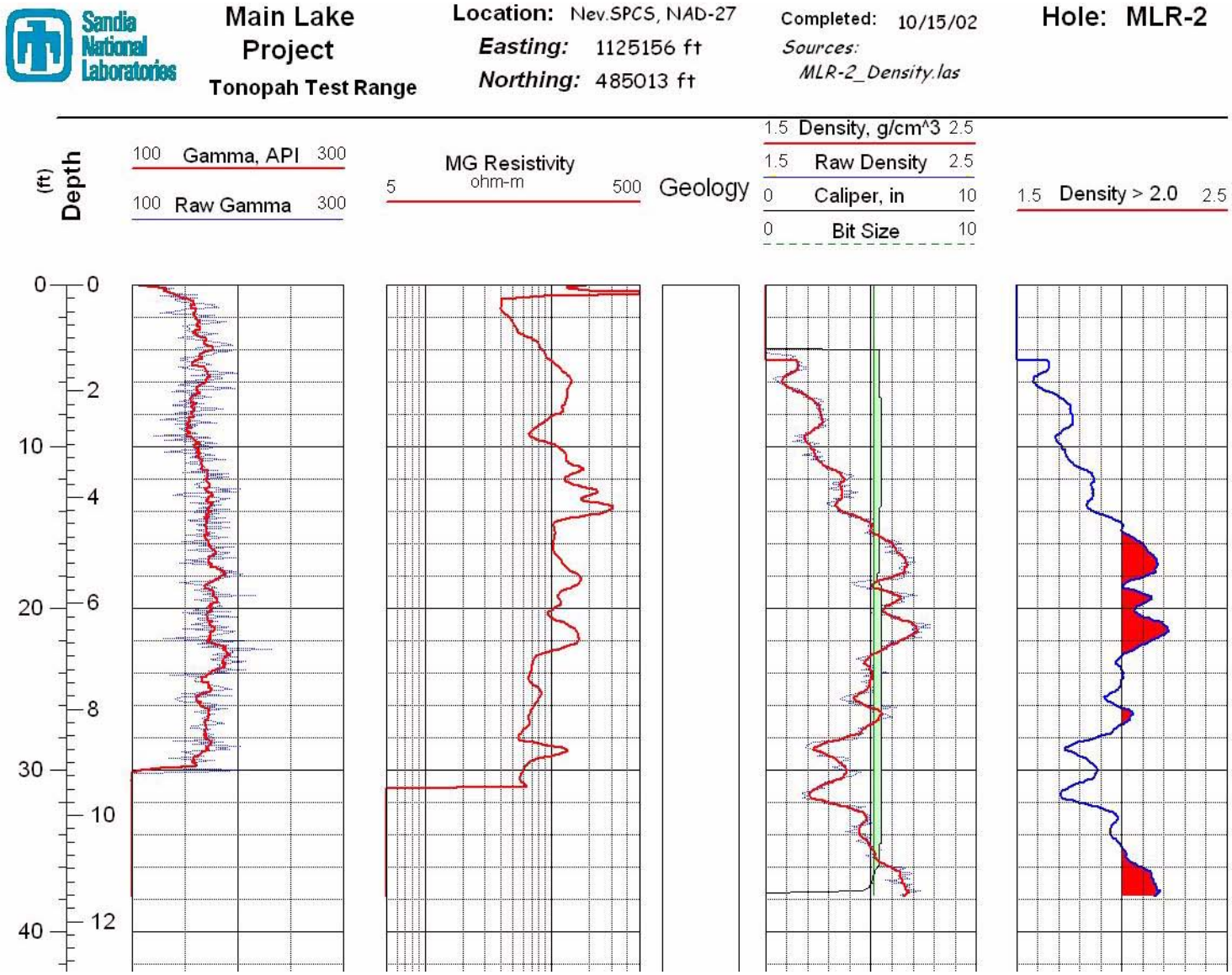

Figure C-18 Geophysical logs for drill hole MLR-2

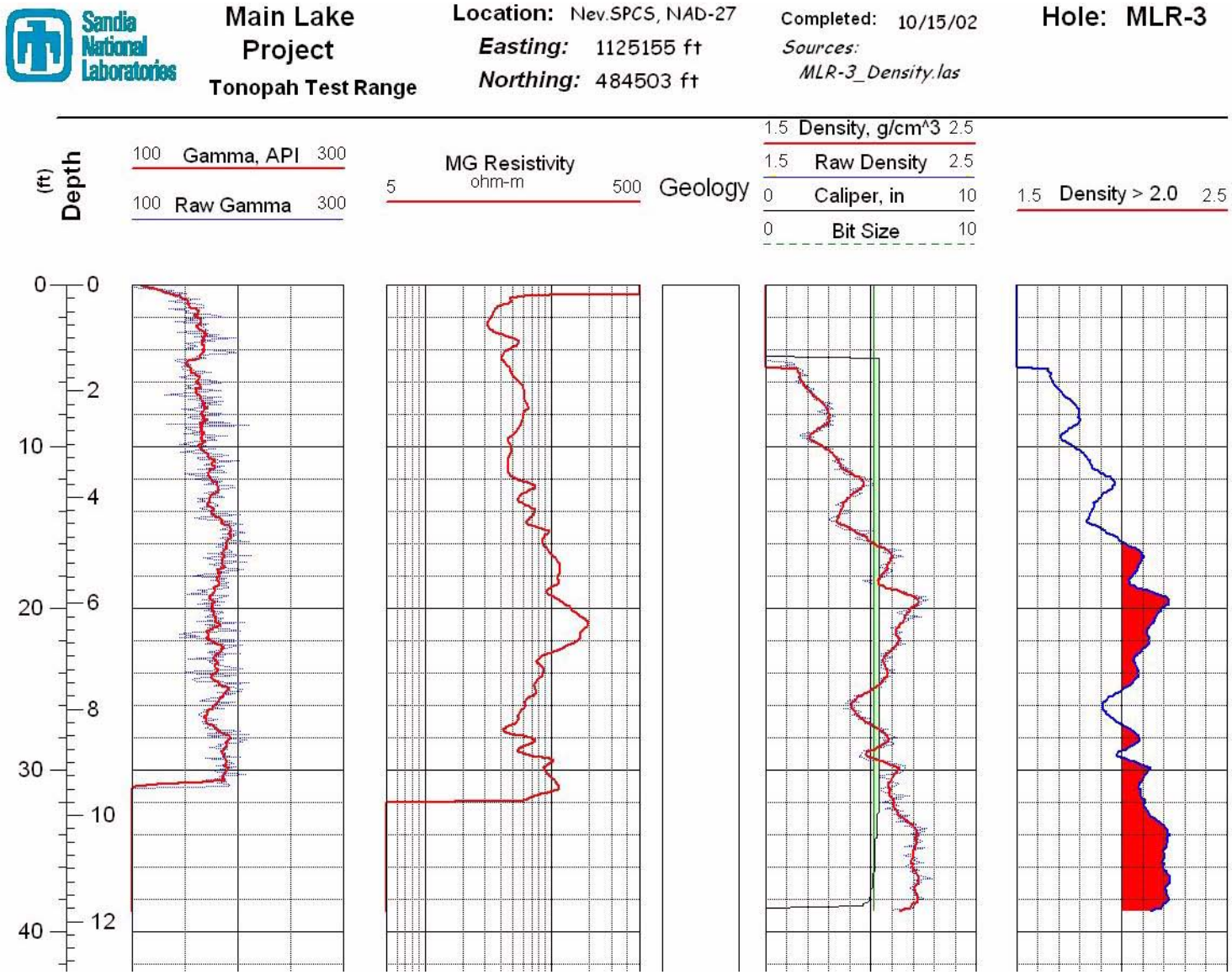

Figure C-19 Geophysical logs for drill hole MLR-3

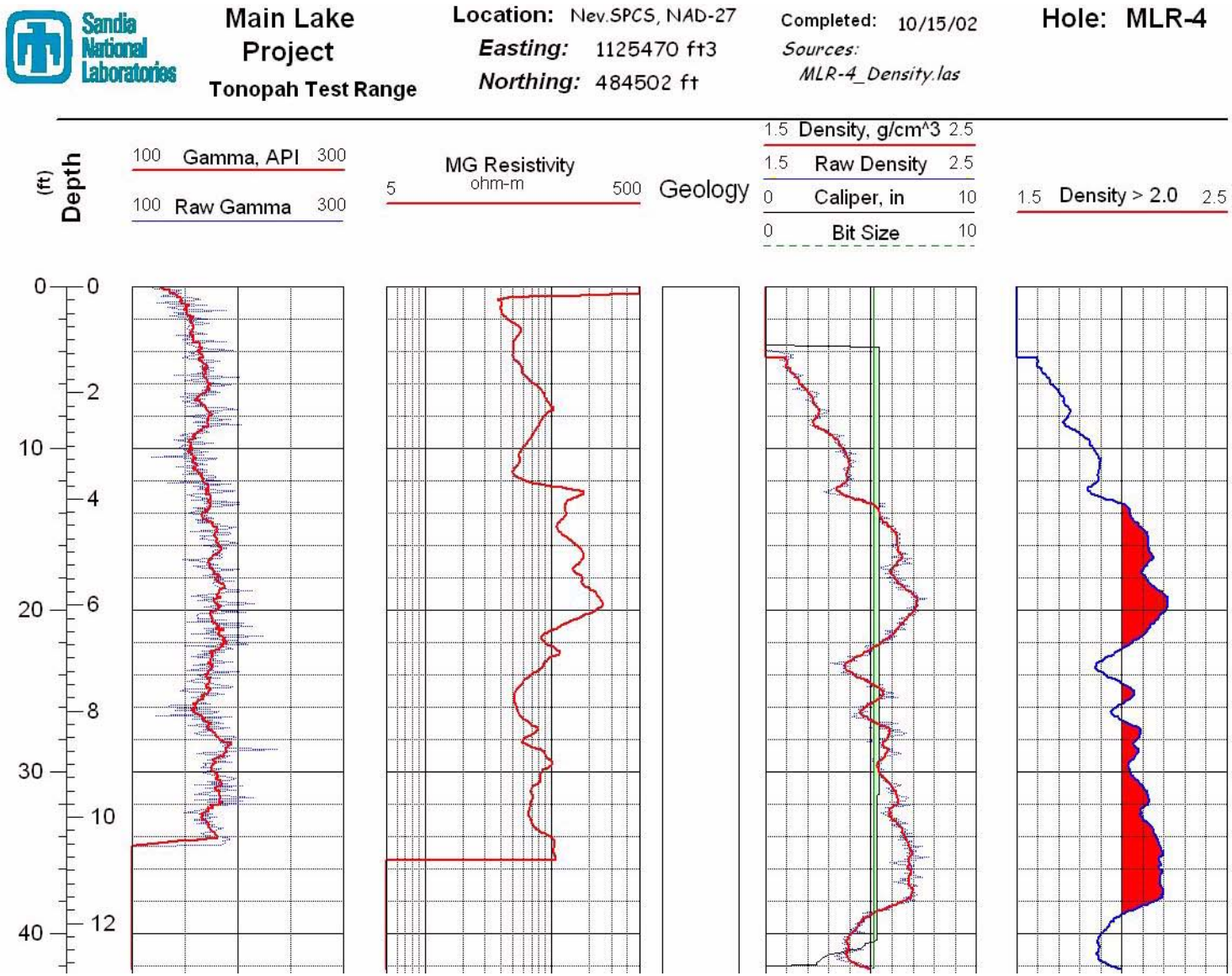

Figure C-20 Geophysical logs for drill hole MLR-4

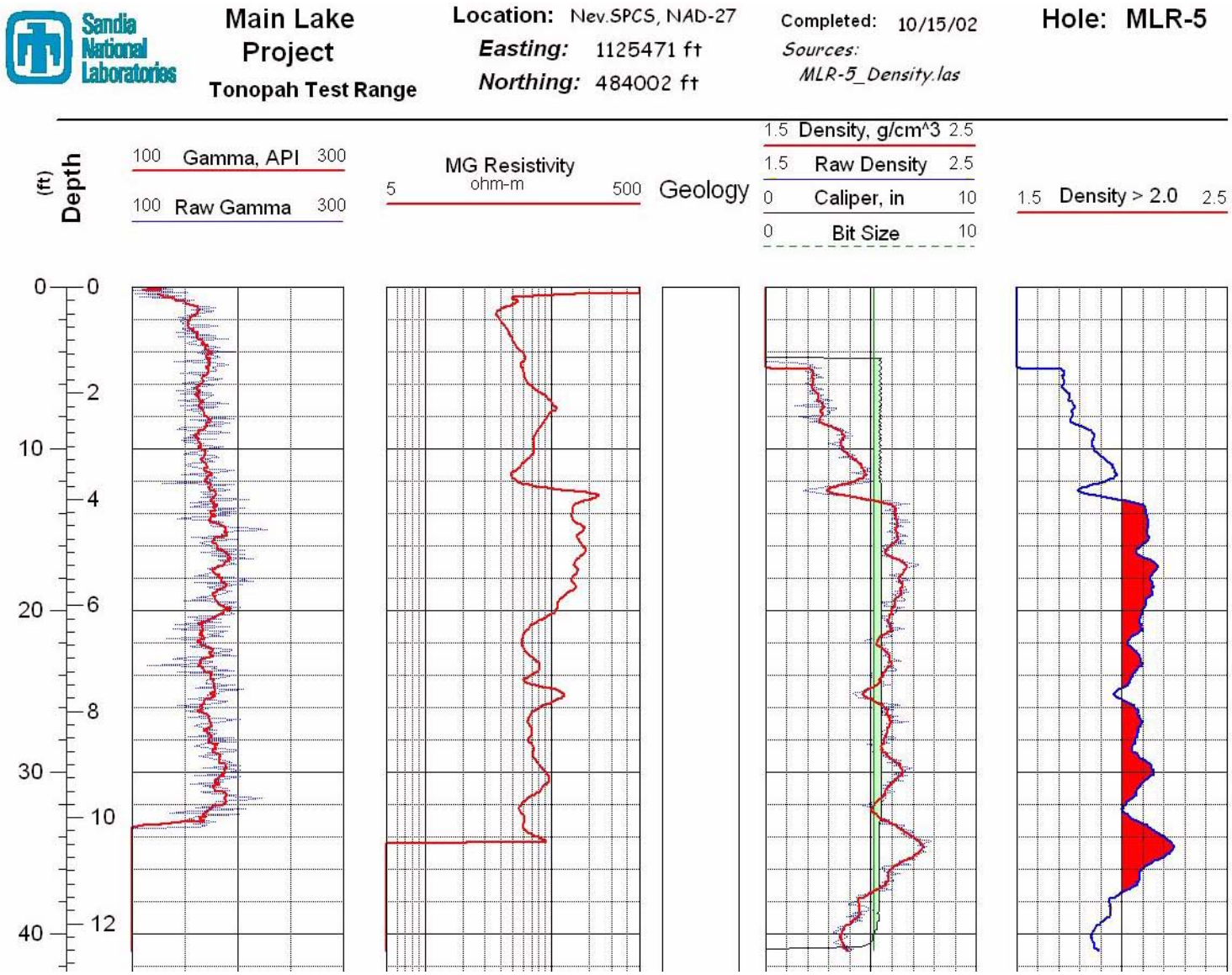

Figure C-21 Geophysical logs for drill hole MLR-5

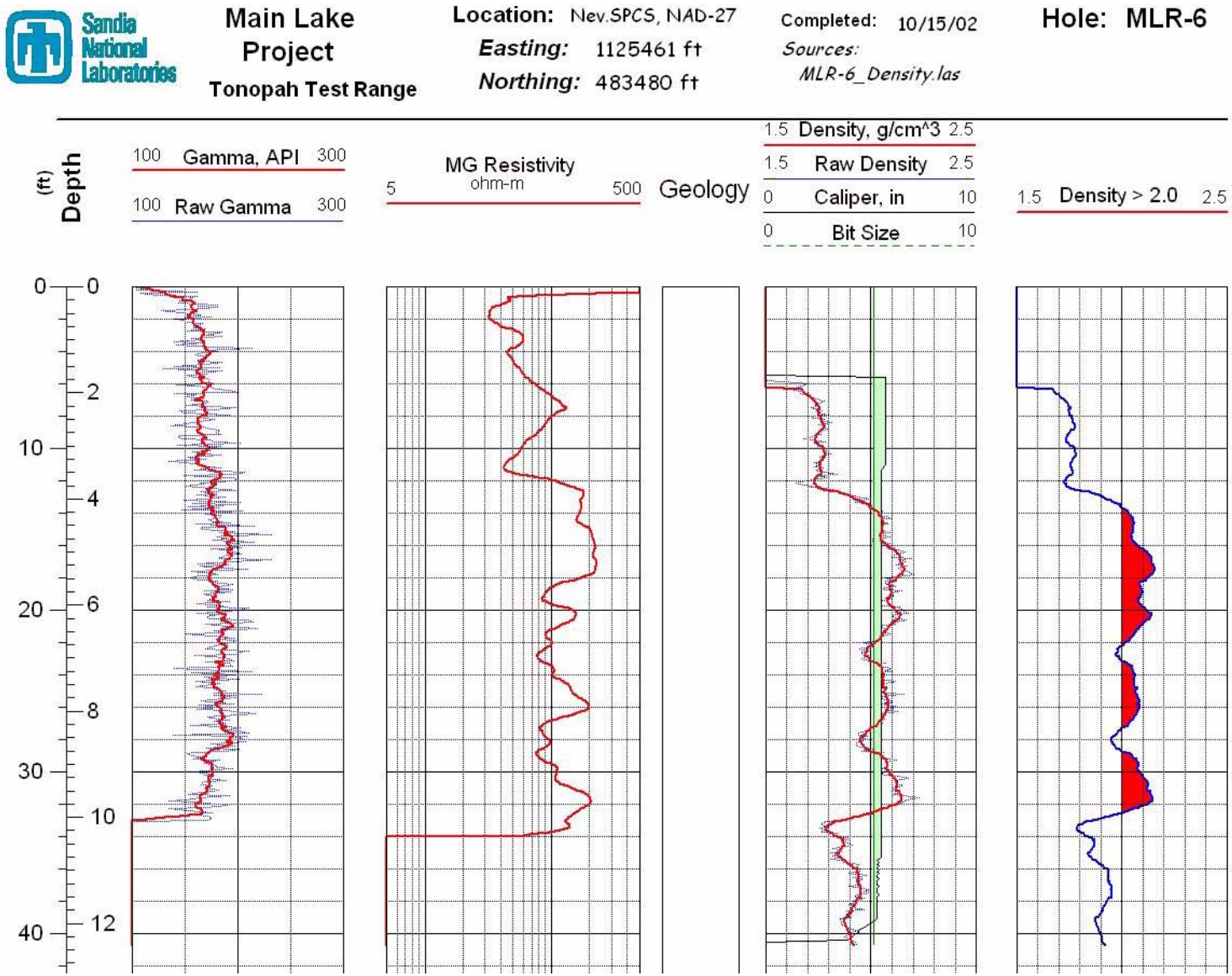

Figure C-22 Geophysical logs for drill hole MLR-6

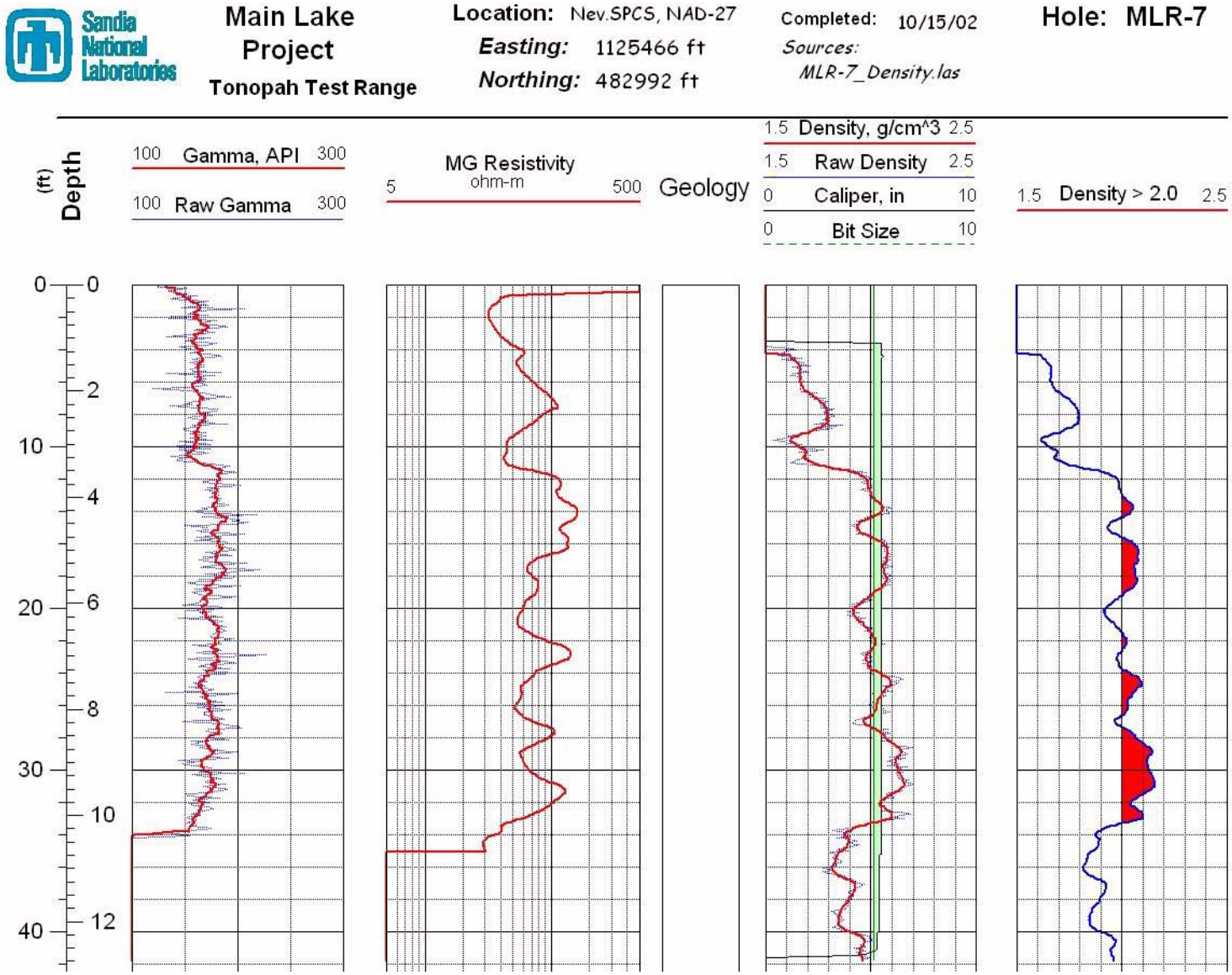

Figure C-23 Geophysical logs for drill hole MLR-7

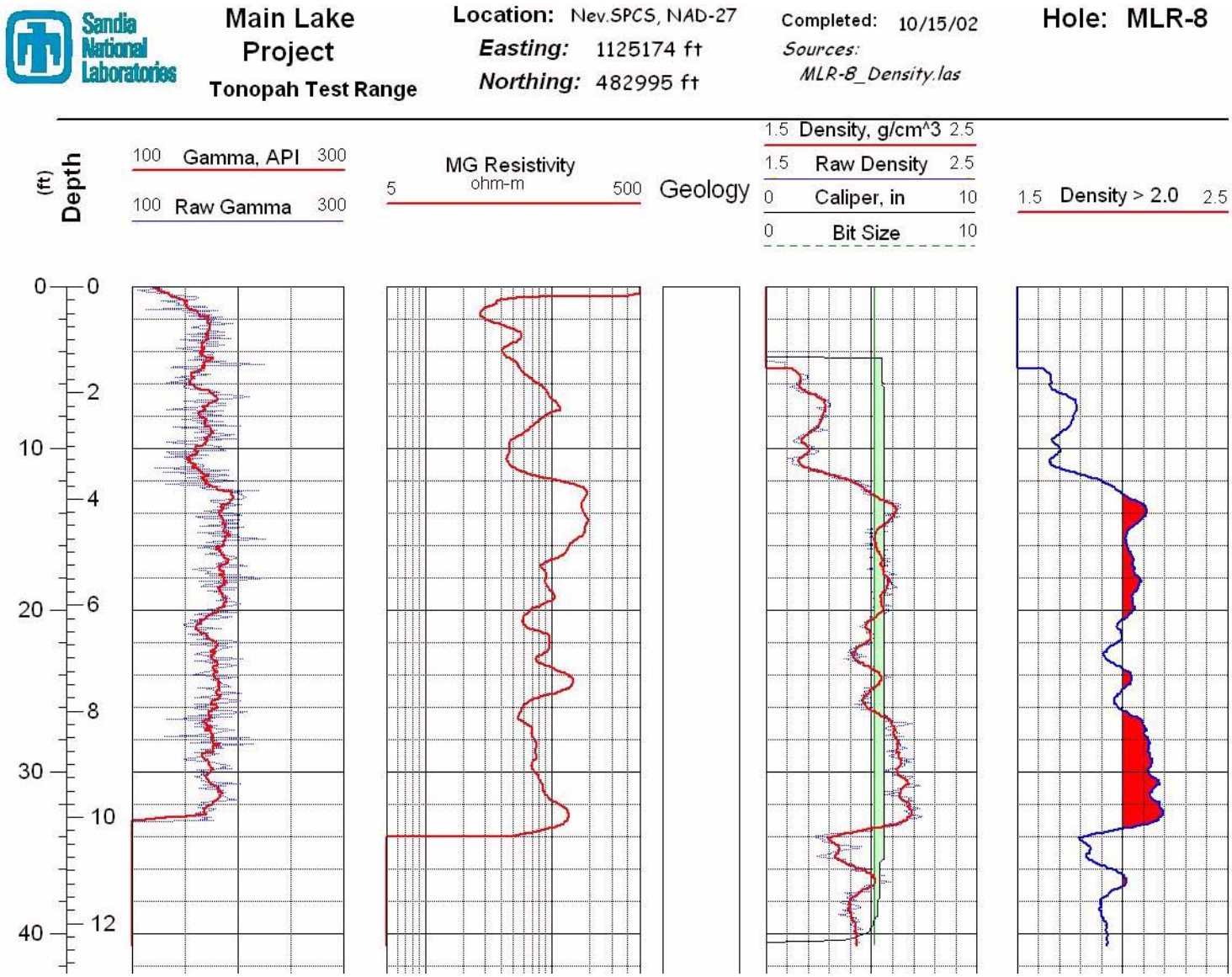

Figure C-24 Geophysical logs for drill hole MLR-8

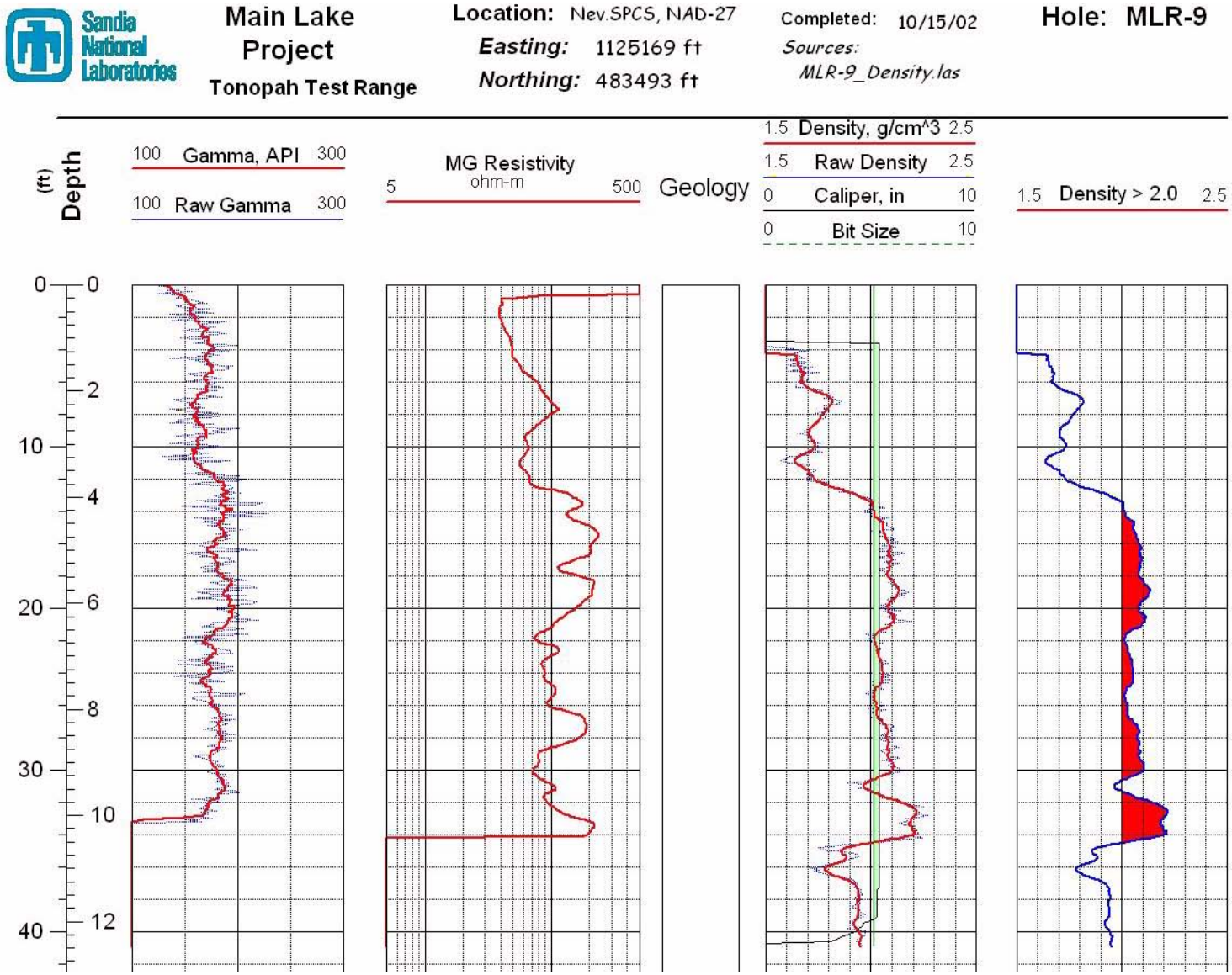

Figure C-25 Geophysical logs for drill hole MLR-9

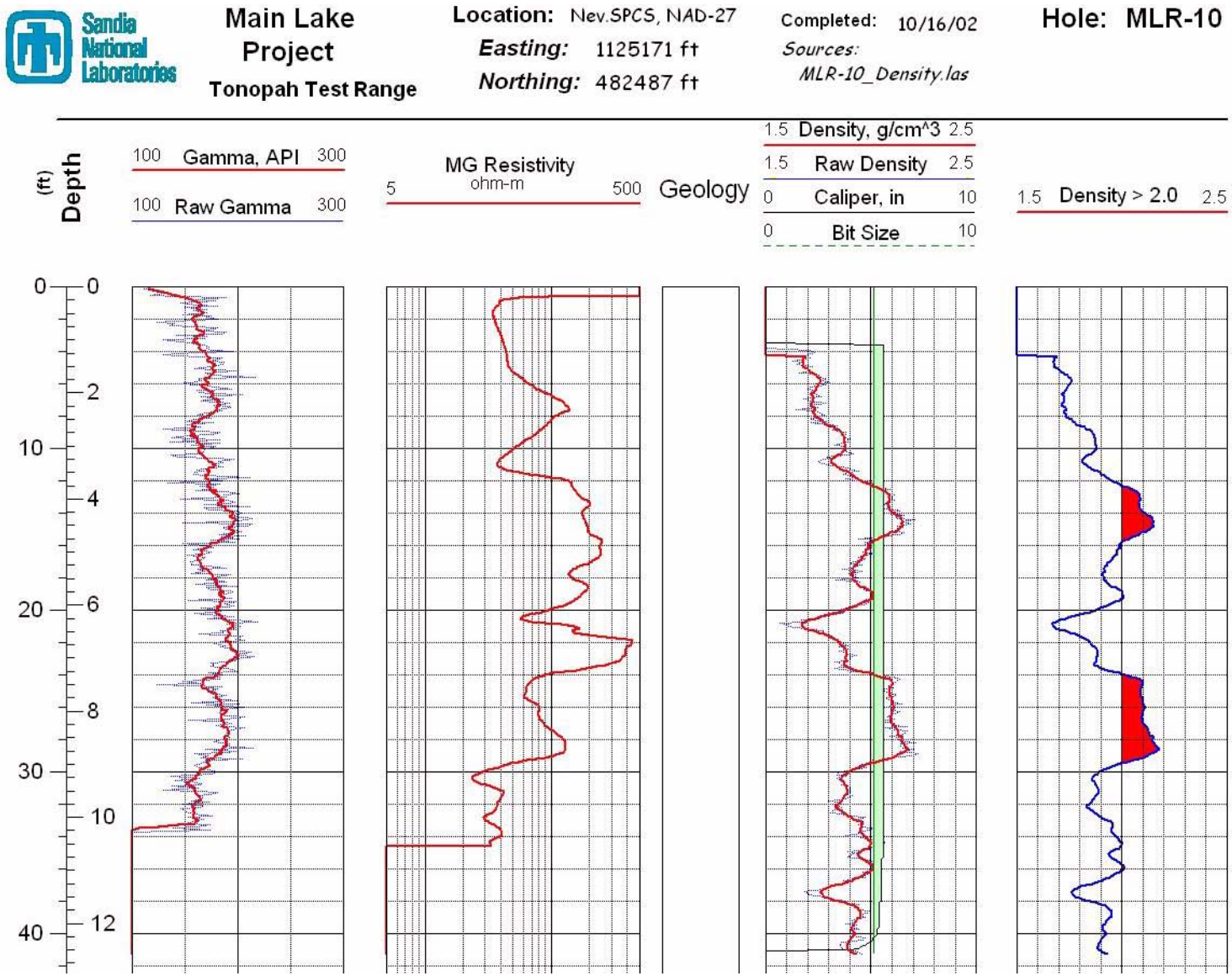

Figure C-26 Geophysical logs for drill hole MLR-10

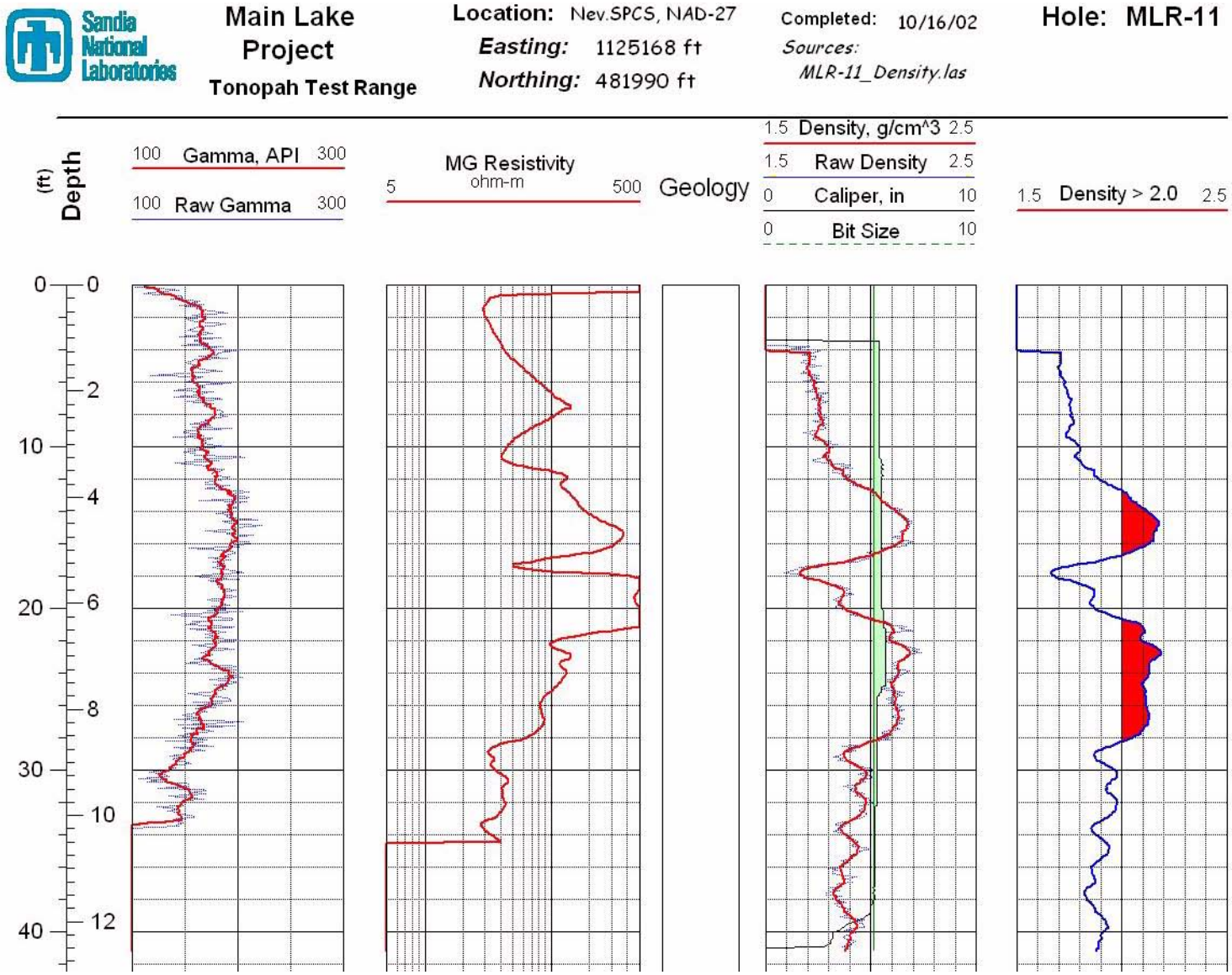

Figure C-27 Geophysical logs for drill hole MLR-11

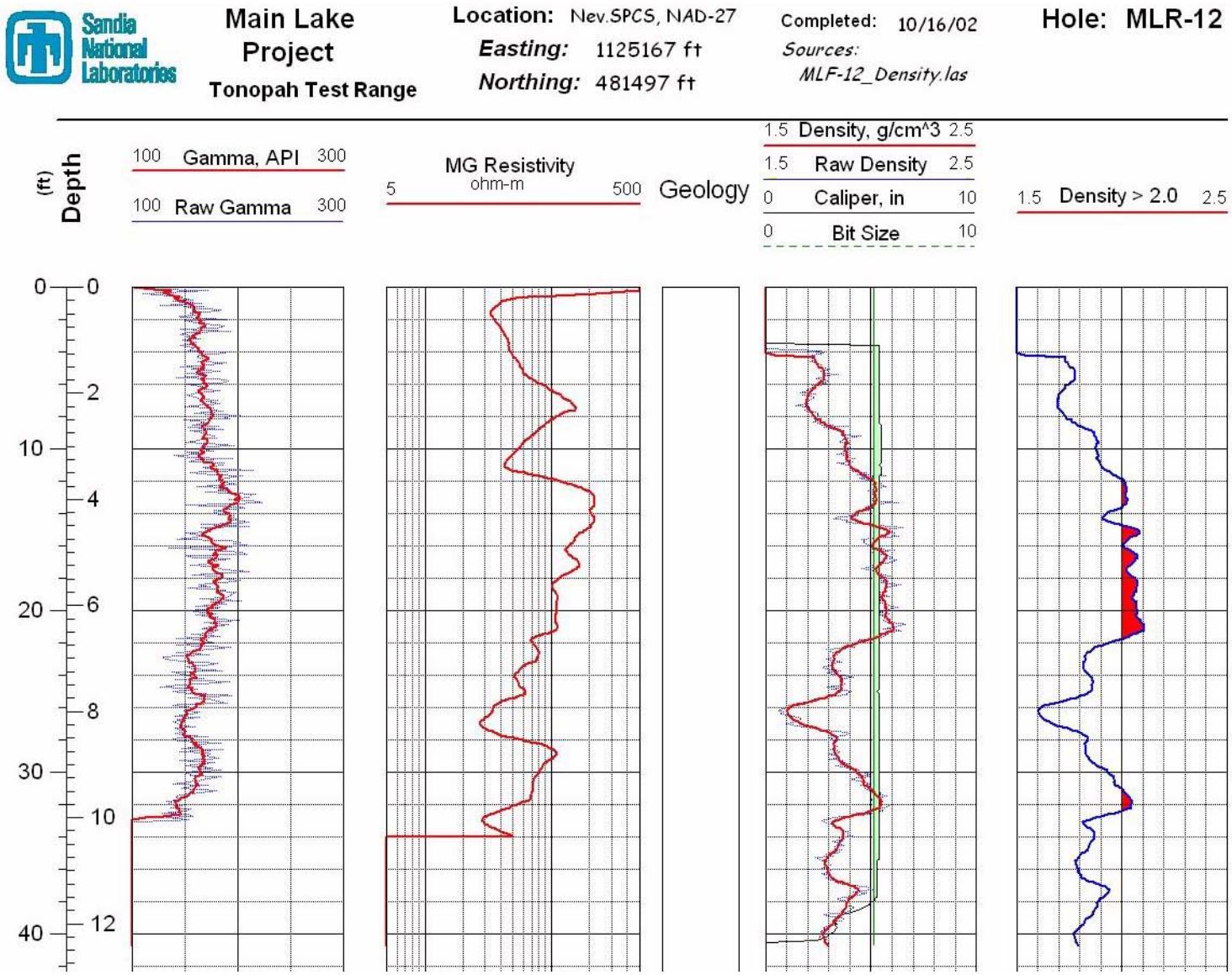

Figure C-28 Geophysical logs for drill hole MLR-12

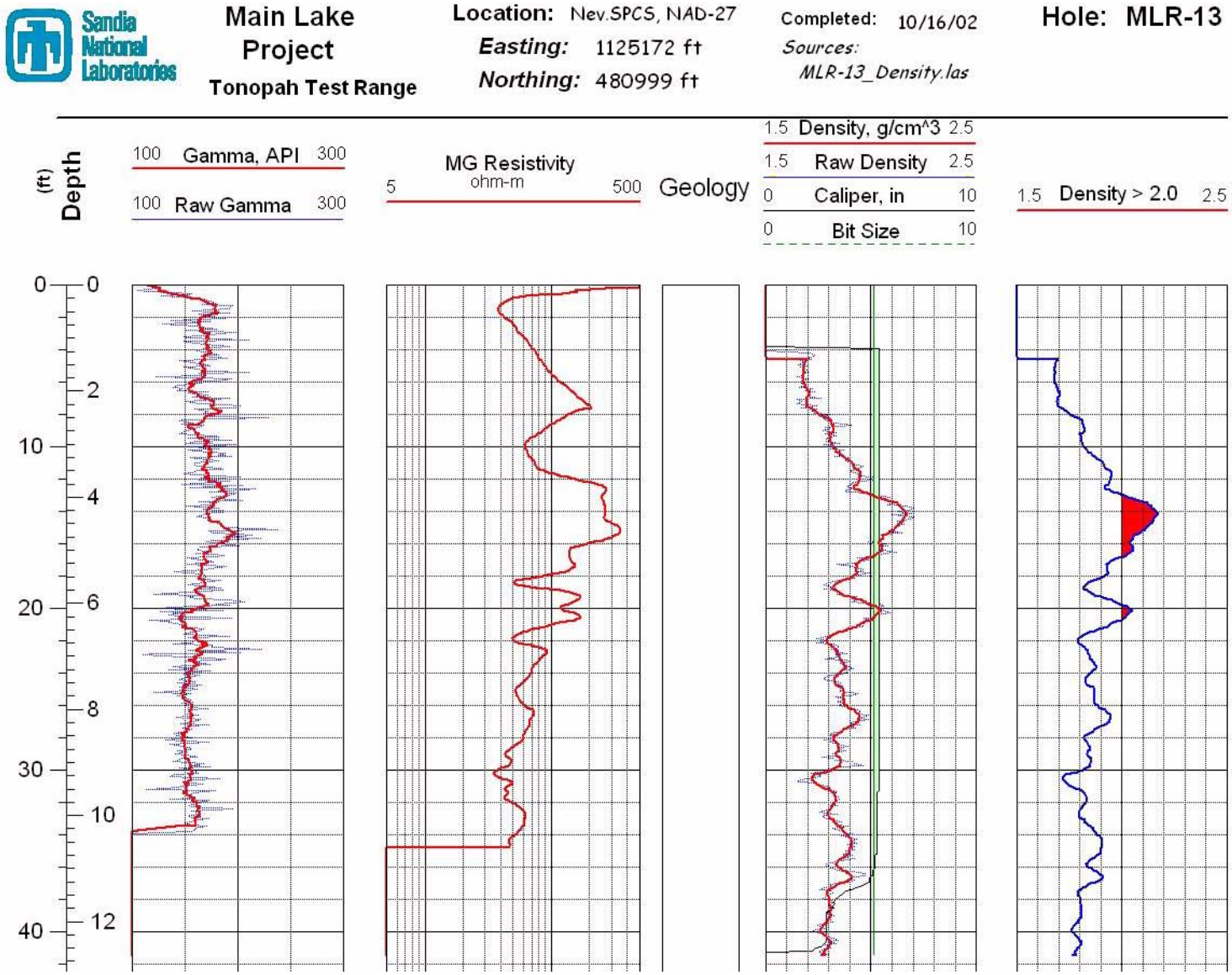

Figure C-29 Geophysical logs for drill hole MLR-13

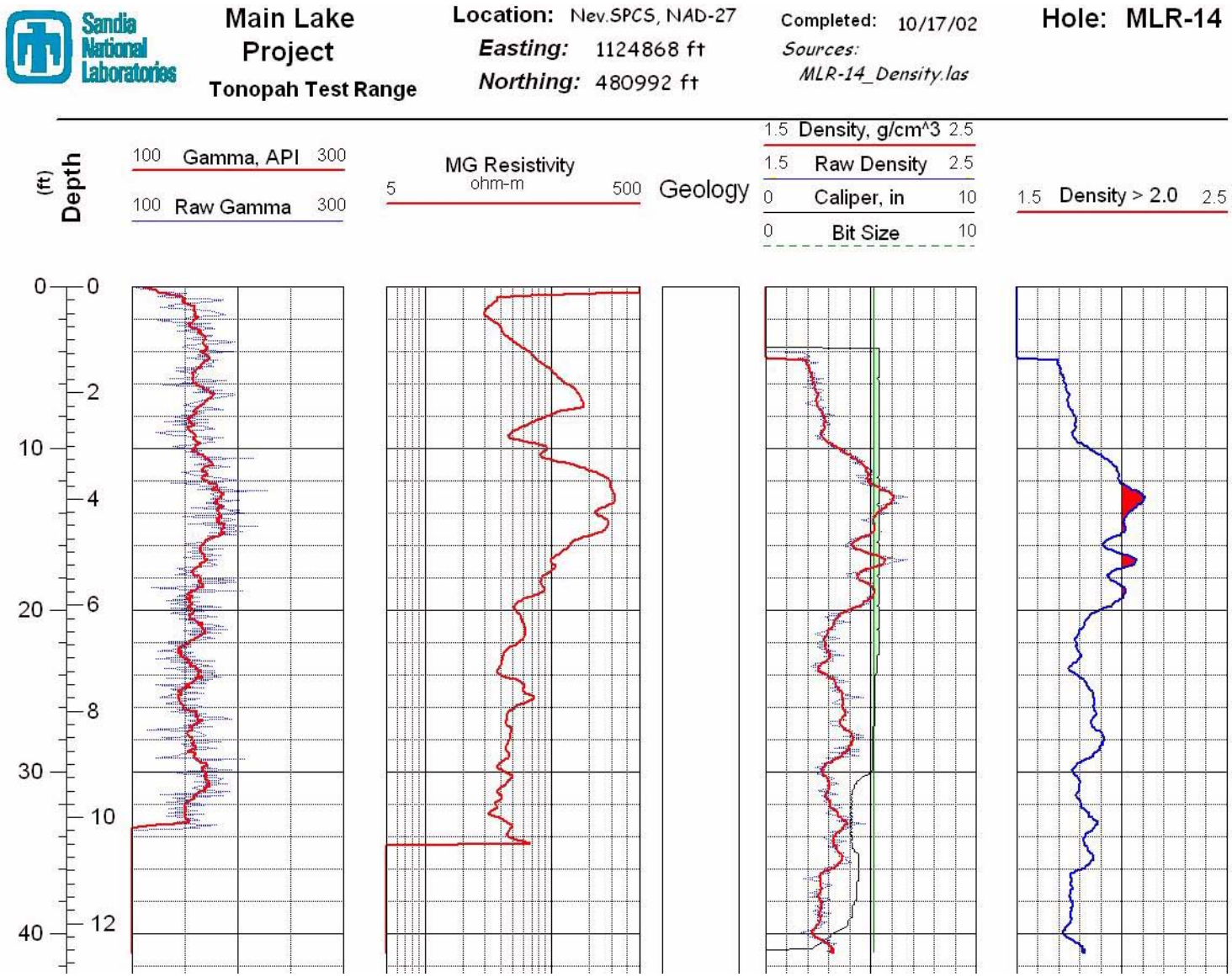

Figure C-30 Geophysical logs for drill hole MLR-14

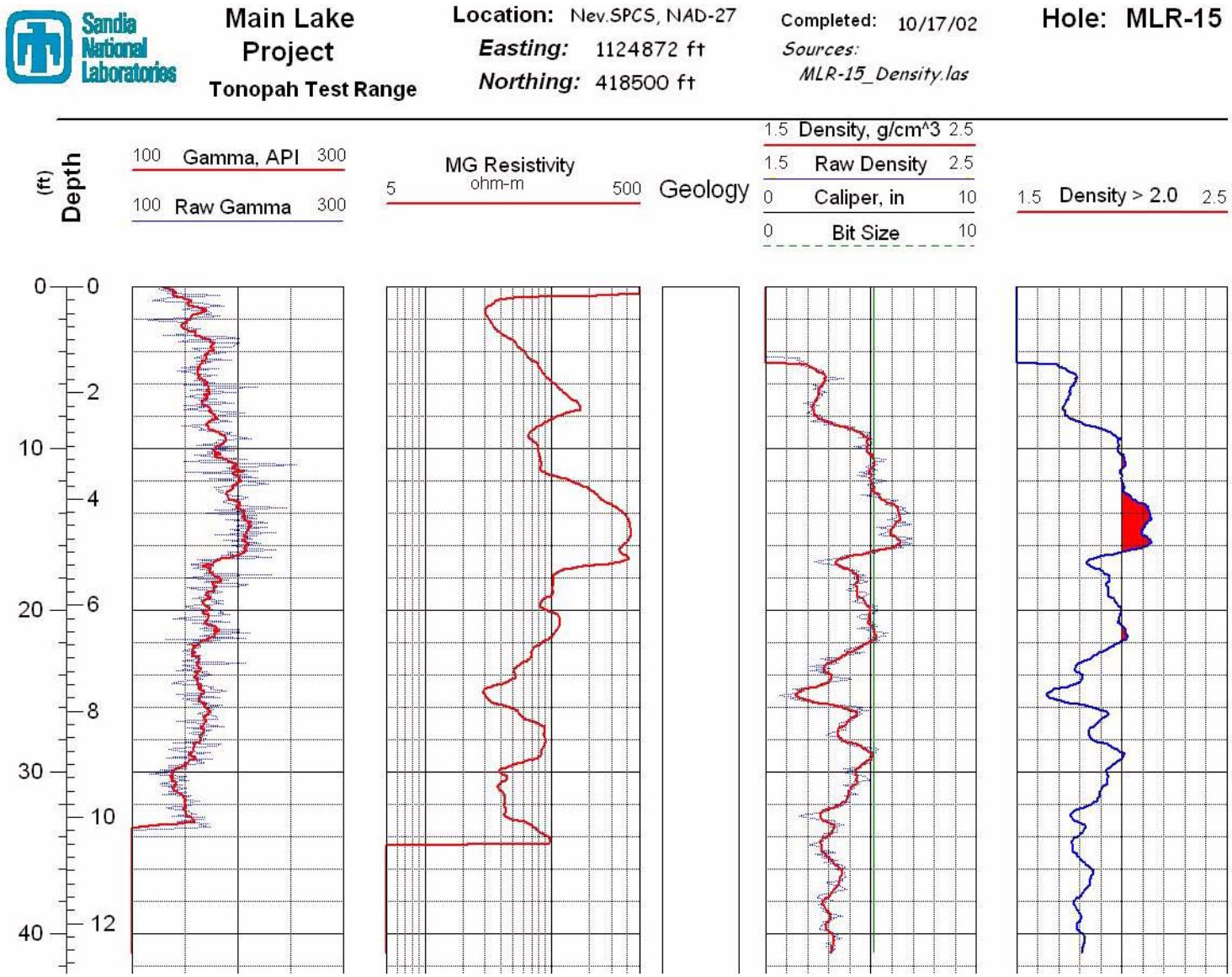

Figure C-31 Geophysical logs for drill hole MLR-15

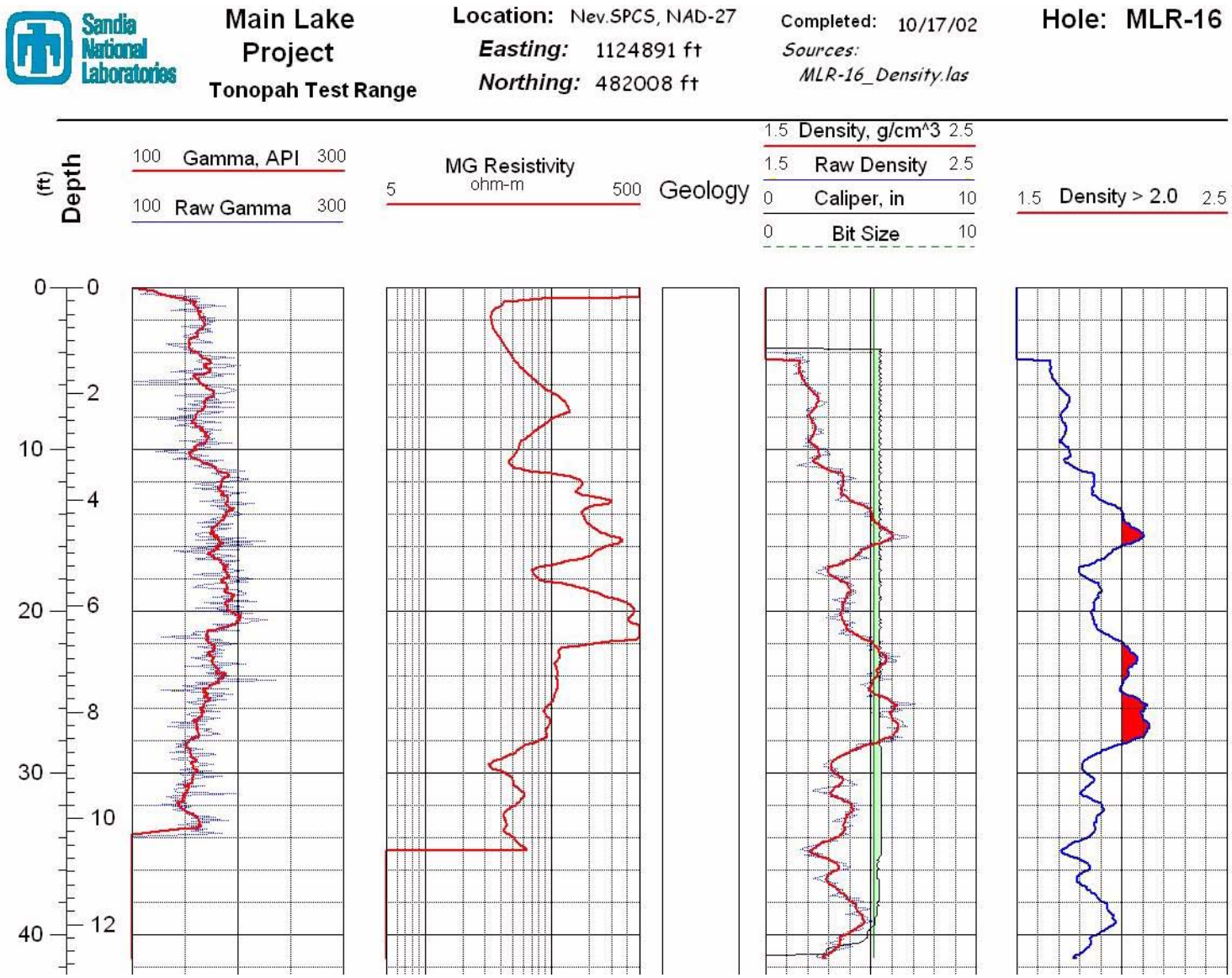

Figure C-32 Geophysical logs for drill hole MLR-16

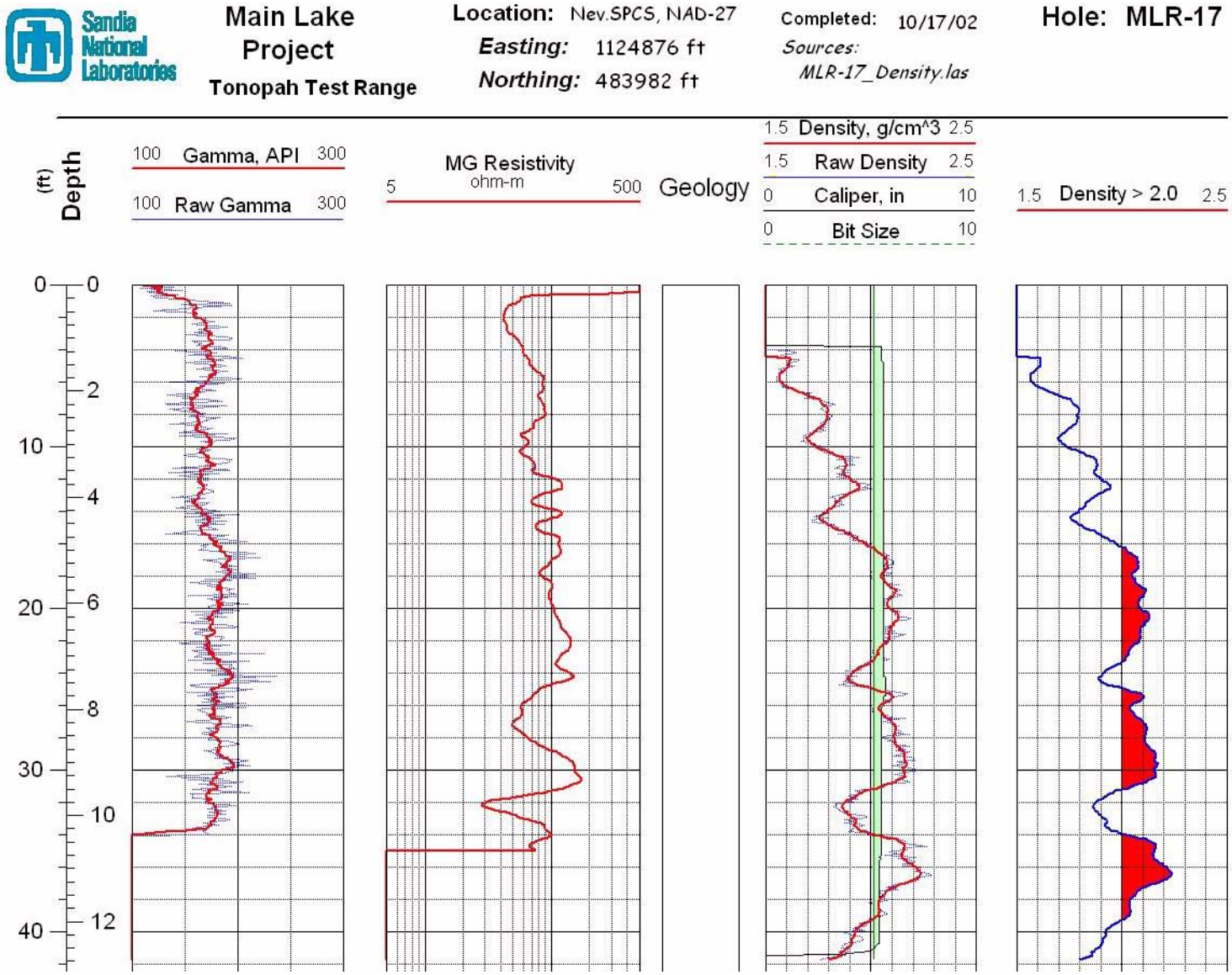

Figure C-33 Geophysical logs for drill hole MLR-17

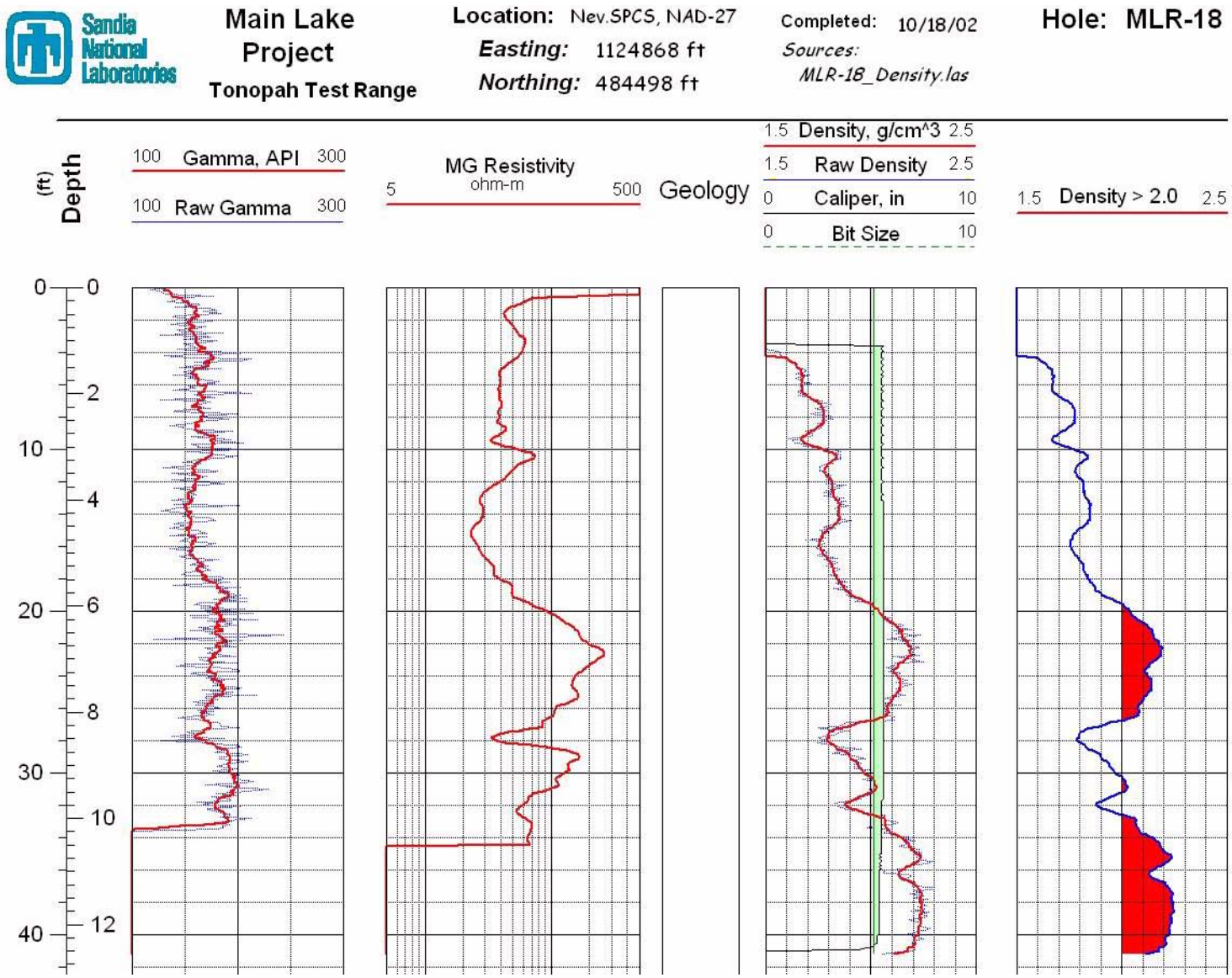

Figure C-34 Geophysical logs for drill hole MLR-18

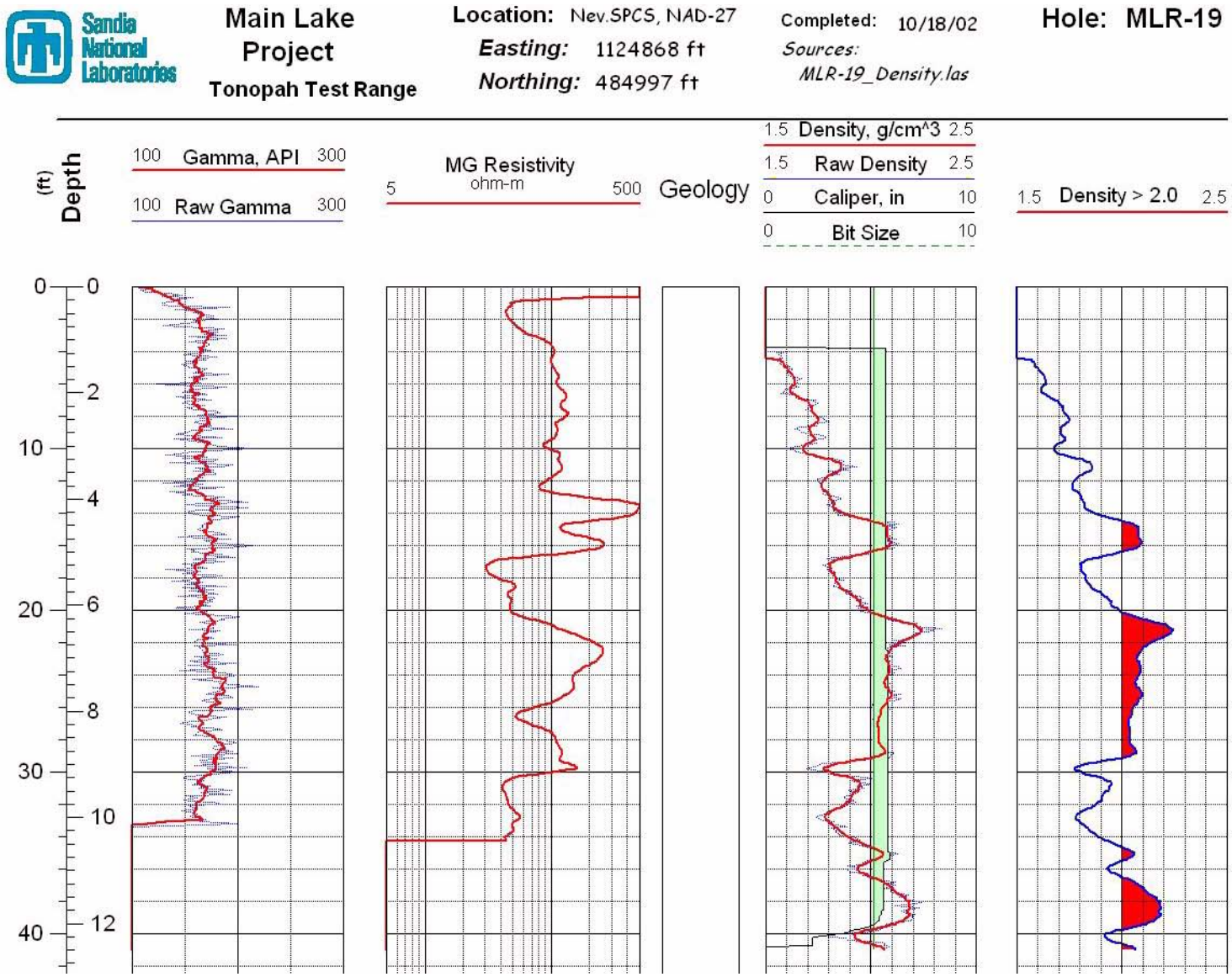

Figure C-35 Geophysical logs for drill hole MLR-19

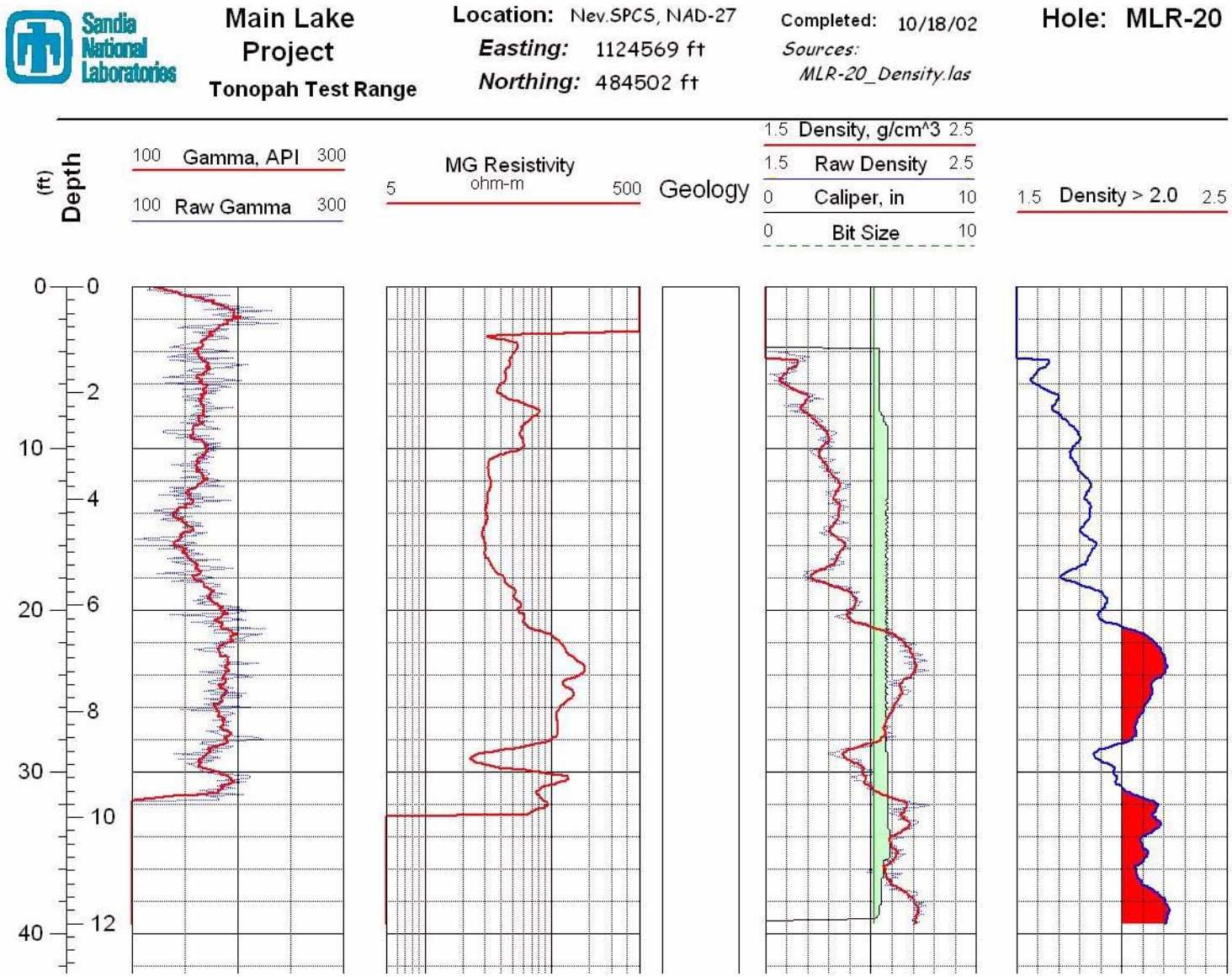

Figure C-36 Geophysical logs for drill hole MLR-20

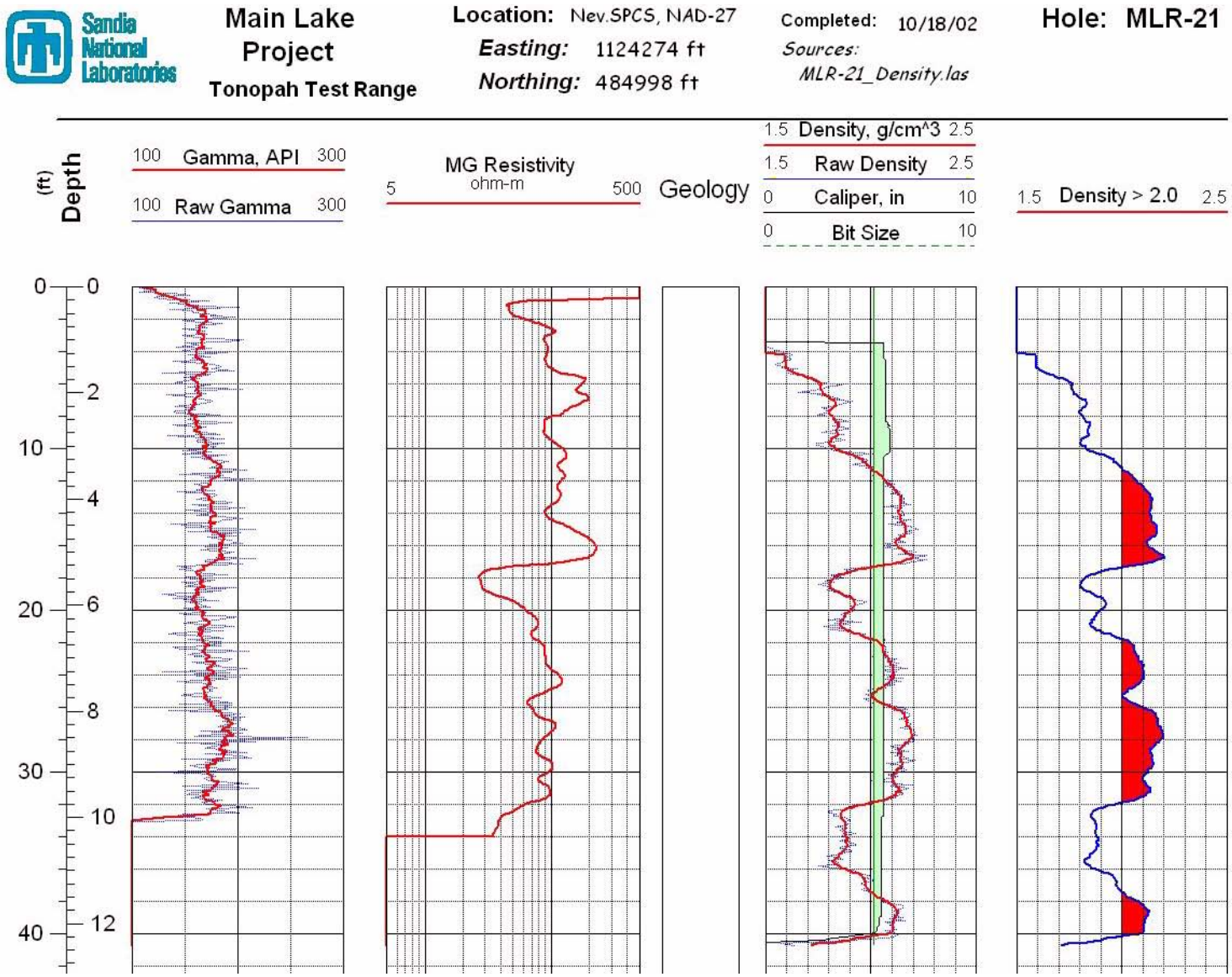

Figure C-37 Geophysical logs for drill hole MLR-21

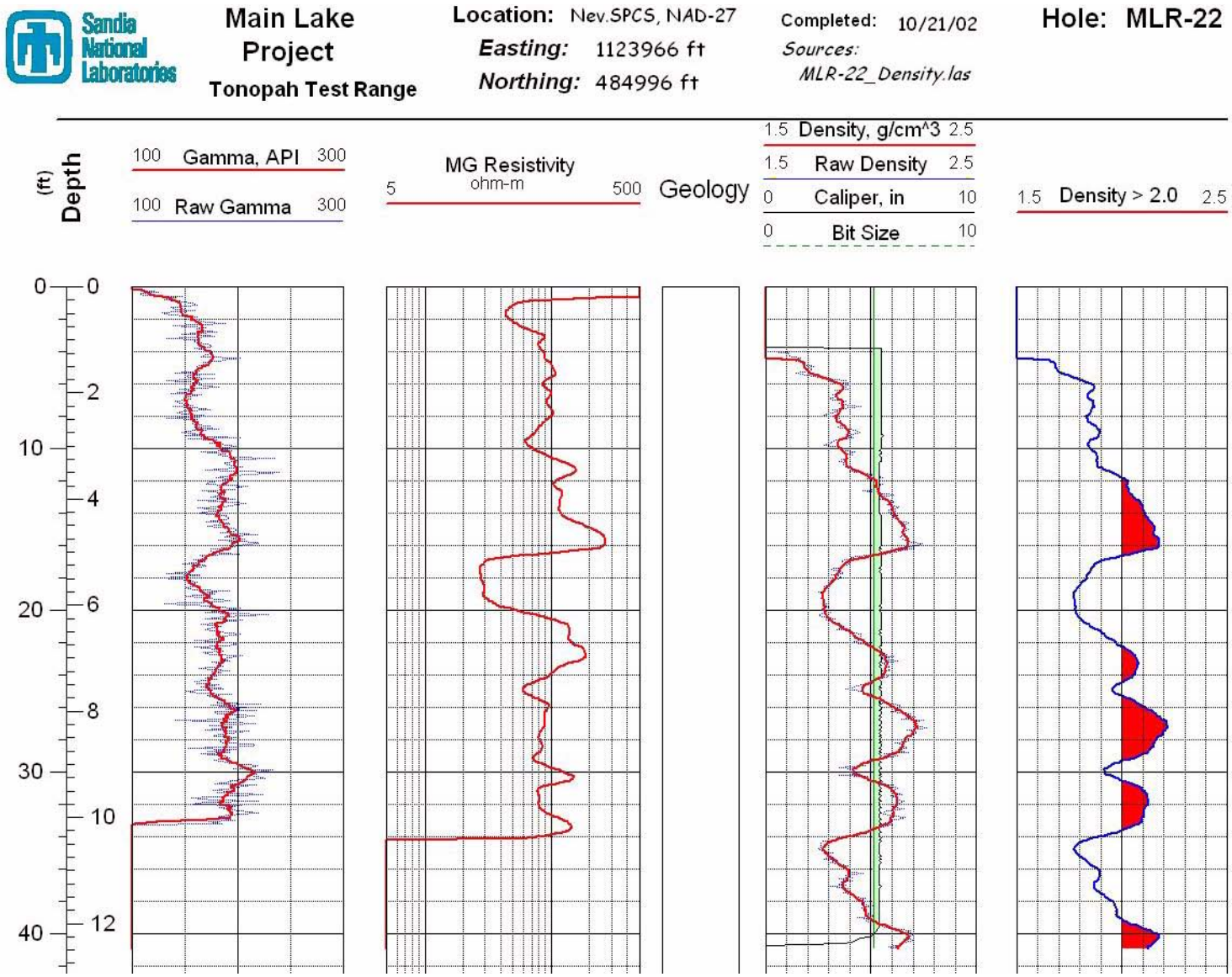

Figure C-38 Geophysical logs for drill hole MLR-22

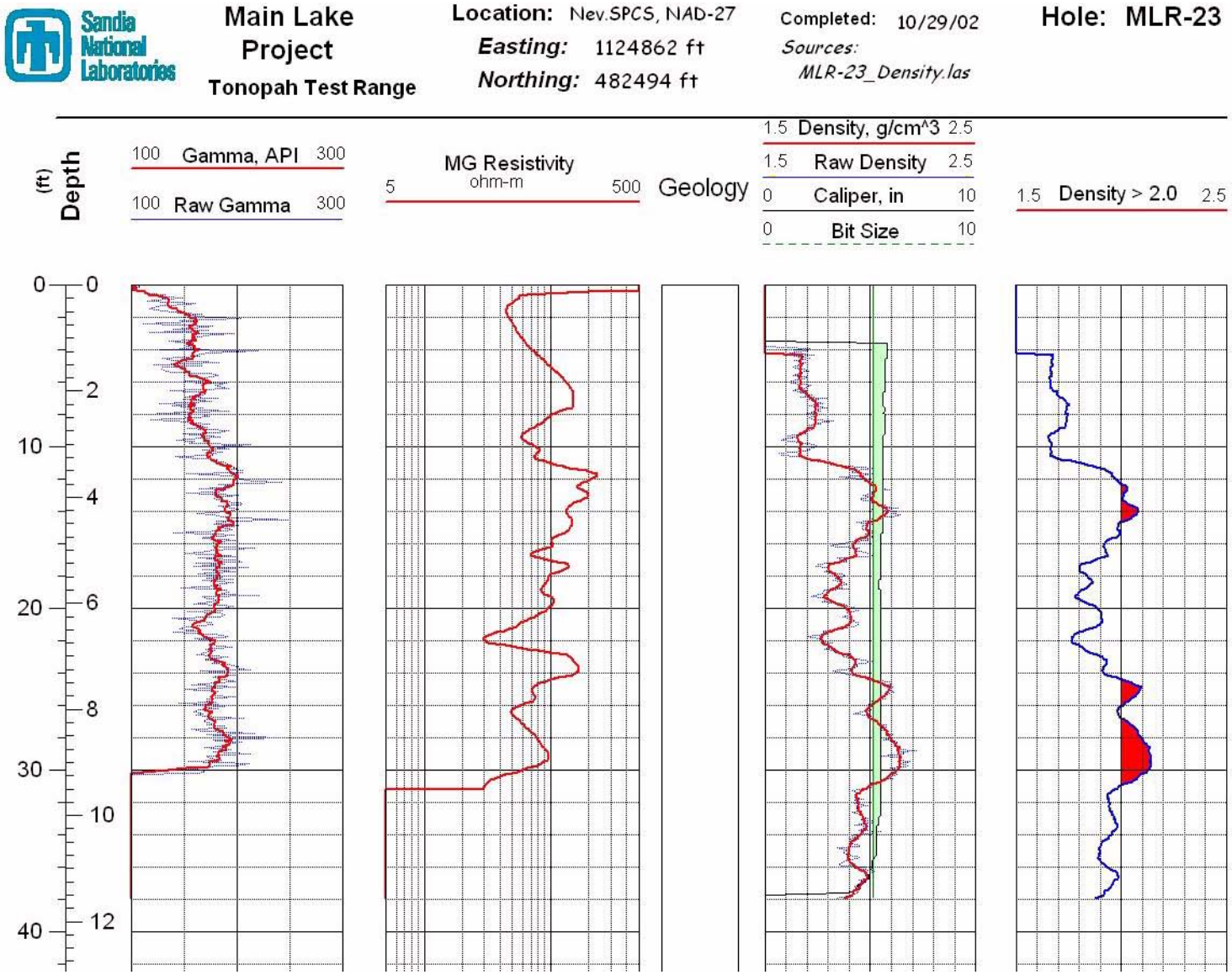

Figure C-39 Geophysical logs for drill hole MLR-23

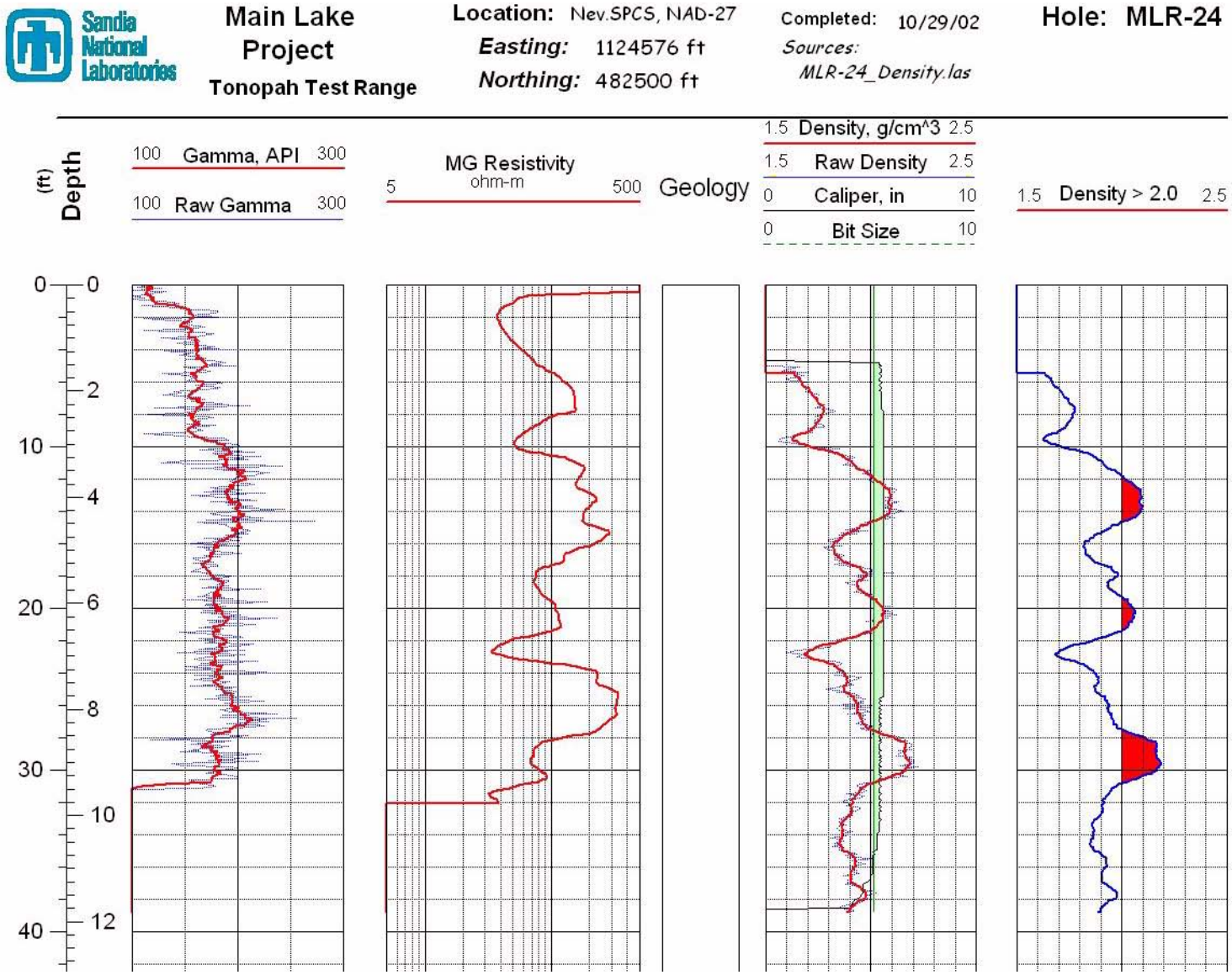

Figure C-40 Geophysical logs for drill hole MLR-24

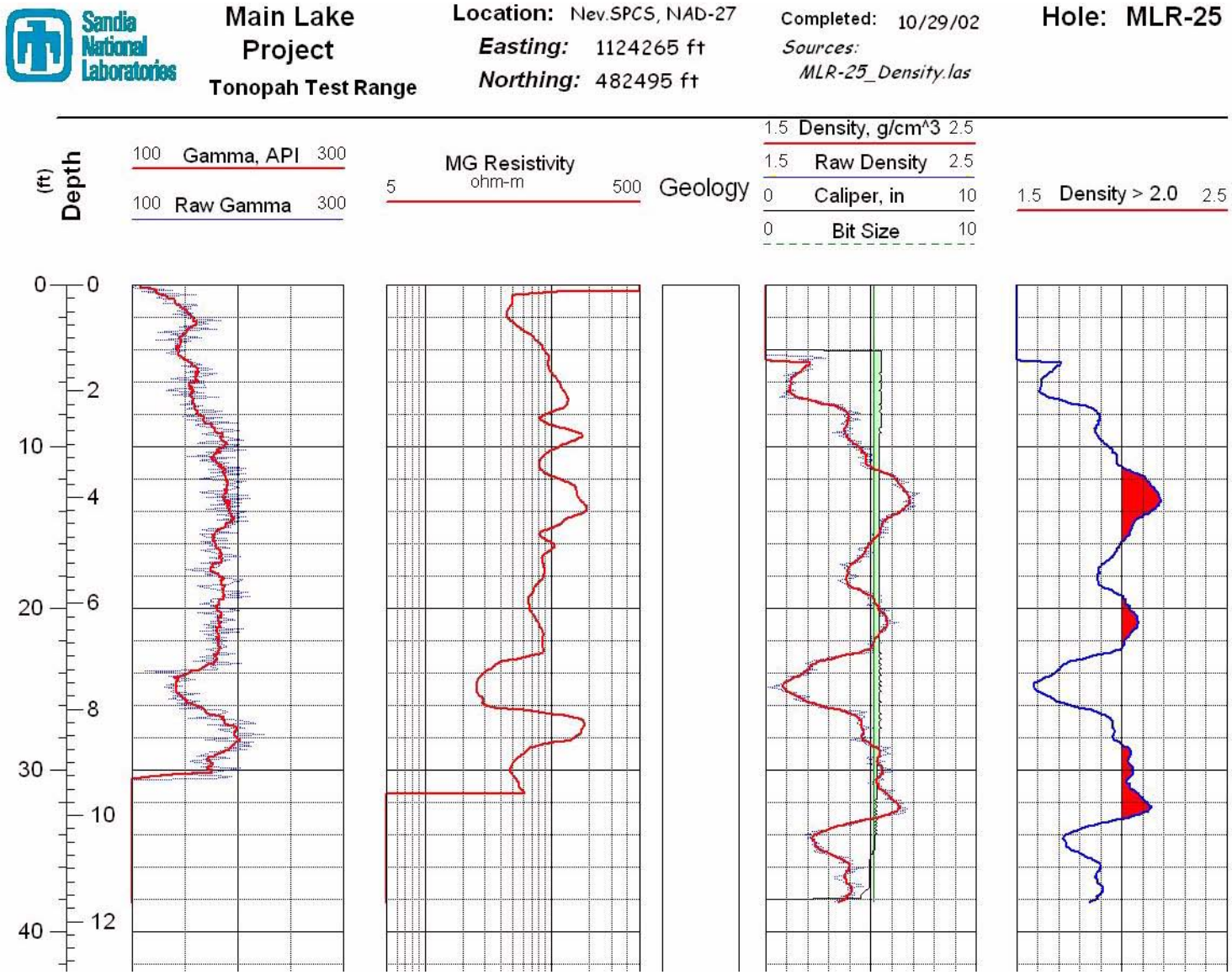

Figure C-41 Geophysical logs for drill hole MLR-25

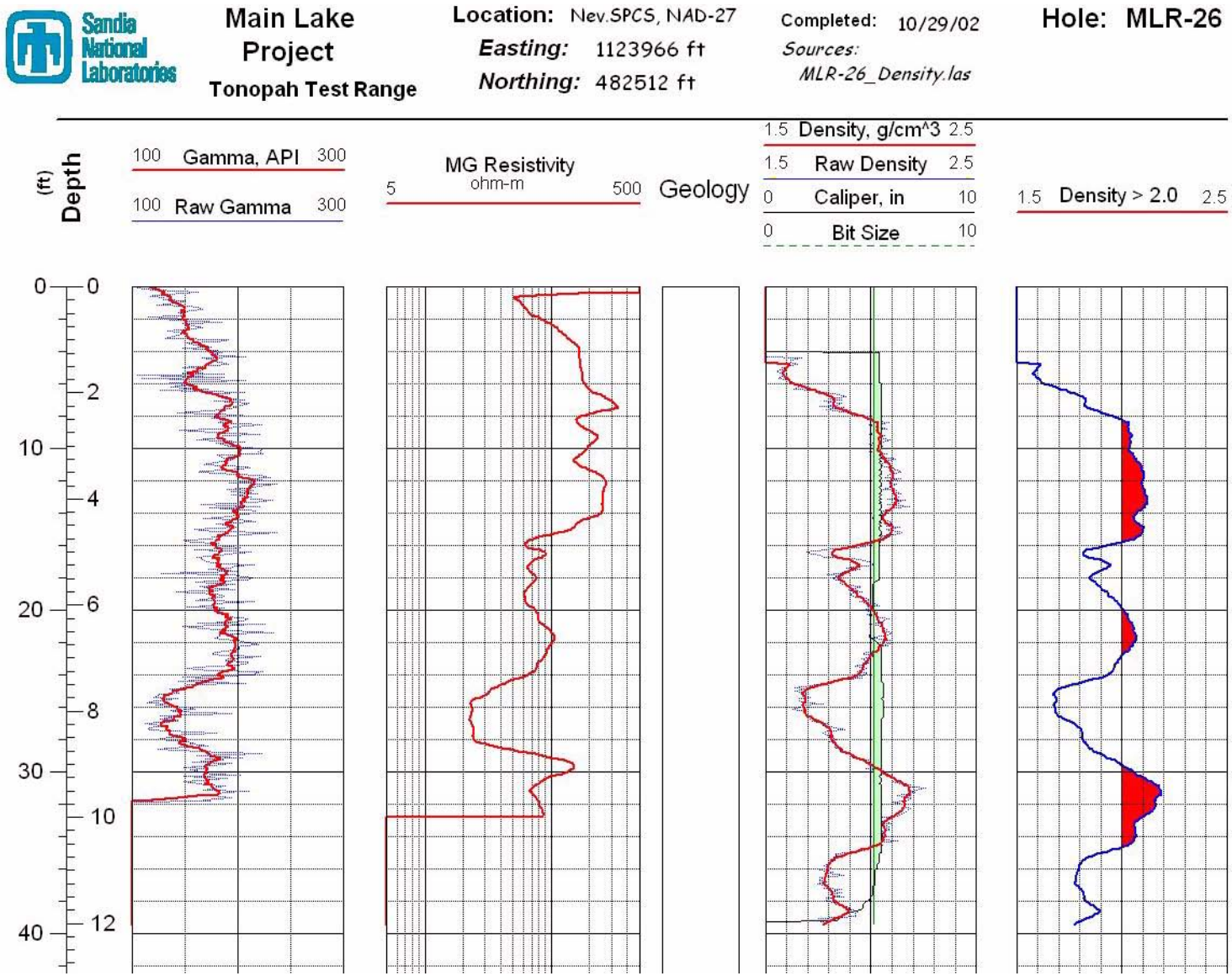

Figure C-42 Geophysical logs for drill hole MLR-26

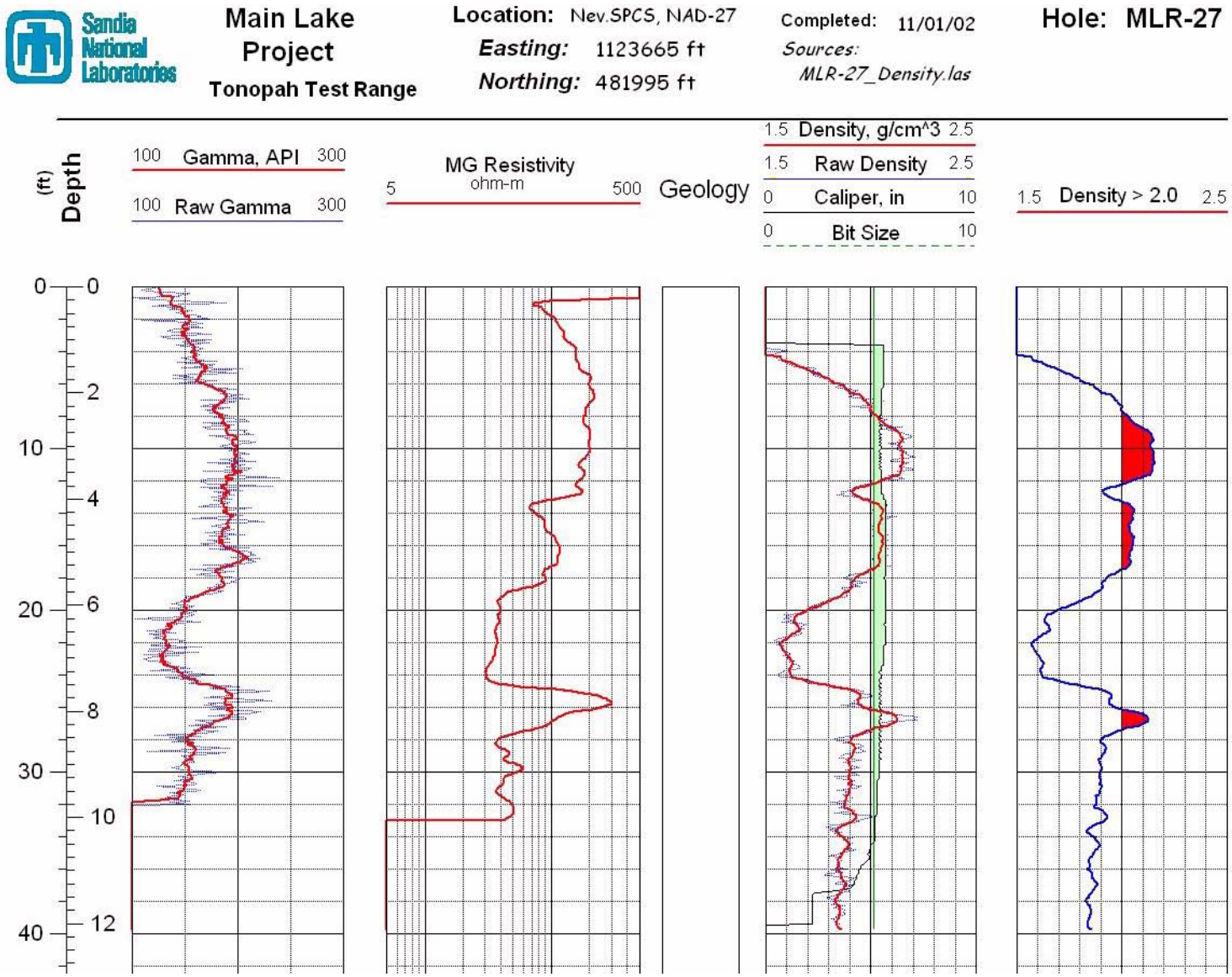

Figure C-43 Geophysical logs for drill hole MLR-27

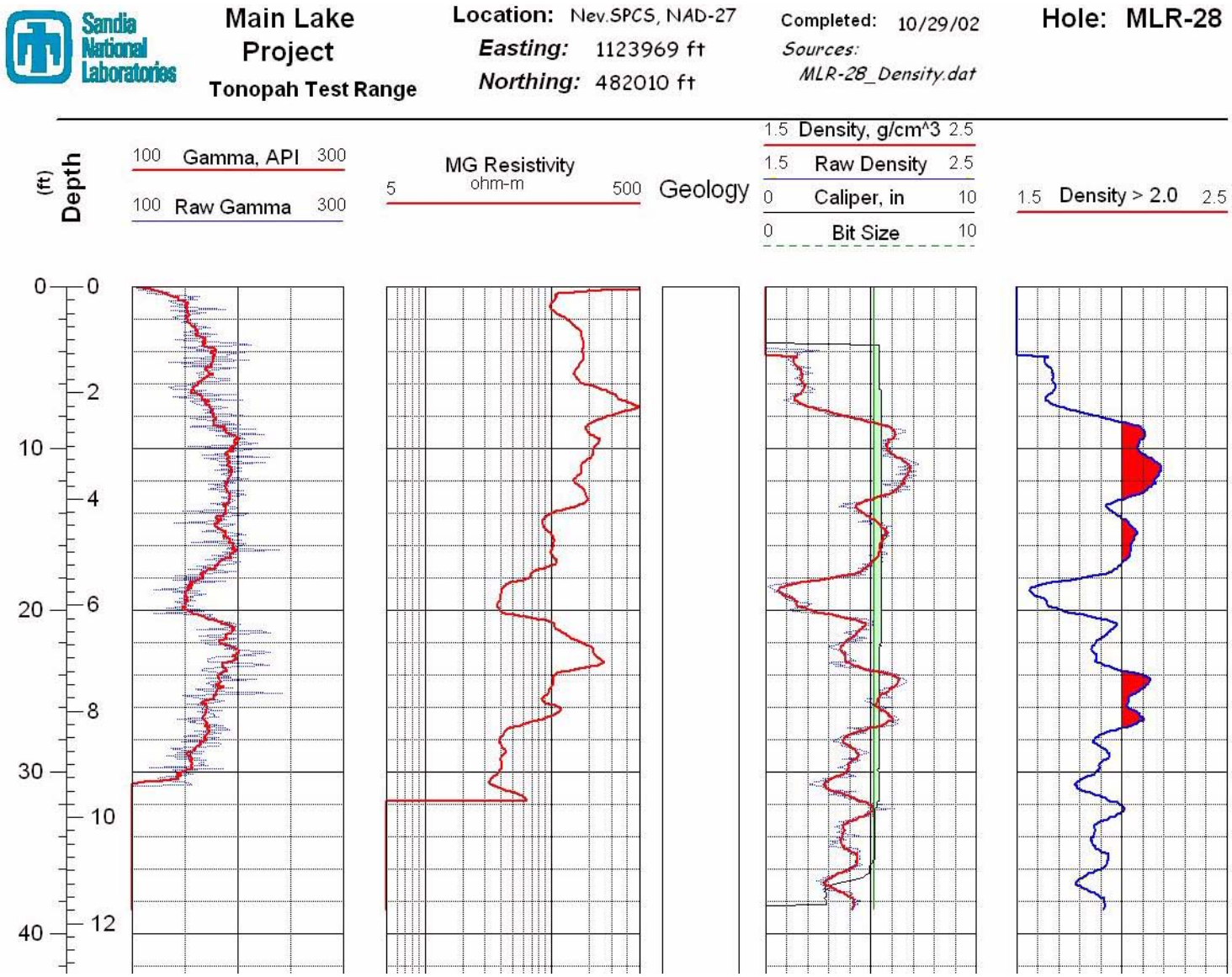

Figure C-44 Geophysical logs for drill hole MLR-28

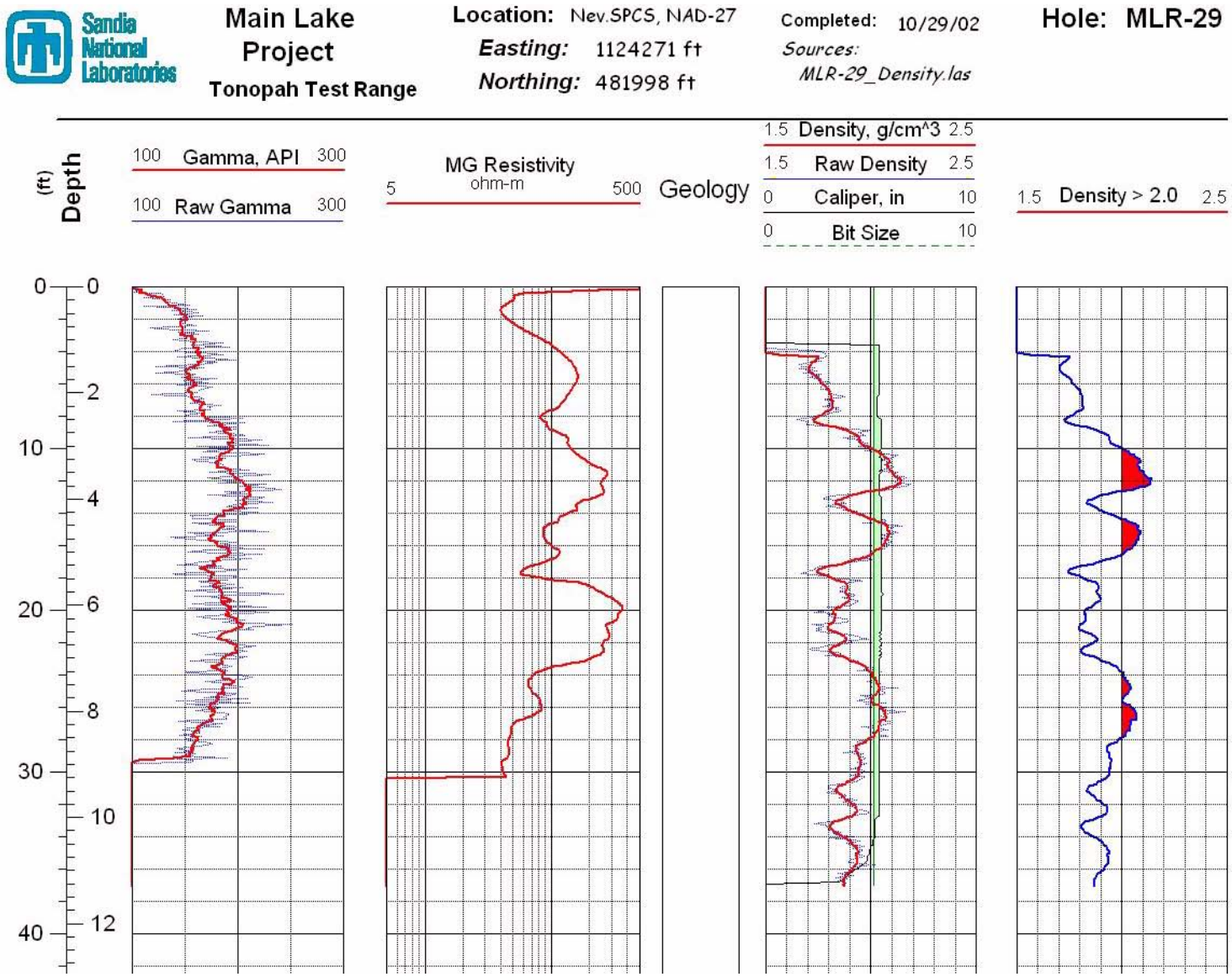

Figure C-45 Geophysical logs for drill hole MLR-29

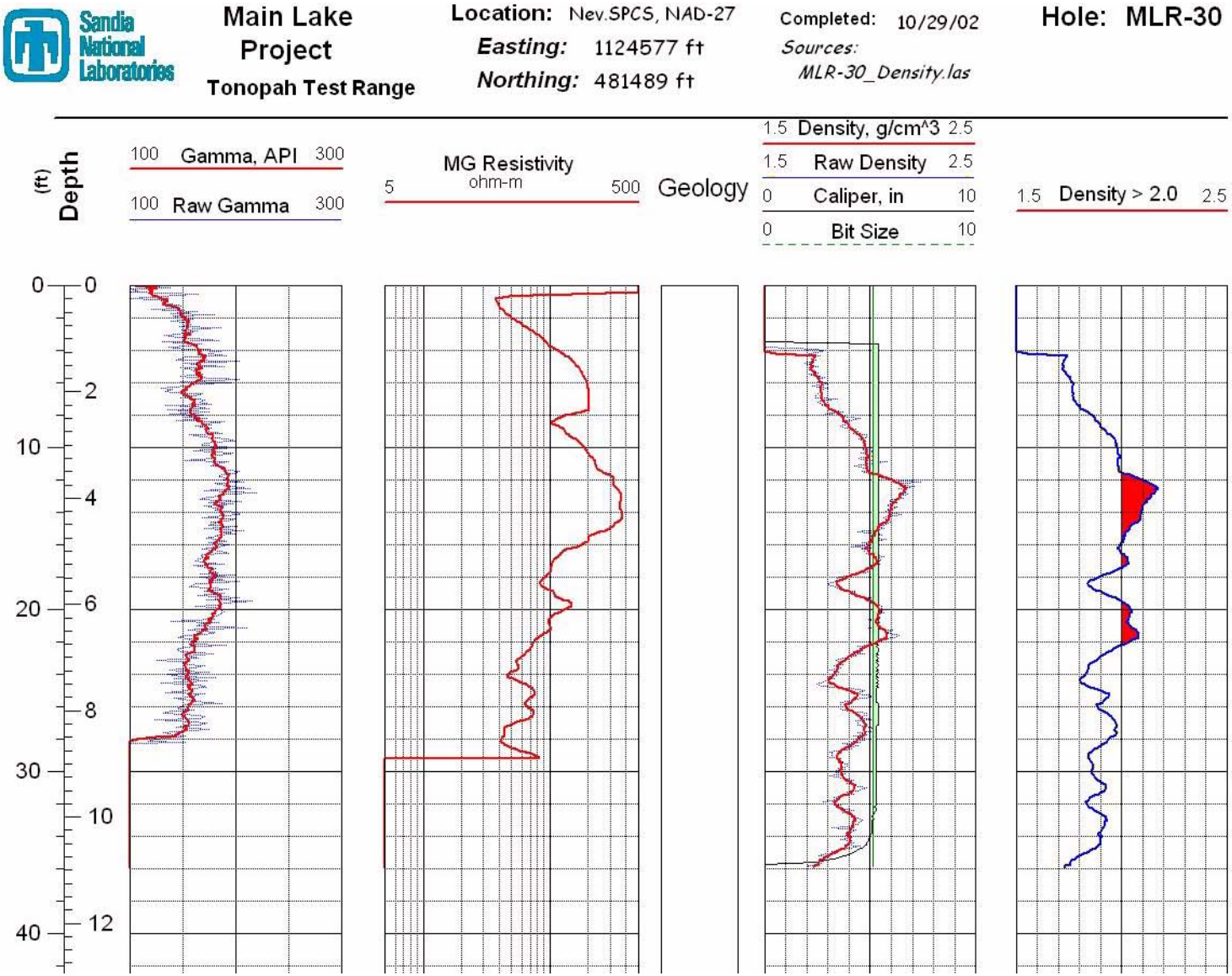

Figure C-46 Geophysical logs for drill hole MLR-30

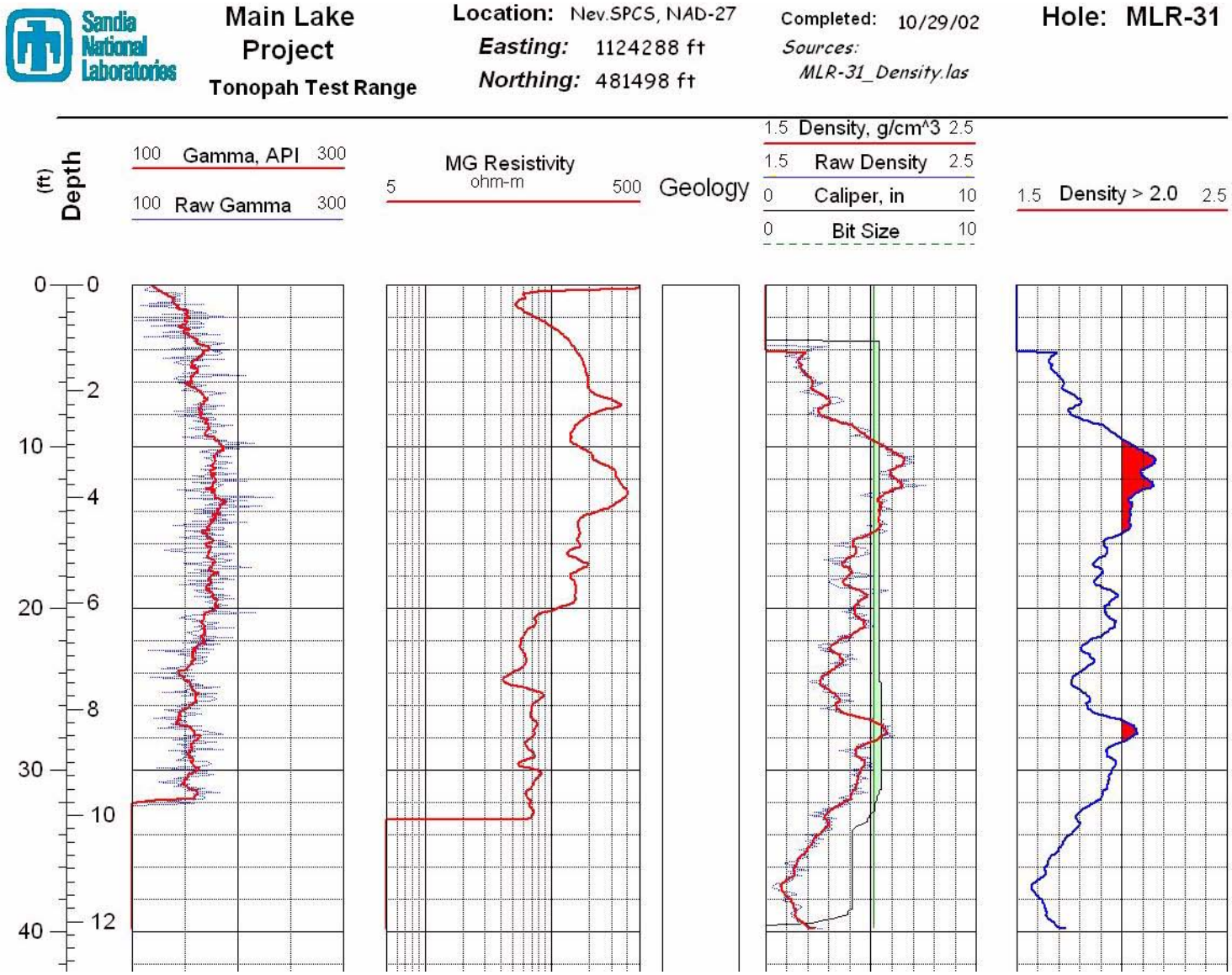

Figure C-47 Geophysical logs for drill hole MLR-31

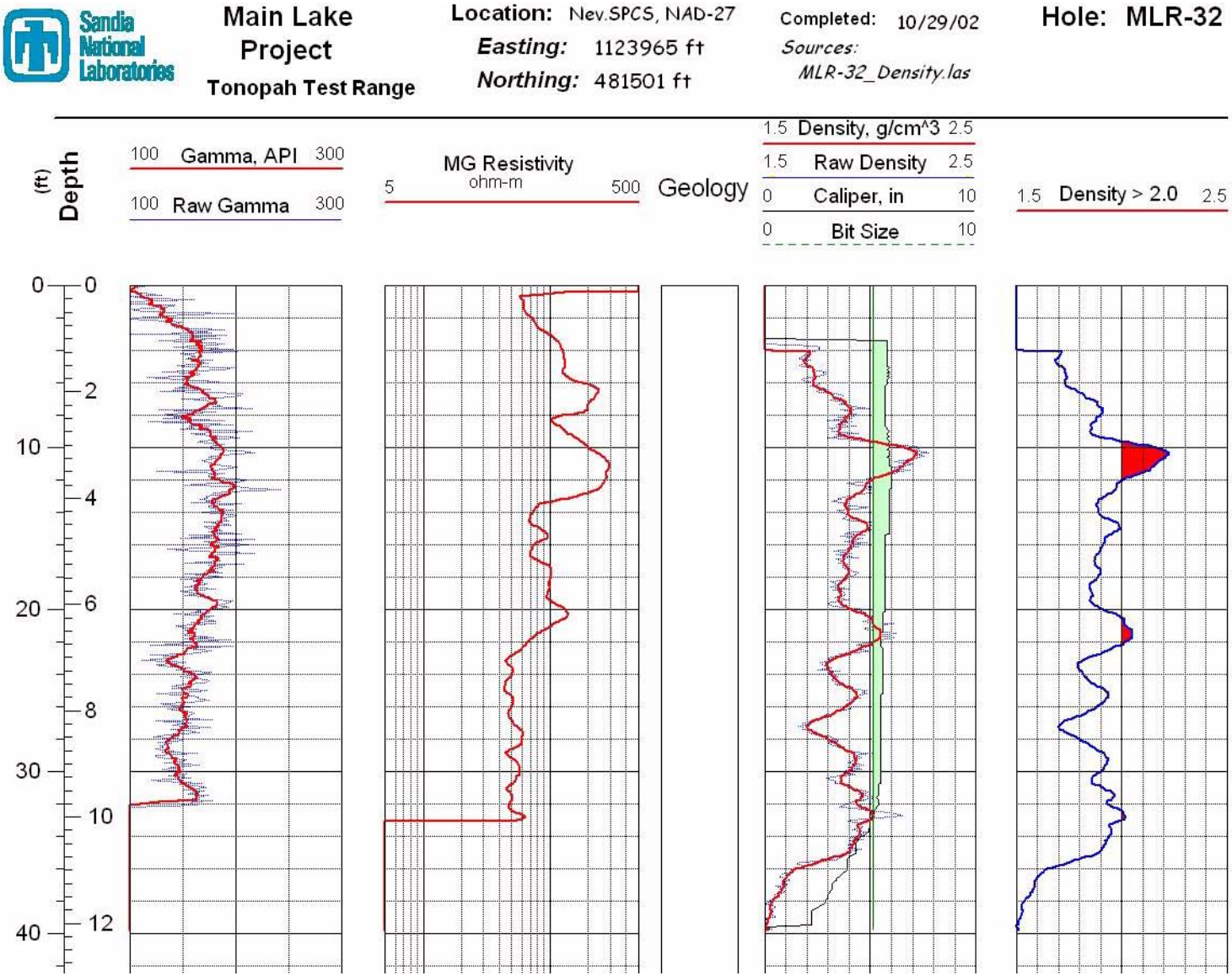

Figure C-48 Geophysical logs for drill hole MLR-32

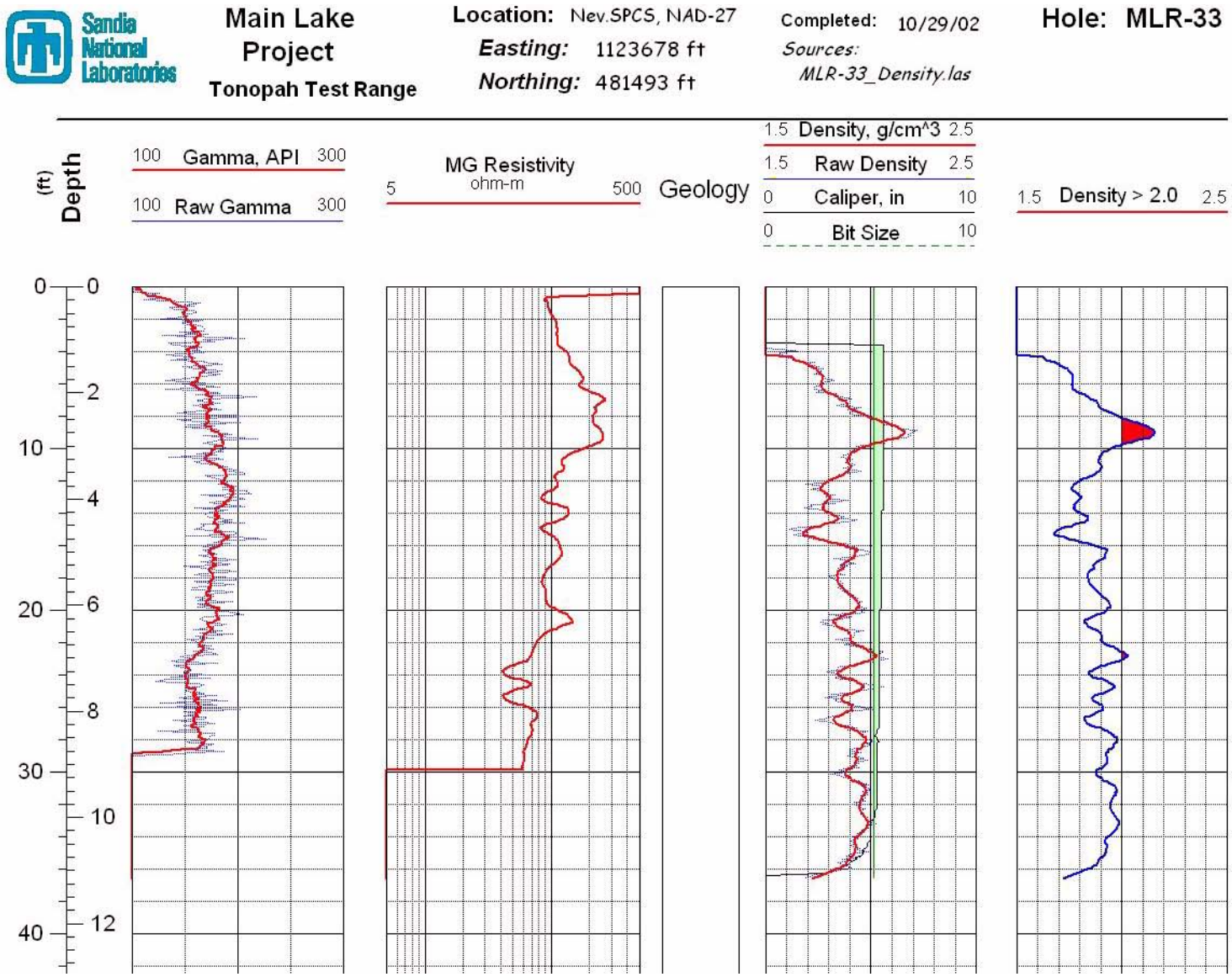

Figure C-49 Geophysical logs for drill hole MLR-33

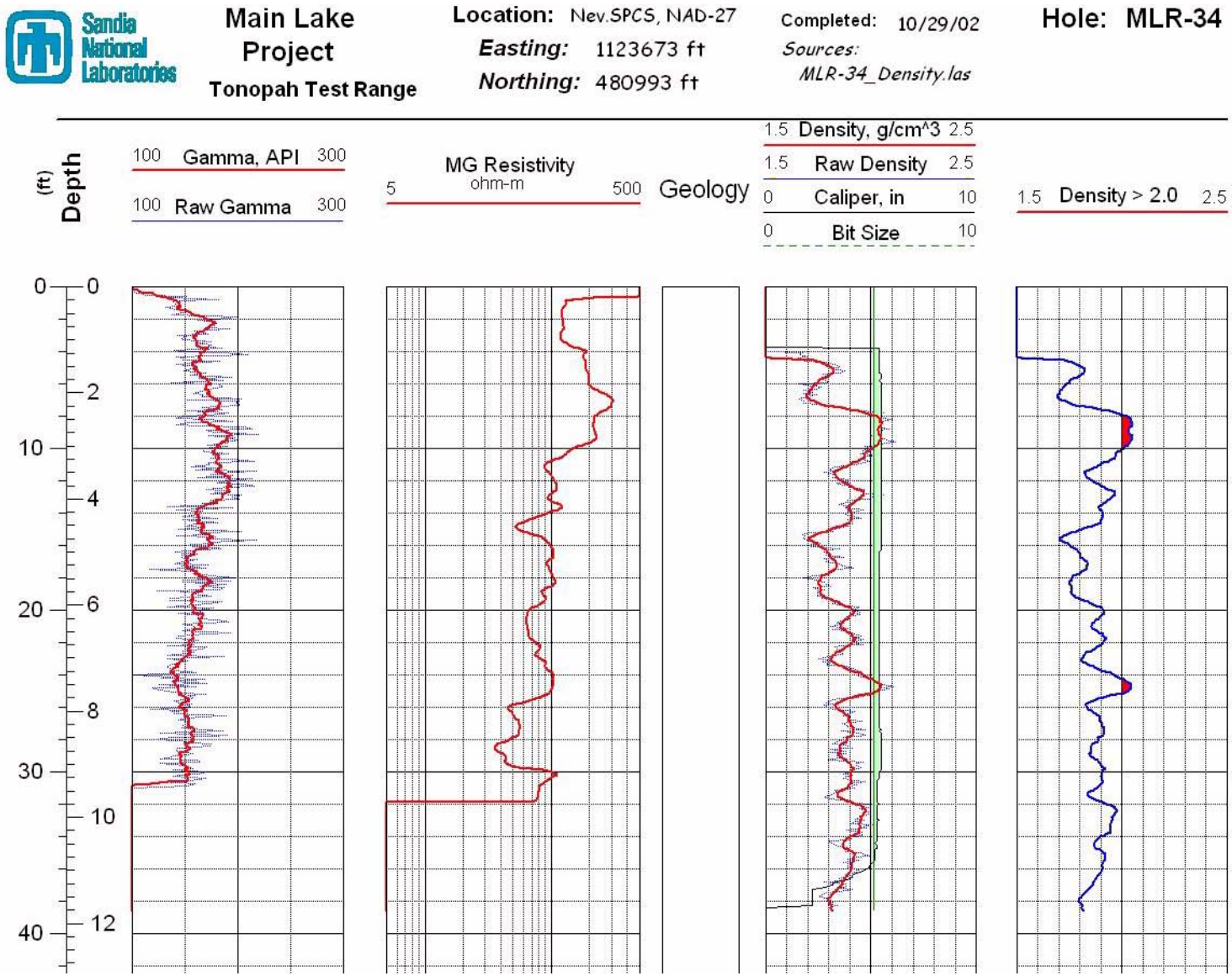

Figure C-50 Geophysical logs for drill hole MLR-34

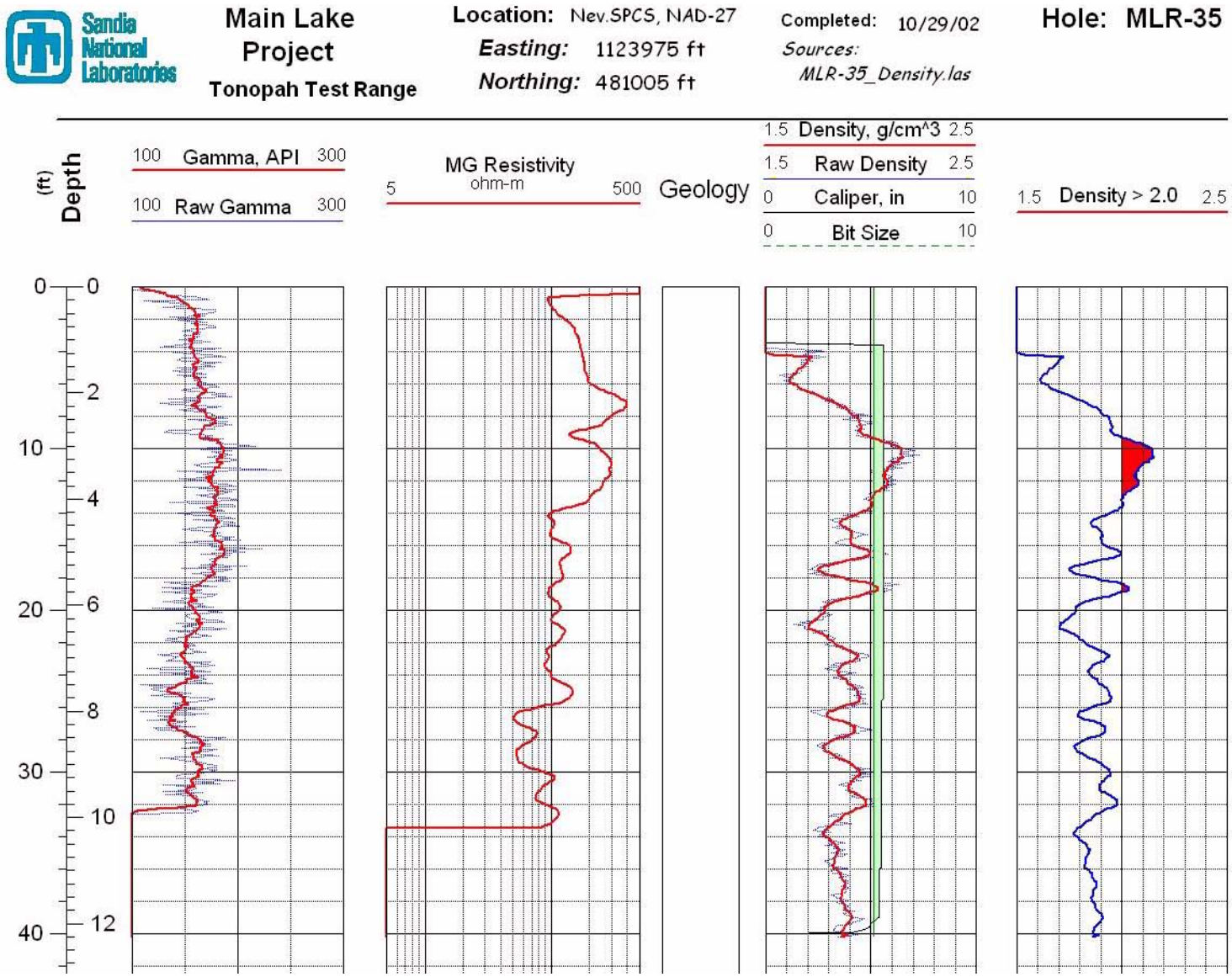

Figure C-51 Geophysical logs for drill hole MLR-35

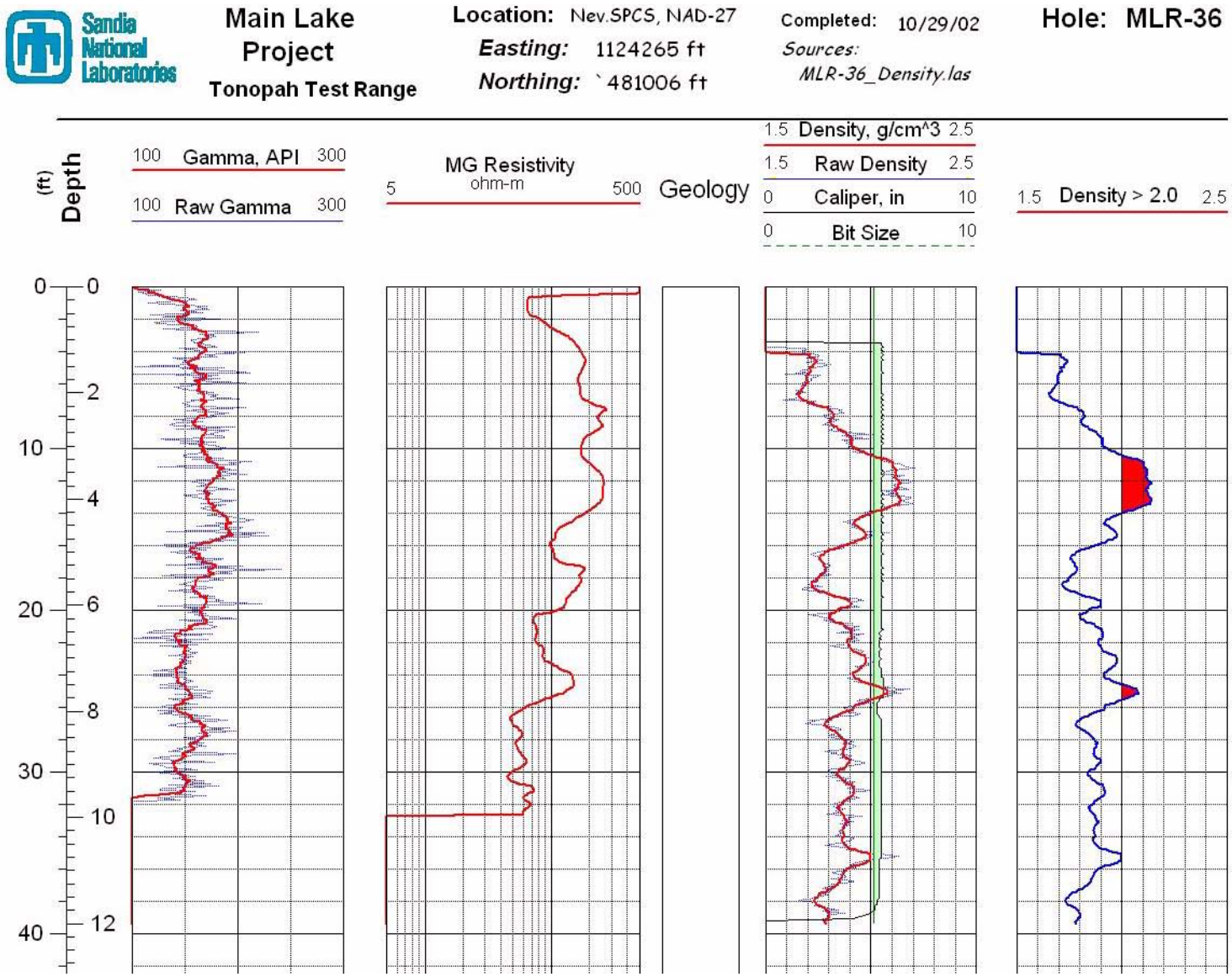

Figure C-52 Geophysical logs for drill hole MLR-36

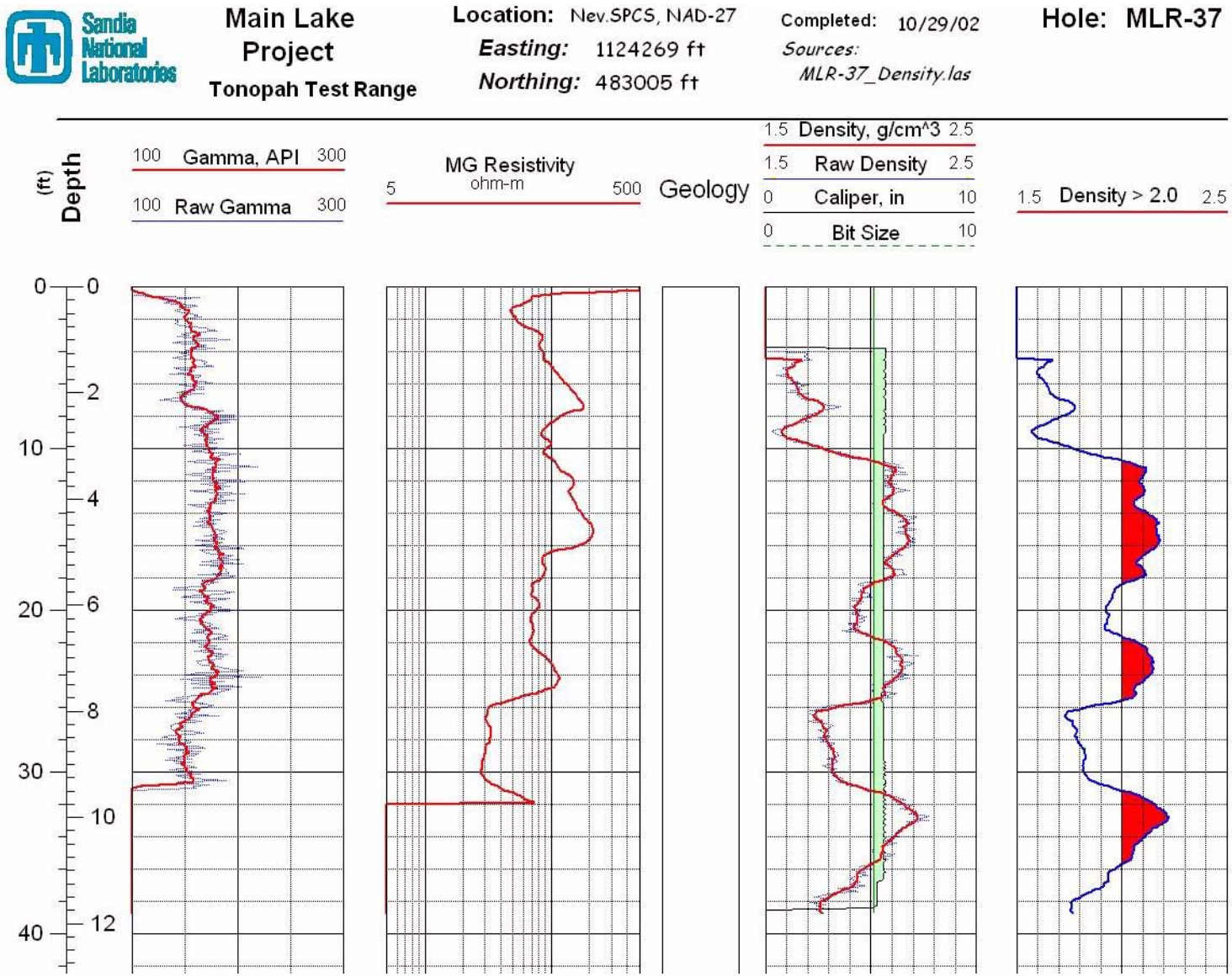

Figure C-53 Geophysical logs for drill hole MLR-37

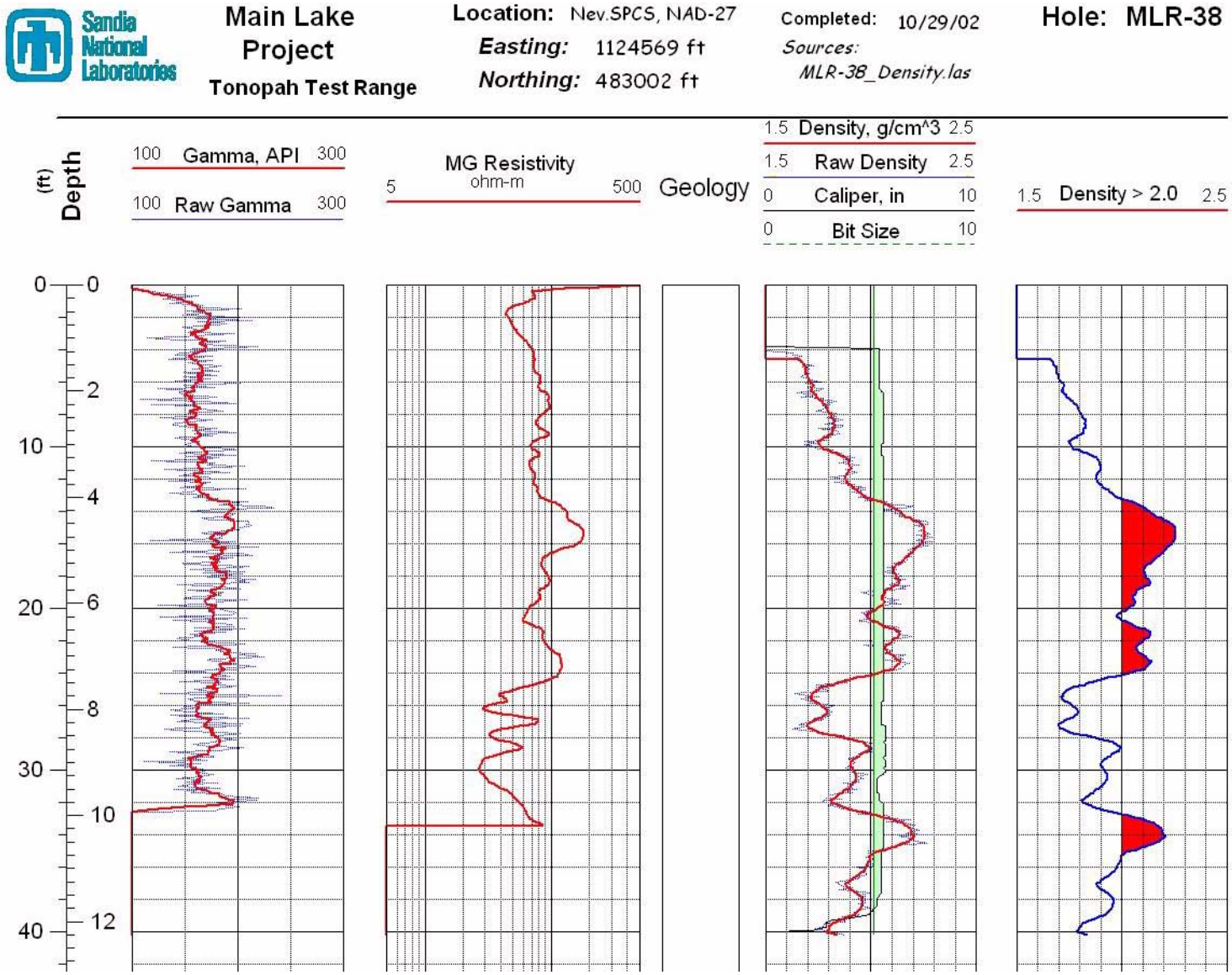

Figure C-54 Geophysical logs for drill hole MLR-38

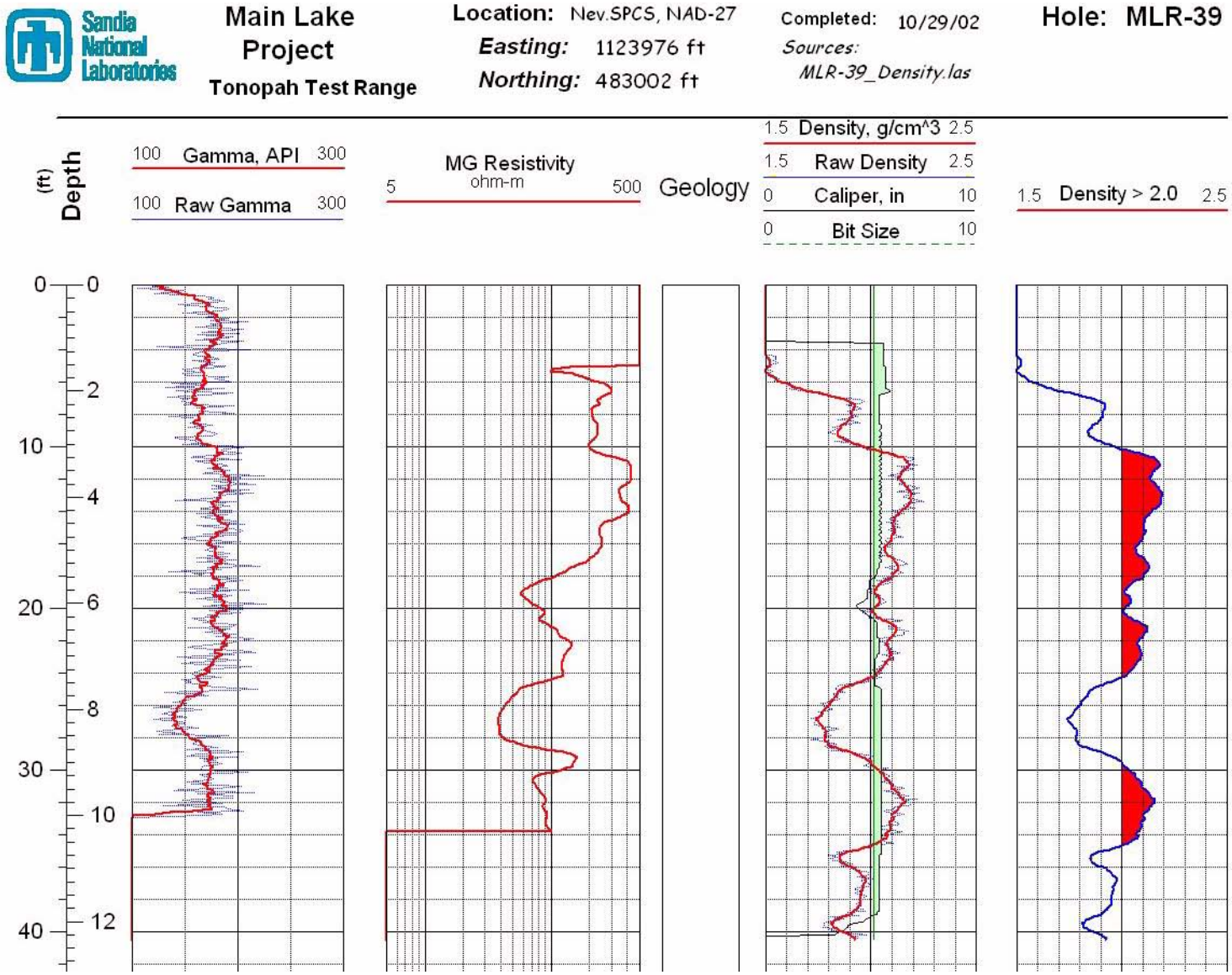

Figure C-55 Geophysical logs for drill hole MLR-39

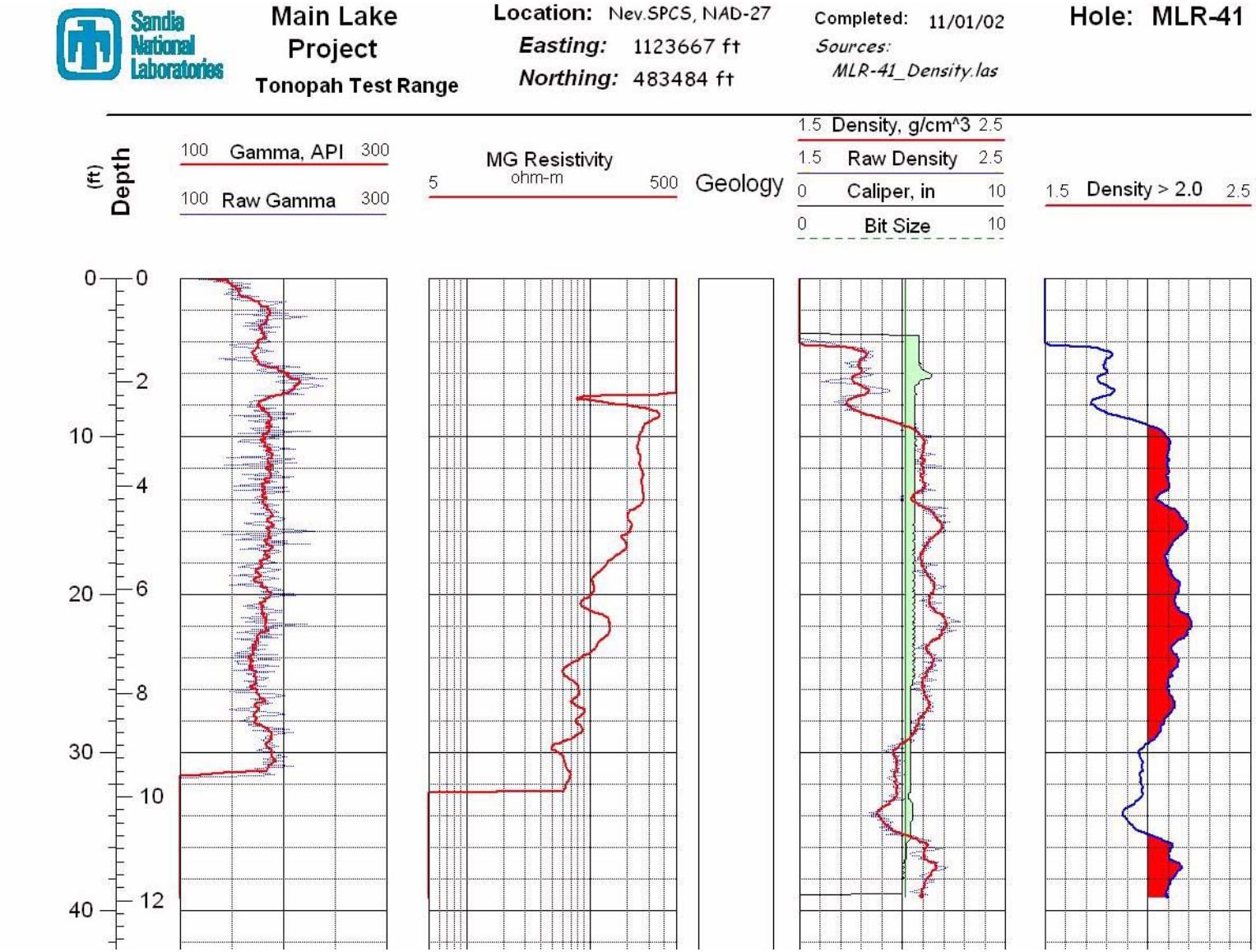

Figure C-56 Geophysical logs for drill hole MLR-41

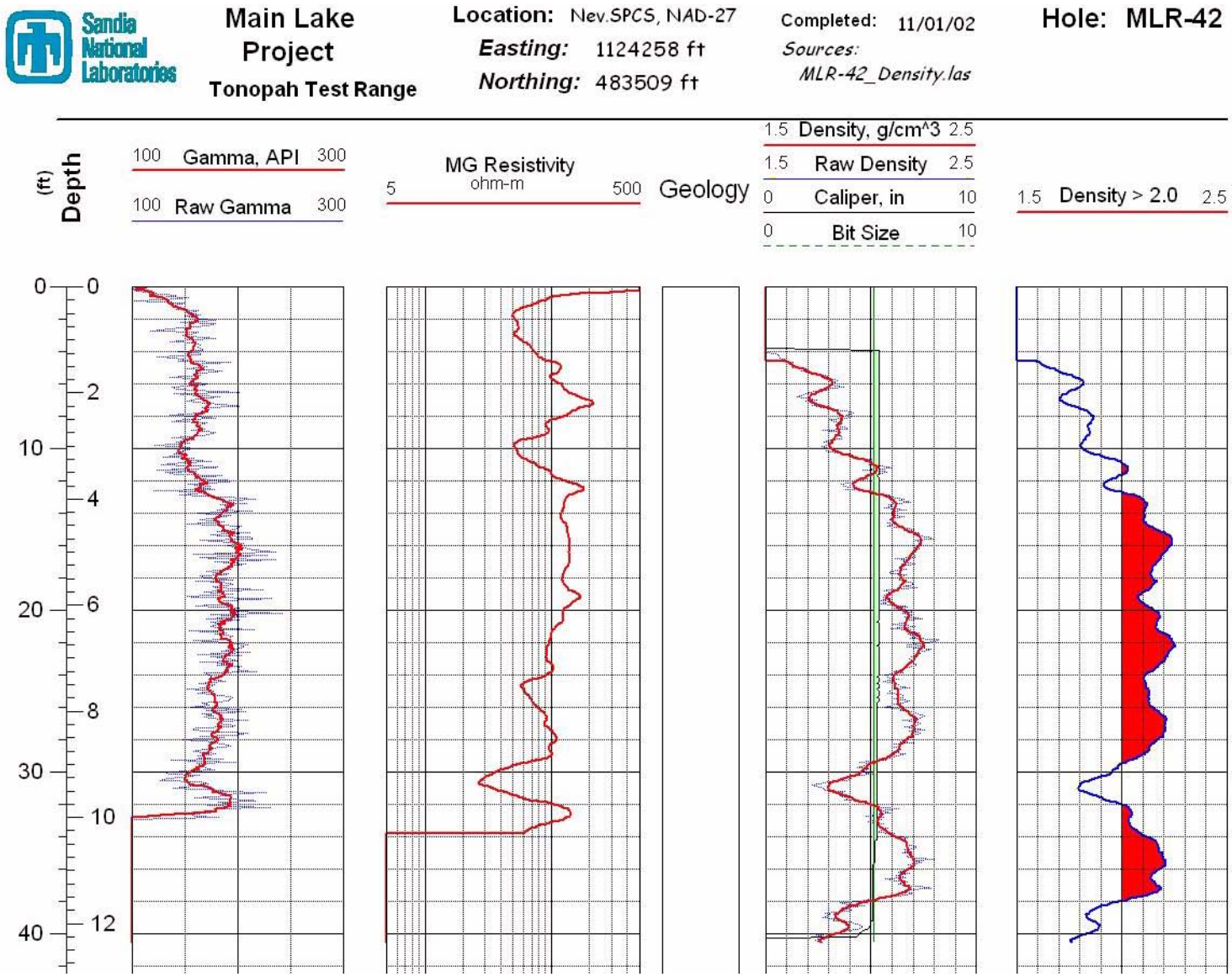

Figure C-57 Geophysical logs for drill hole MLR-42

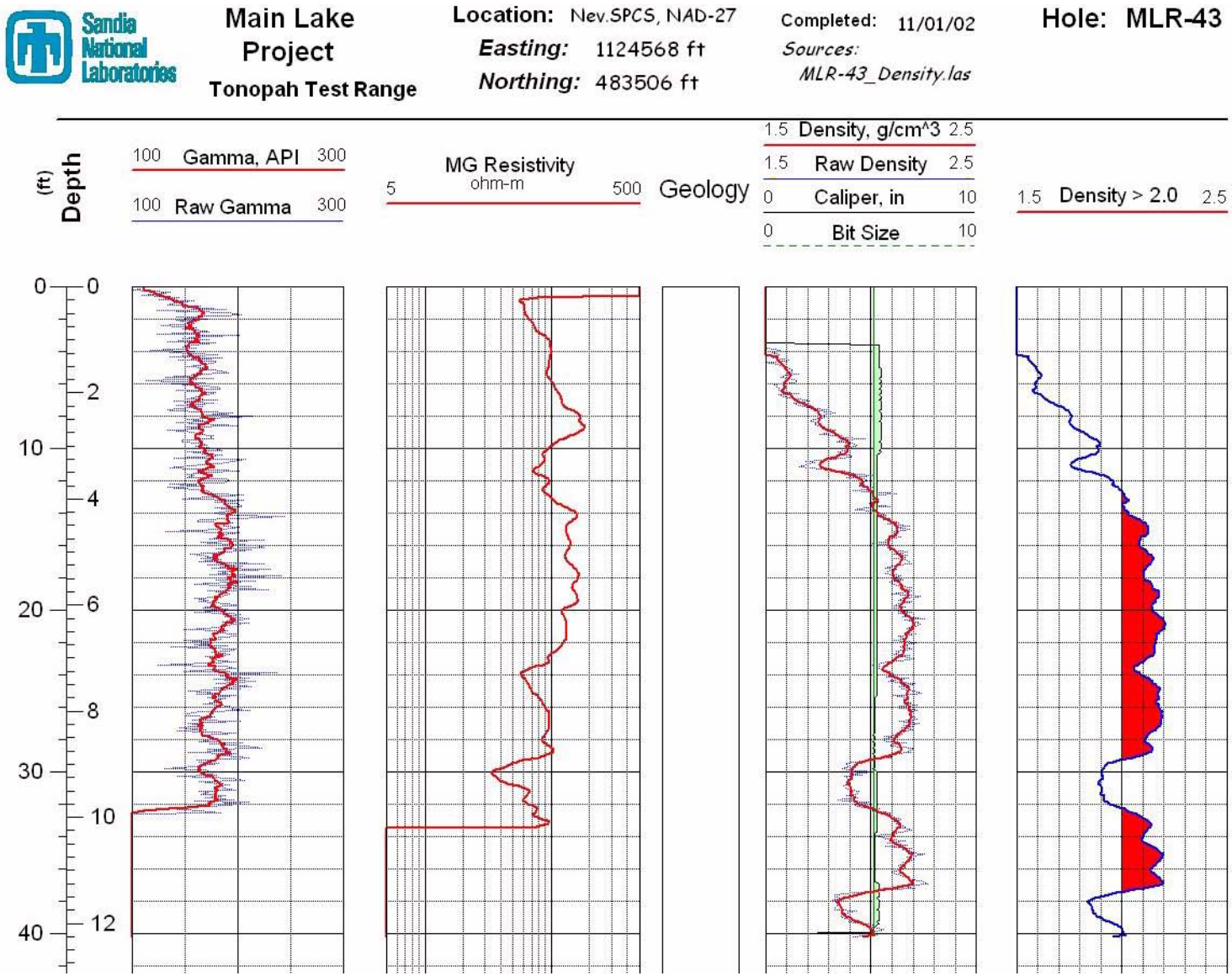

Figure C-58 Geophysical logs for drill hole MLR-43

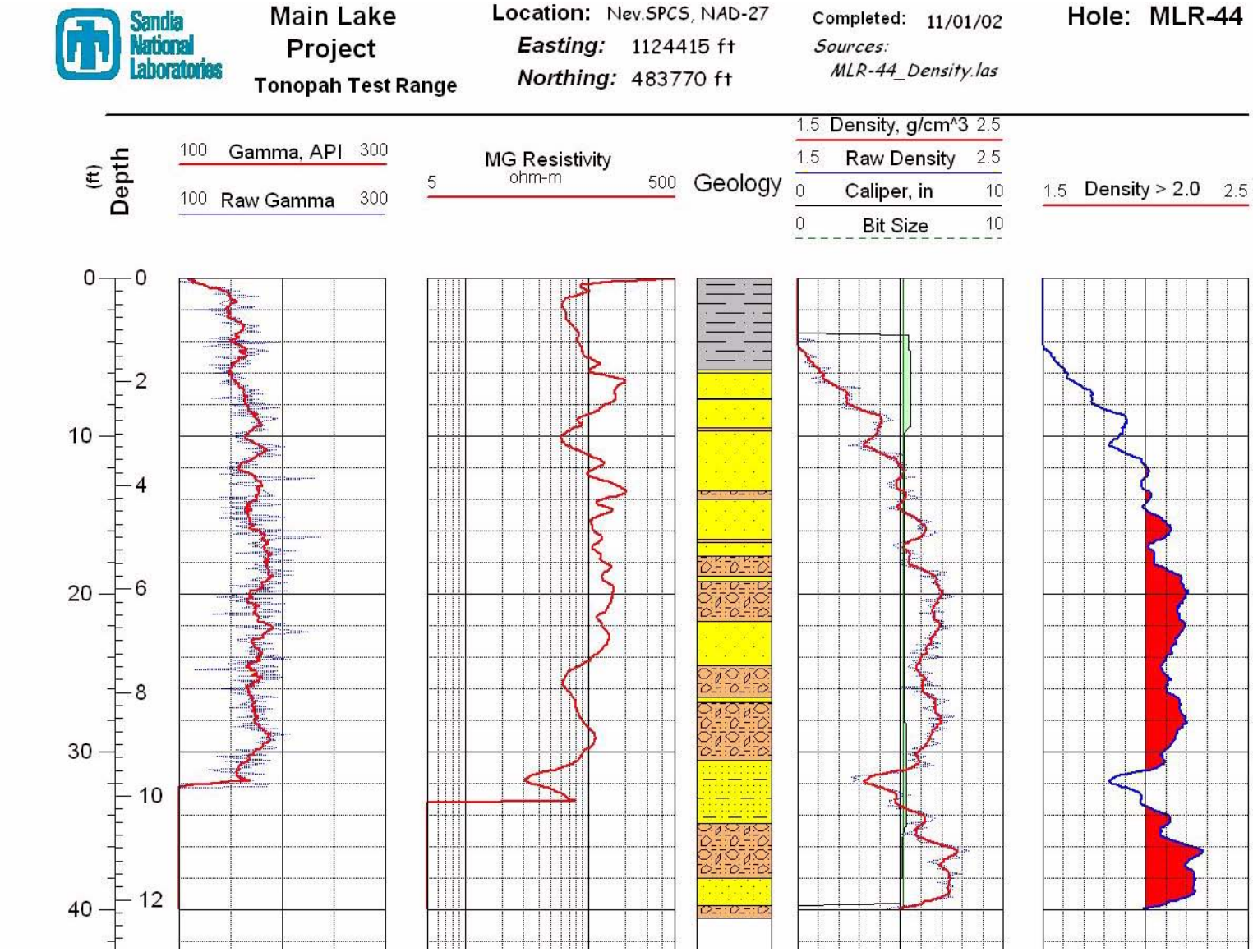

Figure C-59 Geophysical logs for drill hole ML-44. Hole MLR-44 is a rotary hole but the geology is shown for nearby core hole ML-1.

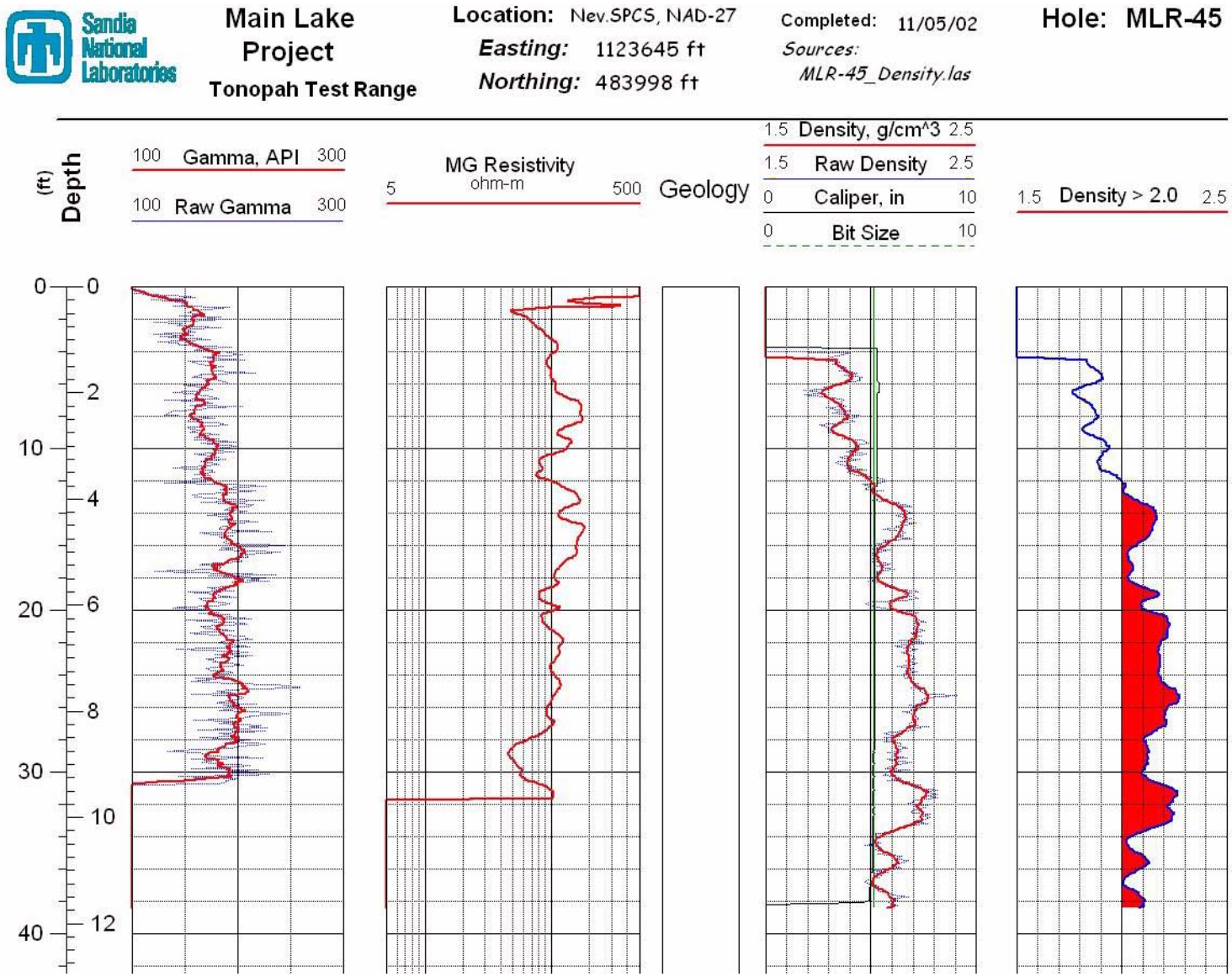

Figure C-60 Geophysical logs for drill hole MLR-45

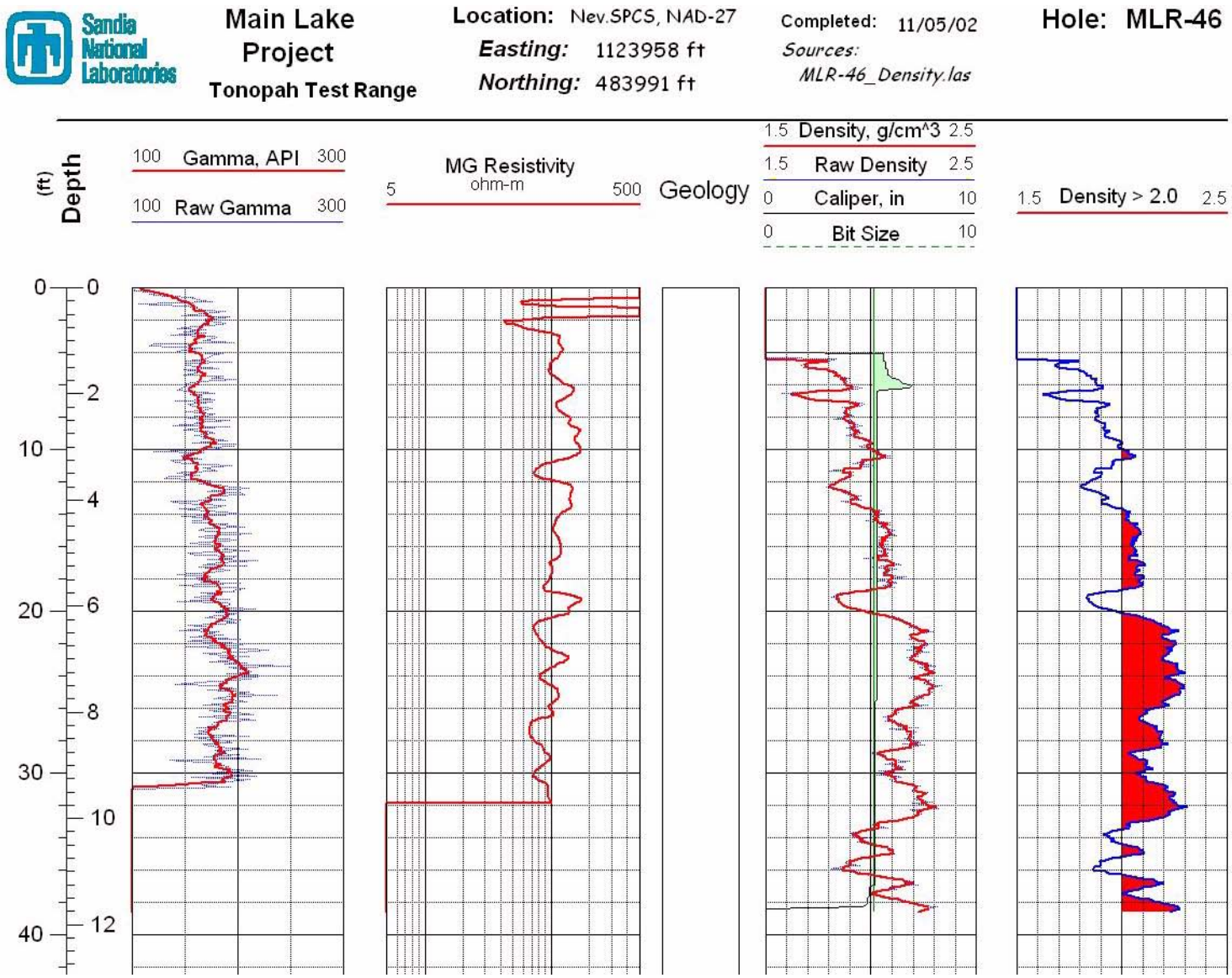

Figure C-61 Geophysical logs for drill hole MLR-46

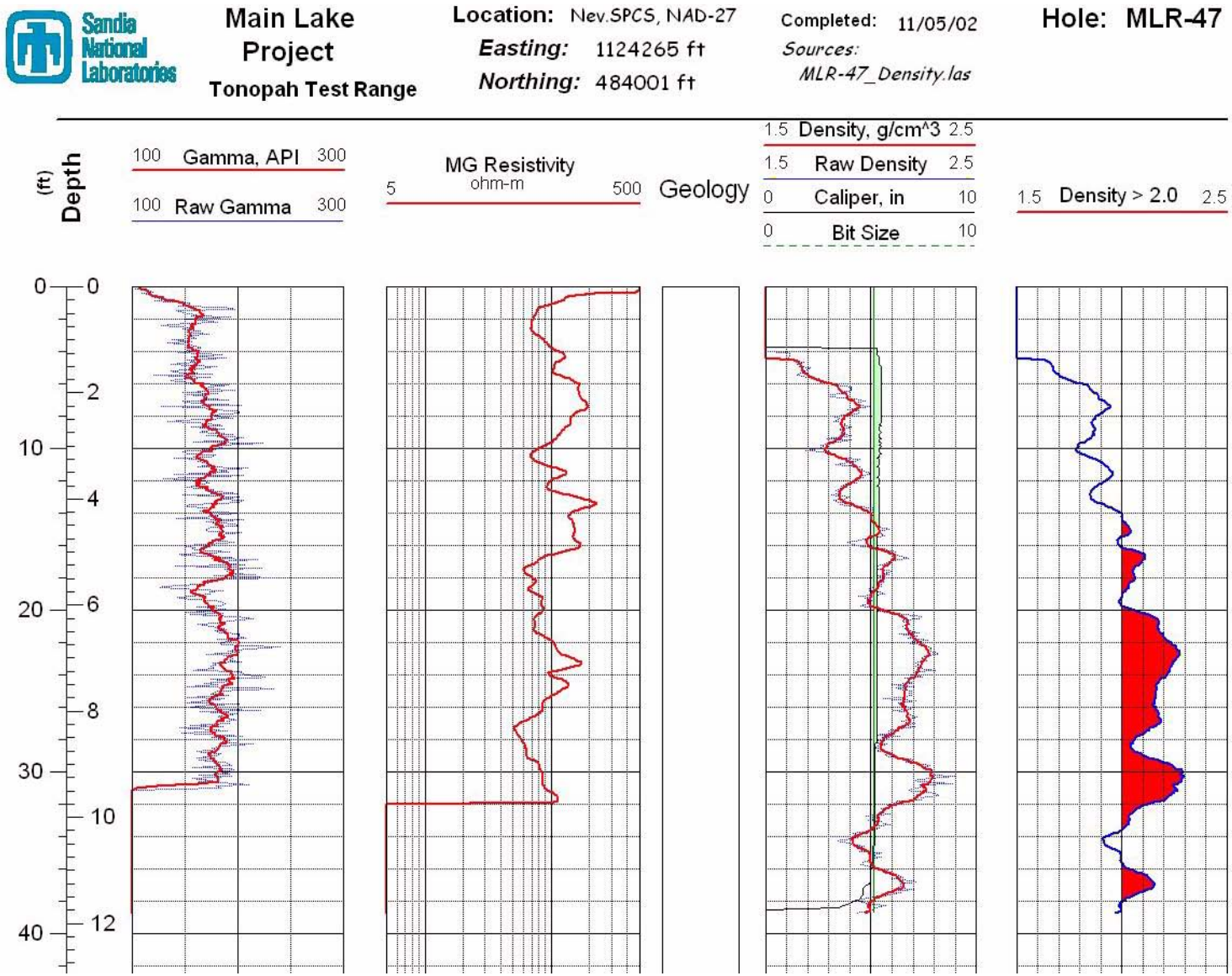

Figure C-62 Geophysical logs for drill hole MLR-47

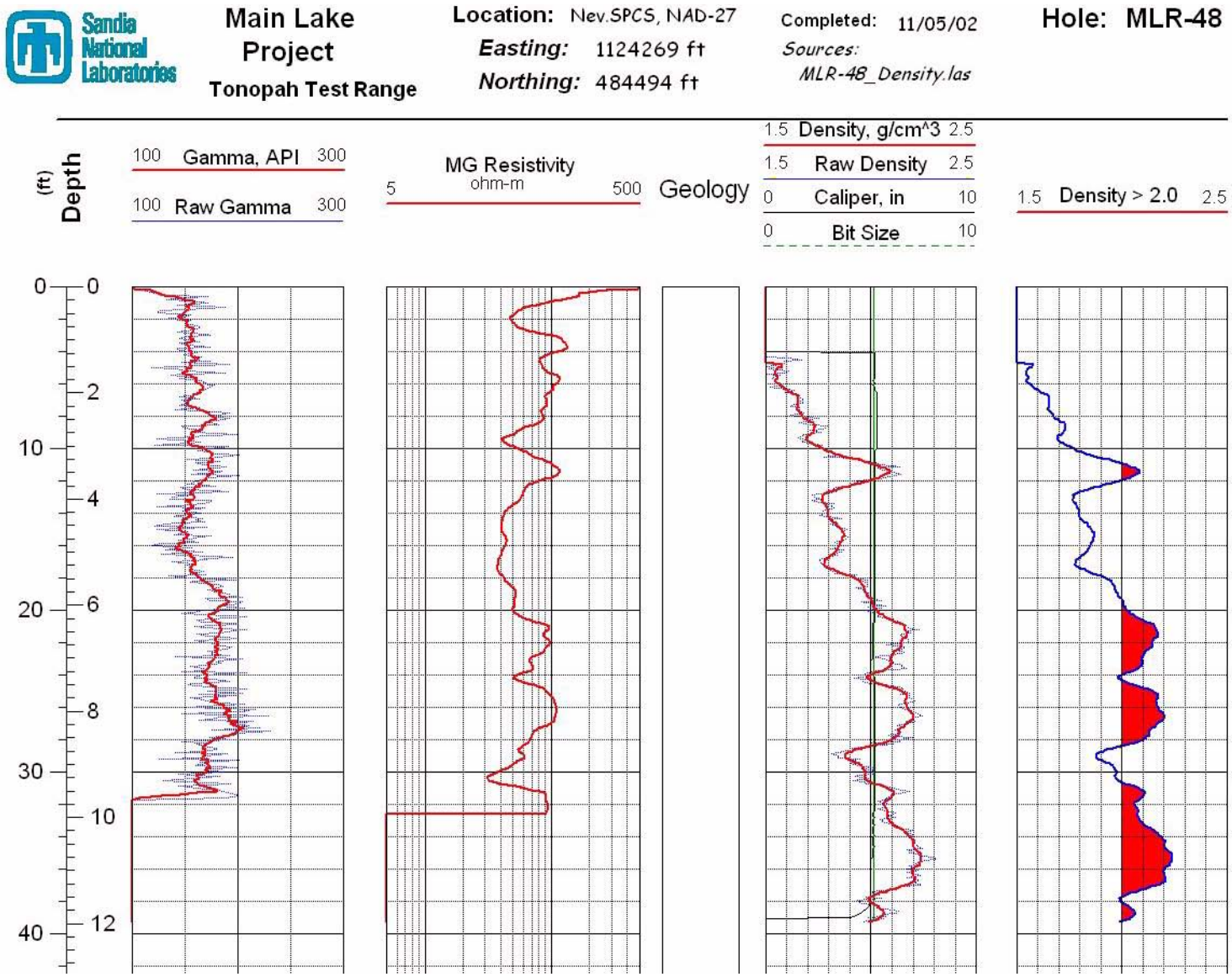

Figure C-63 Geophysical logs for drill hole MLR-48

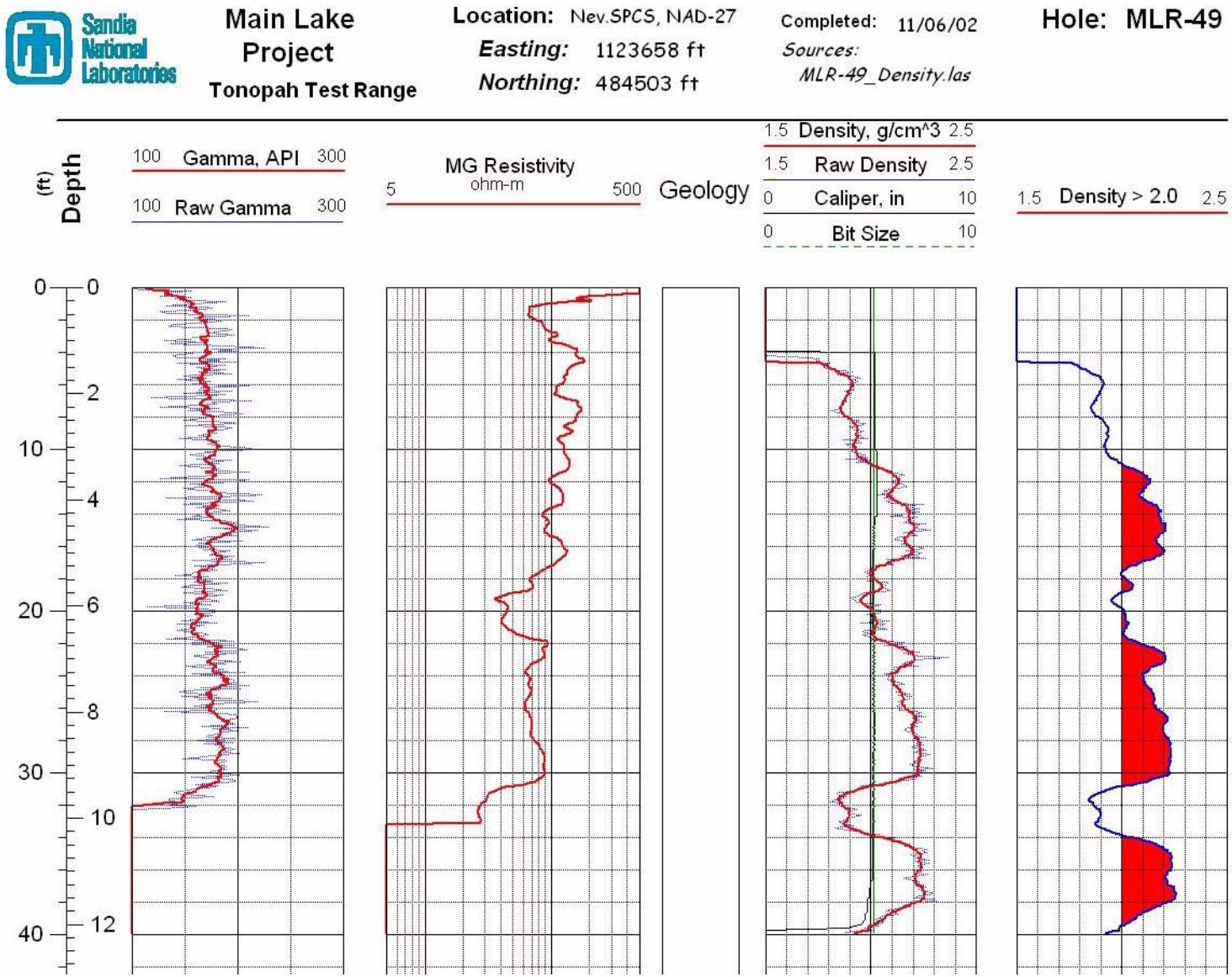

Figure C-64 Geophysical logs for drill hole MLR-49

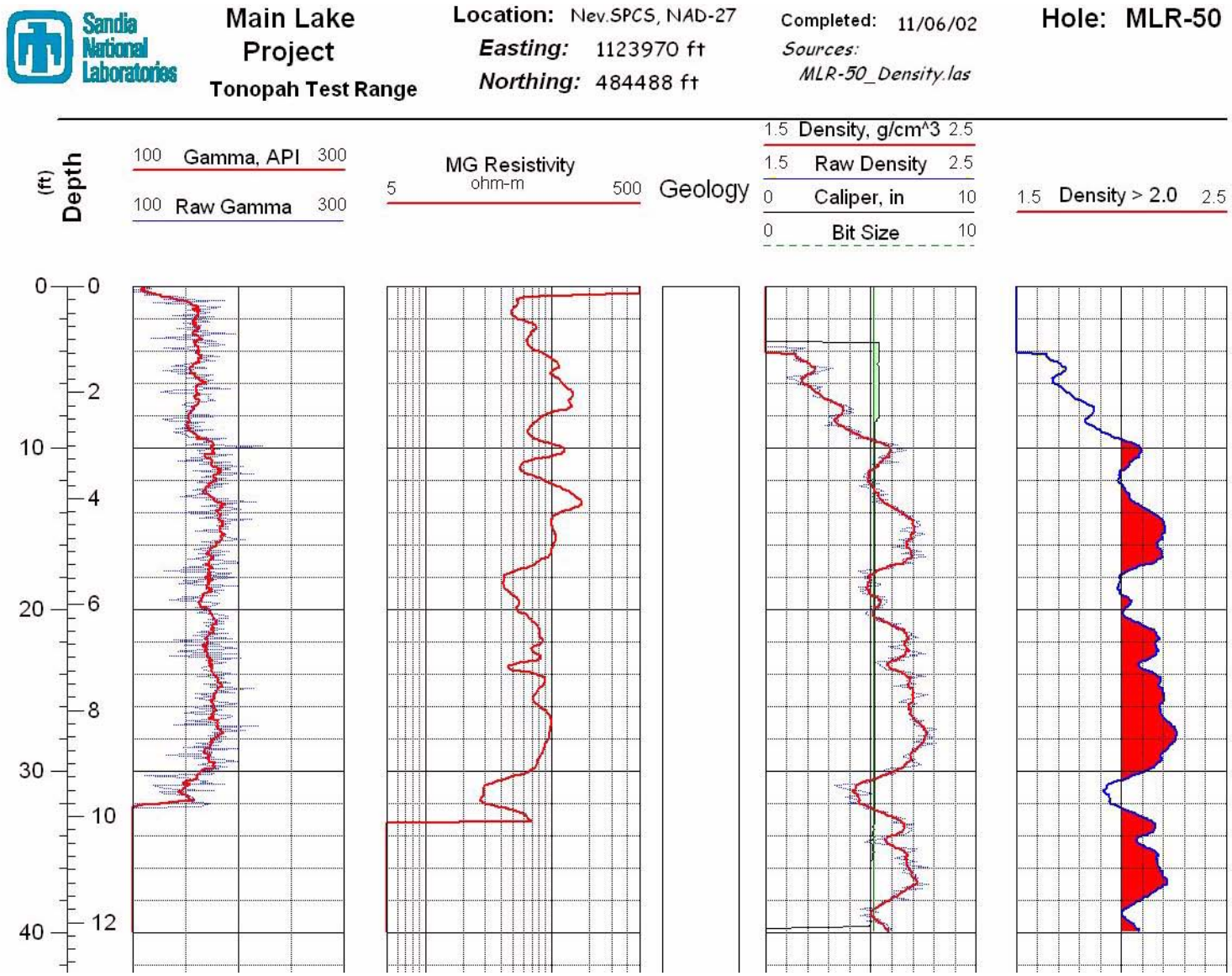

Figure C-65 Geophysical logs for drill hole MLR-50

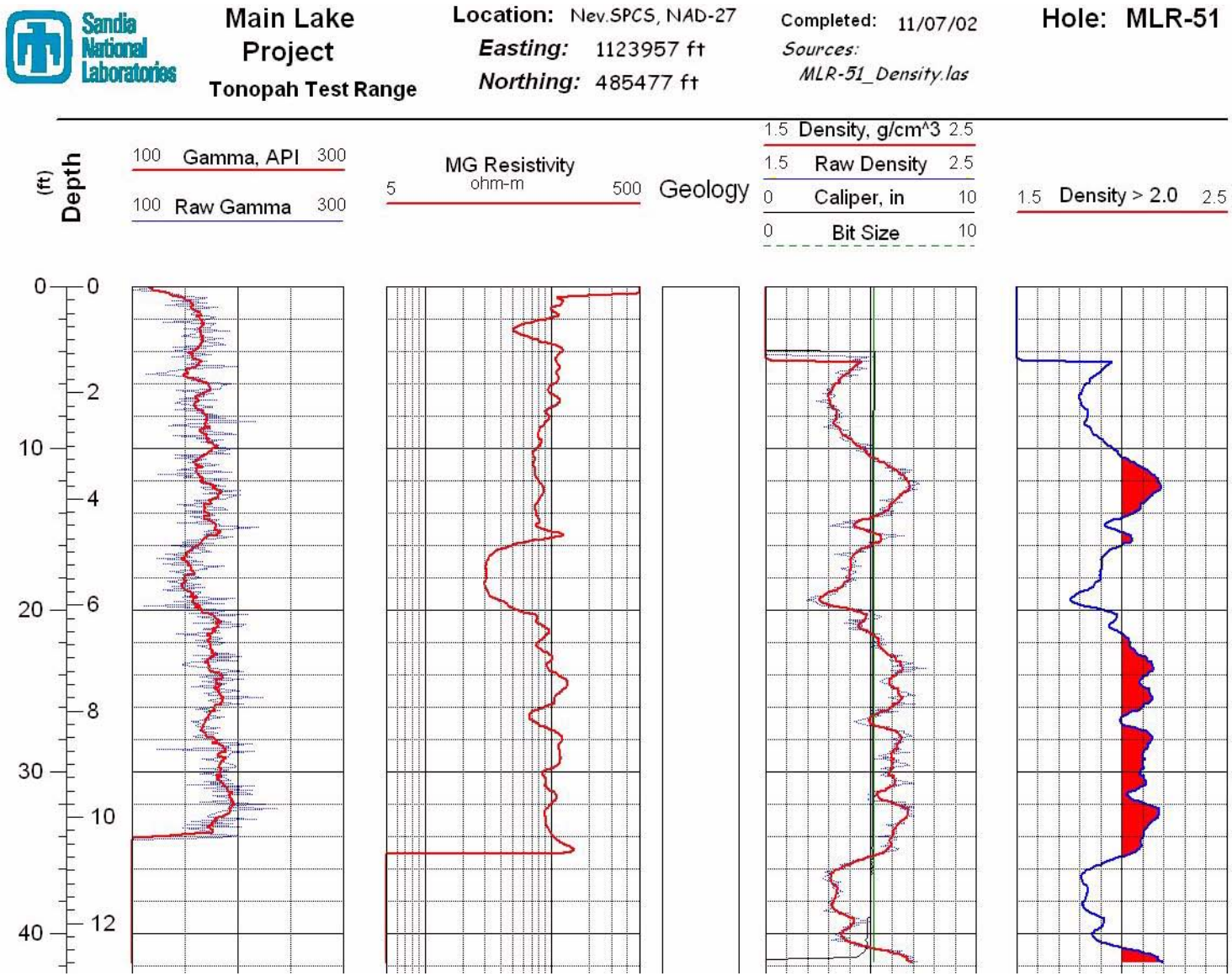

Figure C-66 Geophysical logs for drill hole MLR-51

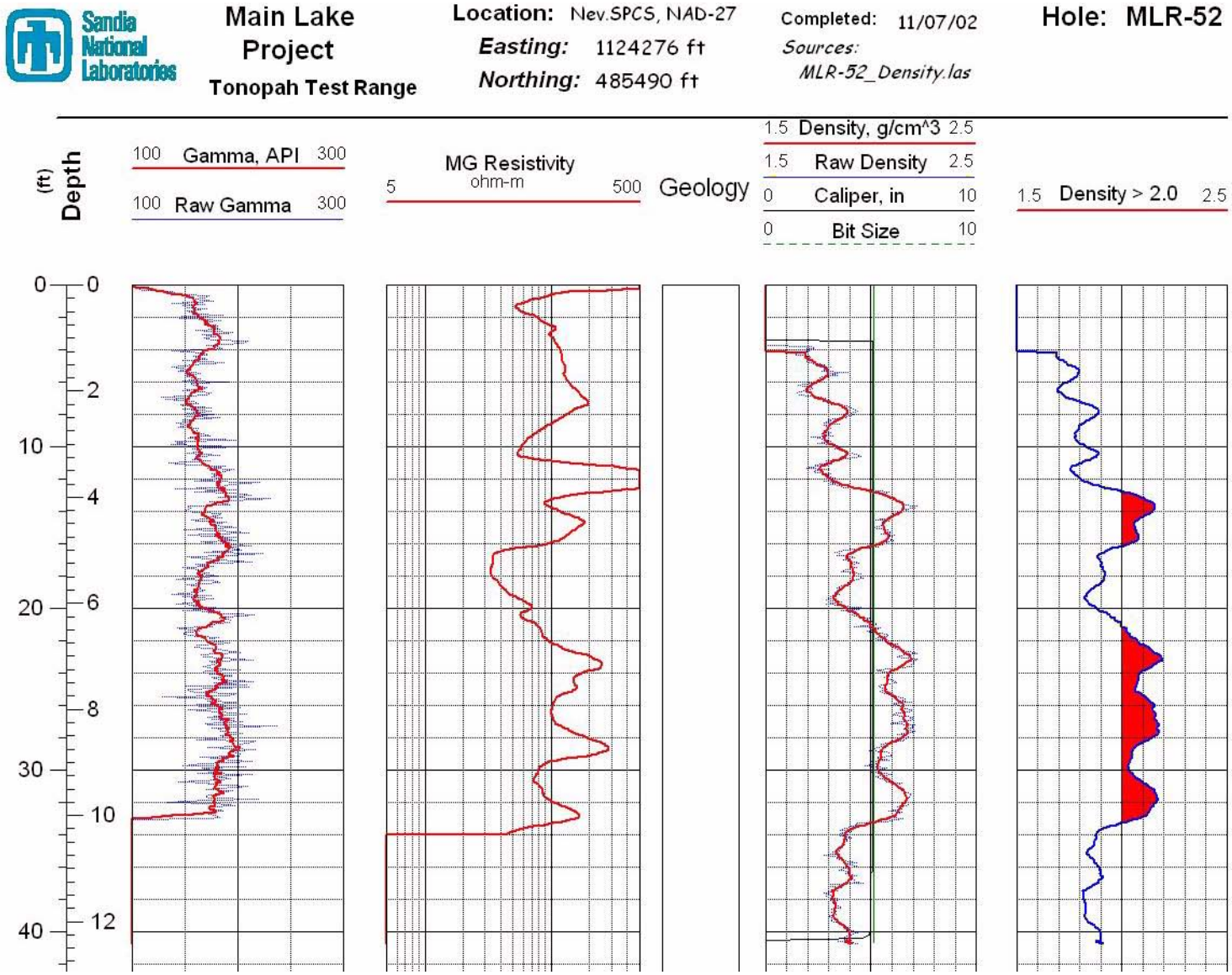

Figure C-67 Geophysical logs for drill hole MLR-52

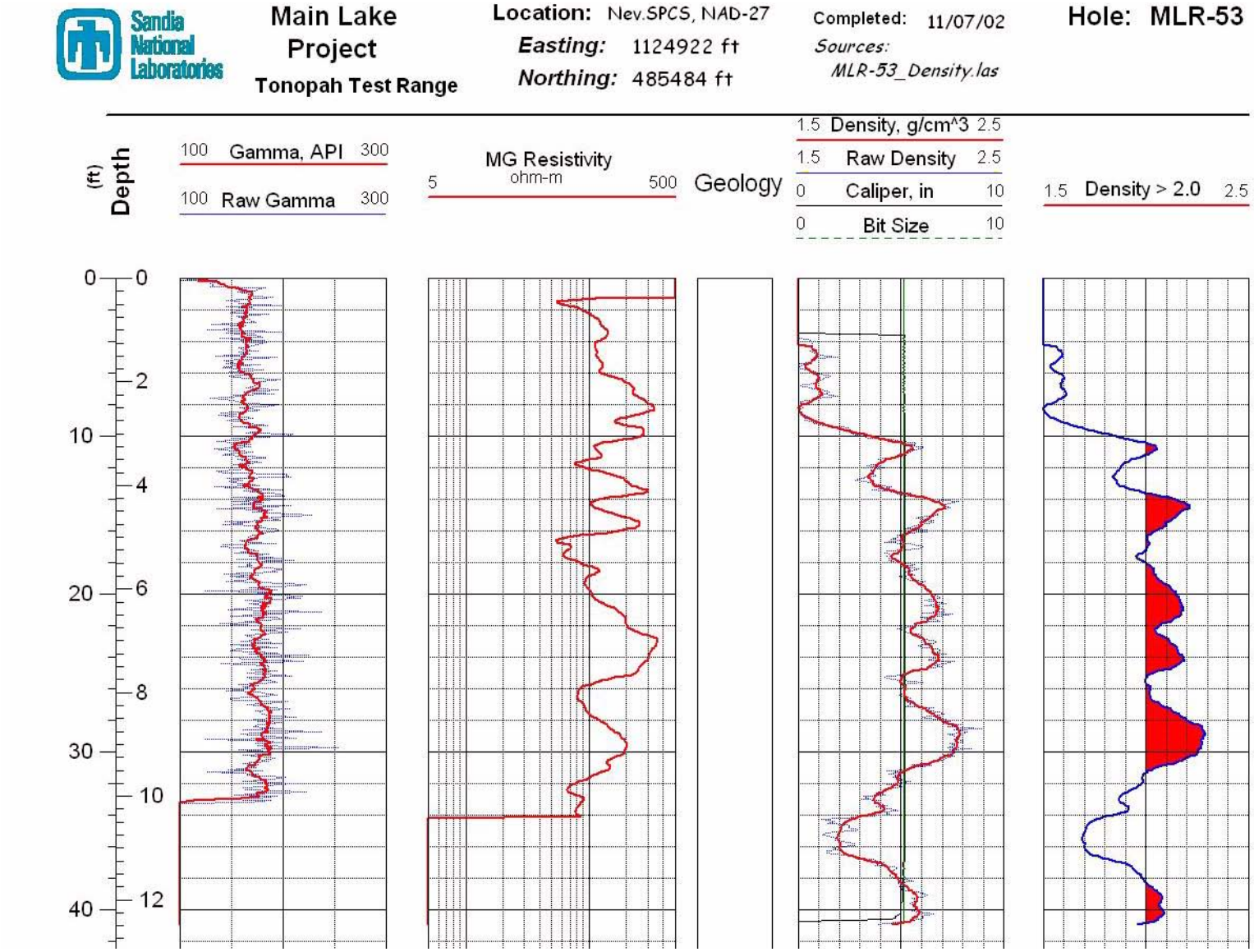

Figure C-68 Geophysical logs for drill hole MLR-53

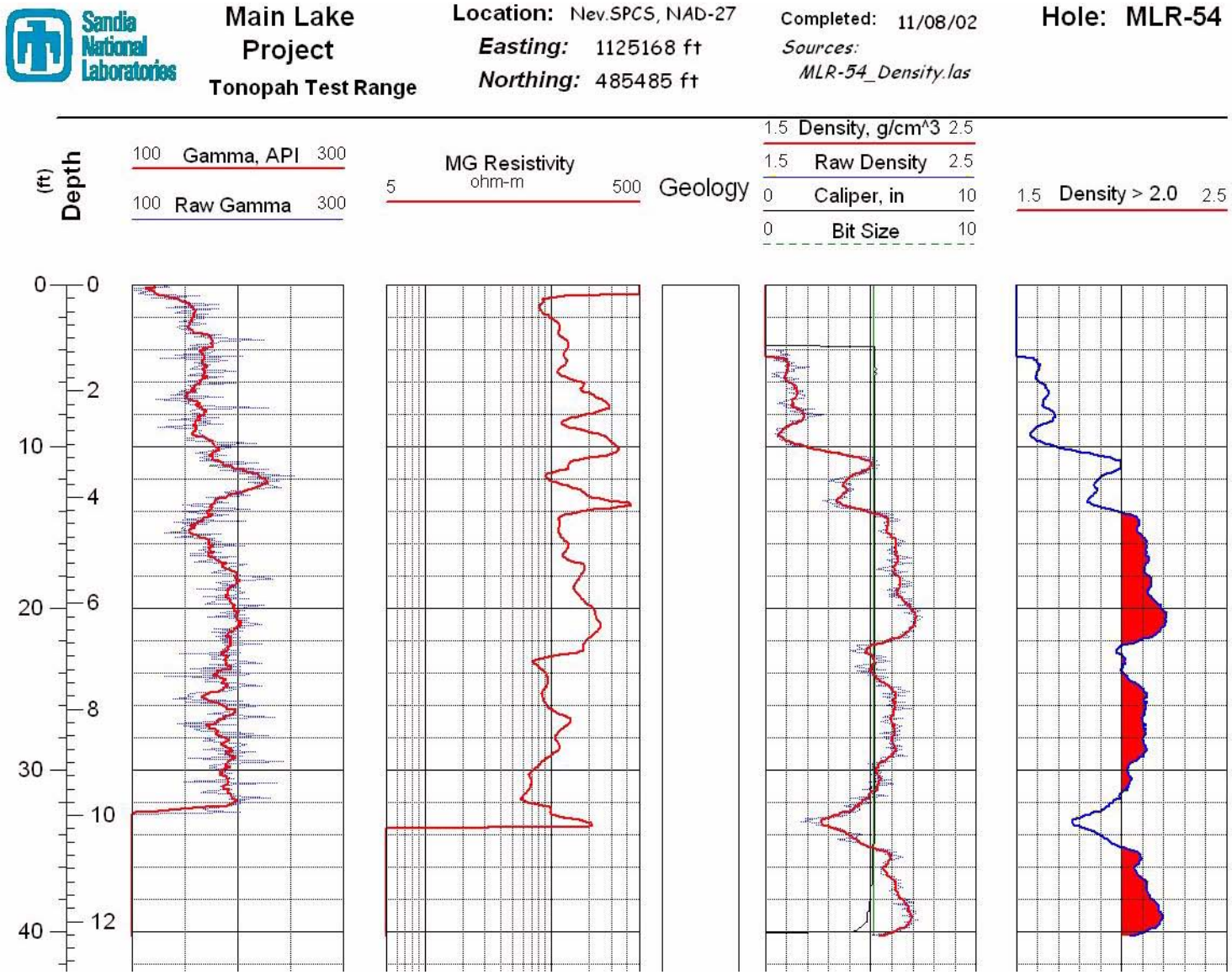

Figure C-69 Geophysical logs for drill hole MLR-54

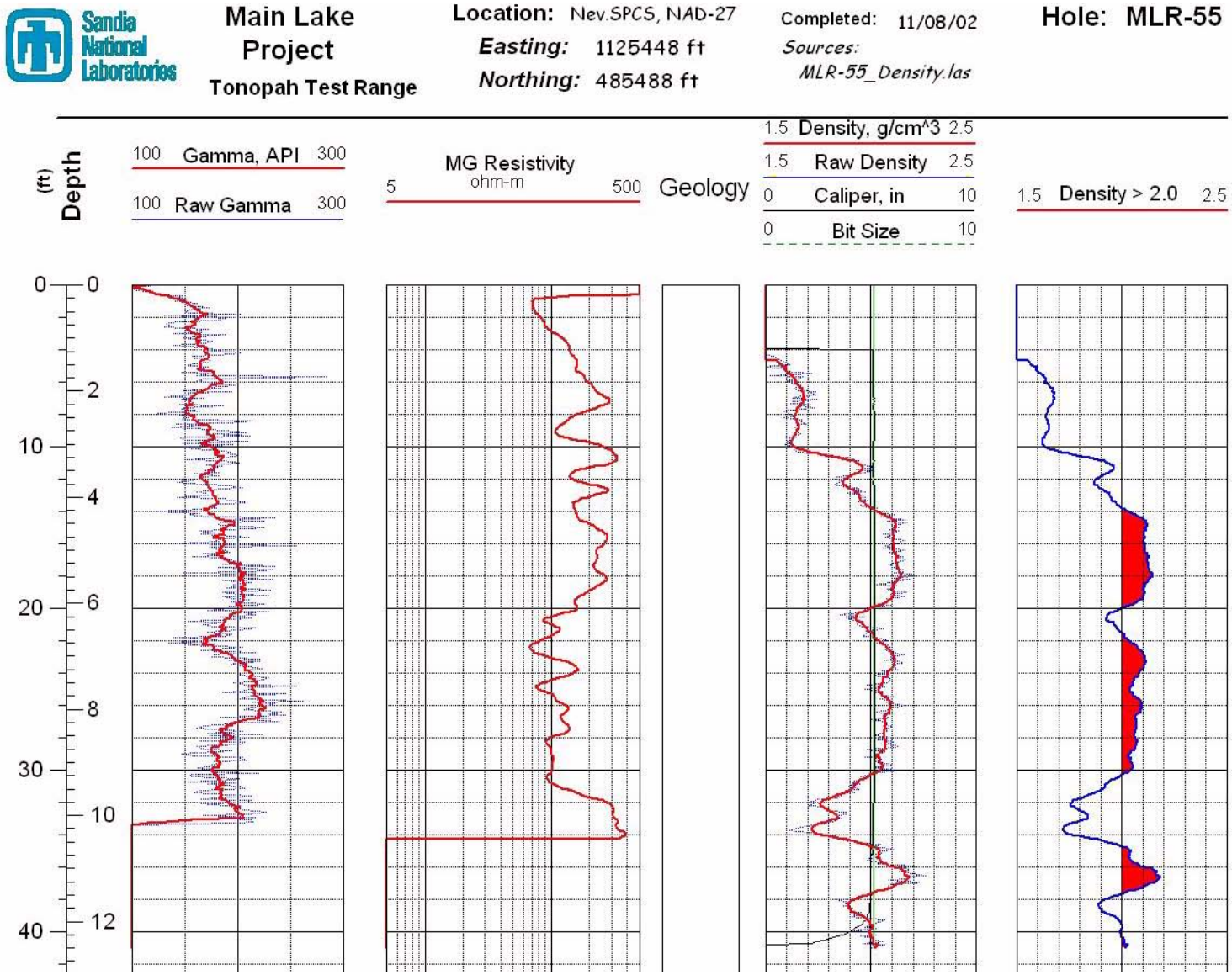

Figure C-70 Geophysical logs for drill hole MLR-55

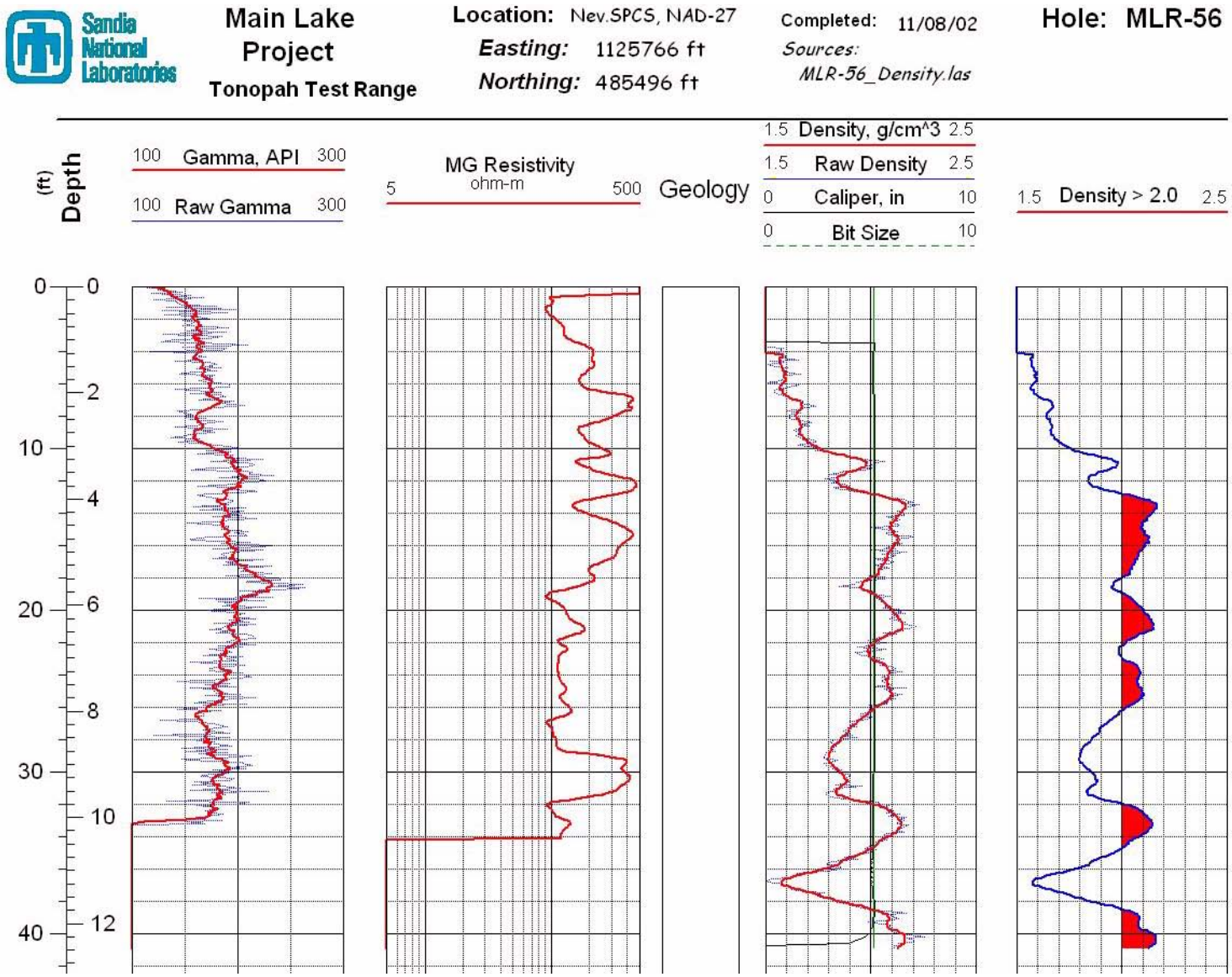

Figure C-71 Geophysical logs for drill hole MLR-56

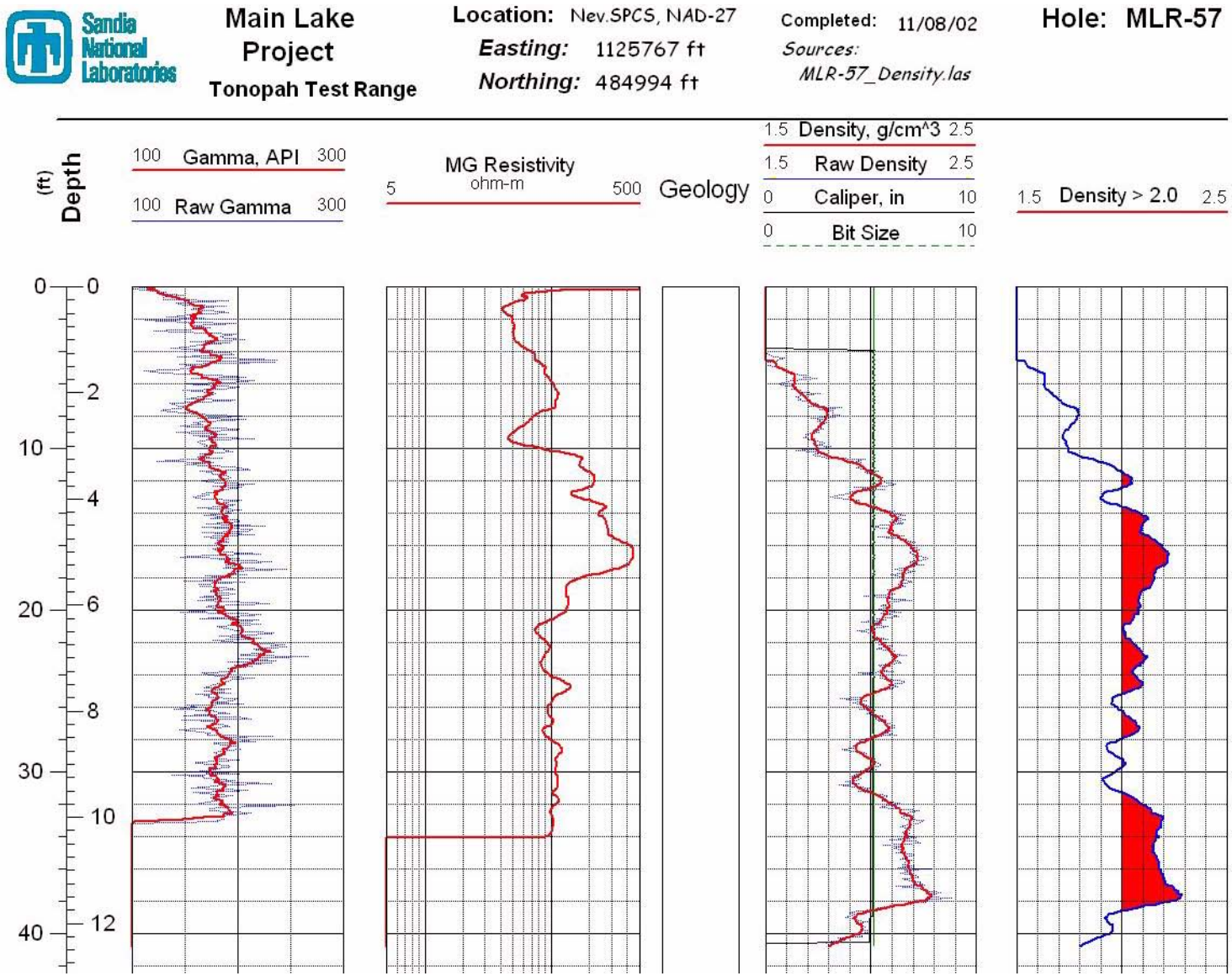

Figure C-72 Geophysical logs for drill hole MLR-57

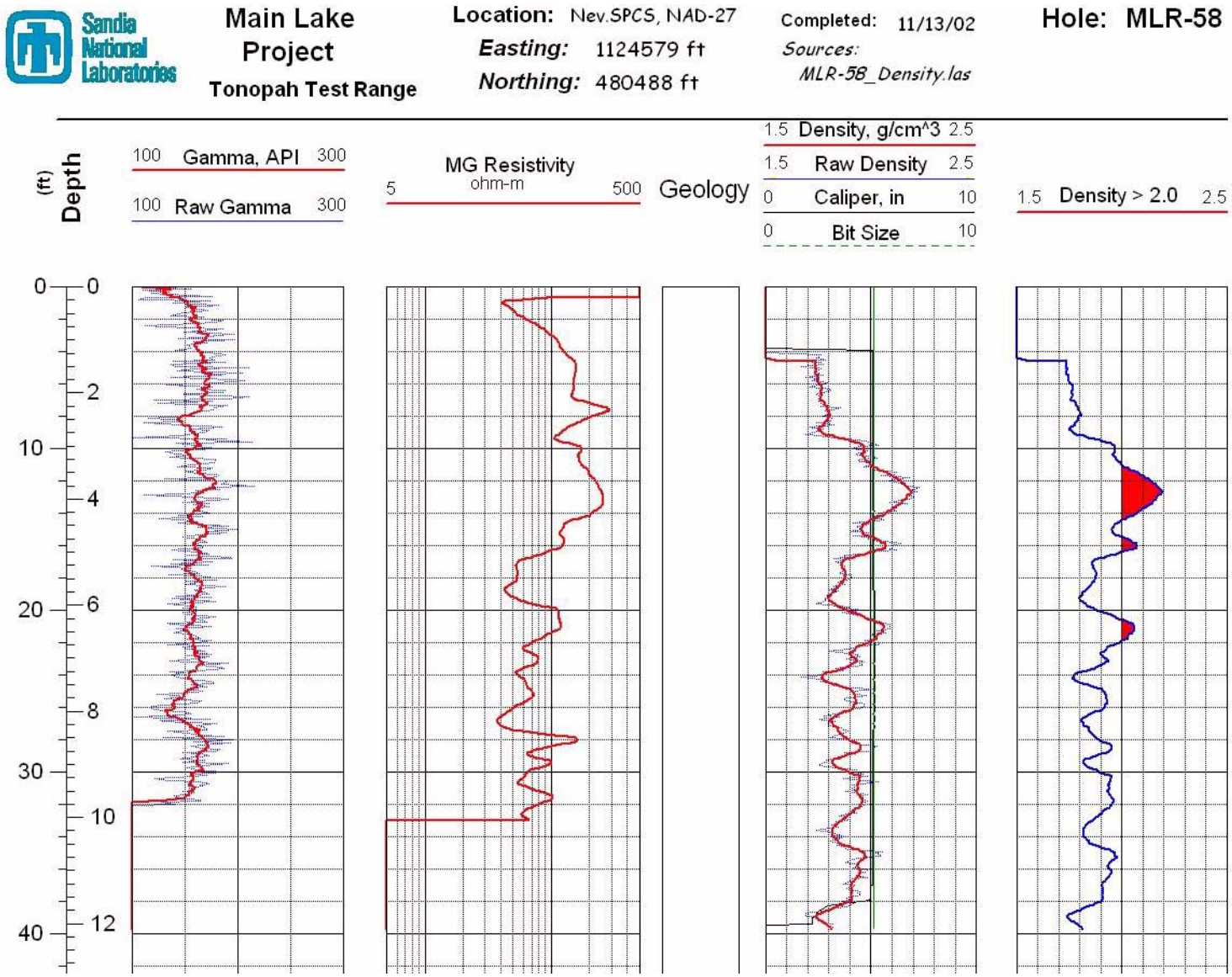

Figure C-73 Geophysical logs for drill hole MLR-58

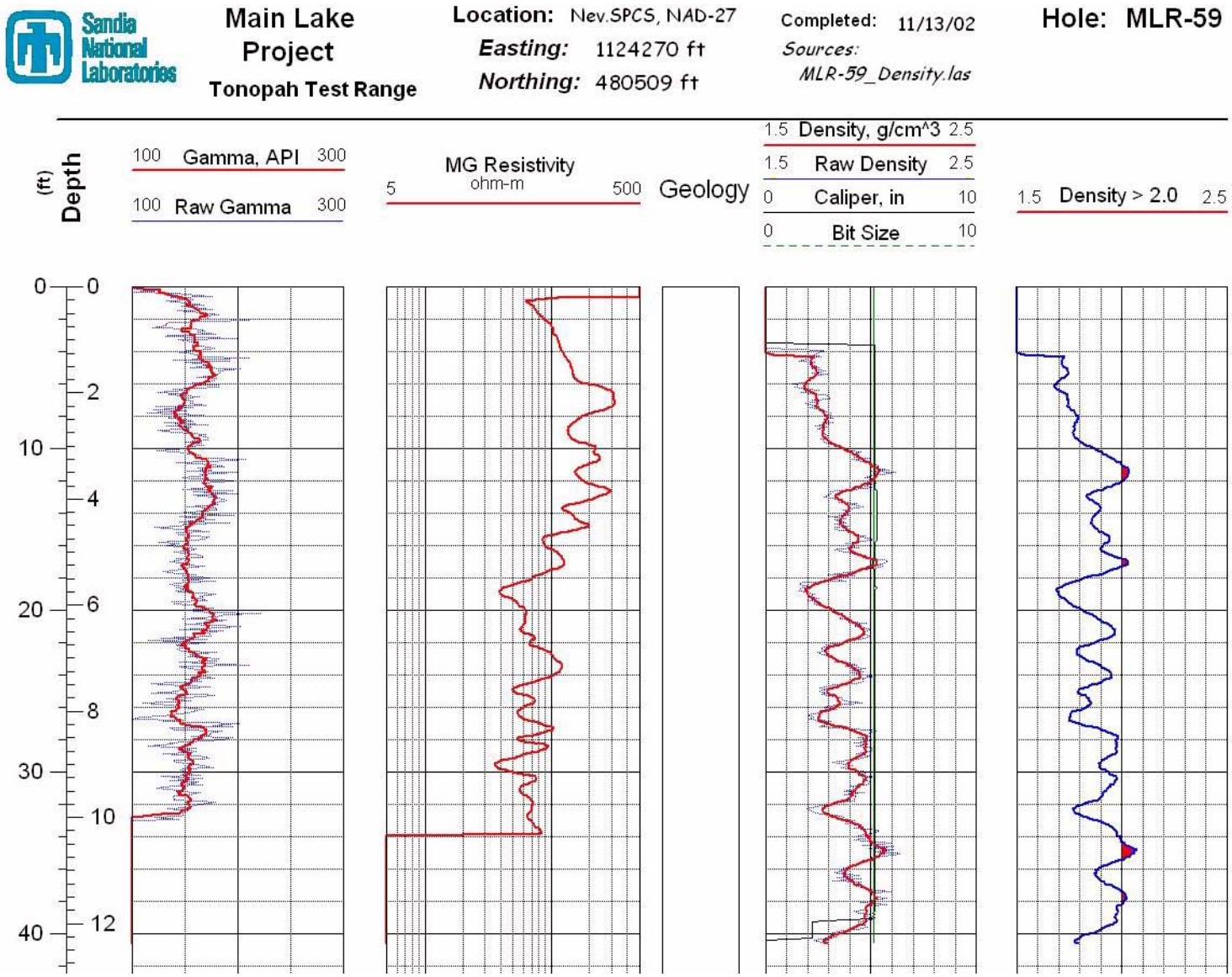

Figure C-74 Geophysical logs for drill hole MLR-59

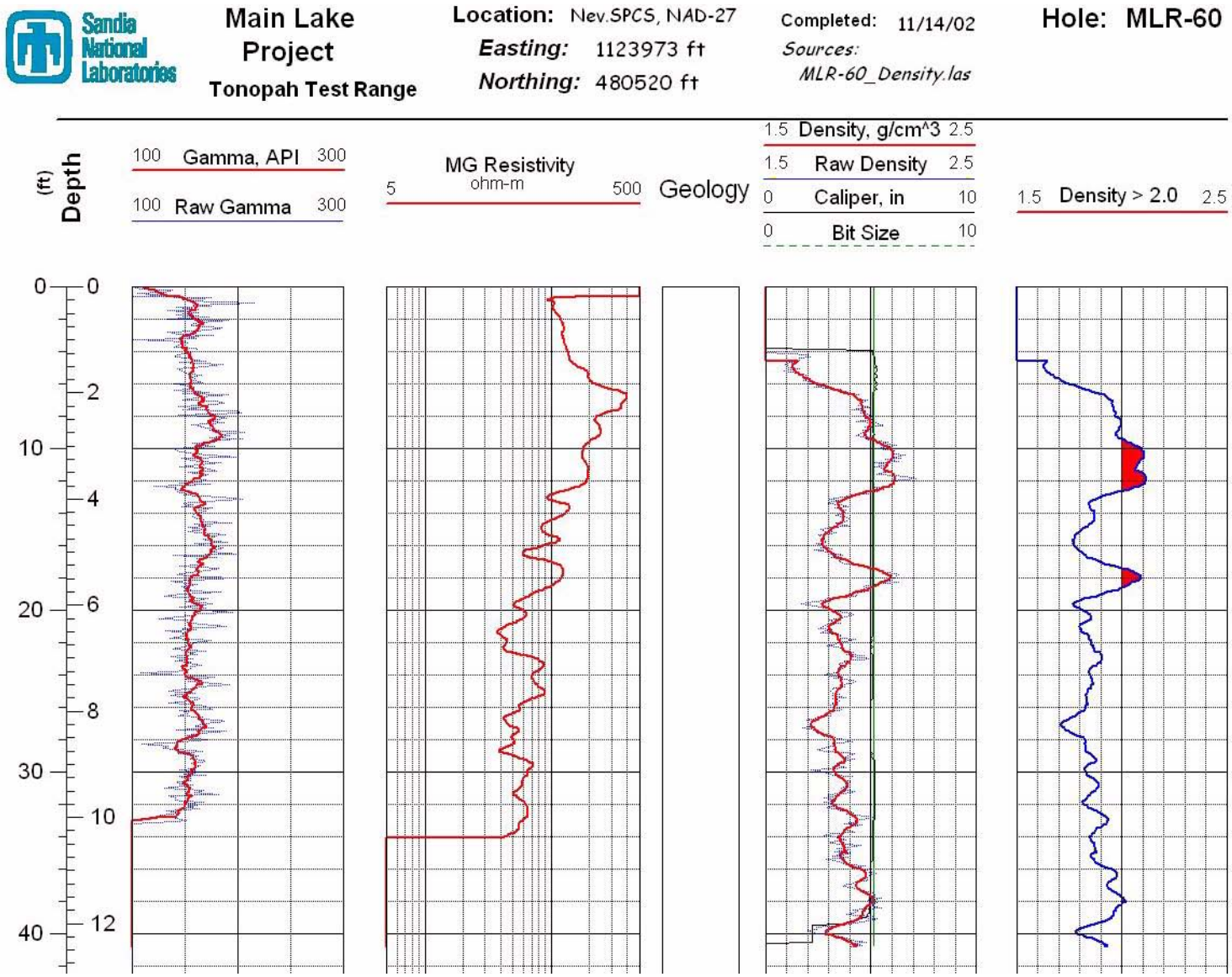

Figure C-75 Geophysical logs for drill hole MLR-60

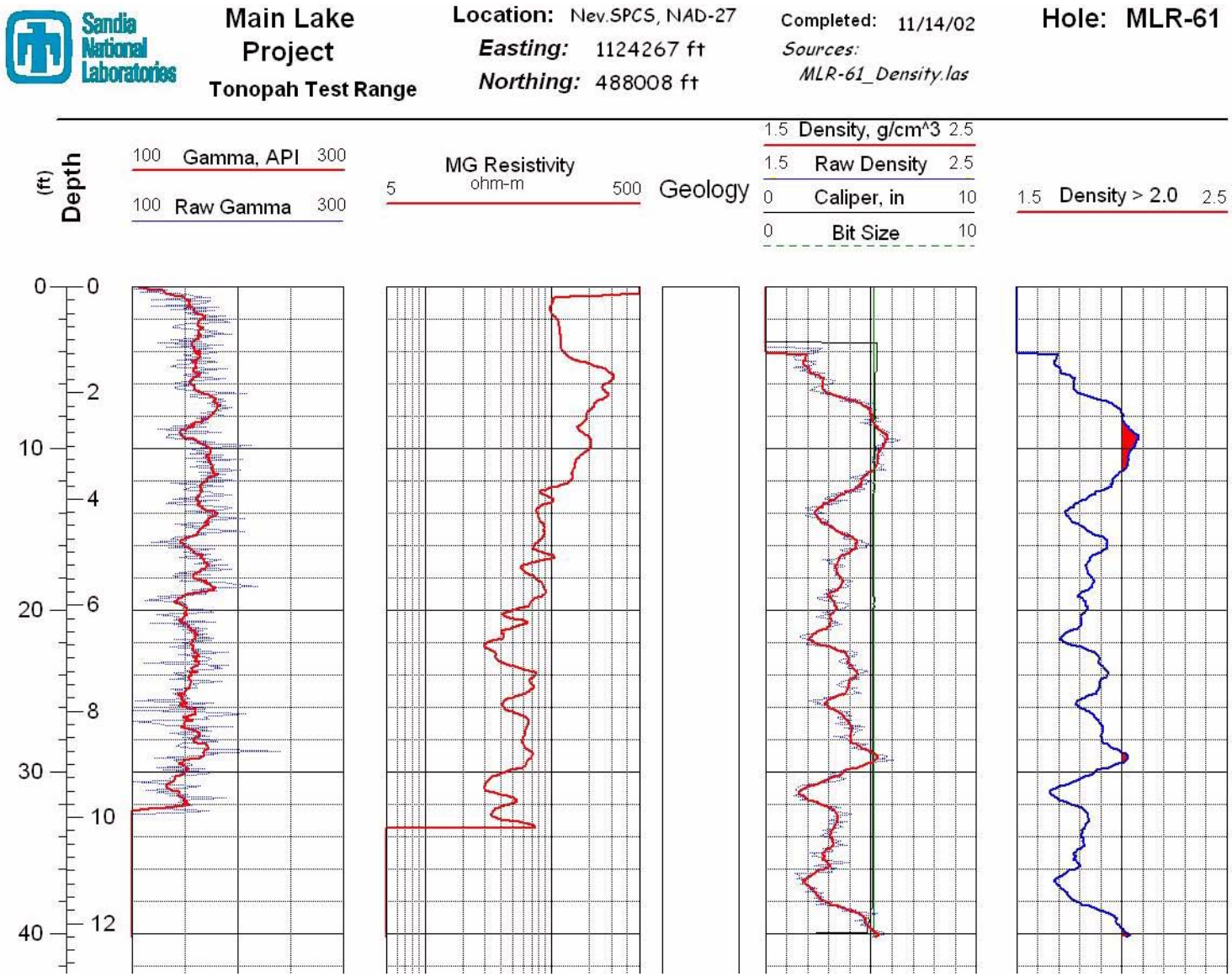

Figure C-76 Geophysical logs for drill hole MLR-61

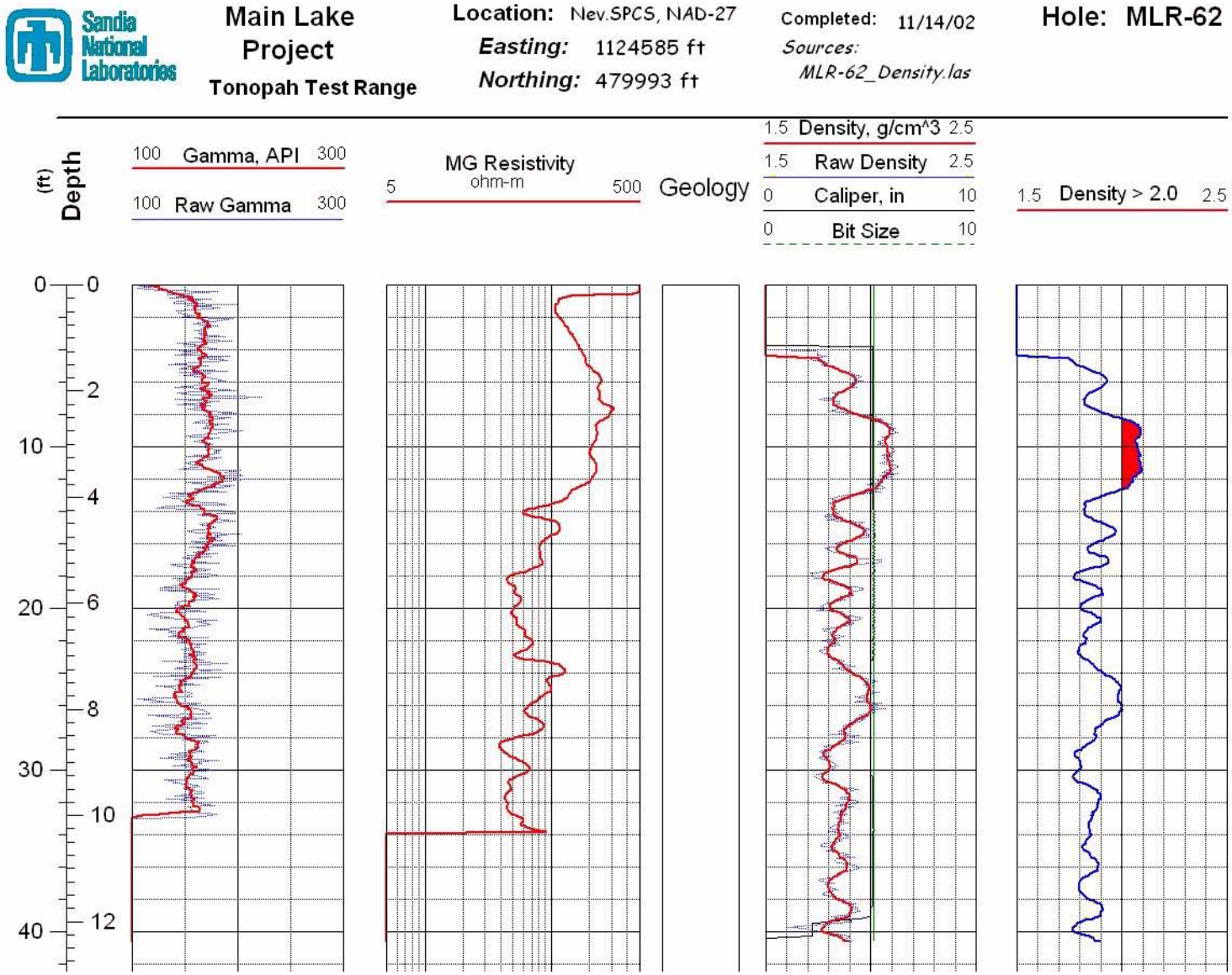

Figure C-77 Geophysical logs for drill hole MLR-62

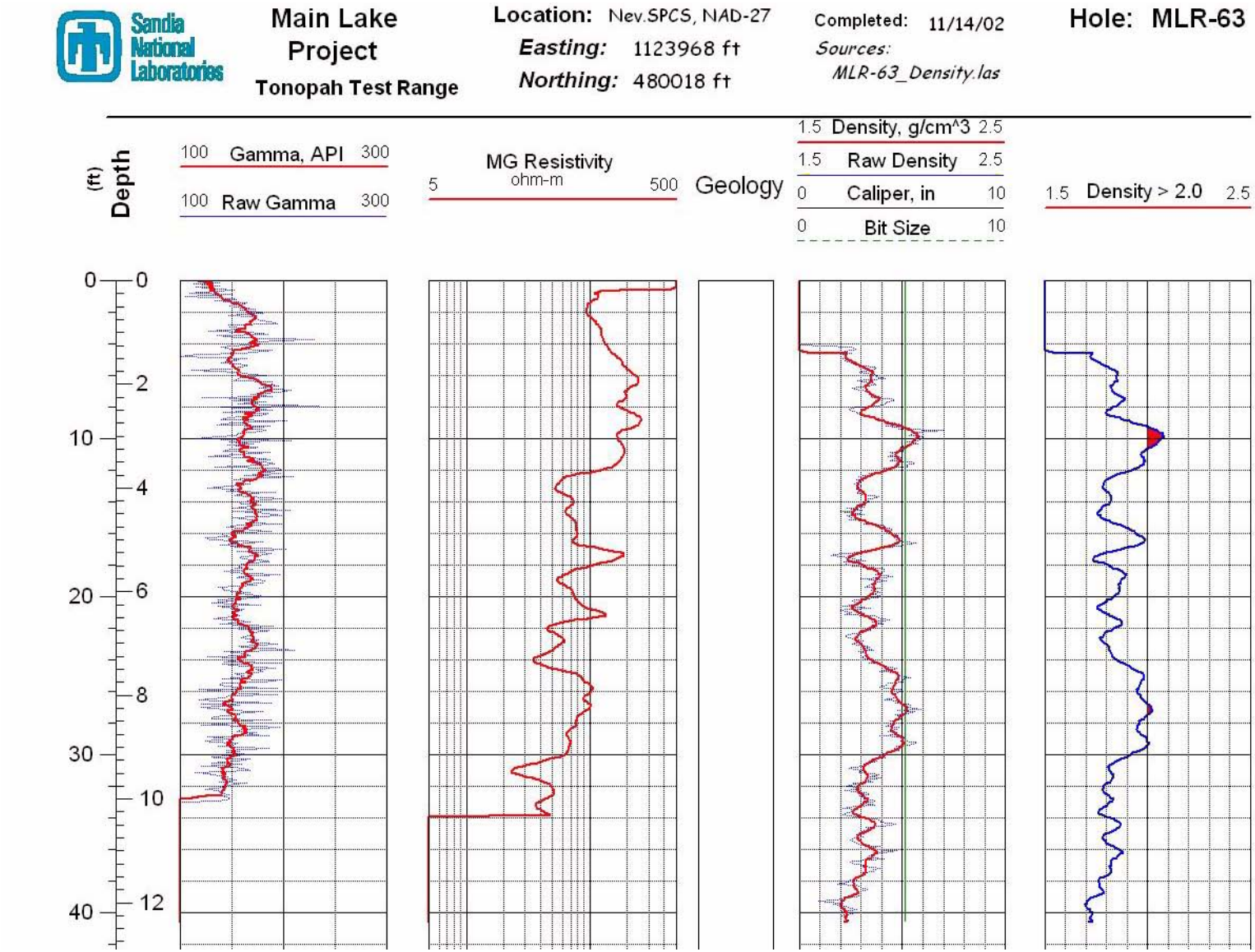

Figure C-78 Geophysical logs for drill hole MLR-63

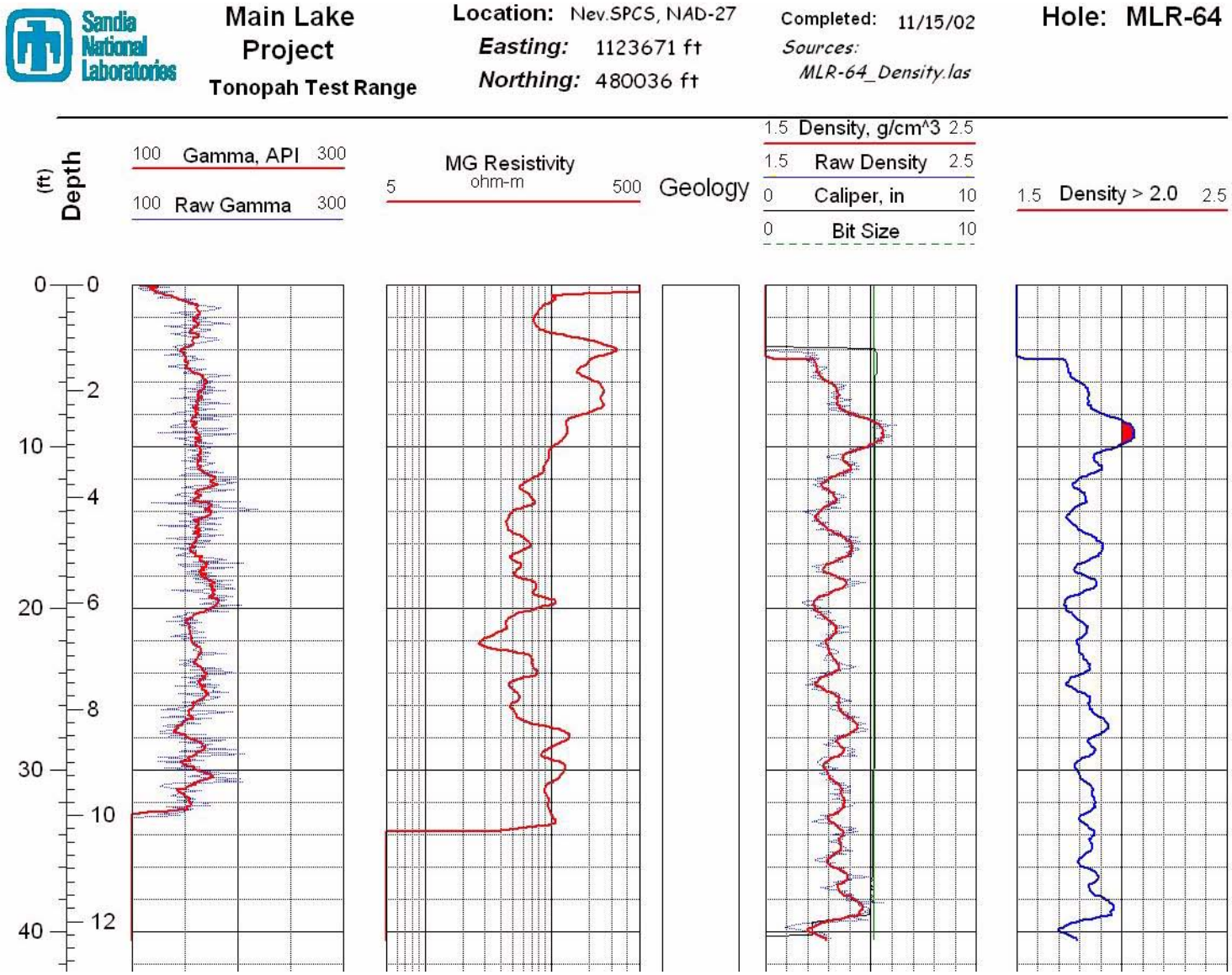

Figure C-79 Geophysical logs for drill hole MLR-64

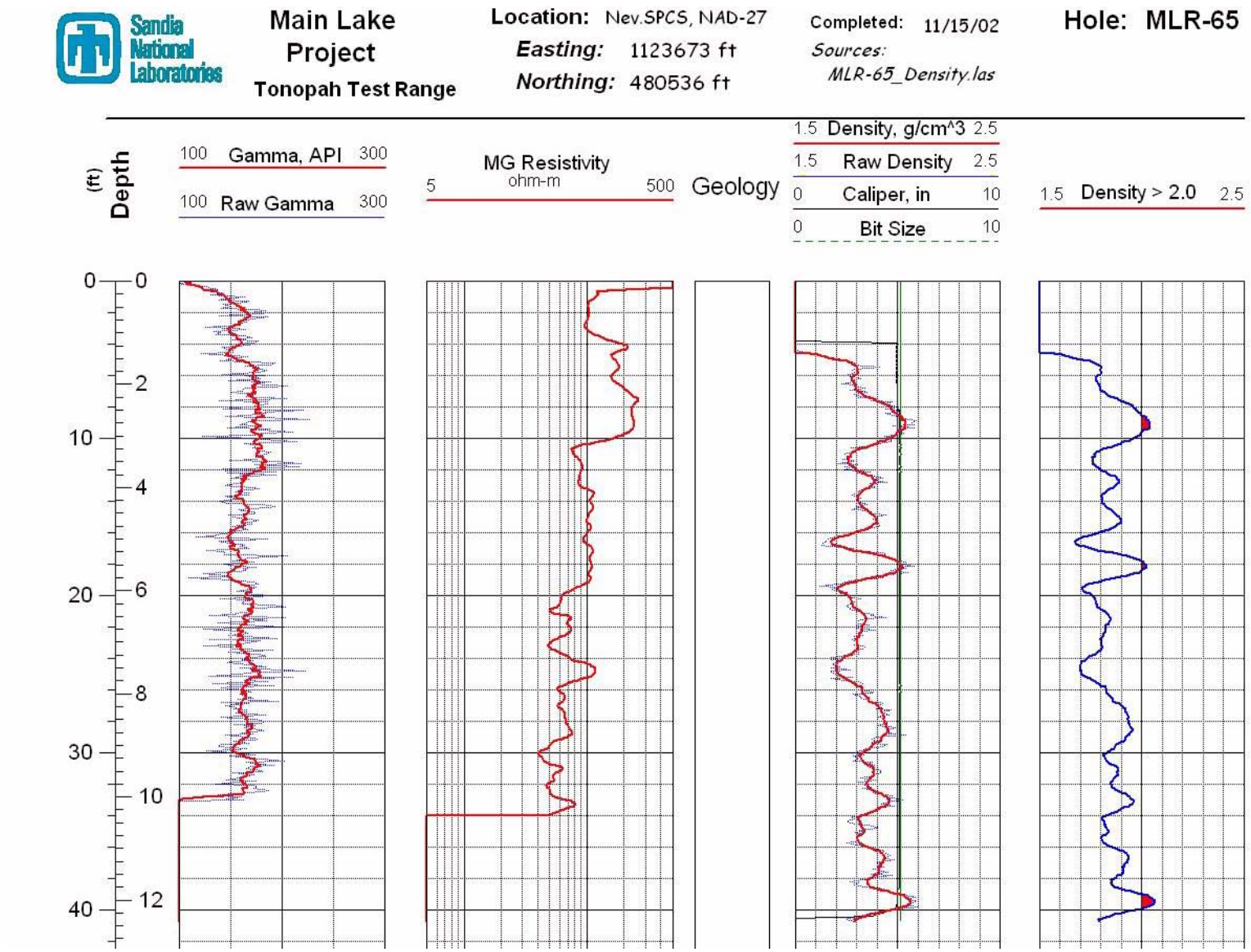

Figure C-80 Geophysical logs for drill hole MLR-65

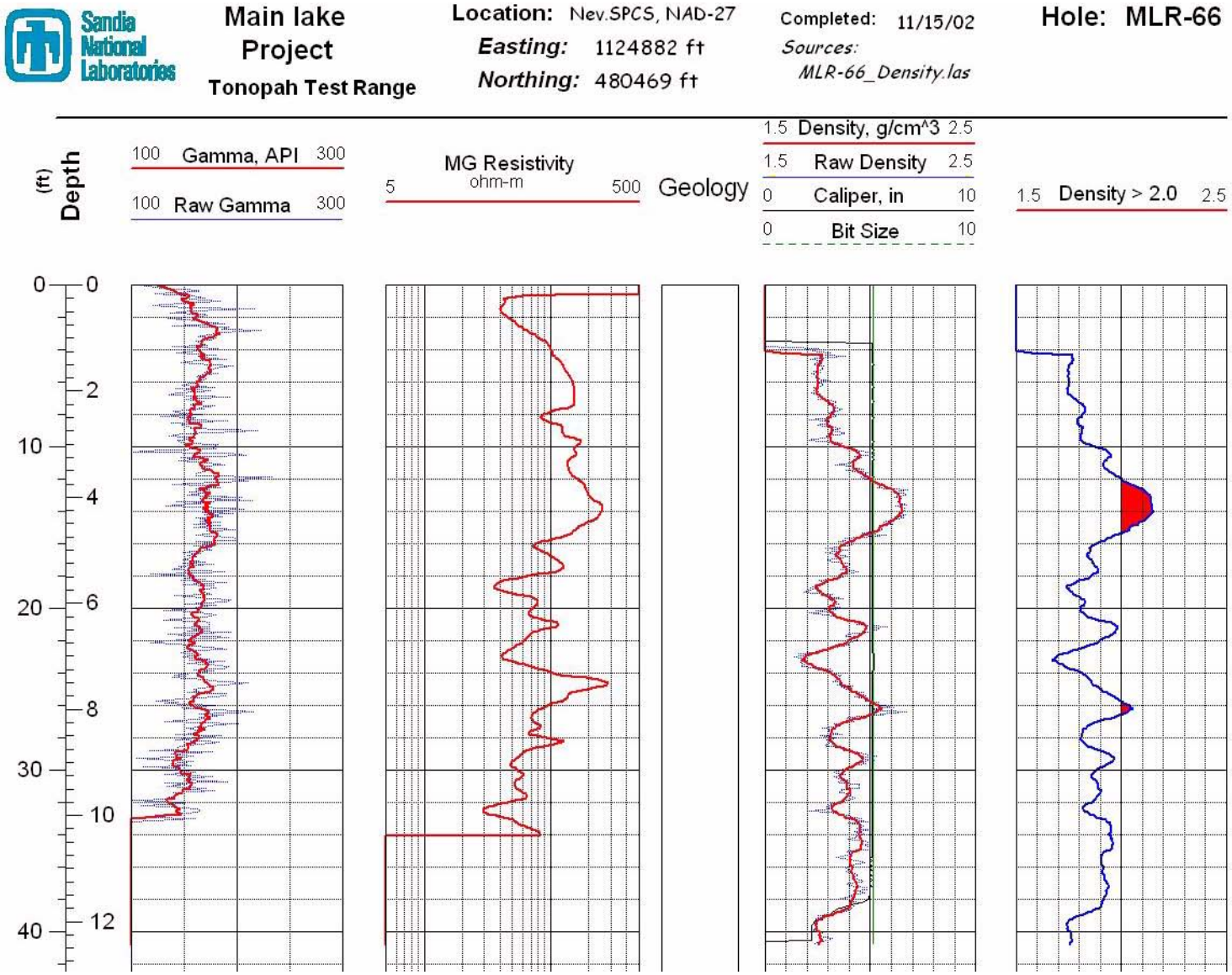

Figure C-81 Geophysical logs for drill hole MLR-66

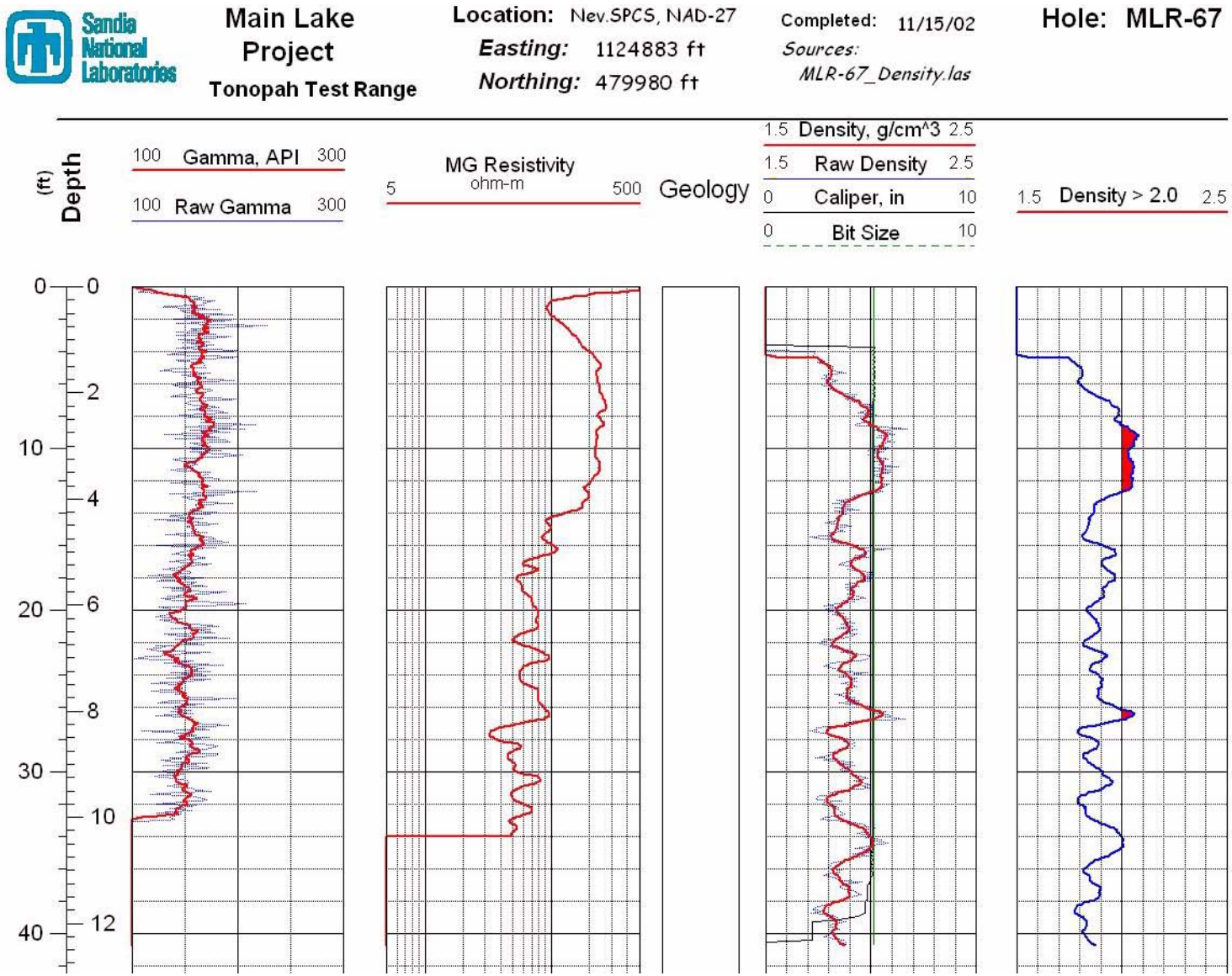

Figure C-82 Geophysical logs for drill hole MLR-67

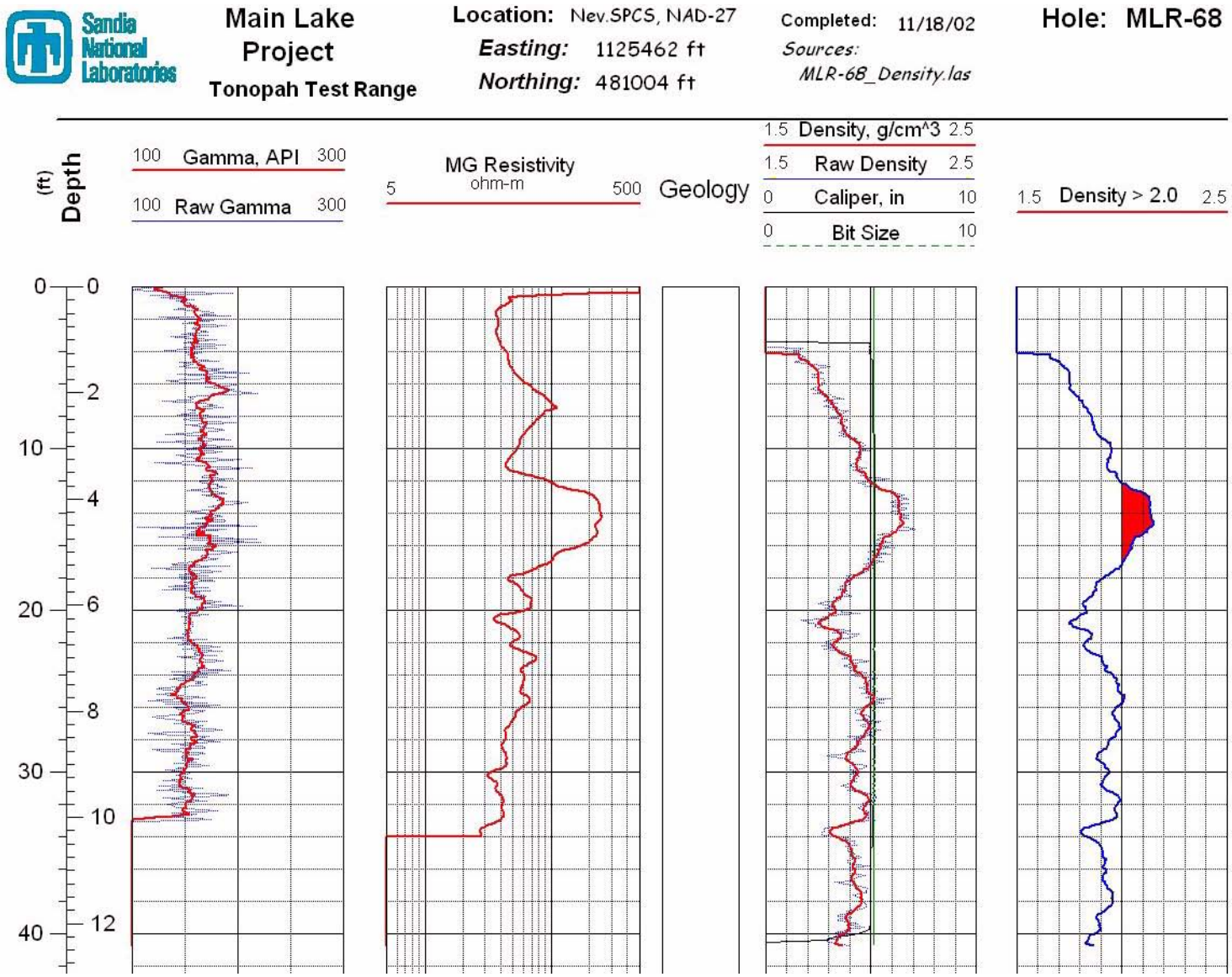

Figure C-83 Geophysical logs for drill hole MLR-68

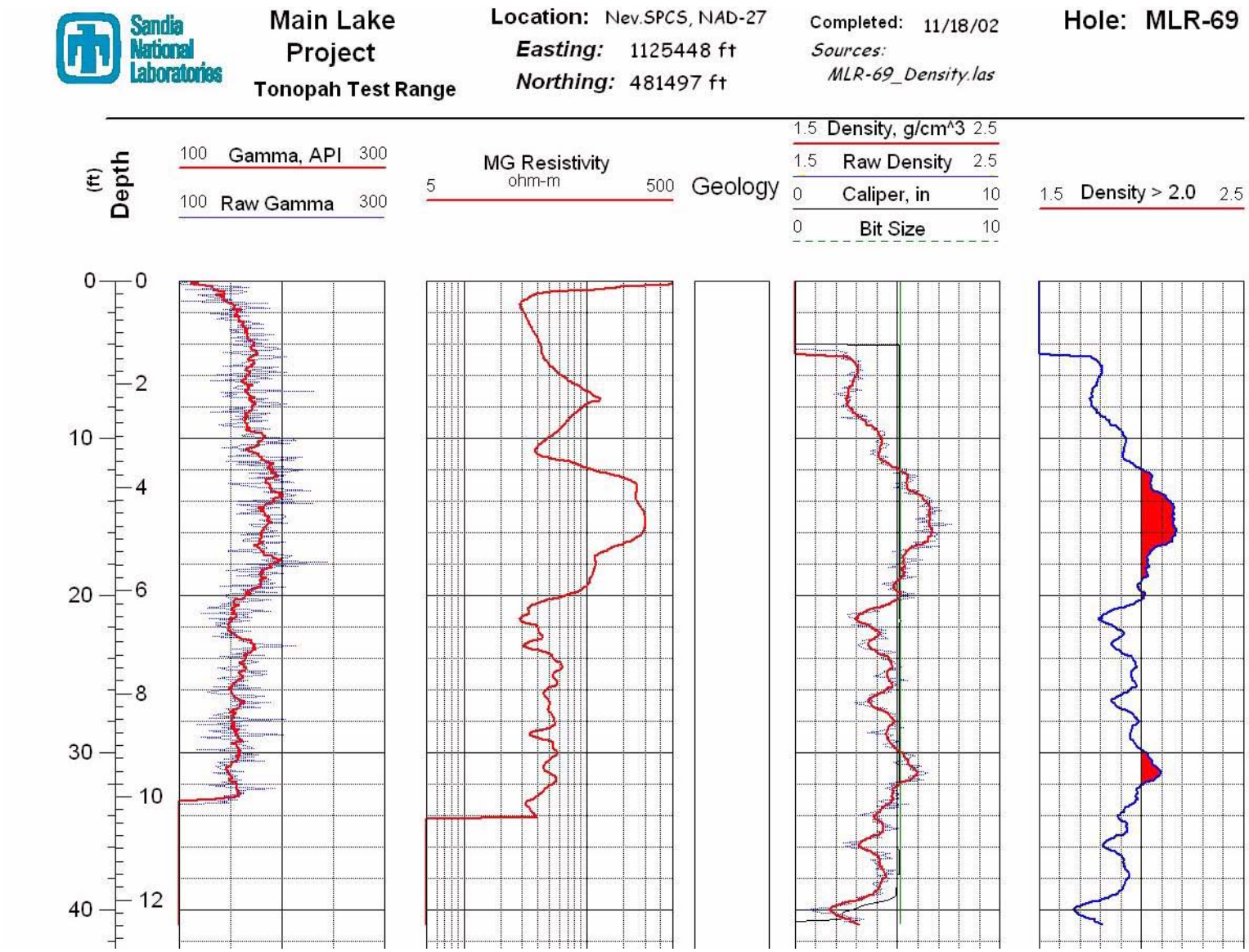

Figure C-84 Geophysical logs for drill hole MLR-69

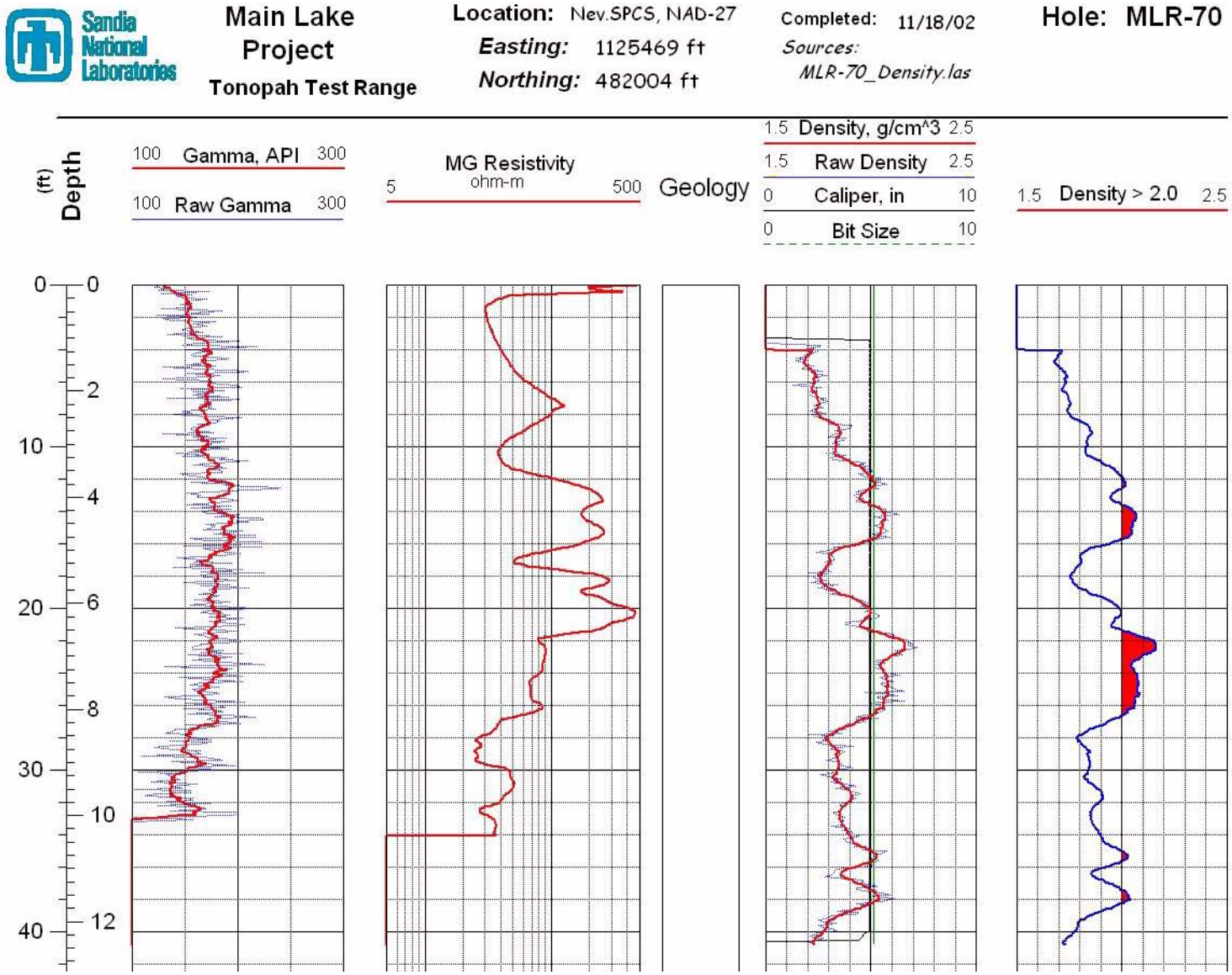

Figure C-85 Geophysical logs for drill hole MLR-70

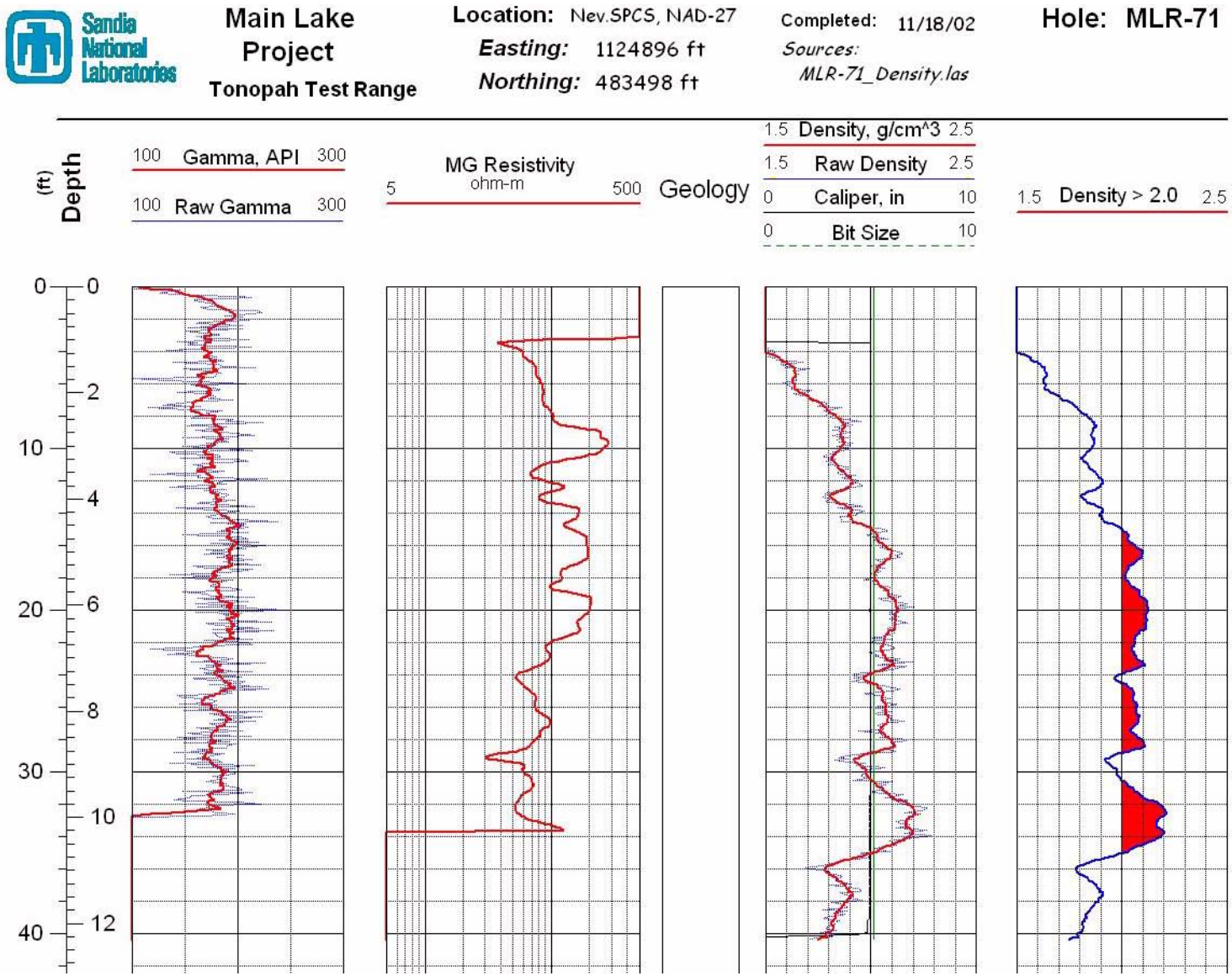

Figure C-86 Geophysical logs for drill hole MLR-71

This page intentionally left blank.

Appendix D: Logs for Cored Drill Holes on the Main Lake

This page intentionally left blank.

INTRODUCTION

This appendix presents graphical geologic logs of the core that was obtained from drill holes ML-1 through ML-19. Emphasis is primarily on the geology — lithology, grain size, fractures (if any), and other visually observable features — of the core itself. Core recovery is also presented, as this value reflects the maximum possible "quality" of the core description. Lost core cannot be described, and thus descriptions from intervals of severe core loss are potentially suspect. A simplified version of the geophysical log suite from Appendix C is also presented for direct comparison with the lithologic descriptions.

LOGGING METHOD

Geologic logging of shallow core holes, such as drilled at the Main Lake, is a fairly simple activity. The core is typically arranged in core boxes in the field in a manner such that the core reads "like a book," from left to right and from top to bottom. Each box nominally holds 10 feet of core, although generally the actual amount of core in a box is less because one usually desires not to generate any more artificial breaks in the core than is absolutely necessary. Natural breaks are therefore used for dividing the core. If the "next" core segment will not fit entirely within the last two-foot core tray, it is typically placed in a new box.

The boxed core is laid out for logging either in the field or in the laboratory, and it is examined for changes in rock type and other features of interest. Core from the Main Lake was examined visually and with a 10x hand lens only. No binocular microscopic or thin-section study was performed. Grain size was determined visually with reference to standard geologic size categorizations ("fine sand," "silt," "granules," etc.), as were percentages of different materials (e.g., AGI Data Sheets, 1989). Lithologic symbols used on the logs in this appendix are shown on page 190.

Depth Determination

The depth of lithologic changes and other entities is determined from the value recorded on the core blocks (literally, small wooden blocks) placed in the box during drilling at the end of each core run marked with the depth. These run depths are determined by totaling the cumulative length of the core barrel plus all rods in the hole and subtracting the "stick-up" of the last rod above ground level (or other reference position). These depth markers are the only depths known for certain, as the core recovered between two drilling breaks may have come from anywhere within that interval.

For drilling runs with good core recovery, it is very simple to measure upward (or downward) from the nearest core block; usually even-foot depths are marked on the core with a felt-tip marker. However, if only a small amount of core has been recovered from a given run — for example, 1.3 feet of core for a 5-ft run — the assignment of depths in the subsurface to the core is not so simple. A common convention is to assign arbitrarily all core loss to the end (bottom) of the run. However, at the Main Lake, a more geologically reasonable assumption would be to assign the core loss to the *top* of the run. The rationale for this latter interpretation is that during retrieval of the inner tube from the bottom of the hole, the undrilled rock below the static core bit is exposed to the fluids in the hole, which may infiltrate into permeable portions of the rock mass. In unconsolidated materials, such as these playa sediments, this addition of water/mud softens the material. Thus, the softer material near the top of the next run is more likely to be washed out of the bit face when drilling resumes than material near the end of a run that has been exposed to the drilling fluid only briefly.

Core Recovery Computation

Core recovery is simply the cumulative length of physically recovered material divided by the length of the cored interval and expressed as a percentage. If the core material is severely broken (or, in the case of the Main Lake material, disaggregated to granular material), the approximate length of equivalent "whole" core is used. In essence, disaggregated sediments are heaped up to the approximate size (diameter) of intact core and the length of the reformed material is measured. The associated core-block depths are shown on the geologic core logs next to the column showing recovery.

Geophysical Logs

Three of the more important geophysical log traces are shown on the core logs: smoothed natural gamma, smoothed density, and MicroGuard resistivity. The caliper log and bit size are not shown, nor are the raw gamma and density curves. These latter traces are available on the geophysical log figures in Appendix C. The intent of including the major geophysical curves on the core logs is to allow correlation of the lithologic descriptions with potentially diagnostic geophysical signatures. Such correlations are fairly well exhibited for the density and resistivity traces. However, in some cases the correlations need to be adjusted for missing core intervals and the resulting uncertainty in the depth position of the core and lithologic descriptions. Natural gamma appears to correlate much less well with the lithology, a fact which is probably no too surprising because all of the sediments are derived from the same volcanic rocks in the source terrane. Compositional homogeneity appears to be the result.

Note that officially there are no geophysical logs for drill holes ML-1, ML-2, and ML-3. However, as noted elsewhere in this report, rotary hole MLR-44 was drilled within 25 or 30 ft of all three core holes. Therefore, we do show the small-scale MLR-44 geophysical data on figures D-1 through D-3. The source of the geophysical data is identified as from MLR-44.

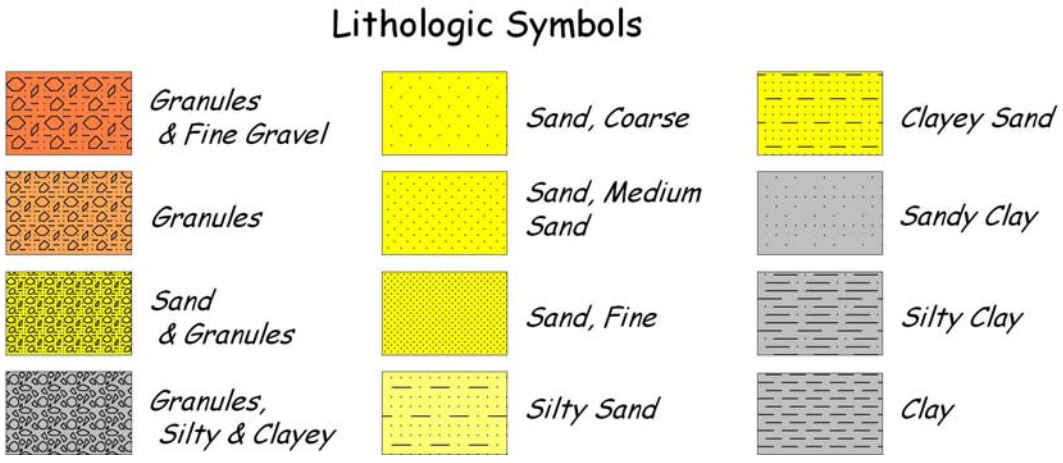

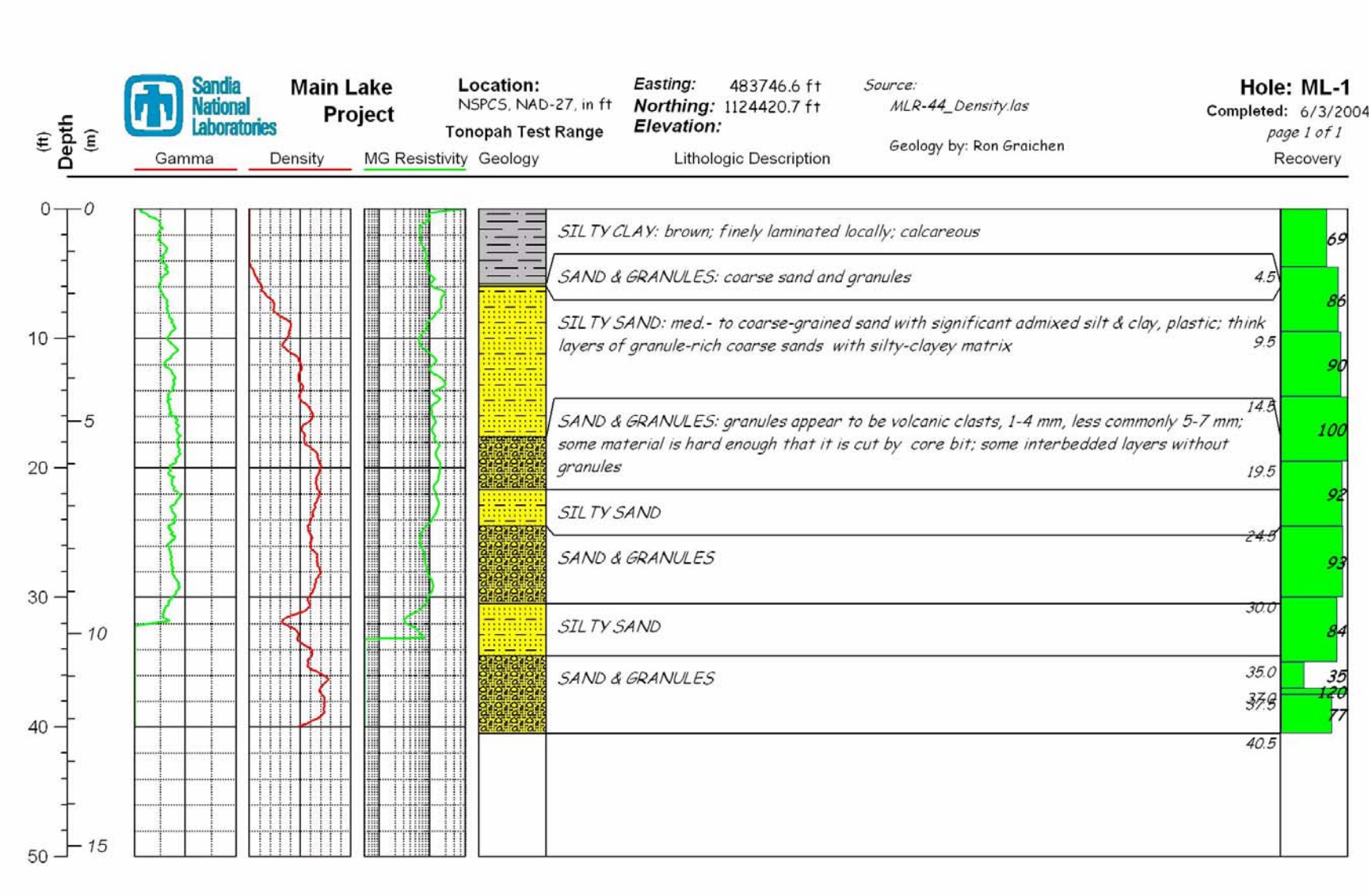

Figure D-1 Geologic core log for drill hole ML-1.

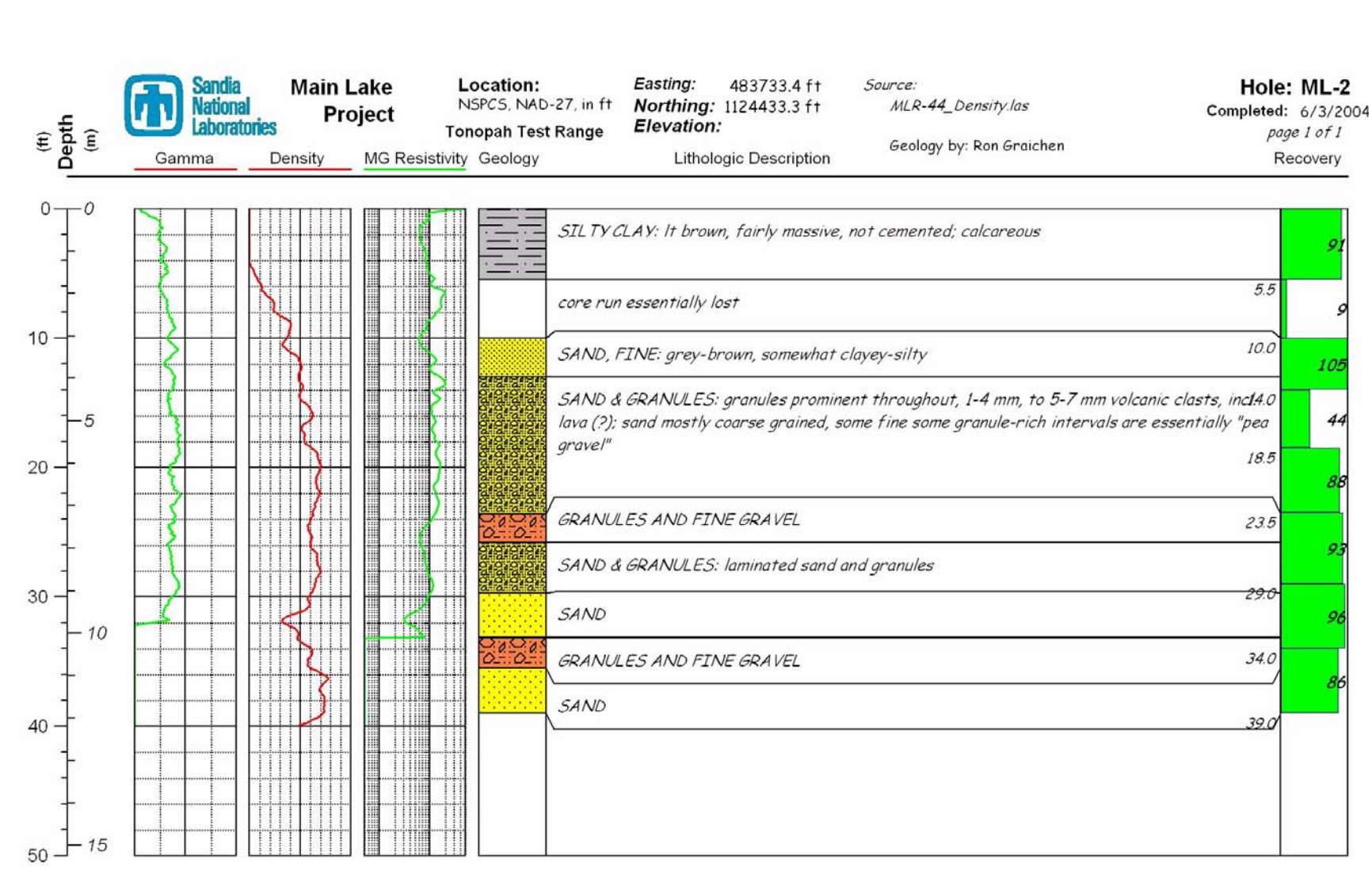

Figure D-2 Geologic core log for drill hole ML-2.

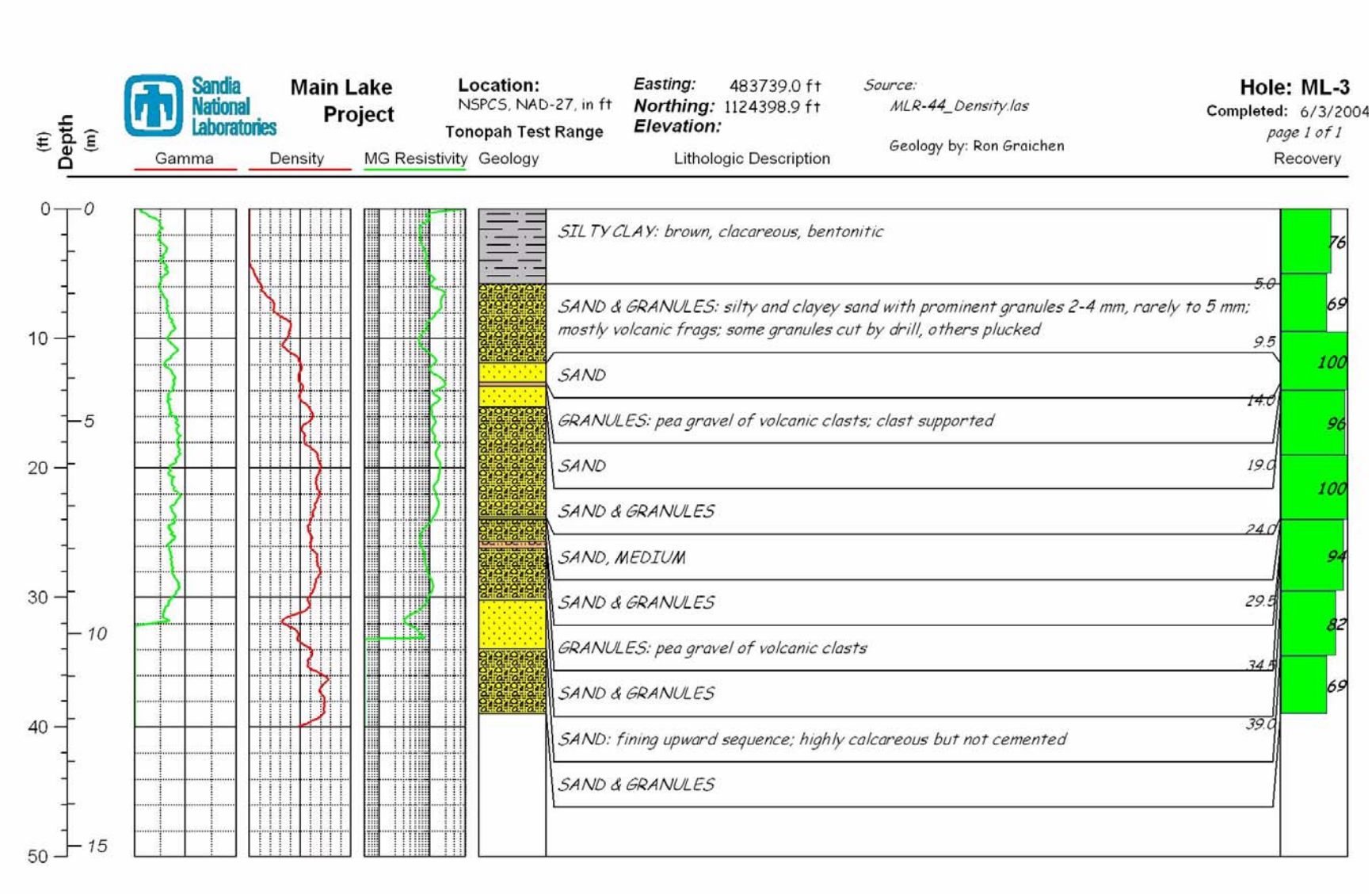

Figure D-3 Geologic core log for drill hole ML-3.

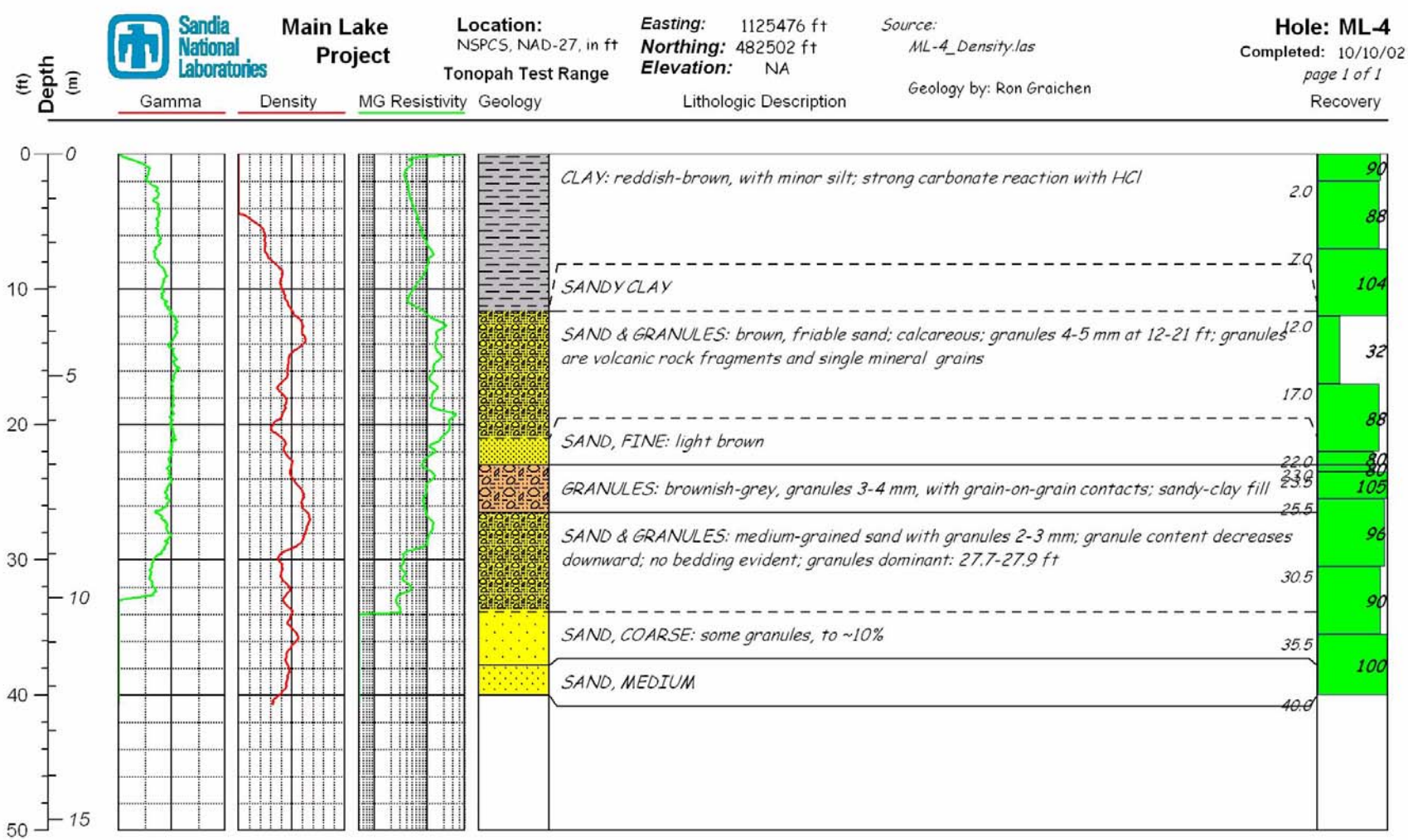

Figure D-4 Geologic core log and geophysical logs for drill hole ML-4.

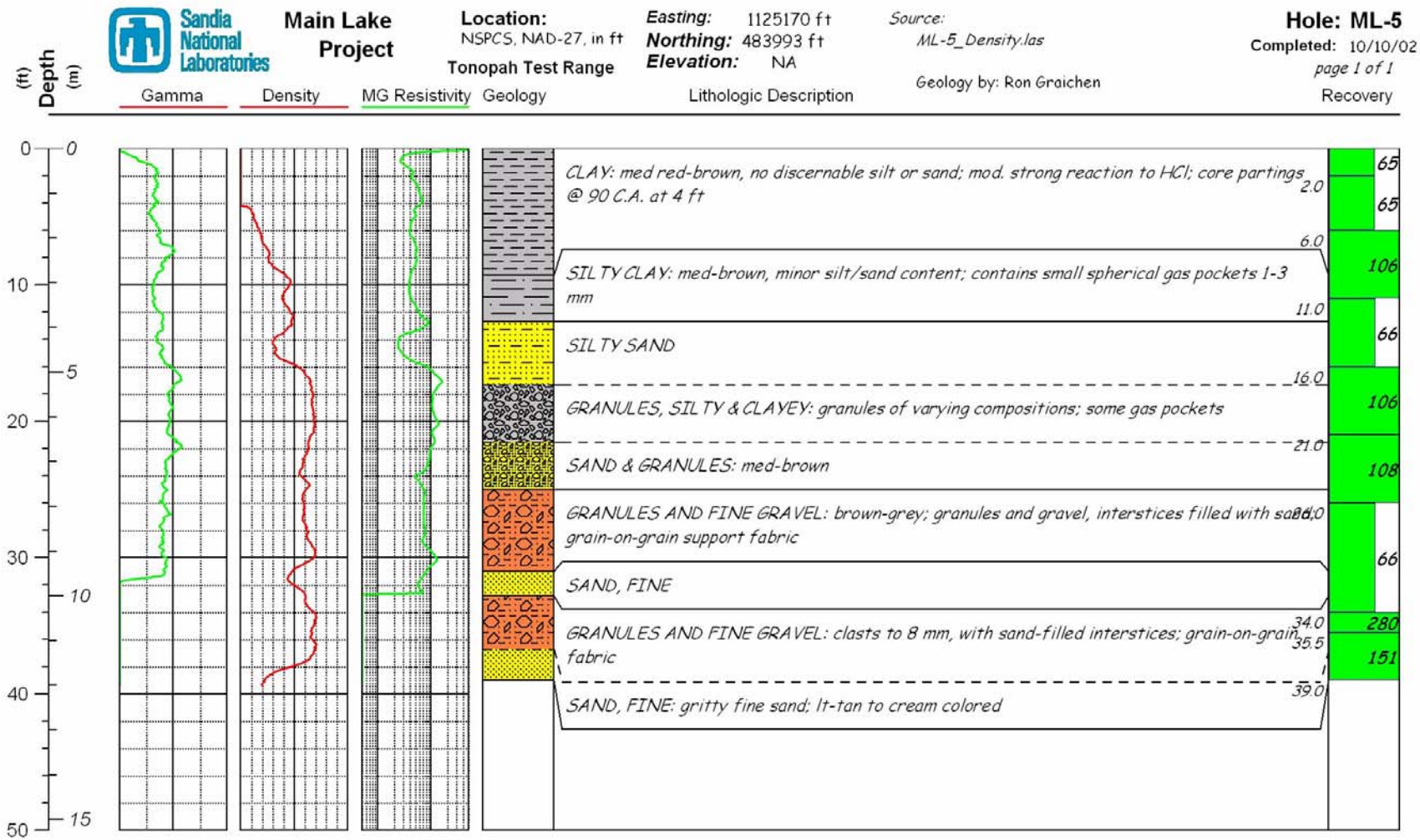

Figure D-5 Geologic core log and geophysical logs for drill hole ML-5.

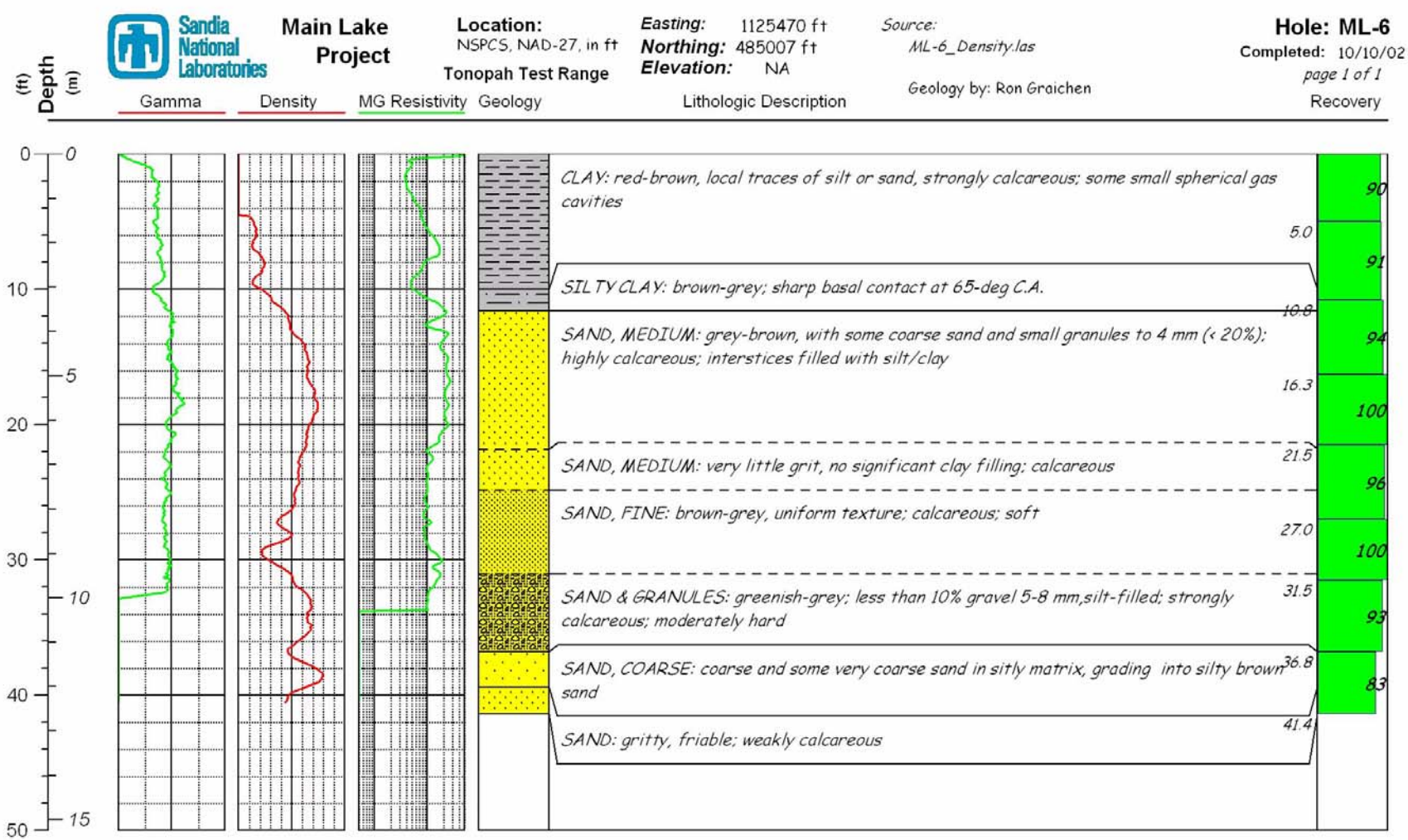

Figure D-6 Geologic core log and geophysical logs for drill hole ML-6.

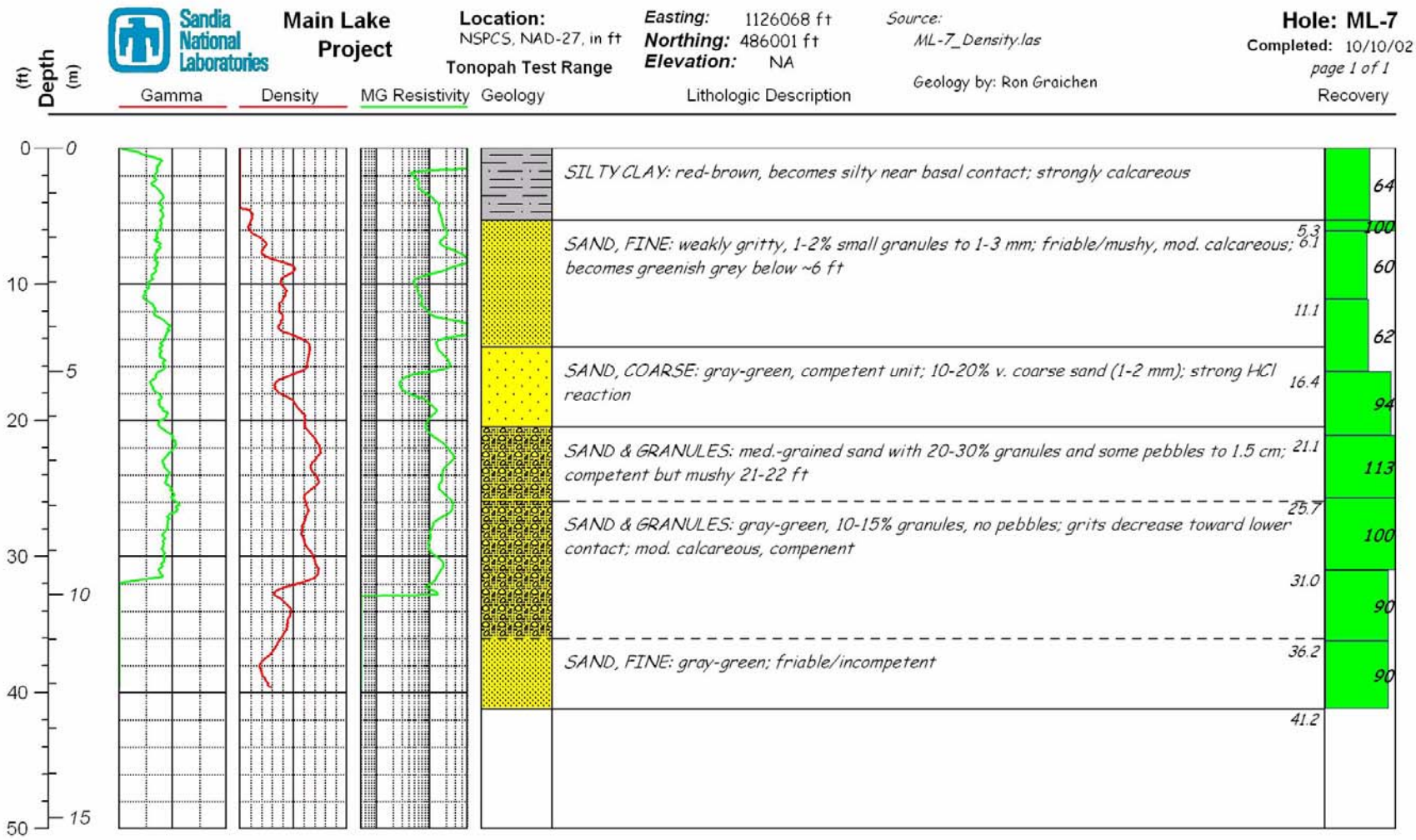

Figure D-7 Geologic core log and geophysical logs for drill hole ML-7.

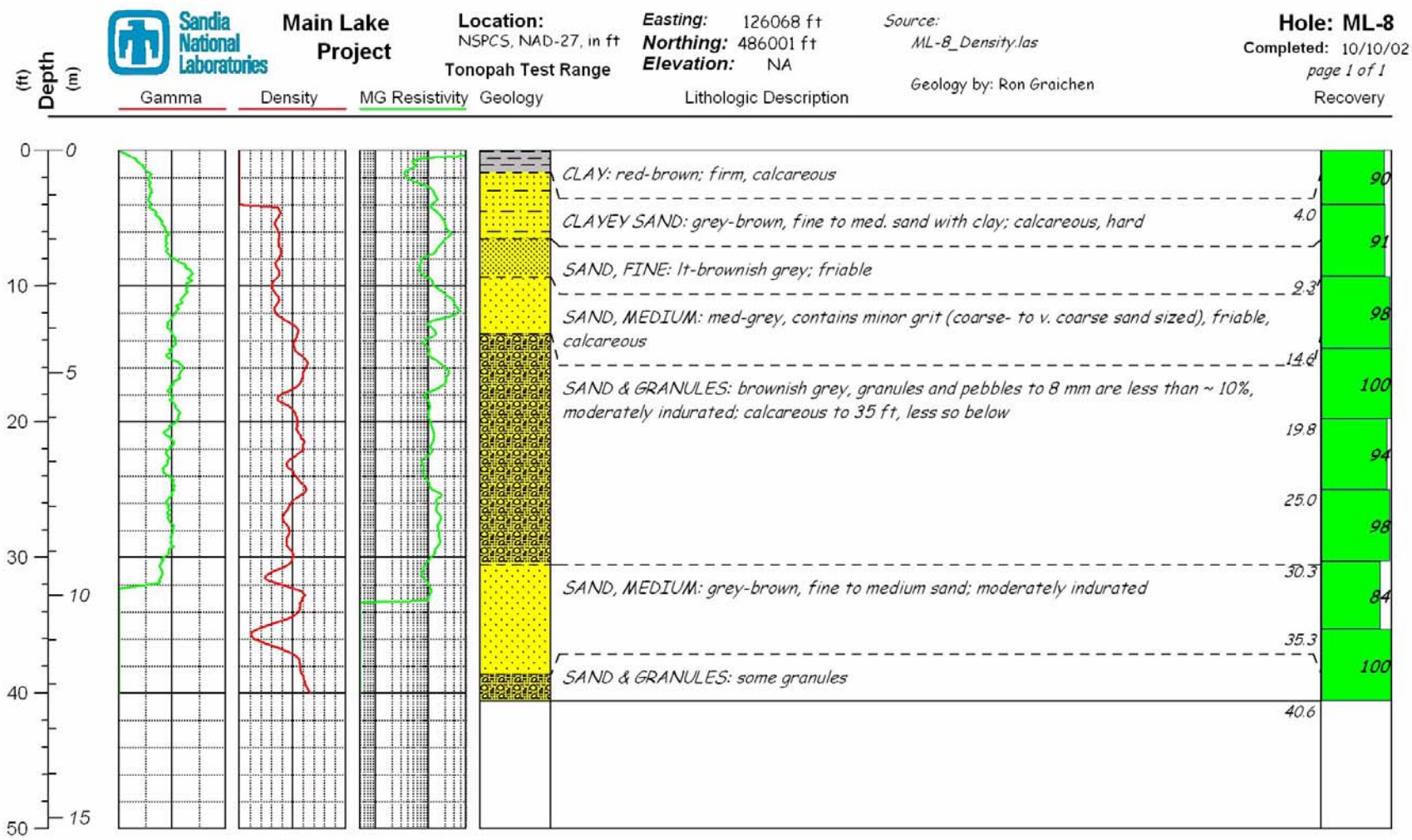

Figure D-8 Geologic core log and geophysical logs for drill hole ML-8.

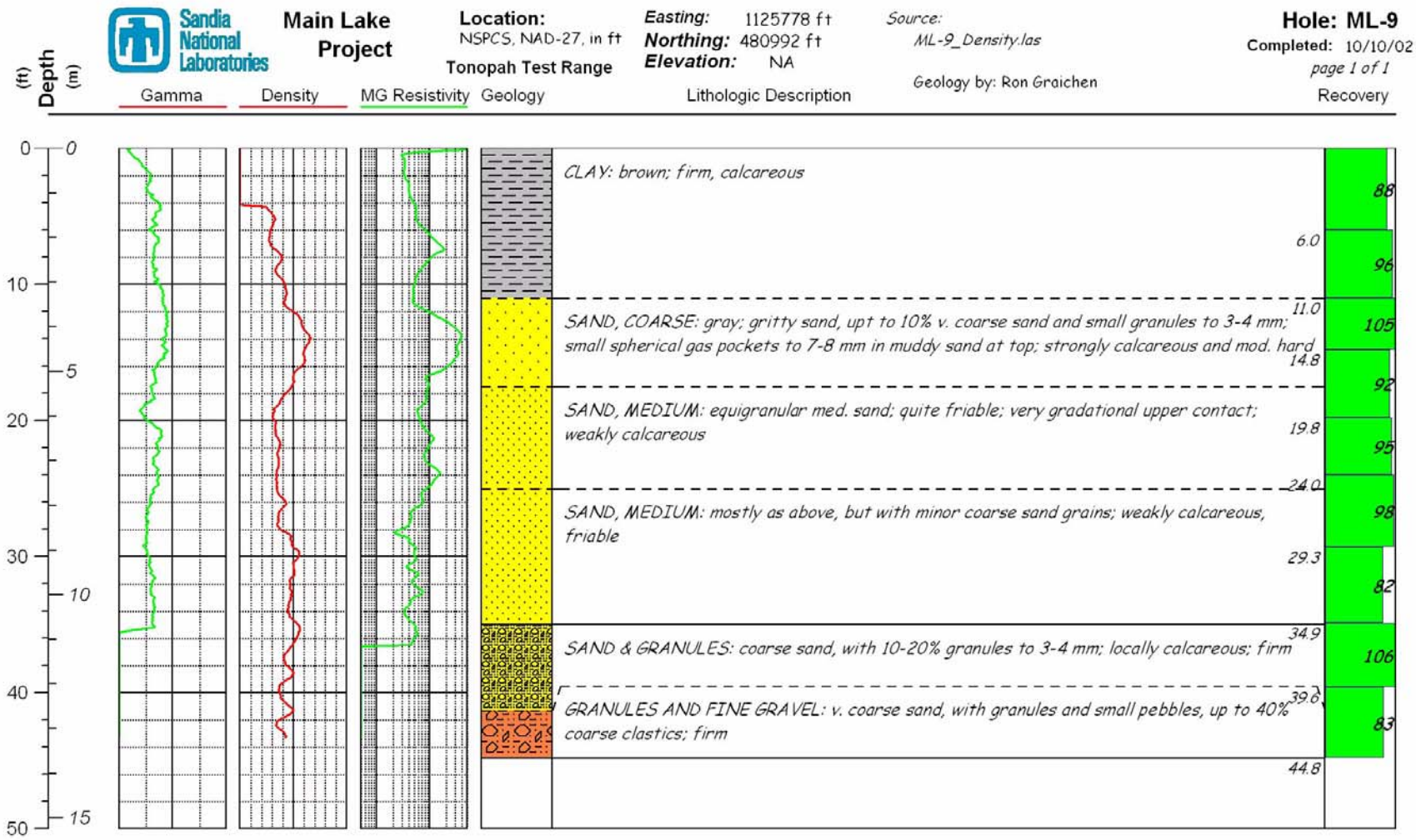

Figure D-9 Geologic core log and geophysical logs for drill hole ML-9.

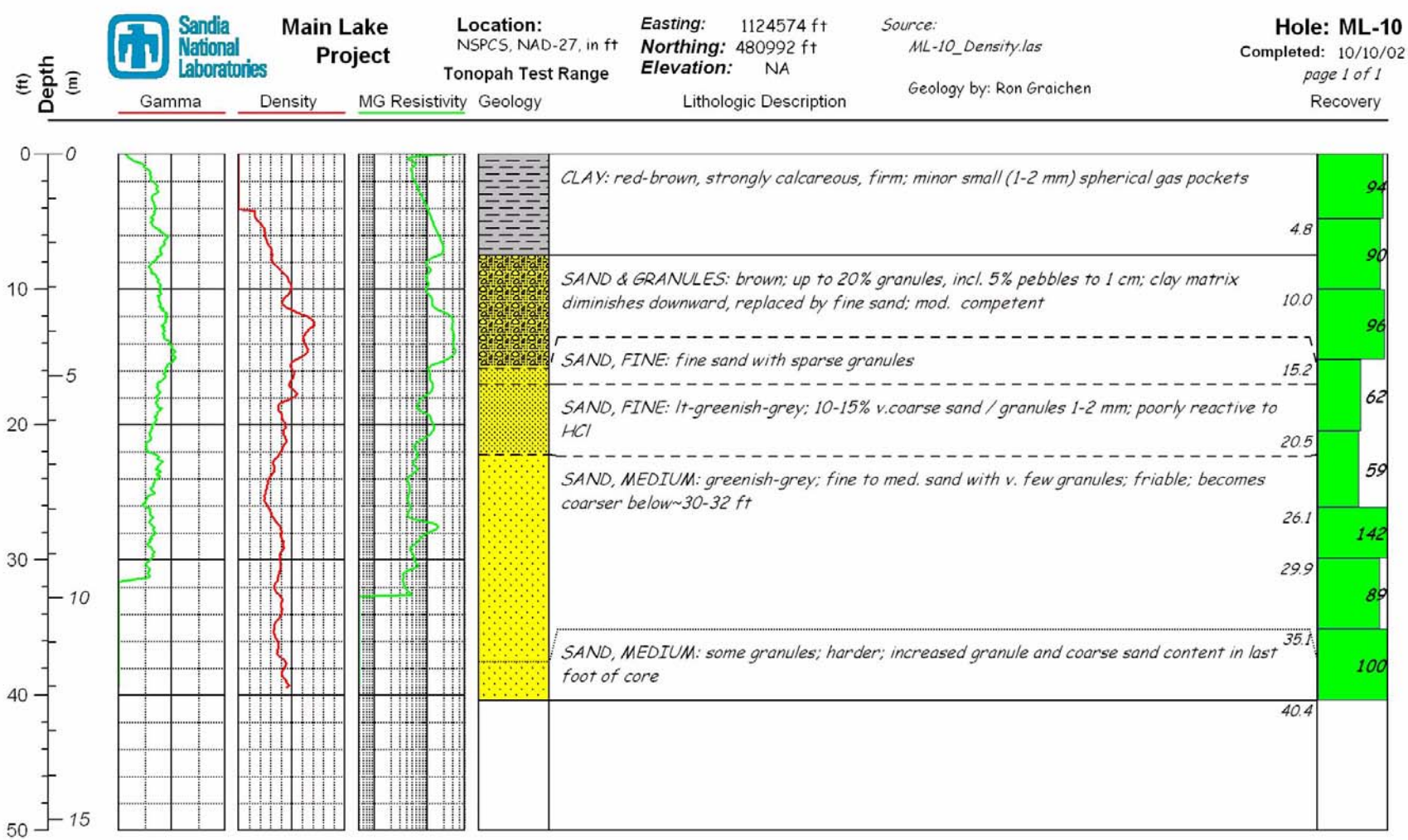

Figure D-10 Geologic core log and geophysical logs for drill hole ML-10.

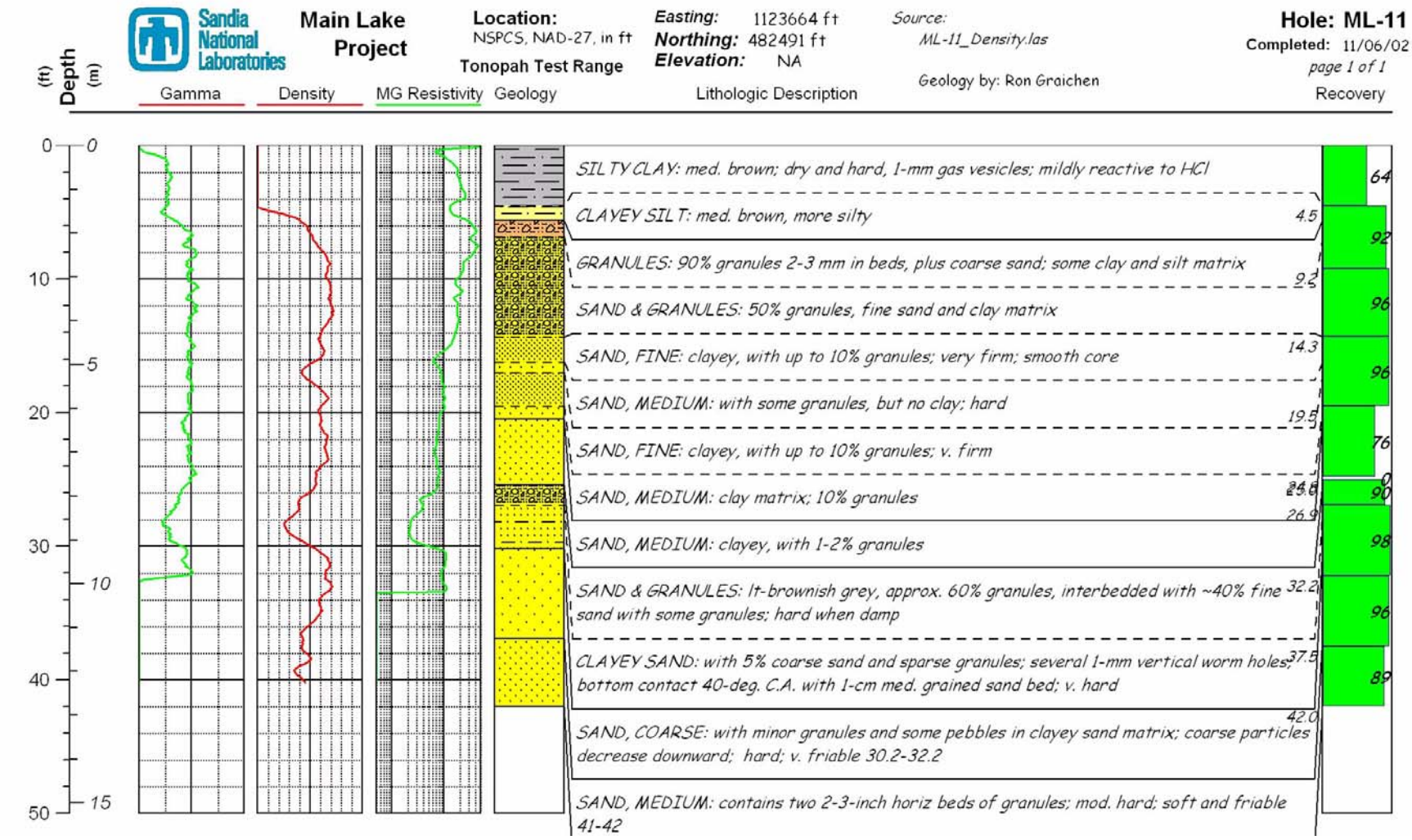

Figure D-11 Geologic core log and geophysical logs for drill hole ML-11.

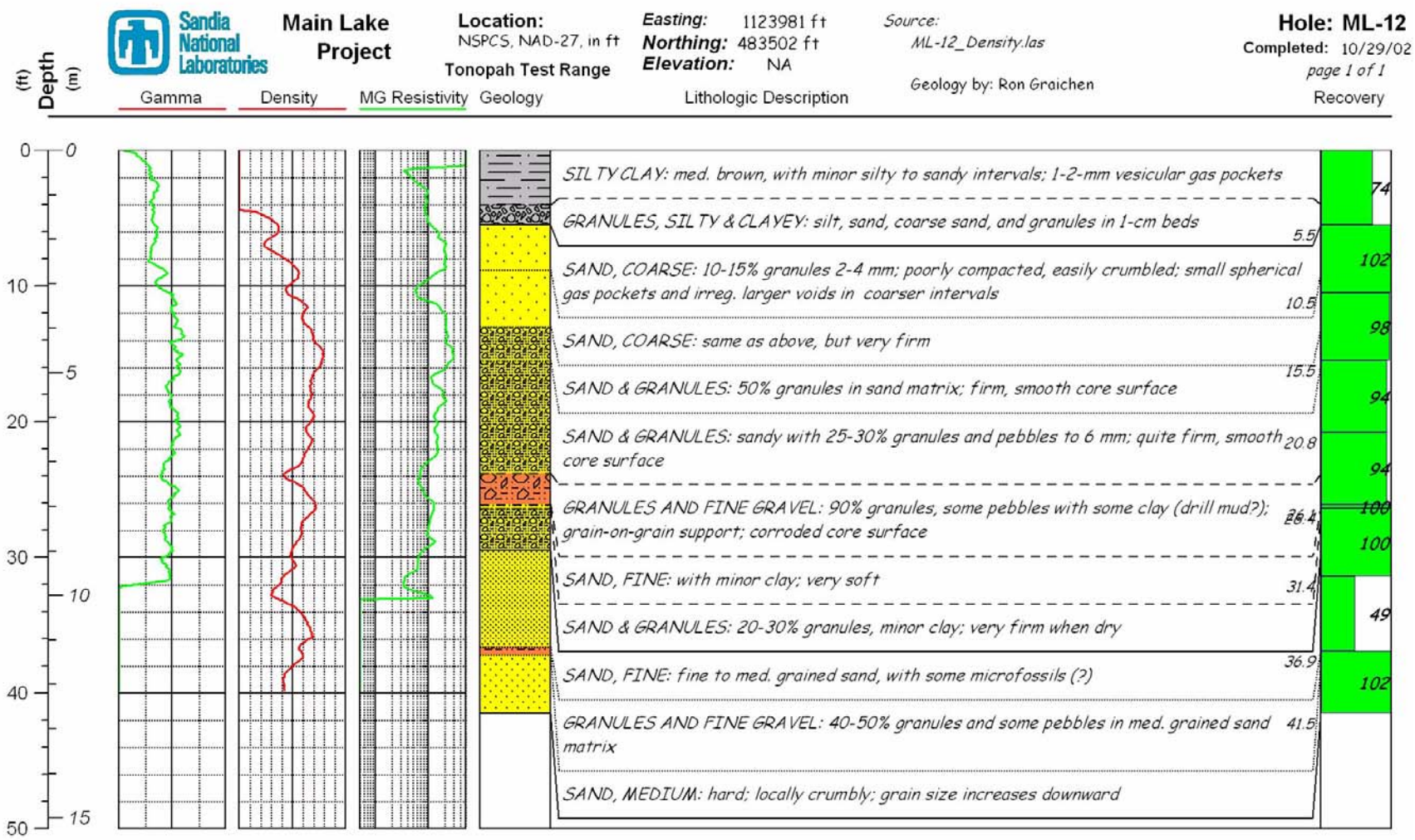

Figure D-12 Geologic core log and geophysical logs for drill hole ML-12.

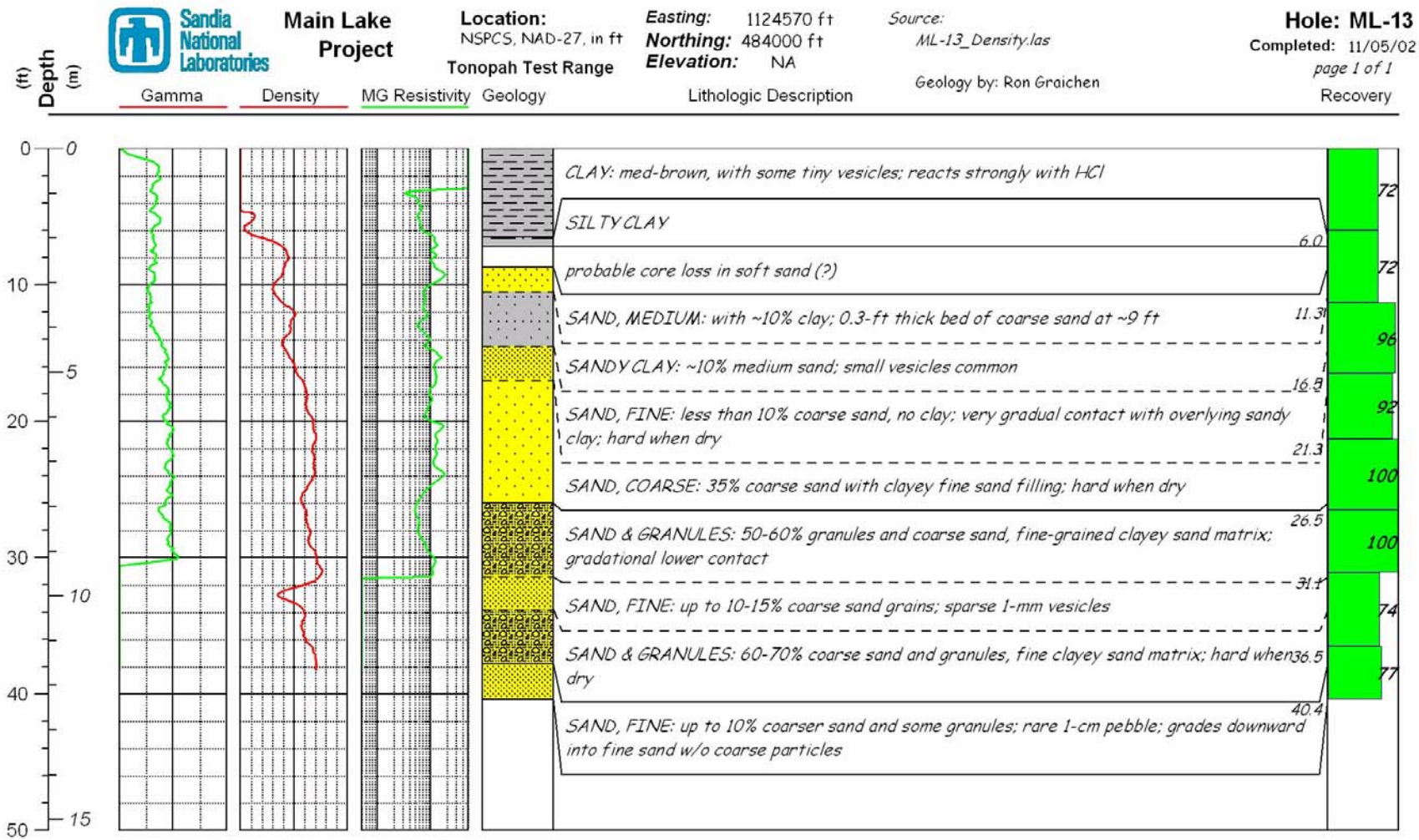

Figure D-13 Geologic core log and geophysical logs for drill hole ML-13.

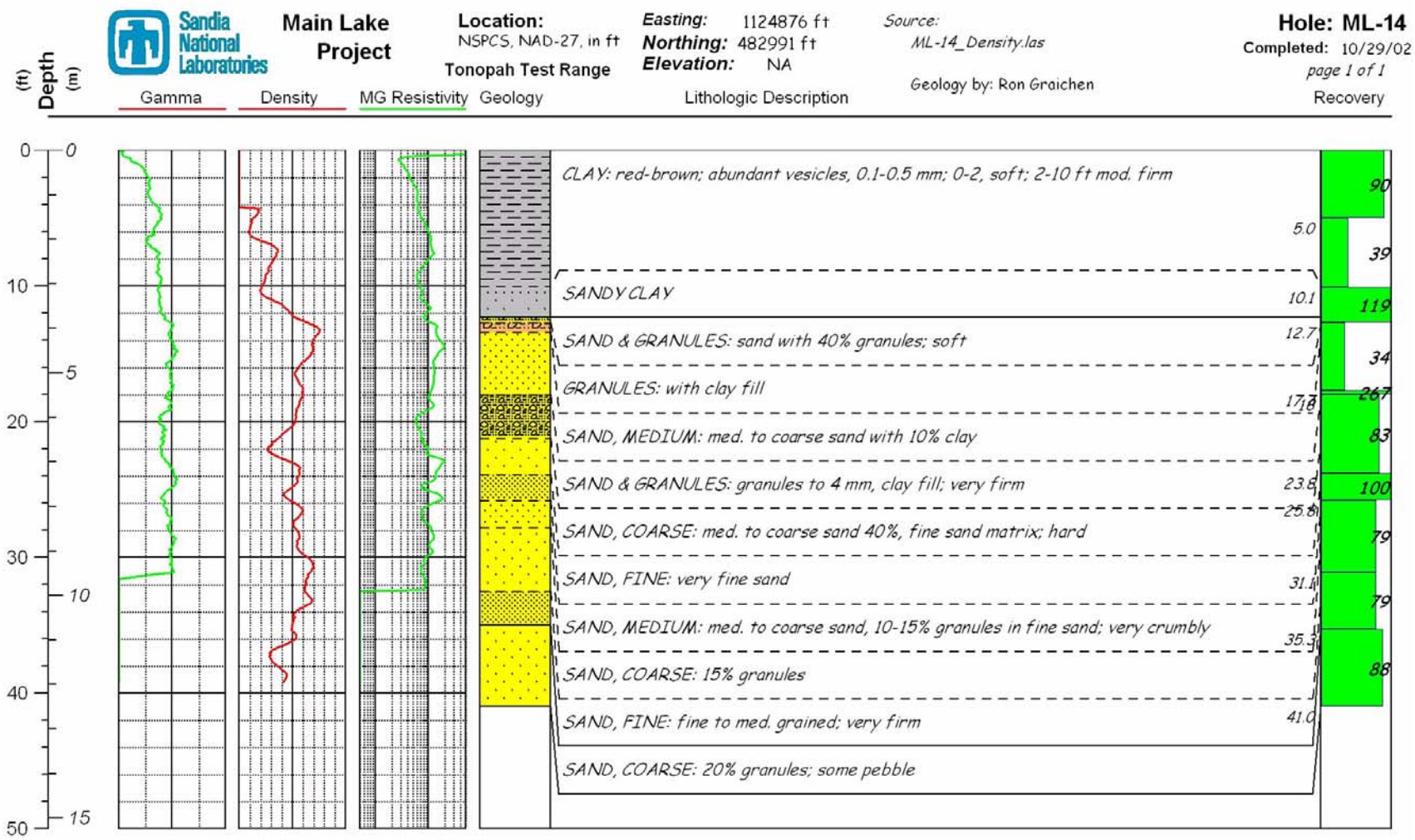

Figure D-14 Geologic core log and geophysical logs for drill hole ML-14.

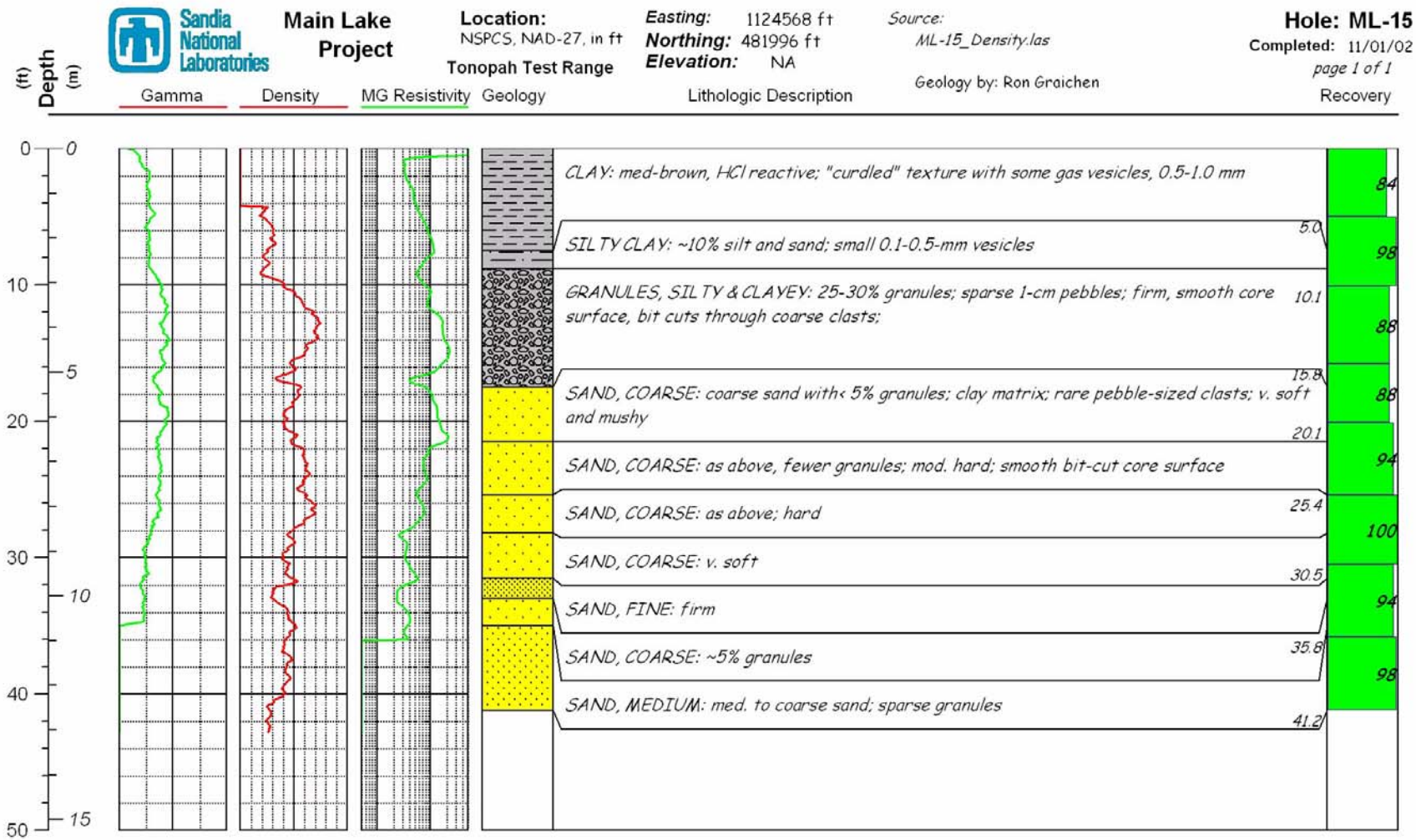

Figure D-15 Geologic core log and geophysical logs for drill hole ML-15.

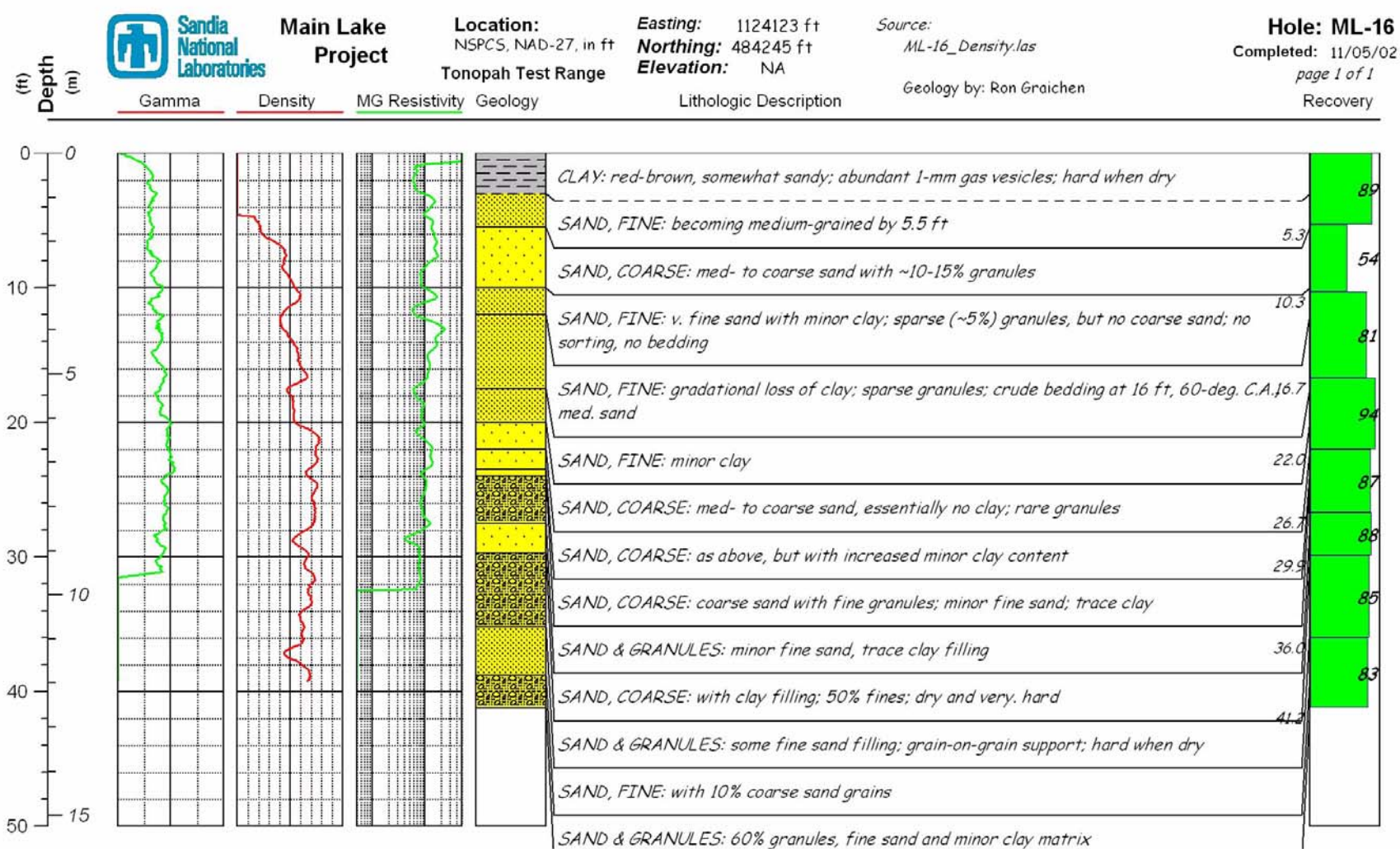

Figure D-16 Geologic core log and geophysical logs for drill hole ML-16.

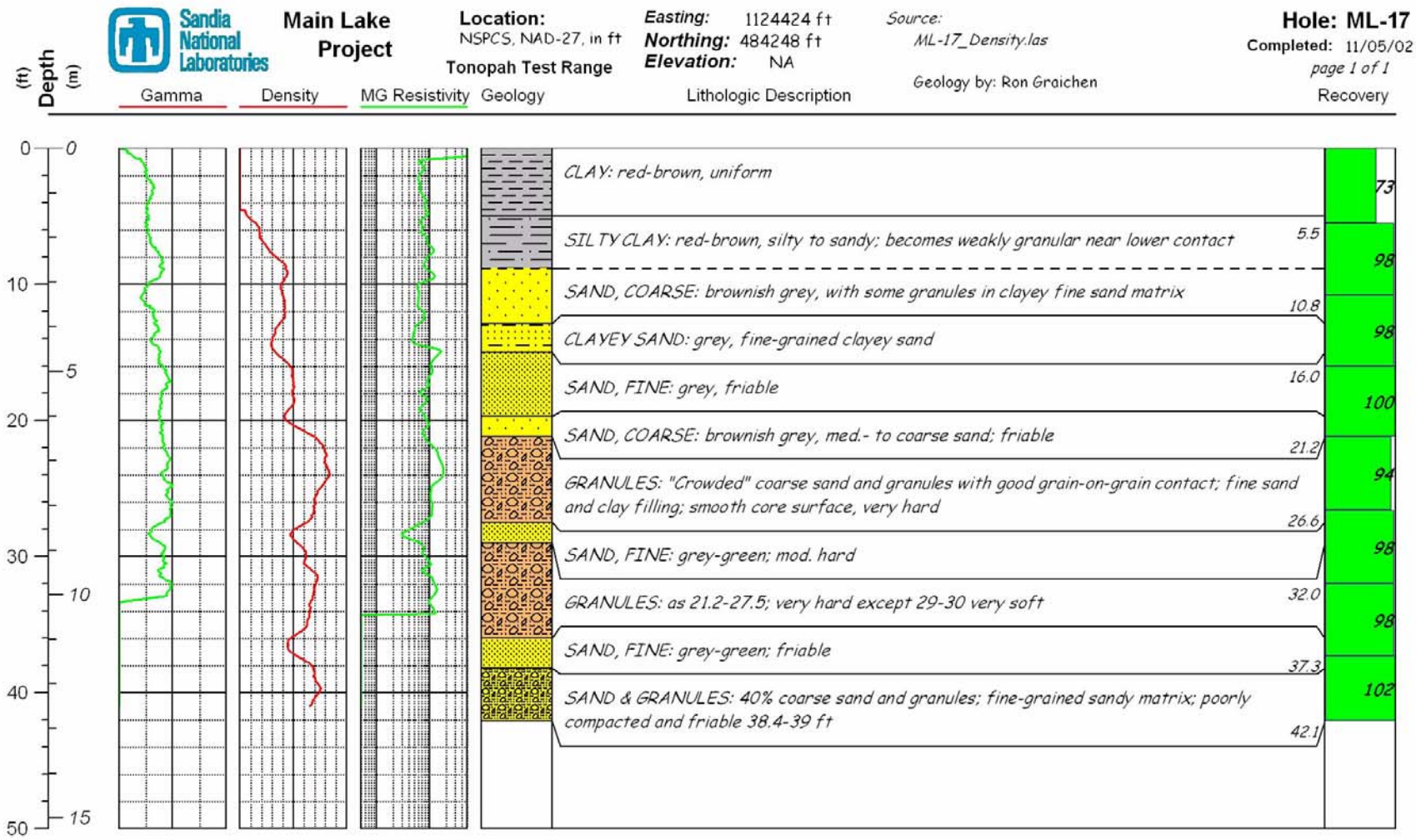

Figure D-17 Geologic core log and geophysical logs for drill hole ML-17.

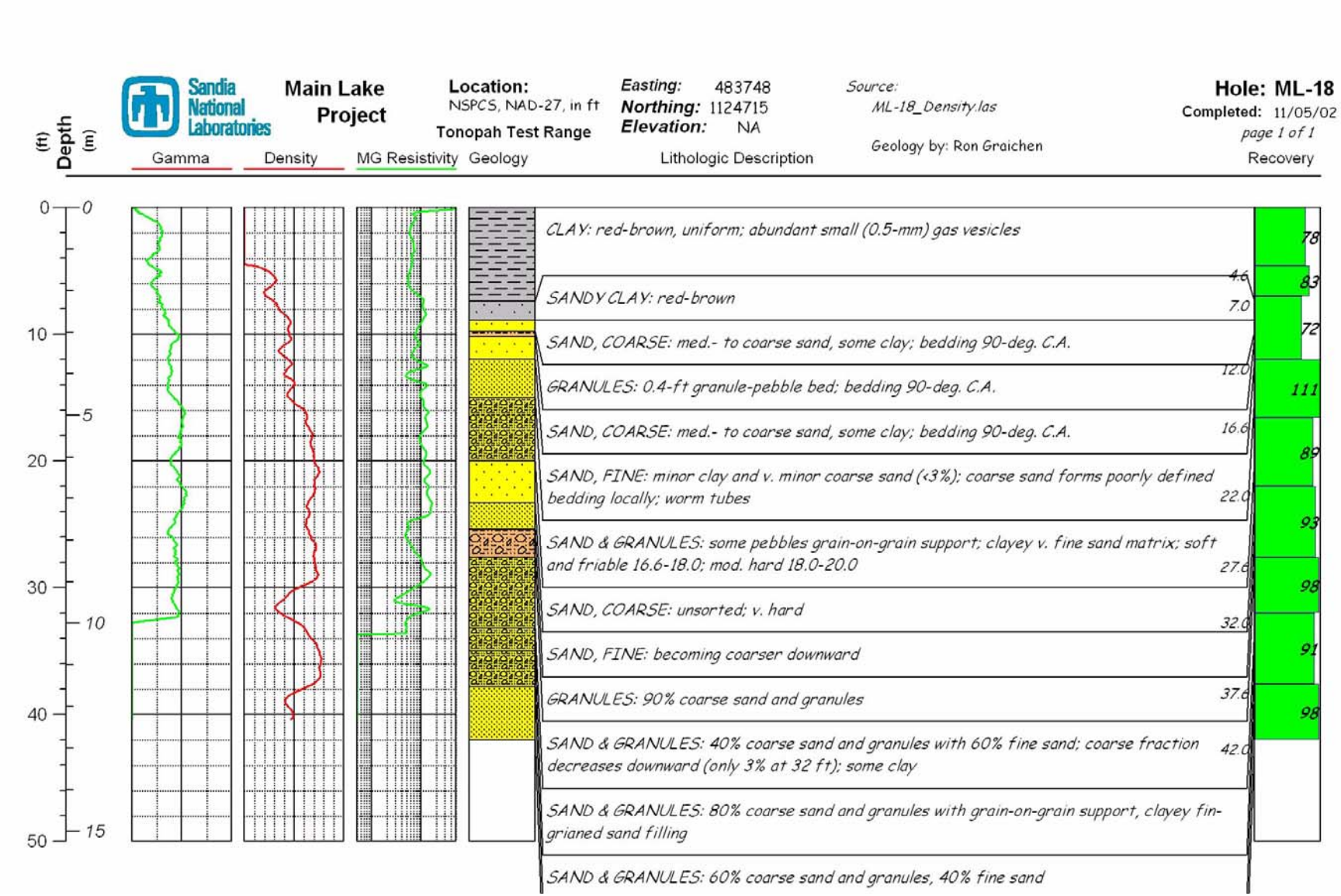

Figure D-18 Geologic core log and geophysical logs for drill hole ML-18.

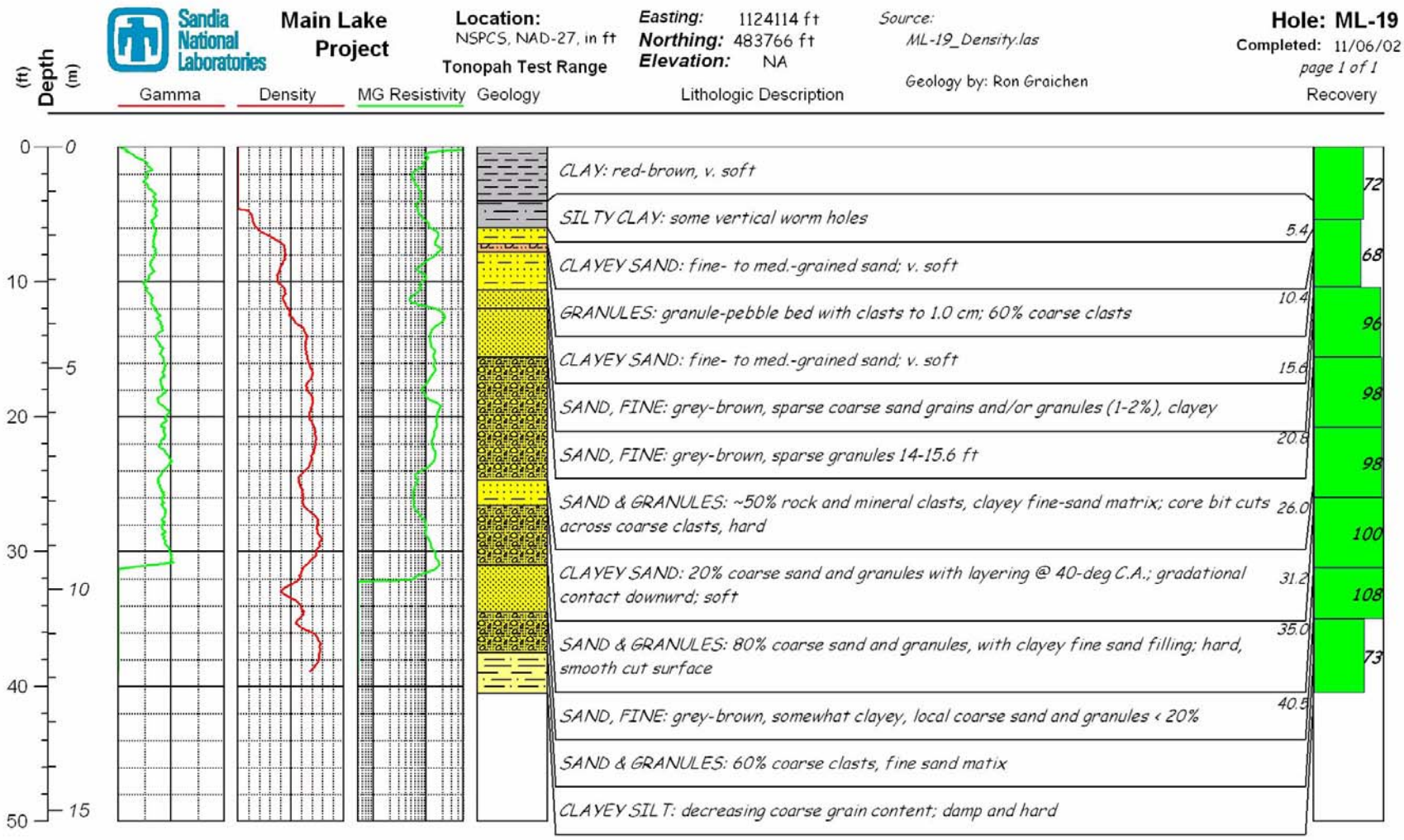

Figure D-19 Geologic core log and geophysical logs for drill hole ML-19.

This page intentionally left blank.

Appendix E: Material Properties Data from Main Lake Samples

This page intentionally left blank.

INTRODUCTION

This appendix contains the results of laboratory material-properties testing on specimens removed from the core drilled at the TTR Main Lake. Specimens were tested both in hydrostatic compression, in unconfined compression and in triaxial compression. The final laboratory values are given in table E-1. A full discussion of the laboratory testing procedure and the implications of the results is beyond the scope of this data report. An inventory listing of all core samples shipped to Sandia National Laboratories in Albuquerque is presented in table E-2.

Electronic Data Storage

The underlying data, as well as the testing results are currently (2004) stored on the Sandia National Laboratories web fileshare system for authorized users. The relevant materials may be found at https://wfsprod01.sandia.gov/ by entering the term *Main Lake* as a substring within the *Title* search field.

Table E-1: Laboratory test data for samples collected from Main Lake drill holes

[Core samples tested by the rock mechanics laboratory at Sandia National Laboratories, M.Y. Lee and D.R. Bronowski, analysts. --: not applicable]

Test ID	Drill Hole	Depth Interval		Diameter (mm)	Length (mm)	Weight (g)	Density (g/cm3)	Wt. Percent Water[1]	Confining Pressure (MPa)	Peak Axial Stress (MPa)
		Top (ft)	Bottom (ft)							
Hydrostatic Compression Tests										
TTR-HC01	ML-2	21.7	22.0	61.0	88.7	508.0	1.96	--	400	--
TTR-HC02[2]	ML-3	23.2	23.6	61.2	107.2	633.1	2.01	4.6	400	--
Unconfined Compression Test										
TTR-UC01	ML-3	21.3	21.7	61.1	100.7	--	--	--	0	0.55
Triaxial Compression Tests										
TTR-TA01[3]	--	--	--	61.0	152.5	--	--	--	20	--
TTR-TA02	ML-1	21.0	21.6	61.1	123.4	768.9	2.13	3.5	20	65.7
TTR-TA03	ML-1	21.6	22.0	61.1	108.7	676.0	2.12	2.9	40	162.8
TTR-TA04[2]	ML-3	23.2	23.6	61.2	107.2	633.1	2.01	--	400	691.8
TTR-TA05	ML-1	22.0	22.4	61.1	103.9	605.0	1.99	2.2	10	52.8
TTR-TA06	ML-3	22.8	23.3	61.2	122.2	730.0	2.03	2.2	2	13.7
TTR-TA07	ML-1	23.3	23.8	61.1	125.8	760.0	2.06	3.0	0.54	6.5

1. Weight-percent water = W_{H2O}/W_{sample}
2. These two tests are on the same physical specimen; triaxial compression test conducted after hydrostatic compression.
3. Test TTR-TA01 was never conducted.

Table E-2: Inventory listing of core specimens from Main Lake core at Sandia National Laboratories, 2004

Borehole	Interval Top (ft)	Interval Base (ft)	Length (inch)	Interval Top (m)	Interval Base (m)	Length (cm)
ML-1	13.30	14.00	8.40	4.27	2.56	21.34
	17.65	18.25	7.20	5.56	2.19	18.29
	28.60	29.00	4.80	8.84	1.46	12.19
	29.20	29.60	4.80	9.02	1.46	12.19
ML-2	12.00	12.60	7.20	3.84	2.19	18.29
	13.80	14.25	5.40	4.34	1.65	13.72
	19.60	20.00	4.80	6.10	1.46	12.19
	19.95	20.30	4.20	6.19	1.28	10.67
	20.30	21.10	9.60	6.43	2.93	24.38
	24.75	25.35	7.20	7.73	2.19	18.29
	26.20	26.60	4.80	8.11	1.46	12.19
ML-3	11.85	12.20	4.20	3.72	1.28	10.67
	26.15	26.65	6.00	8.12	1.83	15.24
	27.25	27.70	5.40	8.44	1.65	13.72
	28.25	28.75	6.00	8.76	1.83	15.24
ML-4	12.70	13.10	4.80	3.99	1.46	12.19
	27.90	28.50	7.20	8.69	2.19	18.29
	29.40	30.00	7.20	9.14	2.19	18.29
	37.00	37.40	4.80	11.40	1.46	12.19
	37.80	38.50	8.40	11.73	2.56	21.34
ML-5	19.30	19.70	4.80	6.00	1.46	12.19
	20.30	20.80	6.00	6.34	1.83	15.24
	26.90	27.80	10.80	8.47	3.29	27.43
	27.90	28.50	7.20	8.69	2.19	18.29
	30.00	30.50	6.00	9.30	1.83	15.24
	36.10	39.90	45.60	12.16	13.90	115.82
ML-6	13.80	14.50	8.40	4.42	2.56	21.34
	17.40	18.00	7.20	5.49	2.19	18.29
	19.10	19.70	7.20	6.00	2.19	18.29
	20.80	21.20	4.80	6.46	1.46	12.19
	32.70	33.30	7.20	10.15	2.19	18.29
	33.90	34.50	7.20	10.52	2.19	18.29
	34.80	35.40	7.20	10.79	2.19	18.29
ML-7	18.80	19.30	6.00	5.88	1.83	15.24
	19.60	20.00	4.80	6.10	1.46	12.19
	24.20	24.80	7.20	7.56	2.19	18.29
	27.90	28.70	9.60	8.75	2.93	24.38
	32.20	32.60	4.80	9.94	1.46	12.19

Table E-2: Inventory listing of core specimens from Main Lake core at Sandia National Laboratories, 2004 (continued)

Borehole	Interval Top (ft)	Interval Base (ft)	Length (inch)	Interval Top (m)	Interval Base (m)	Length (cm)
ML-8	7.80	8.40	7.20	2.56	2.19	18.29
	15.50	16.00	6.00	4.88	1.83	15.24
	18.50	19.20	8.40	5.85	2.56	21.34
	27.10	27.80	8.40	8.47	2.56	21.34
	27.80	28.30	6.00	8.63	1.83	15.24
	29.00	29.60	7.20	9.02	2.19	18.29
	31.60	32.20	7.20	9.81	2.19	18.29
ML-9	15.20	15.70	6.00	4.79	1.83	15.24
	18.50	19.20	8.40	5.85	2.56	21.34
	25.40	26.60	14.40	8.11	4.39	36.58
	35.00	35.70	8.40	10.88	2.56	21.34
	37.80	38.50	8.40	11.73	2.56	21.34
ML-10	18.10	18.75	7.80	5.72	2.38	19.81
	27.00	28.00	12.00	8.53	3.66	30.48

Appendix F: Coordinate Locations of Drill Holes on Antelope Lake

This page intentionally left blank.

INTRODUCTION

This appendix contains the collar coordinates of all holes drilled on Antelope Lake at the Tonopah Test Range. Locations are reported in latitude and longitude, UTM coordinates, and Nevada state plane coordinate system eastings and northings. Note that the geographic datum used for latitude/longitude and the UTM coordinates is different than that for the Nevada state plane system. Use of coordinate values from one datum with reference to another datum can result in errors of up to several hundred feet.

The collar locations were surveyed using a Trimble Pro XRS global positioning satellite (GPS) receiver using real-time correction signals, either from the Wide-Area Augmentation System (WAAS) or beacon signals, probably transmitted by the military. WAAS corrections are generally considered of lower precision than beacon corrections, although the difference is most likely to be meaningless for purposes of drill hole location in the field. The GPS equipment records locations in native WGS-84 latitude and longitude, but can export the data in virtually any desired coordinate system.

Because of the numbering scheme employed for drilling at Antelope Lake, coordinates for both cored and rotary holes are contained in a single table, table F-1. However, rotary (non-cored) drill holes have a suffix, *R*, appended to the hole number in table F-1. Drill holes without this suffix are core holes.

Table F-1: Drill hole coordinate locations for holes drilled on Antelope Lake

[Geographic coordinates are WGS-84 values by Global Positioning Satellite. UTM coordinates are WGS-84, Zone 11. State Plane Coordinates are Nevada Coordinate System, Central Zone, NAD-27. An "R" suffix to the Hole ID indicates a rotary drill hole]

Hole Id	Depth	Latitude	Longitude	UTM East	UTM North	Horizontal Precision	GPS Elevation	Vertical Precision	State Plane East	State Plane North	Elevation
	(ft)	(degrees)	(degrees)	(m)	(m)	(m)	(m)	(m)	(ft)	(ft)	(ft)
AL-1	100	37.691126075	-116.659768662	529996.3	4171600.2	0.40	1633.2	0.63	502254	1070610	5359
AL-2	100	37.685668692	-116.659722274	530002.6	4170994.7	0.40	1633.3	0.63	502268	1068623	5359
AL-3	100	37.685282490	-116.659534702	530019.3	4170951.9	0.46	1633.3	1.06	502322	1068483	5359
AL-4	100	37.683467734	-116.664302216	529599.6	4170749.1	0.37	1633.4	0.56	500943	1067822	5359
AL-5	100	37.681686253	-116.667739342	529297.3	4170550.3	0.37	1633.1	0.57	499948	1067173	5358
AL-6	100	37.678976184	-116.667732319	529299.0	4170249.7	0.39	1634.6	0.69	499950	1066186	5363
AL-7	100	37.676454295	-116.666846199	529378.1	4169970.1	0.51	1633.0	1.10	500206	1065268	5358
AL-8	100	37.676739119	-116.664319133	529600.8	4170002.5	0.38	1633.2	0.63	500938	1065372	5359
AL-9	100	37.680337325	-116.664285492	529602.4	4170401.8	0.29	1634.3	0.48	500947	1066682	5362
AL-10	100	37.679444411	-116.671103180	529001.5	4170300.6	0.38	1634.4	0.66	498975	1066357	5362
AL-11R	100	37.679464484	-116.669975167	529101.0	4170303.1	0.39	1634.8	0.66	499301	1066364	5364
AL-12R	100	37.679434507	-116.668845933	529200.6	4170300.2	0.38	1634.8	0.67	499628	1066353	5364
AL-13R	100	37.679438529	-116.666575771	529400.8	4170301.3	0.35	1634.5	0.54	500285	1066355	5363
AL-14R	100	37.680338366	-116.667665599	529304.3	4170400.8	0.41	1633.7	0.74	499969	1066682	5360
AL-15R	100	37.678545019	-116.671120850	529000.3	4170200.8	0.38	1634.3	0.66	498969	1066029	5362
AL-16R	100	37.678538112	-116.669983607	529100.6	4170200.4	0.39	1635.0	0.66	499298	1066027	5364
AL-17R	100	37.678530036	-116.668878564	529198.1	4170199.8	0.38	1634.6	0.65	499618	1066024	5363
AL-18R	100	37.677670771	-116.669985890	529100.8	4170104.1	0.40	1635.3	0.66	499298	1065711	5365
AL-19R	100	37.677650434	-116.667805449	529293.0	4170102.6	0.38	1634.4	0.65	499929	1065704	5362
AL-20R	100	37.677685233	-116.672168832	528908.3	4170105.1	0.35	1634.0	0.53	498666	1065716	5361
AL-21R	100	37.676795340	-116.669987961	529100.9	4170007.0	0.36	1635.1	0.57	499297	1065392	5365
AL-22R	100	37.680347098	-116.670074428	529091.9	4170401.0	0.39	1634.8	0.66	499272	1066686	5364
AL-23R	100	37.680342385	-116.668806066	529203.7	4170400.9	0.38	1634.8	0.67	499639	1066684	5364

Table F-1: Drill hole coordinate locations for holes drilled on Antelope Lake (continued)

[Geographic coordinates are WGS-84 values by Global Positioning Satellite. UTM coordinates are WGS-84, Zone 11. State Plane Coordinates are Nevada Coordinate System, Central Zone, NAD-27. An "R" suffix to the Hole ID indicates a rotary drill hole]

Hole Id	Depth	Latitude	Longitude	UTM East	UTM North	Horizontal Precision	GPS Elevation	Vertical Precision	State Plane East	State Plane North	Elevation
	(ft)	(degrees)	(degrees)	(m)	(m)	(m)	(m)	(m)	(ft)	(ft)	(ft)
AL-24R	100	37.678306302	-116.667773082	529295.6	4170175.3	0.38	1634.4	0.65	499938	1065942	5362
AL-25R	100	37.680432438	-116.672269108	528898.4	4170409.8	0.37	1634.4	0.65	498637	1066717	5363
AL-26R	100	37.679519186	-116.672253900	528900.0	4170308.5	0.37	1634.3	0.65	498642	1066384	5362
AL-27R	100	37.678605137	-116.672213014	528904.0	4170207.1	0.37	1634.4	0.65	498653	1066051	5362
AL-28	100	37.677623228	-116.671113182	529001.4	4170098.5	0.37	1634.3	0.65	498972	1065694	5362
AL-29R	100										
AL-30R	100	37.676795588	-116.669990757	529100.7	4170007.0	0.36	1633.4	0.50	499296	1065392	5359
AL-31R	100	37.677621006	-116.668838407	529202.0	4170099.0	0.35	1634.1	0.53	499630	1065693	5361
AL-32R	100	37.681229872	-116.669972033	529100.6	4170499.0	0.35	1633.7	0.53	499302	1067007	5360
AL-33R	100	37.680330352	-116.671117303	529000.0	4170398.8	0.35	1633.5	0.54	498970	1066679	5360
AL-34R[1]	100	37.672093876	-116.663621674	529664.2	4169487.4	0.35	1633.5	0.52	501140	1063680	5360

1.Hole AL-34 was drilled immediately adjacent to the location of the experimental drop-test known as "TD-2" (Togami, 2002).

This page intentionally left blank.

Appendix G: Geophysical Logs for Drill Holes on Antelope Lake

This page intentionally left blank.

INTRODUCTION

This appendix contains graphic presentations of the geophysical logs that were acquired from the drill holes on Antelope Lake, both core and rotary. Both types of holes were logged in an identical fashion. Cored holes were reamed to the full diameter of the rotary drill holes (~5.25 inches) prior to logging. The contractor for the geophysical logging activities at Antelope Lake was Century Geophysical Corporation, of Tulsa Oklahoma.

Because both the Main Lake logging program described in Appendix C and this logging program were intended to be essentially the same, much of the descriptive material in Appendix C beginning on page 95 is relevant and will not be repeated here. Rather, emphasis will be placed on the differences between the two logging programs, and in particular upon the additional geophysical log traces that were obtained at Antelope Lake.

THE LOG DATA

Conventional Electrical Logs

In essence, the same, single-tool log suite that was acquired at Main Lake was again acquired at Antelope Lake. In addition, the following major log traces were obtained:

1. 16-inch normal resistivity (ohm-meters)
2. 64-inch normal resistivity (ohm-meters)
3. Lateral resistivity (ohm-meters)
4. Induction resistivity (ohm-meters)
5. Spontaneous (self-) potential (millivolts)
6. Fluid resistivity (ohm-meters)
7. Sonic logs (interval-transit time (microseconds per foot)

All of these curves except for the sonic are "electrical" logs, and as such measure various quantities about the electrical properties of the rocks, the fluids within the formations, or the interaction between the rocks and the fluids in the borehole. A few other traces were also acquired as part of the logging program because the instrumentation was collocated on the tools used for the seven traces described above. These curves are of little value to this characterization program, and are therefore not discussed further. The data, however, are included in the LAS-format log files on the CD-R in the back of this report.

The 16-inch and 64-inch so-called normal resistivity curves are quite "old" logging traces, extensively used in the oil-and-gas exploration industry. They measure the electrical resistivity of the formation and its contained fluids, but the spacing of the electrodes (16 and 64 inches respectively) by which these resistivity measurements are made is different. The intent is to query the resistivity of the rock at differing distances away from the borehole to evaluate the effects of *invasion* — the movement of drilling fluids out of the drill hole and into the rocks themselves. Invasion effects are important to the evaluation of permeability in the oil field.

The "lateral" resistivity is what is known as a *focused* resistivity tool. The principal current-measuring electrodes are flanked by additional electrodes that generate another electrical field thus focusing the lateral resistivity field in a more flattened, ellipsoidal pattern, rather than allowing an unconstrained spherical field. The intent is to focus the resistivity within a thinner vertical interval, thus helping to identify thinner beds than is possible with non-focused tools.

Induction resistivity is yet another measure of the resistance of the rock-fluid combination to electrical flow, only the physics of the measurement is different. Rather than directly measuring the resistance of the formation, a high-frequency alternating current is used to

induce secondary currents in the formation, which are then measured and used to determine the apparent resistivity of the rock-fluid environment. The induction tool may be used in drill holes where the conventional resistivity tools cannot be used (air-filled holes or holes drilled with salt-saturated muds) or in which the formations otherwise exhibit electrical properties that interfere with the direct measurement of resistance. Induction, per se, (recorded as millimohs per meter) has been converted here to its reciprocal, resistivity, in ohm-meters

The *SP* (spontaneous-potential or self-potential) trace is again an older curve derived from oil-and-gas exploration. The presence of fluids of differing salinities in the borehole and in the matrix of the rocks serves as a natural battery, generating small currents. These currents can be detected and measured as voltages. The SP log is most useful in holes drilled with fresh-water muds where the formation fluids are saline. The SP trace is not particularly informative at Antelope Lake, and it is not presented on the figures in this appendix.

The fluid resistivity log represents precisely what the name implies: the resistivity of the fluid in the borehole. Although required to make quantitative calculations of various quantities of interest in oil-and-gas exploration or water-well drilling, the trace is not particularly meaningful in the current situation. Some deflections in this log trace may be observed in a few holes for which fresh water was added after drilling to bring the fluid leve in the hole to ground level.

The Sonic Log

The sonic log was run in the boreholes at Antelope Lake because, under the proper conditions and with certain limiting assumptions, it is possible to make some interpretations of the bulk modulus of the rock formations from the P-wave velocity, one of the quantities obtainable from the sonic-logging process. The sonic tool has a transmitter near one end that emits a high-frequency acoustical signal. This signal propagates through the rocks near the wall of the borehole and is recorded at two receivers on the sonde at different locations separated by a known distance. By analyzing the recovered acoustic signal at both physical locations, an estimate can be made of the time it took the signal to travel between the two receivers. Hence, microseconds per foot, which is easily transformed into a P-wave velocity in feet per second or equivalent velocity units.

The sonic log gave mixed results at Antelope Lake. Because the measurement of interval-transit time requires the recognition and distinguishing of a transmitted signal at two location separated by a time lag, it is critical to be measuring the elapsed time between the diachronous arrival of the exact same signal pulse. The interplay of borehole conditions and the formations being surveyed may work to obscure one or the other signals (near or far spacings), with the consequence that the interval-transit time represents different signal cycles and thus underestimate the true velocity of the formation by some integral multiple of the correct interval-transit-time. This phenomenon is referred to as *cycle-skipping*.

Particularly soft formations may attenuate the signal such that the signal is not recognizable at one or the other receivers. Also, borehole rugosity that breaks the physical connection between the tool and the formation can lead to interpretation of the direct acoustic waveform, travelling through the drilling mud, as the arrival of the signal through the rock and thereby generating erroneous velocity estimates.

Both of these conditions apply at Antelope Lake. The sediments are unconsolidated and

many of the drill holes are significantly out-of-gauge, as indicated by the caliper logs. The sonic-log data are included in digital LAS format on the CD-R for archival purposes, but they are not presented graphically in this data report.

Data Processing

Both the natural gamma and density traces are presented in raw and smoothed form in the figures that follow. This presentation style allows evaluation of the degree of smoothing and allows interpretation of the validity of the geologic features represented, and is consistent with the style of Appendix C.

Many of the drill holes on Antelope Lake are out-of-gauge. Some holes are very badly washed out, particularly close to the surface where the soft sediments were exposed to the rotary motion of the drill string and the passage of circulating drill fluids for the longest times. In fact, the holes became so large at places in the subsurface that the standard caliper attached to the density tool reached its maximum extent and provided no meaningful information regarding the actual diameter of the borehole. Because the density sonde was no longer being pressed against the wall of the hole, the density measurements in these intervals are also suspect.

A non-standard (longer) caliper arm was obtained and run routinely in most of the later drill holes. The tool with the extended arm was also re-run in most (but not all) of the earlier holes drilled and logged before the extended arm could be shipped and received. In these cases, the figures that follow show composite logs reflecting the multiple logging runs. However, the data files on the CD contain the original data by original run. Note that several of the Antelope Lake holes were washed so badly that even the extended caliper exceeded its calibrated limits. This holes and intervals may be identified by a straight-line caliper curve at a maximum value of 12 inches. See for example, the log for AL-4 (fig. G-3).

Discussion

Data Quality

In general, the logs recorded at Antelope Lake are of good quality, although the density log in particular is suspect over intervals that are significantly washed-out. As described in the corresponding section in Appendix C, it is the *rugosity* of the borehole and not the hole *size*, per se, that is the most important factor. If the hole is "generally" enlarged such that the logging sonde still can conform to the shape of the wall, the density readings should be meaningful. Of course, if the hole is sufficiently enlarged that the tool cannot be pressed against the sidewall by the caliper arm, the density values will not be representative of the wall materials. To assist in highlighting the intervals in which the density log may be questionable, the difference between the nominal size of the hole (the bit size) and the actual caliper log has been shaded a light-green color on the figures in this appendix. Density values over intervals thus highlighted should be considered carefully, as the density values shown may be misleading. In general, the density values shown for intervals over which the tool separated from the borehole wall because of excessive rugosity will be lower than the true density. More gamma rays will reach the detector without being attenuated by the rock mass and thus the counts recorded will be higher, suggesting a less-dense material. The density trace is shaded red for those portions of the hole that exceed a density of 2.0 g/cm^3 (the original definition of a "hard" layer on the Main Lake). Lithologic symbols for the generalized core logs that accompany the geophysical data for the relevant holes are presented below.

Missing Data

All of the drill holes at Antelope Lake were logged geophysically. However, hole AL-2, a core hole, was abandoned at only 20 ft when mud circulation was lost. Hole AL-3 is a replacement core hole, drilled only a few tens of feet away. Because hole AL-2 is so shallow, we do not present a figure with these logs, although the original (minimal) log data are contained in a LAS-format file on the CD-R. The standard null value of -999.25 represents data that are missing for other operational reasons.

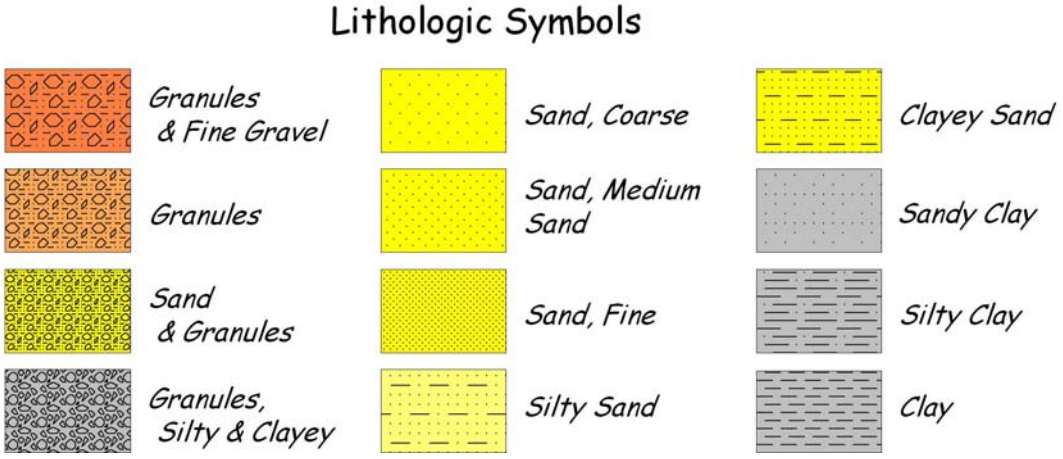

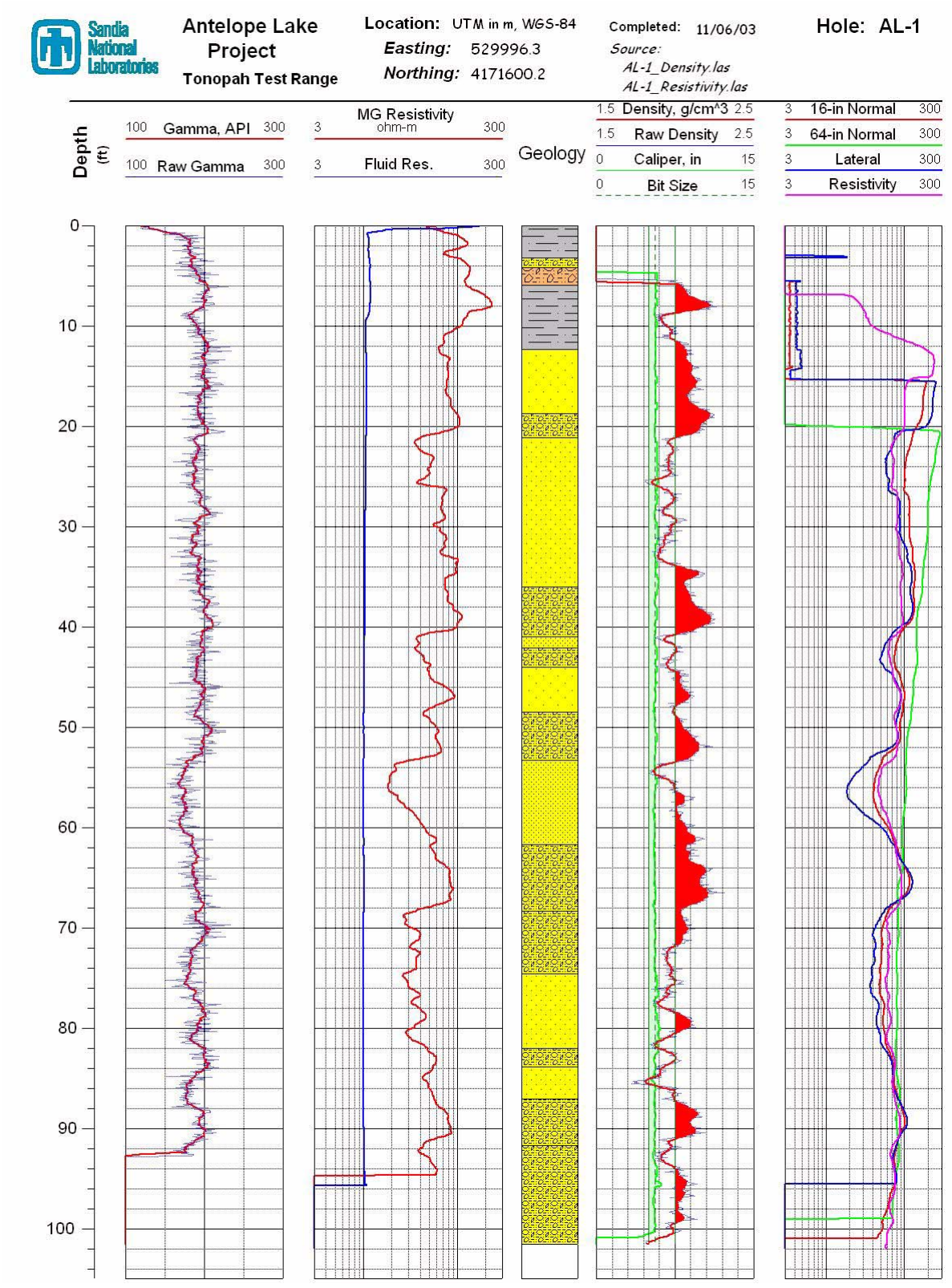

Figure G-1 Geophysical logs for drill hole AL-1.

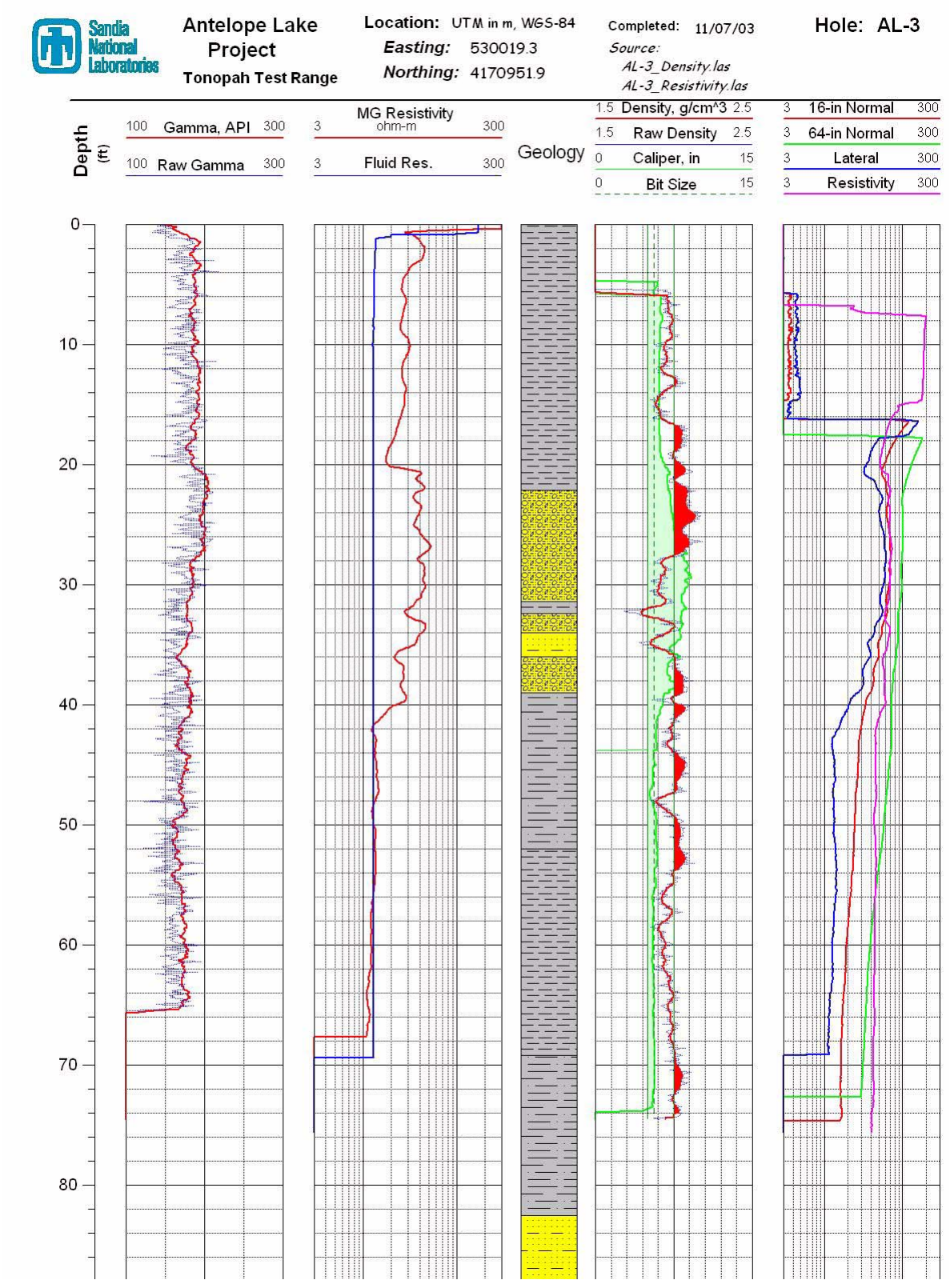

Figure G-2 Geophysical logs for drill hole AL-3.

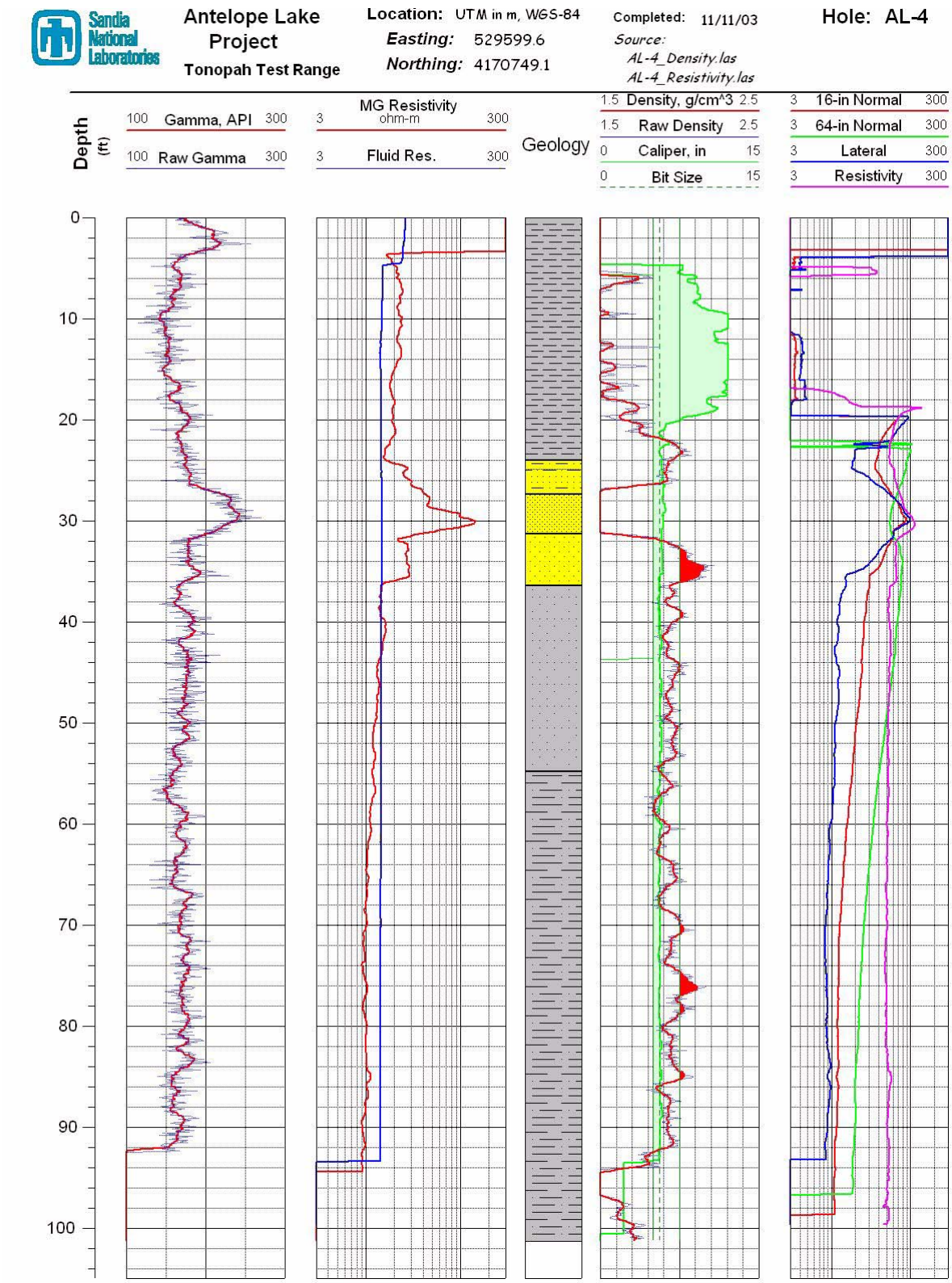

Figure G-3 Geophysical logs for drill hole AL-4.

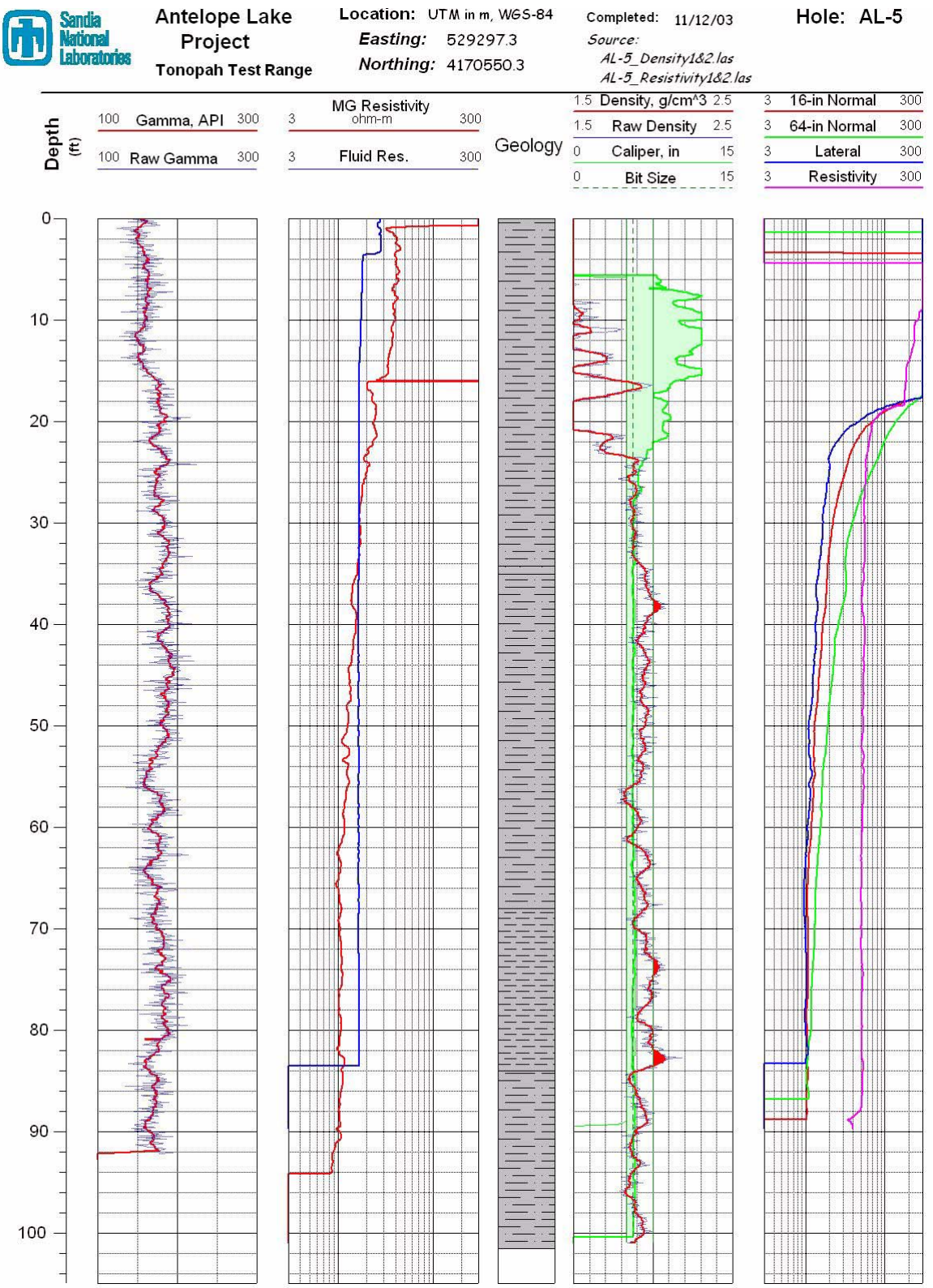

Figure G-4 Geophysical logs for drill hole AL-5.

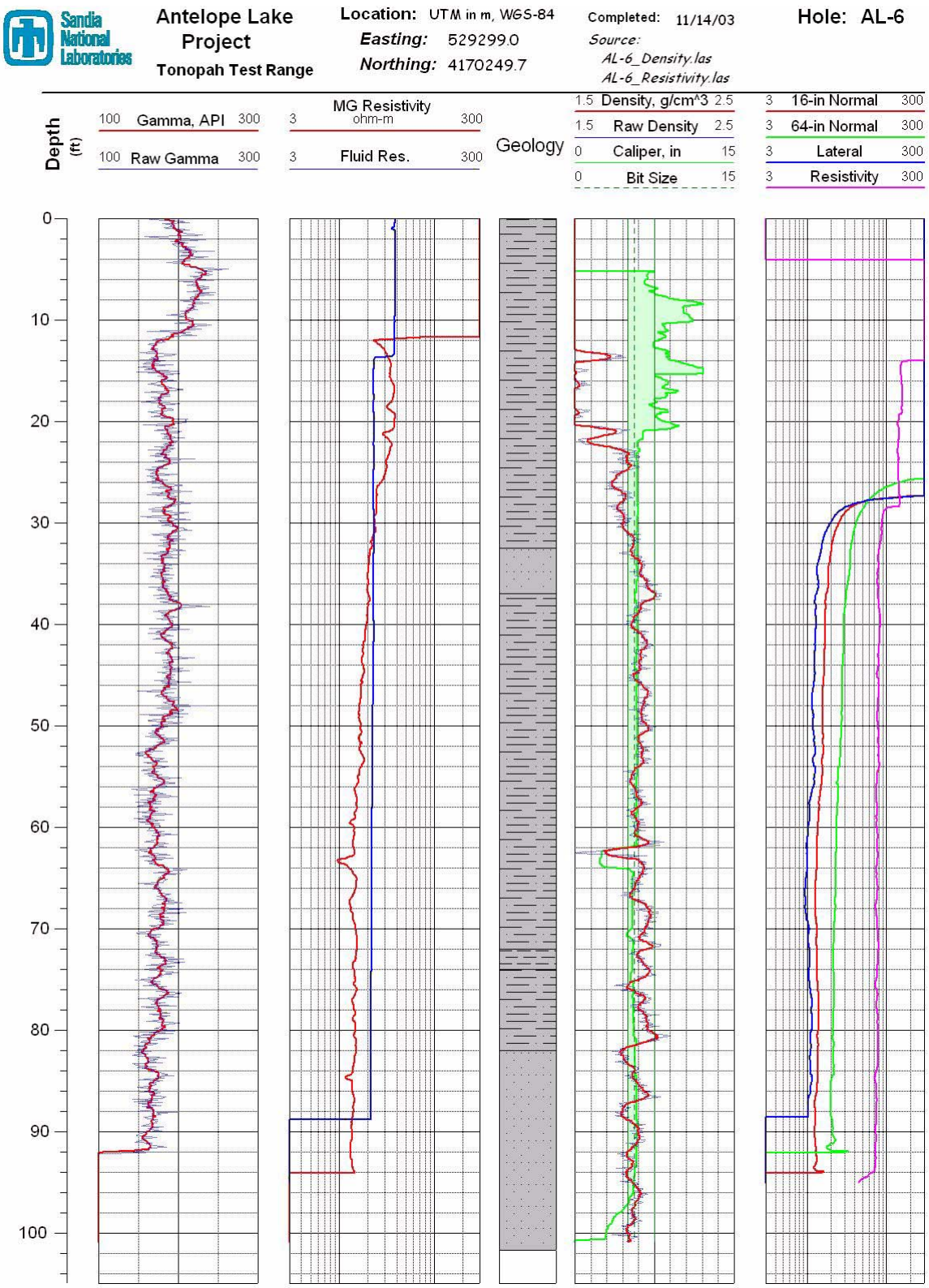

Figure G-5 Geophysical logs for drill hole AL-6.

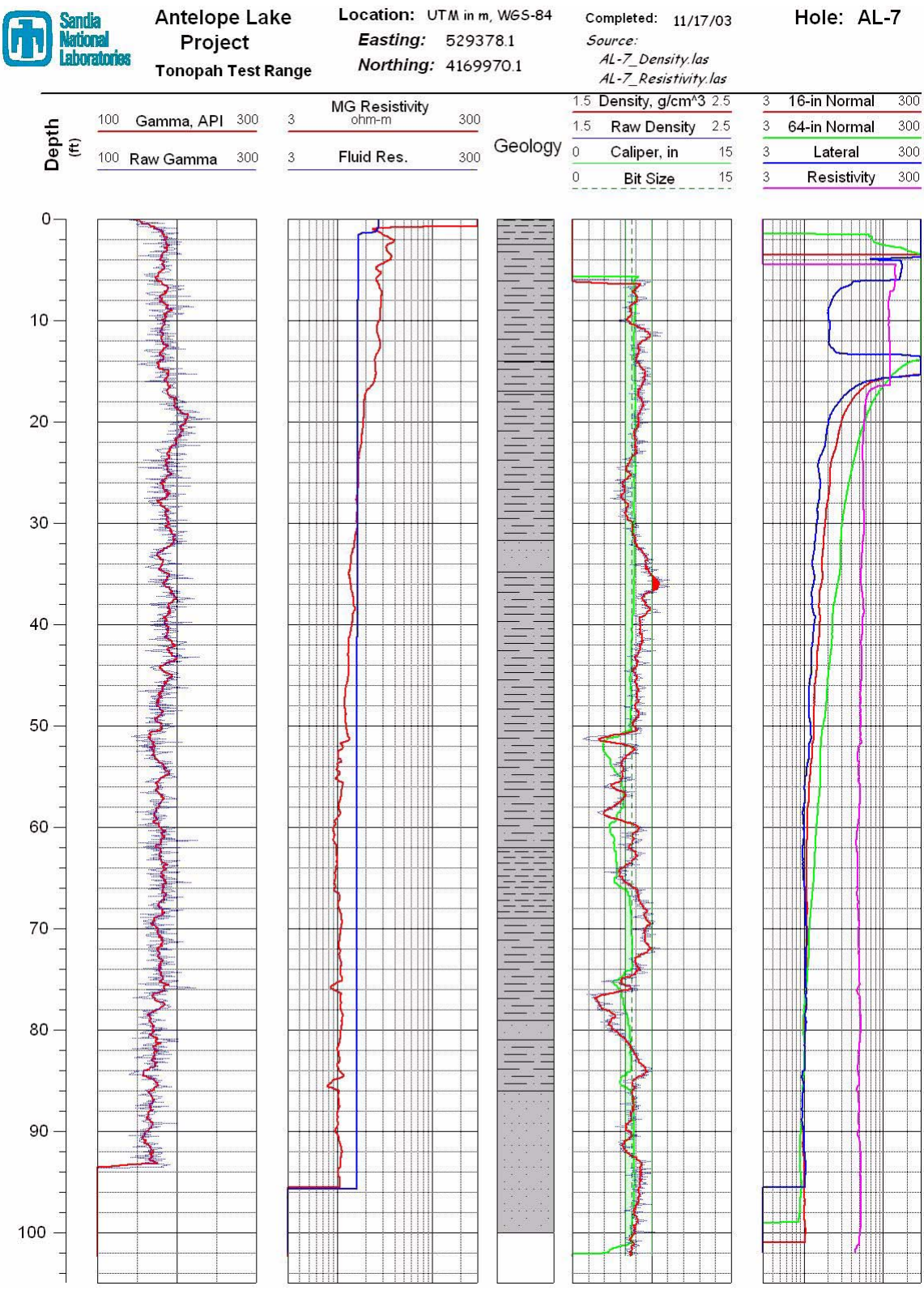

Figure G-6 Geophysical logs for drill hole AL-7.

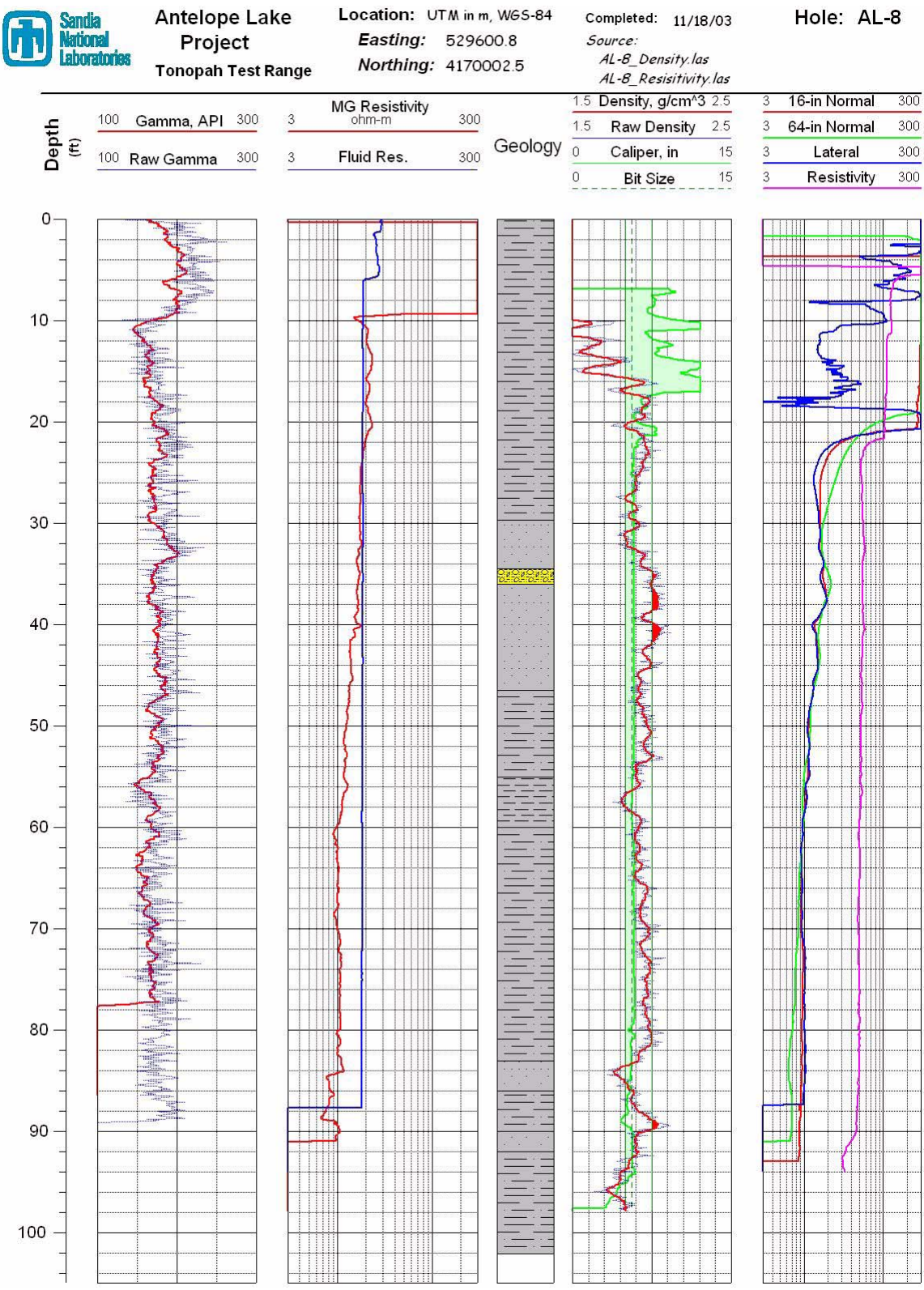

Figure G-7 Geophysical logs for drill hole AL-8.

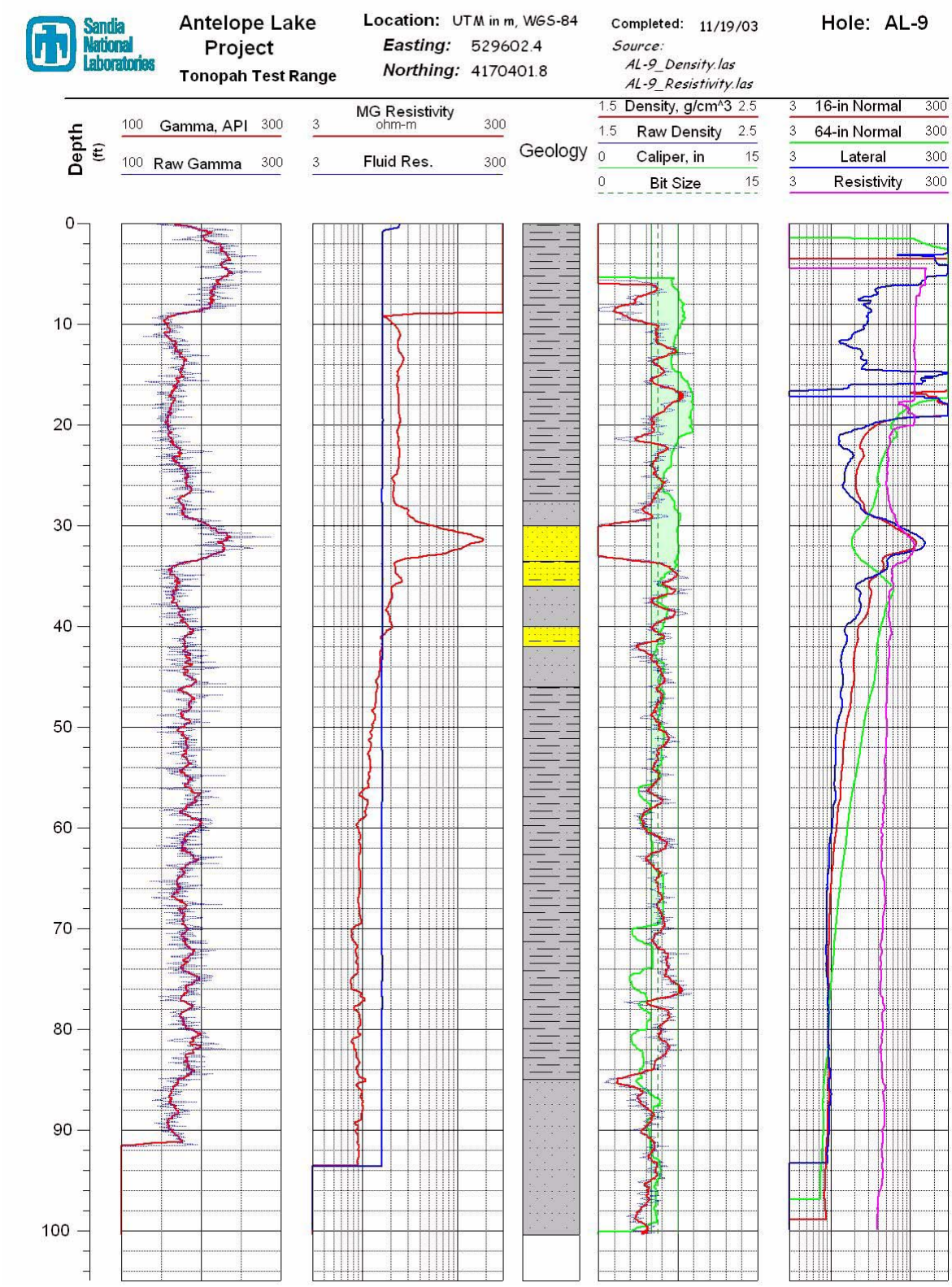

Figure G-8 Geophysical logs for drill hole AL-9.

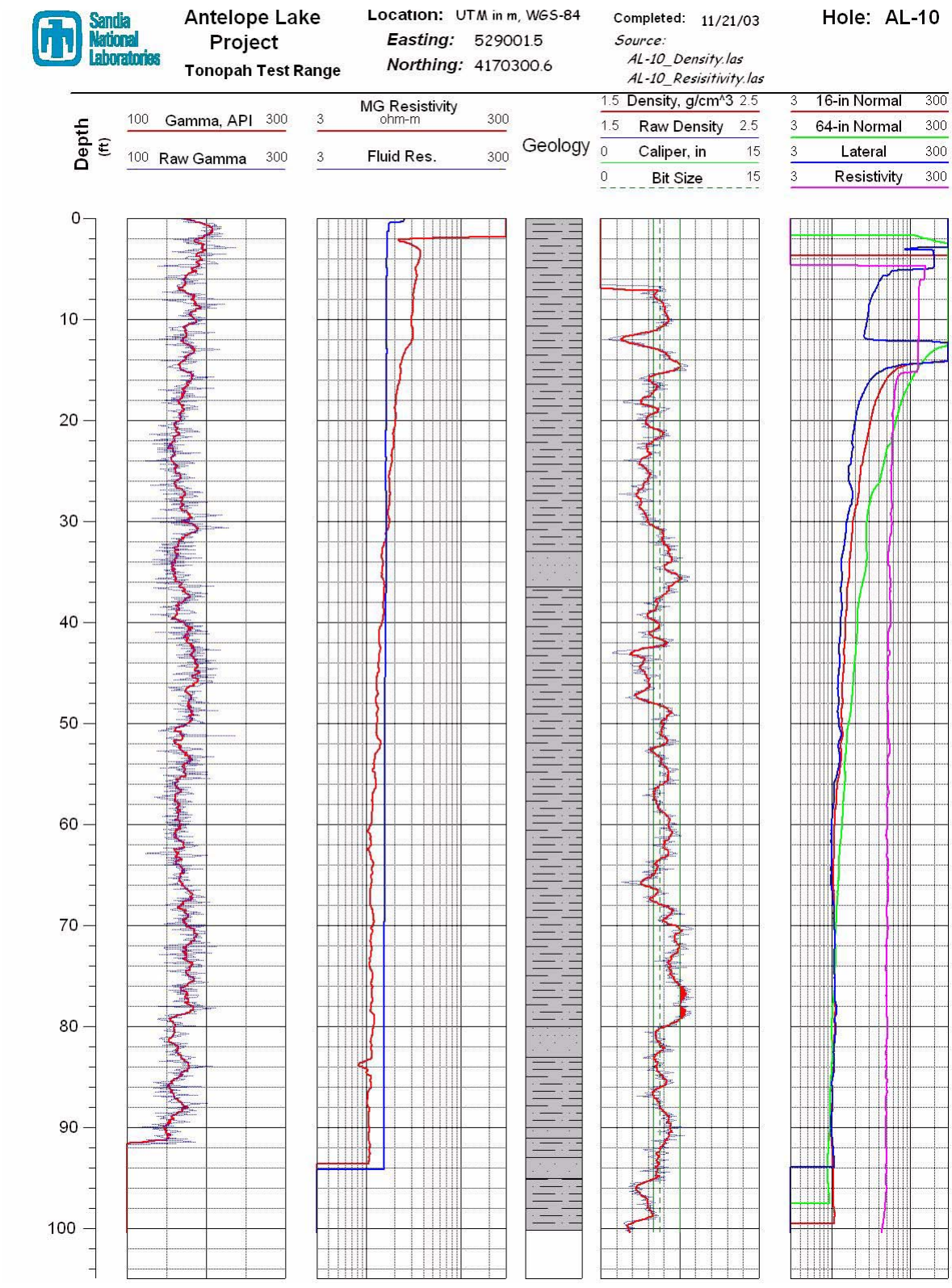

Figure G-9 Geophysical logs for drill hole AL-10.

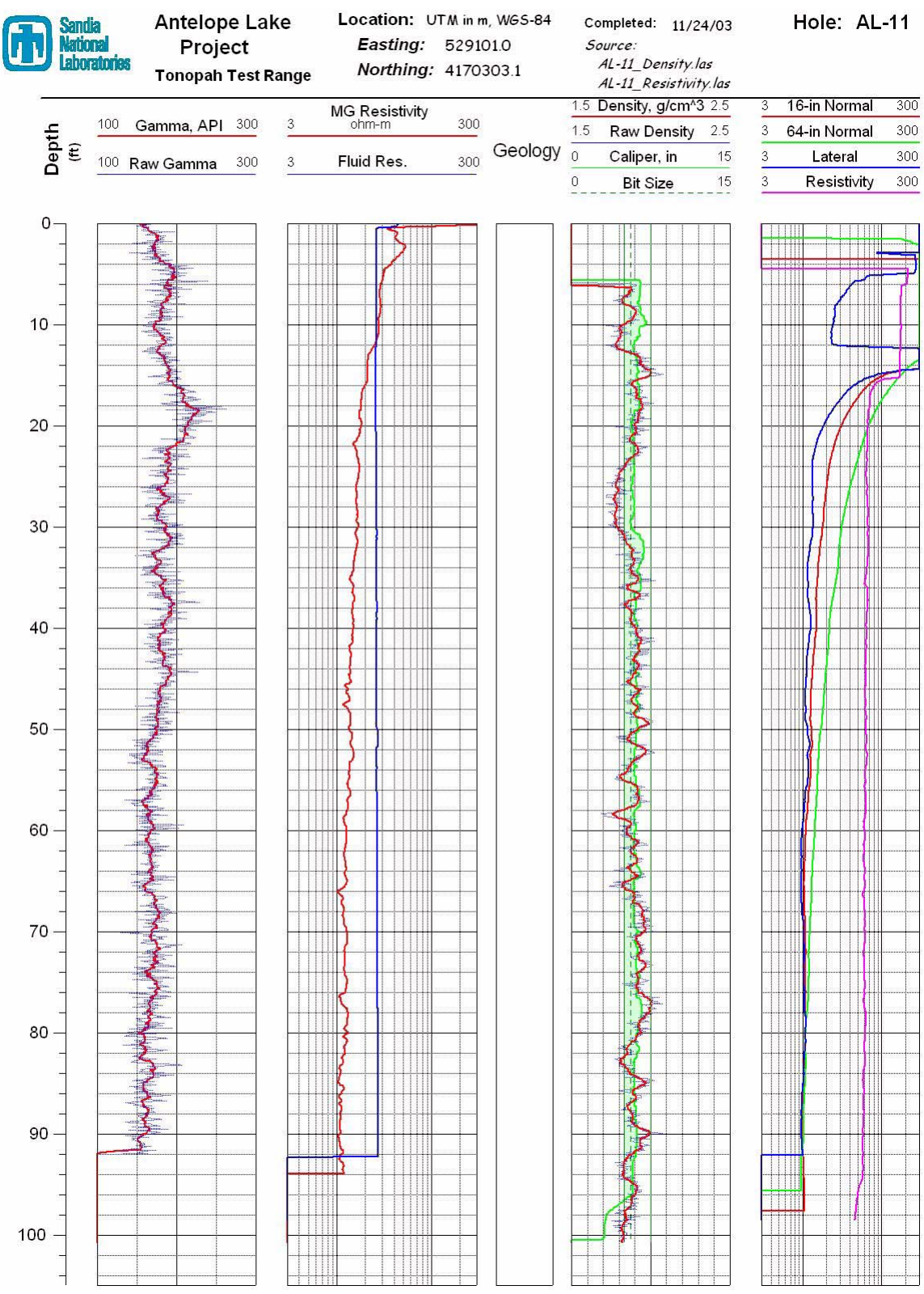

Figure G-10 Geophysical logs for drill hole AL-11.

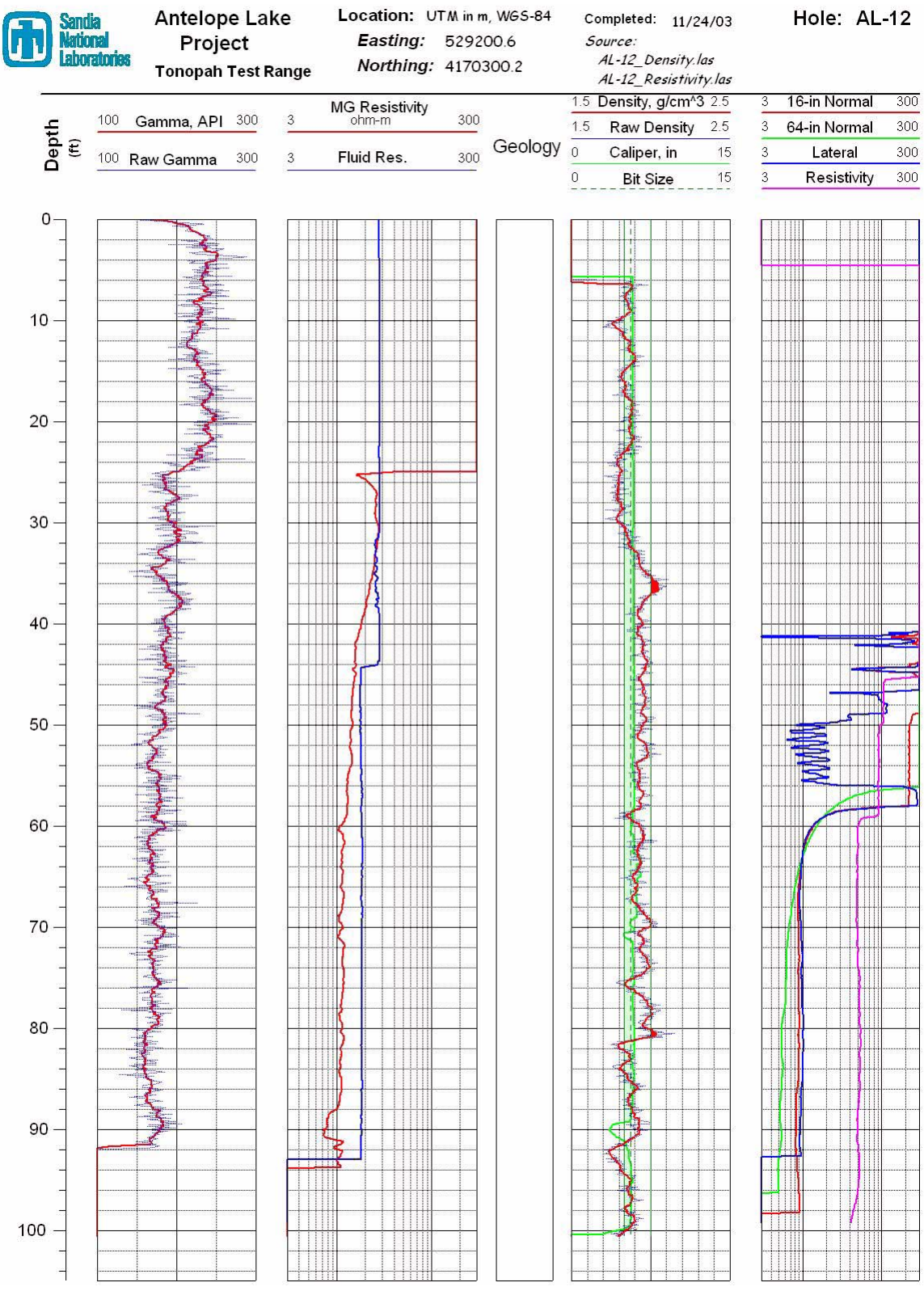

Figure G-11 Geophysical logs for drill hole AL-12.

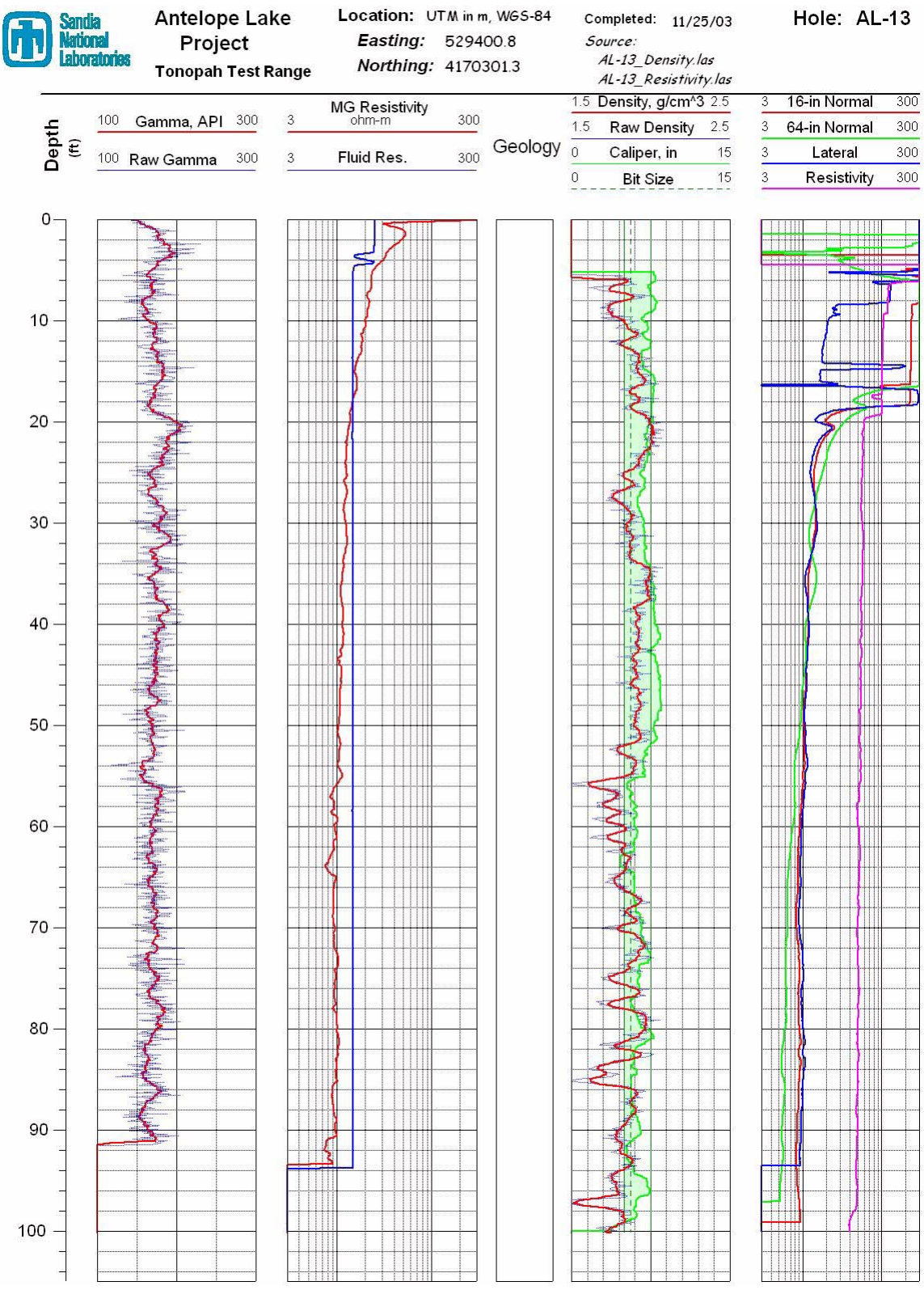

Figure G-12 Geophysical logs for drill hole AL-13

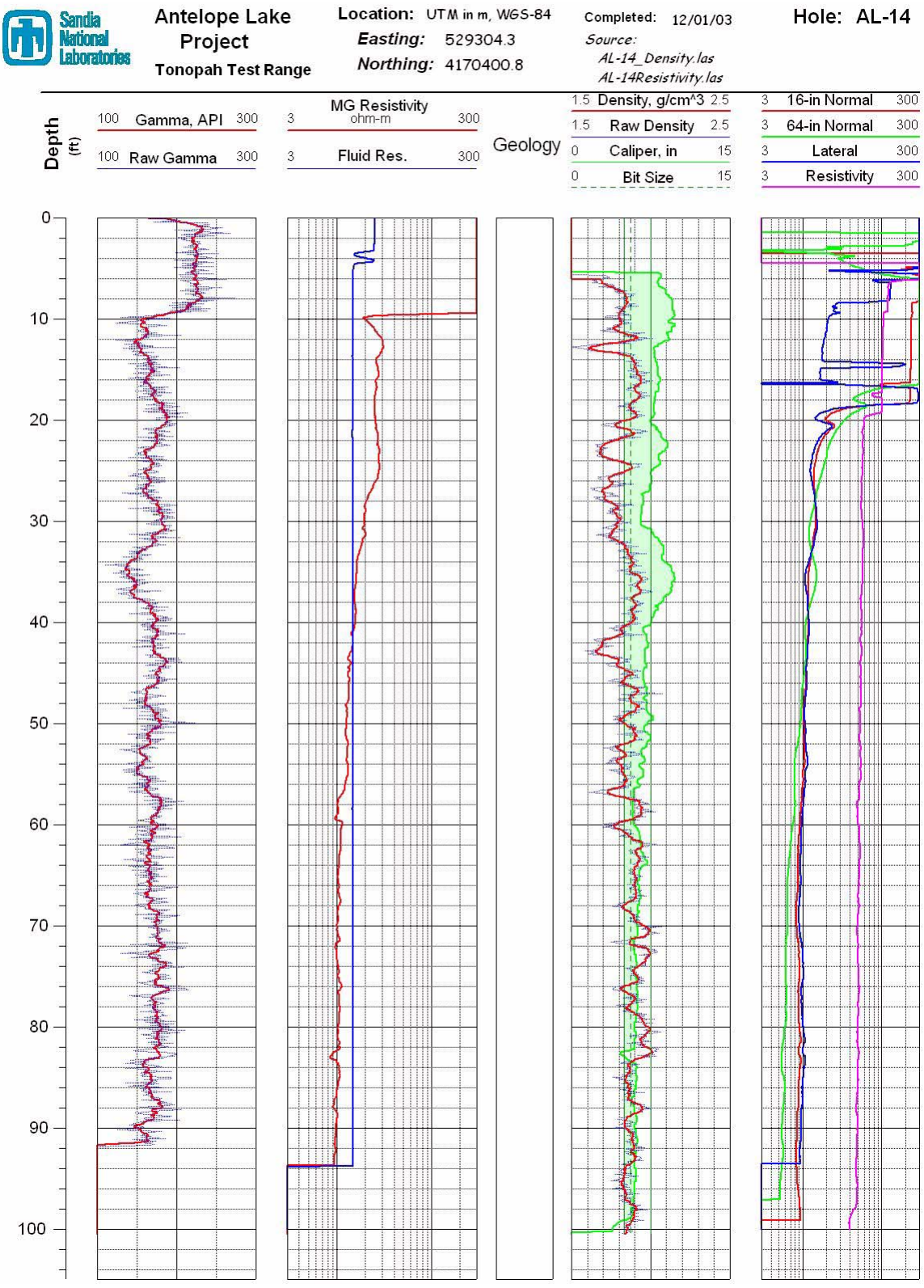

Figure G-13 Geophysical logs for drill hole AL-14.

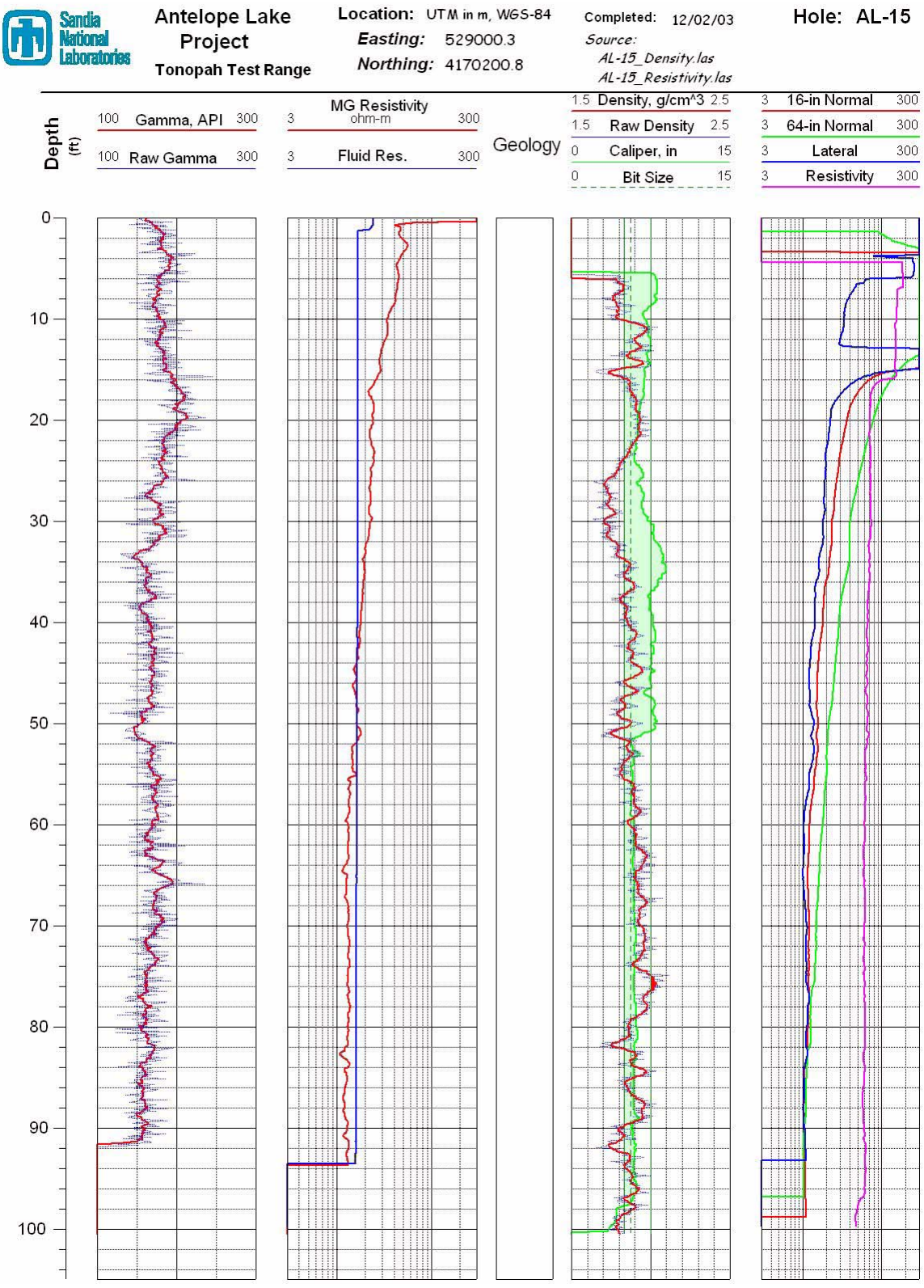

Figure G-14 Geophysical logs for drill hole AL-15.

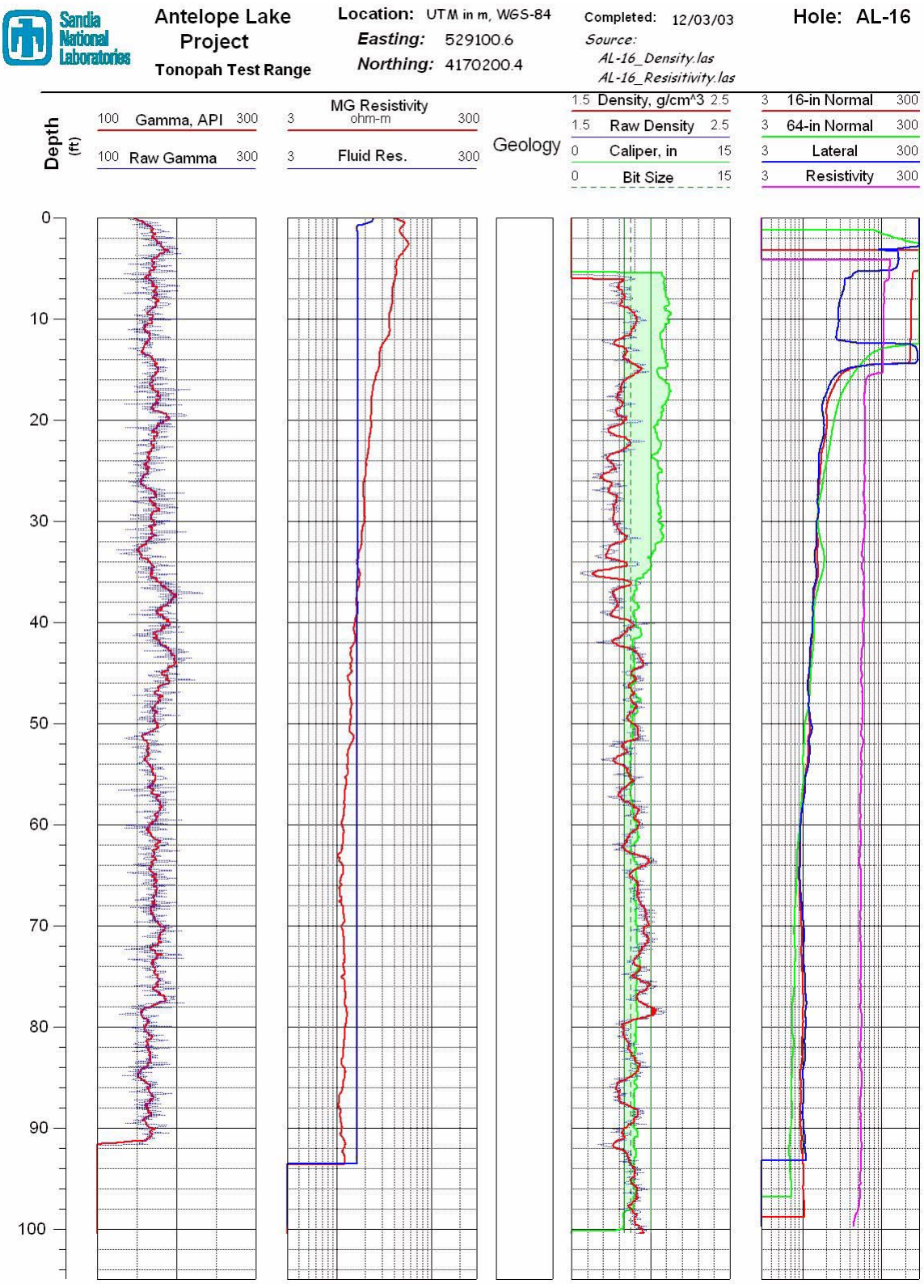

Figure G-15 Geophysical logs for drill hole AL-16.

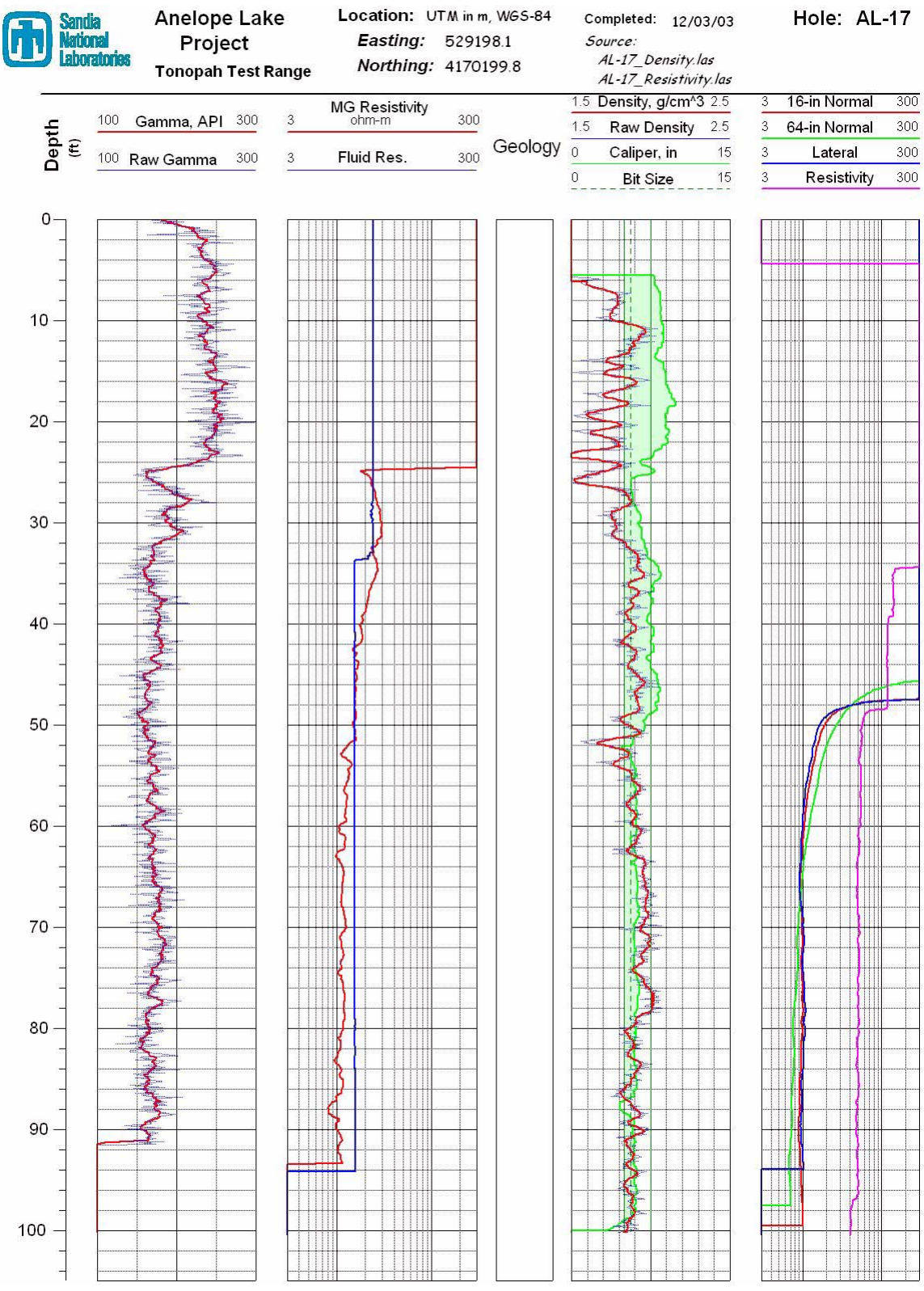

Figure G-16 Geophysical logs for drill hole AL-17.

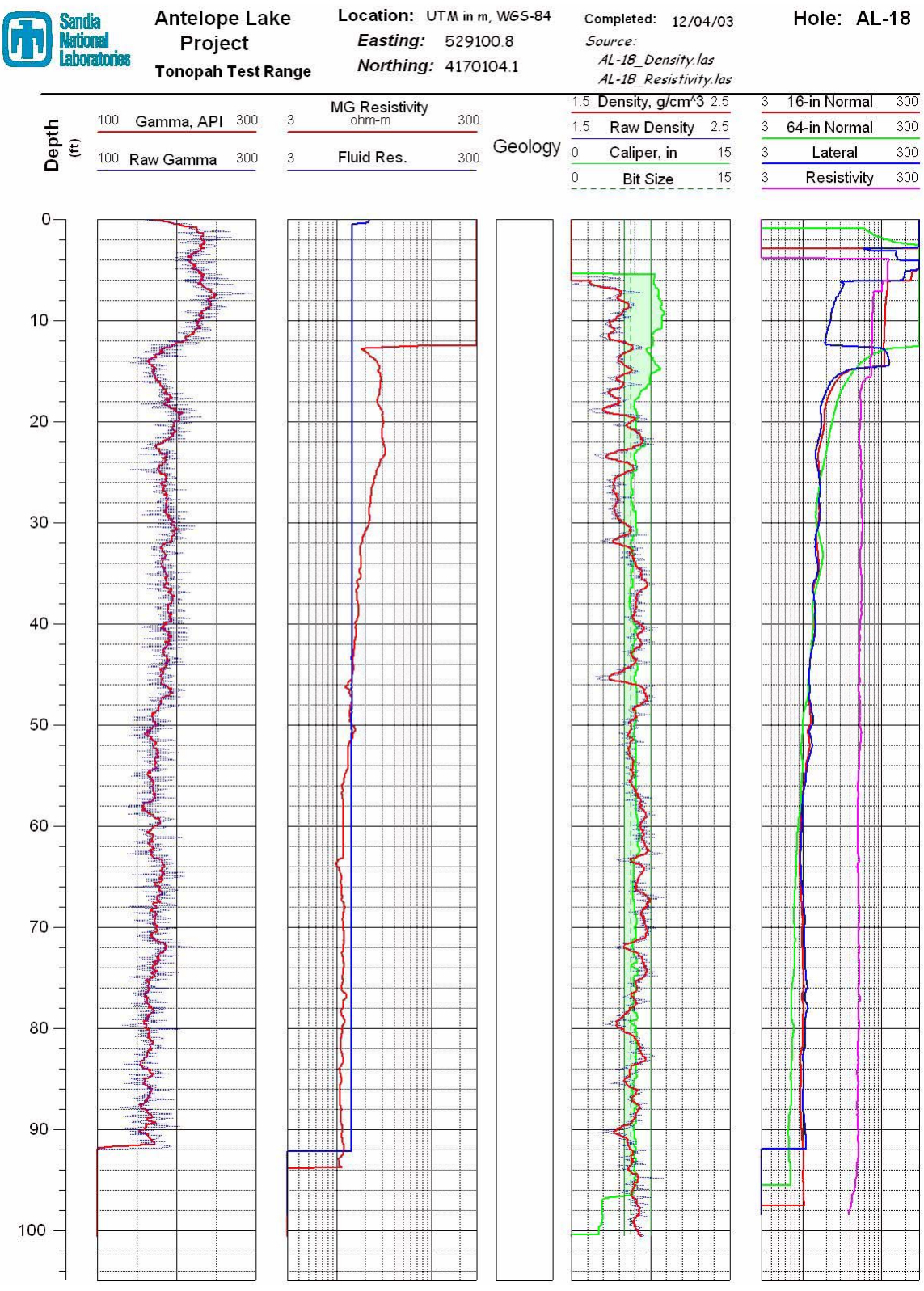

Figure G-17 Geophysical logs for drill hole AL-18.

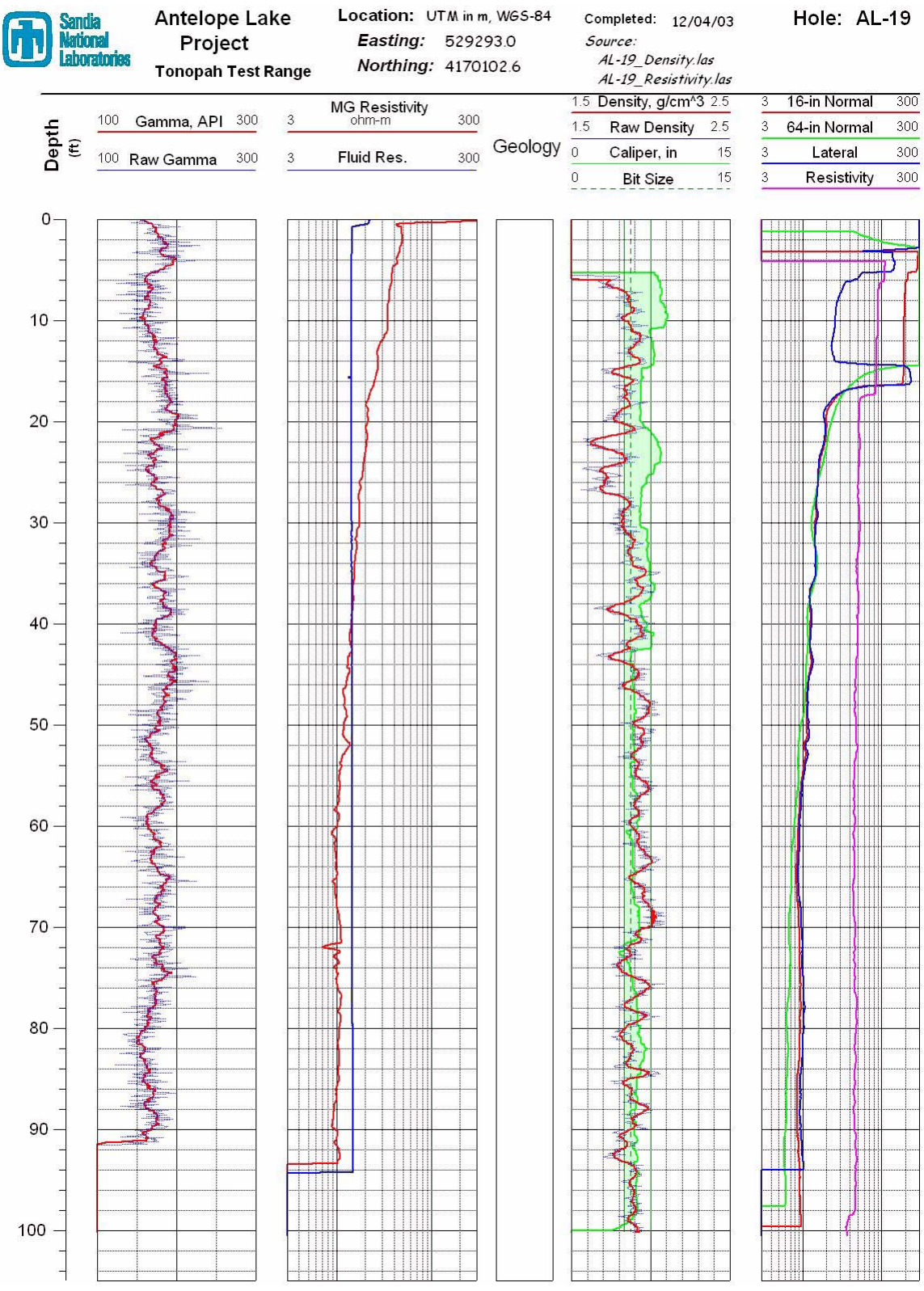

Figure G-18 Geophysical logs for drill hole AL-19.

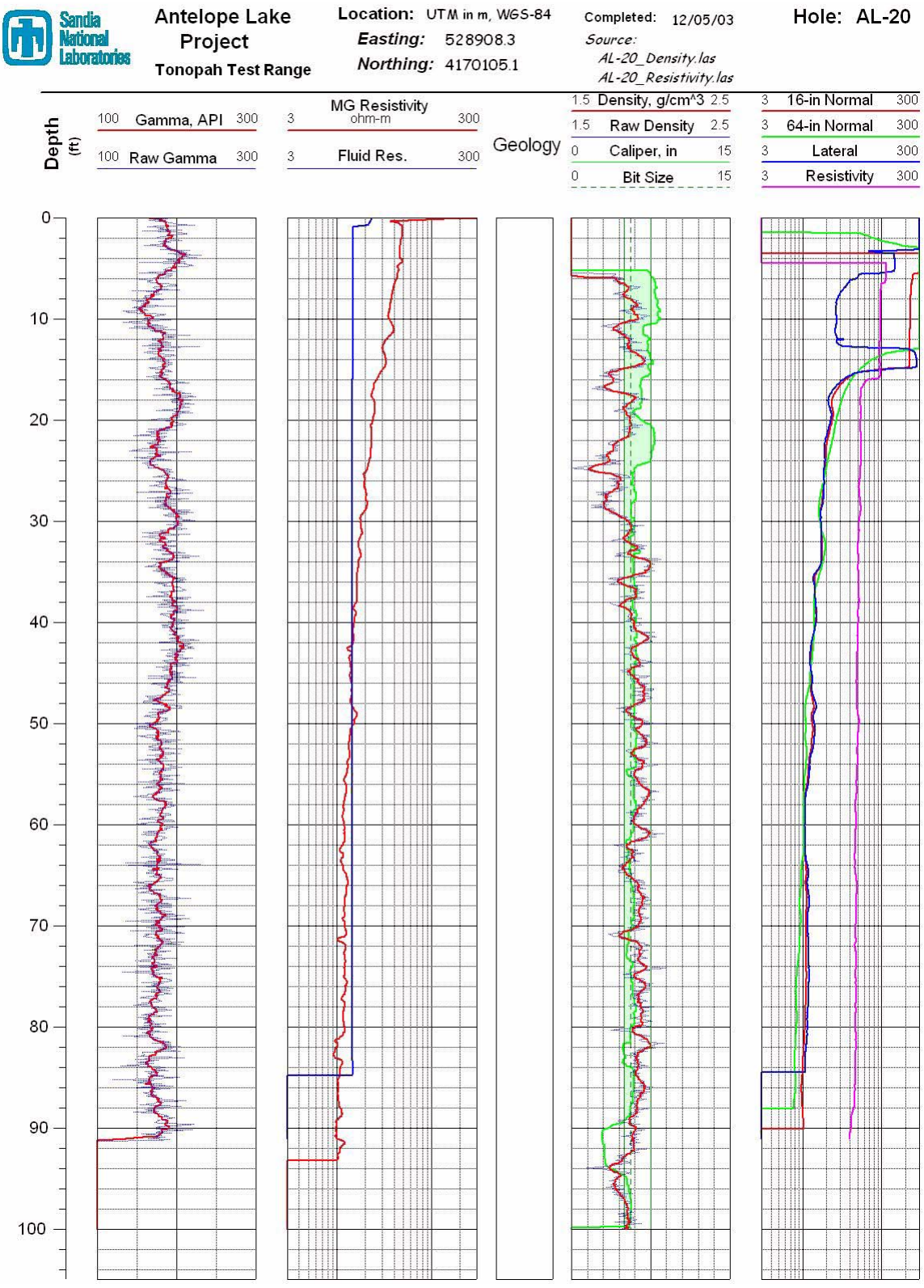

Figure G-19 Geophysical logs for drill hole AL-20.

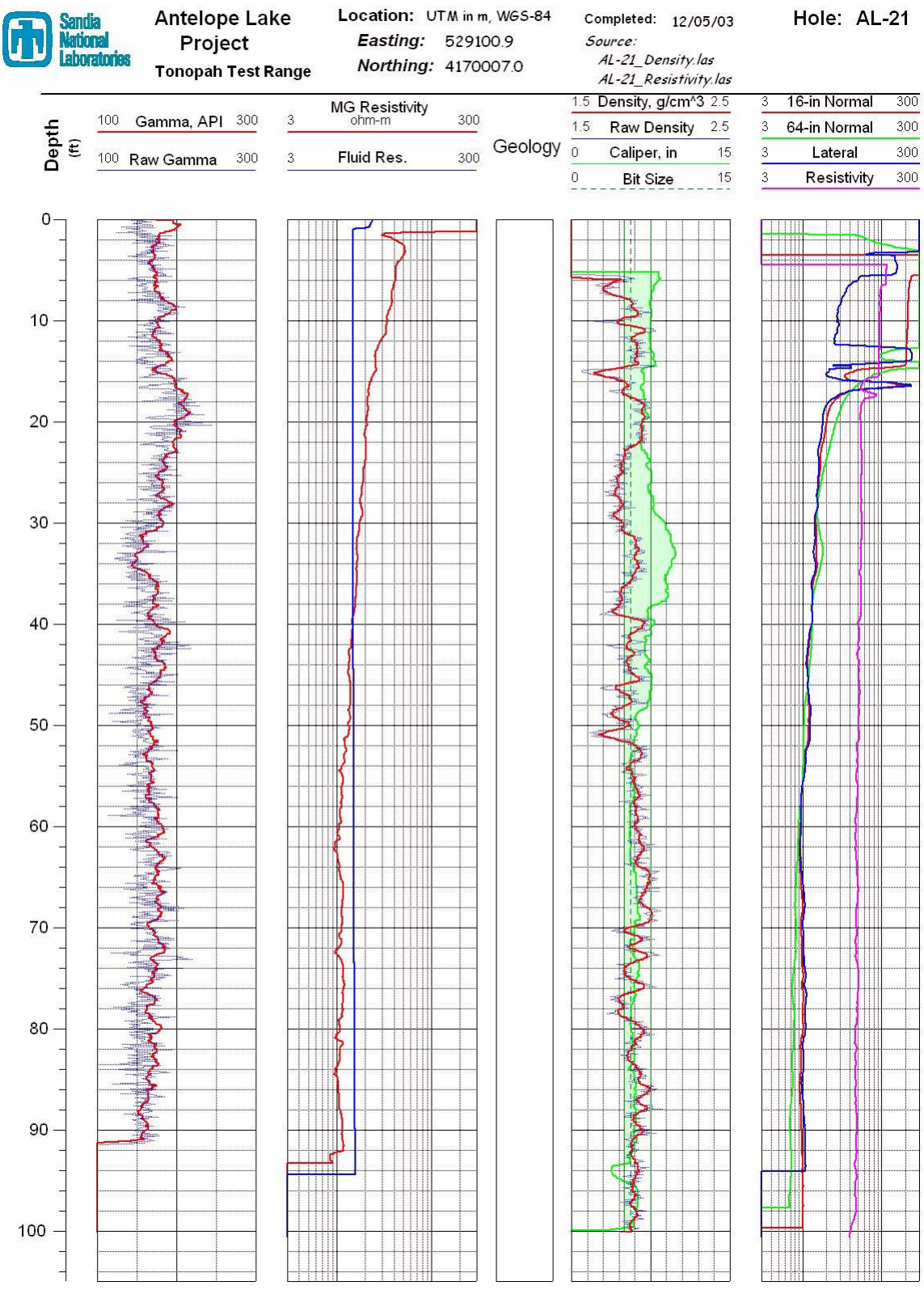

Figure G-20 Geophysical logs for drill hole AL-21.

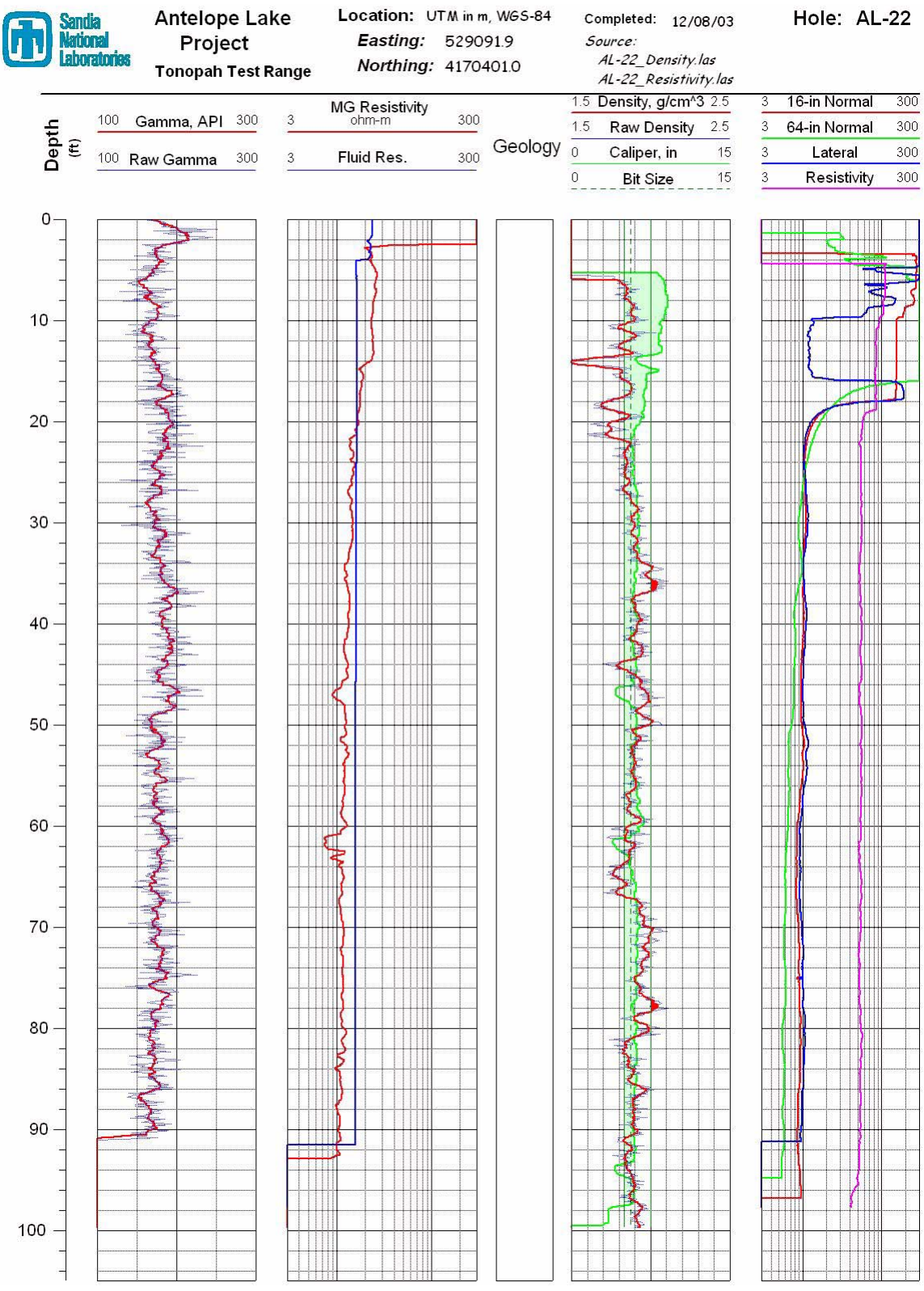

Figure G-21 Geophysical logs for drill hole AL-22.

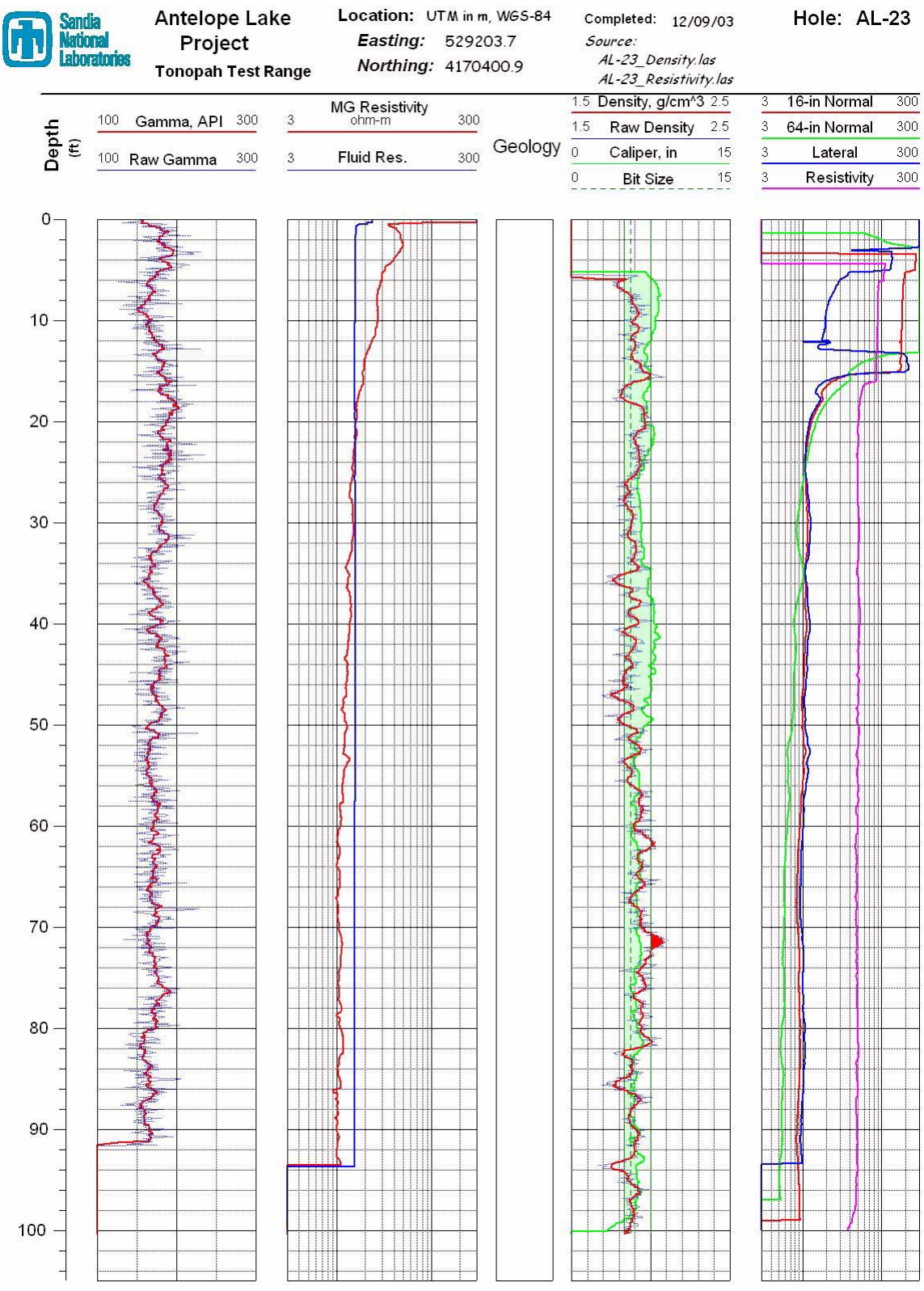

Figure G-22 Geophysical logs for drill hole AL-23.

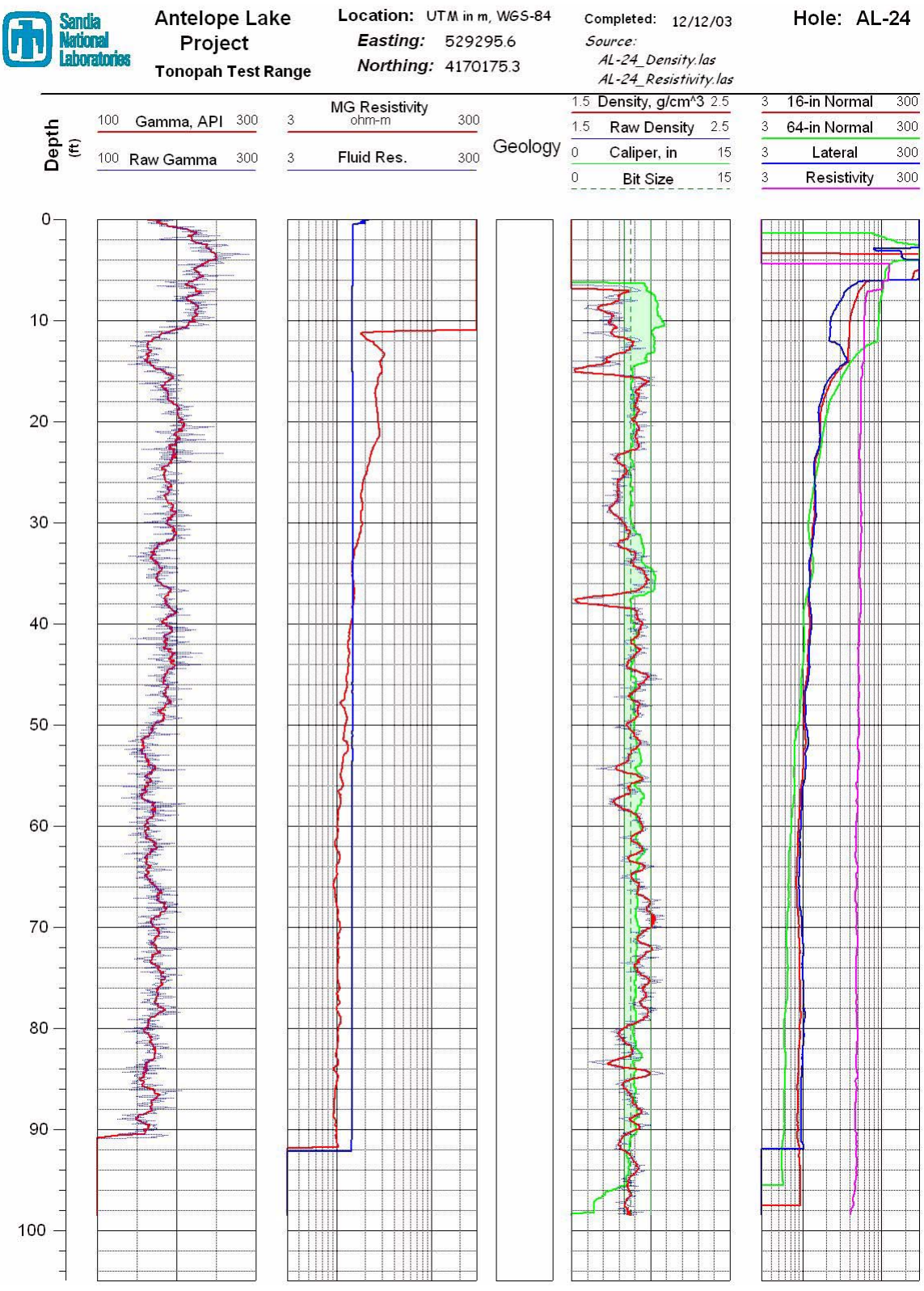

Figure G-23 Geophysical logs for drill hole AL-24.

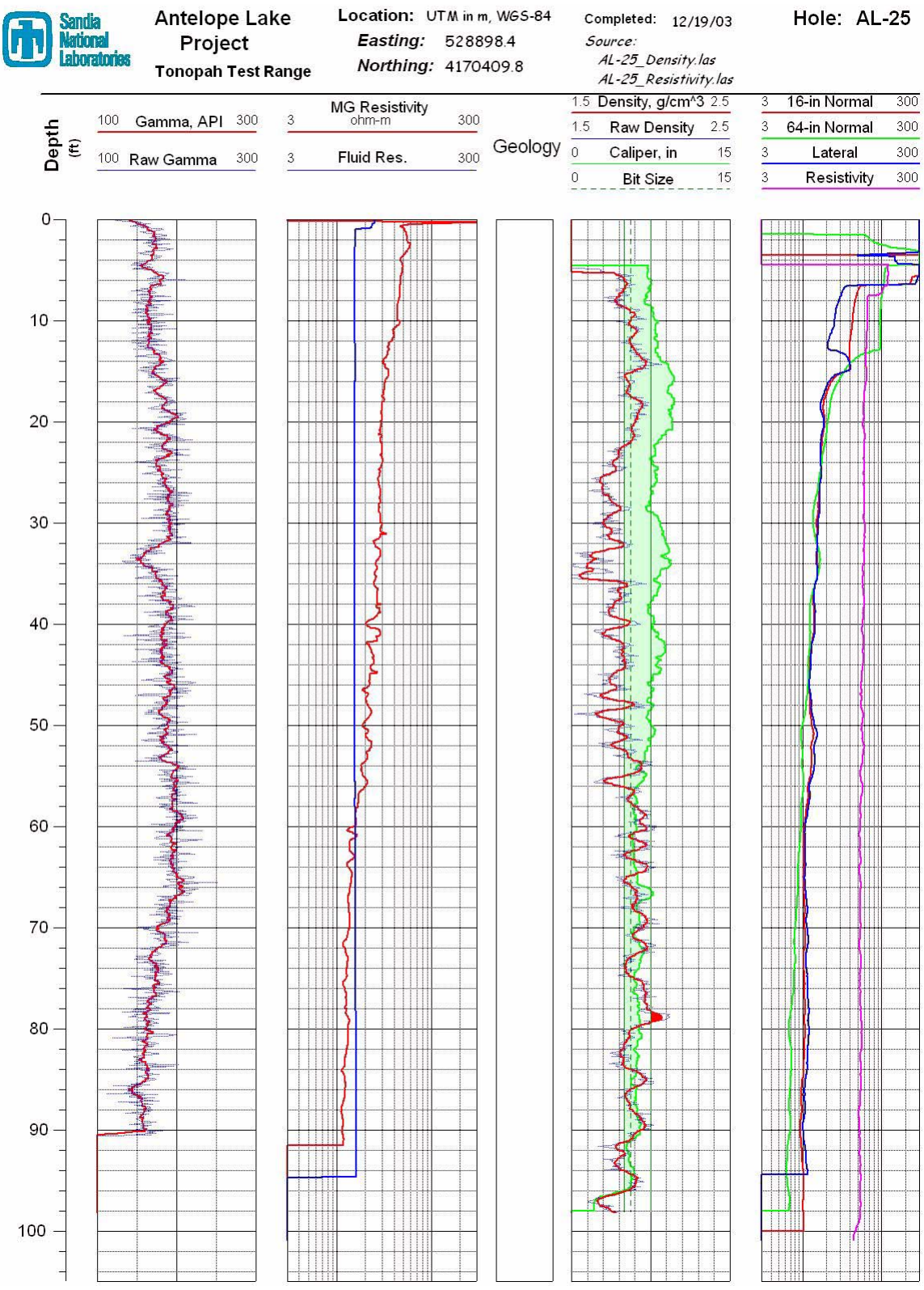

Figure G-24 Geophysical logs for drill hole AL-25.

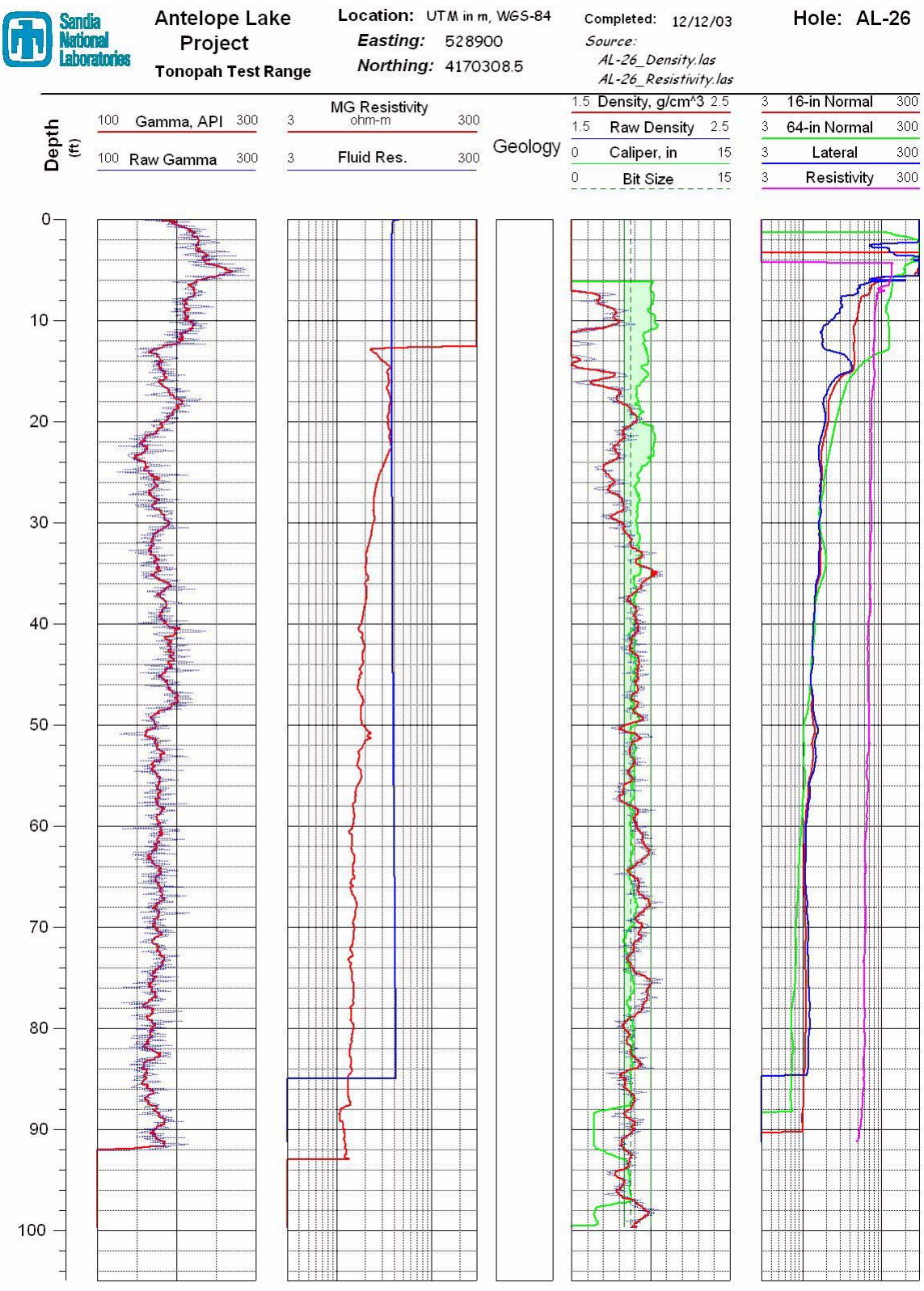

Figure G-25 Geophysical logs for drill hole AL-26.

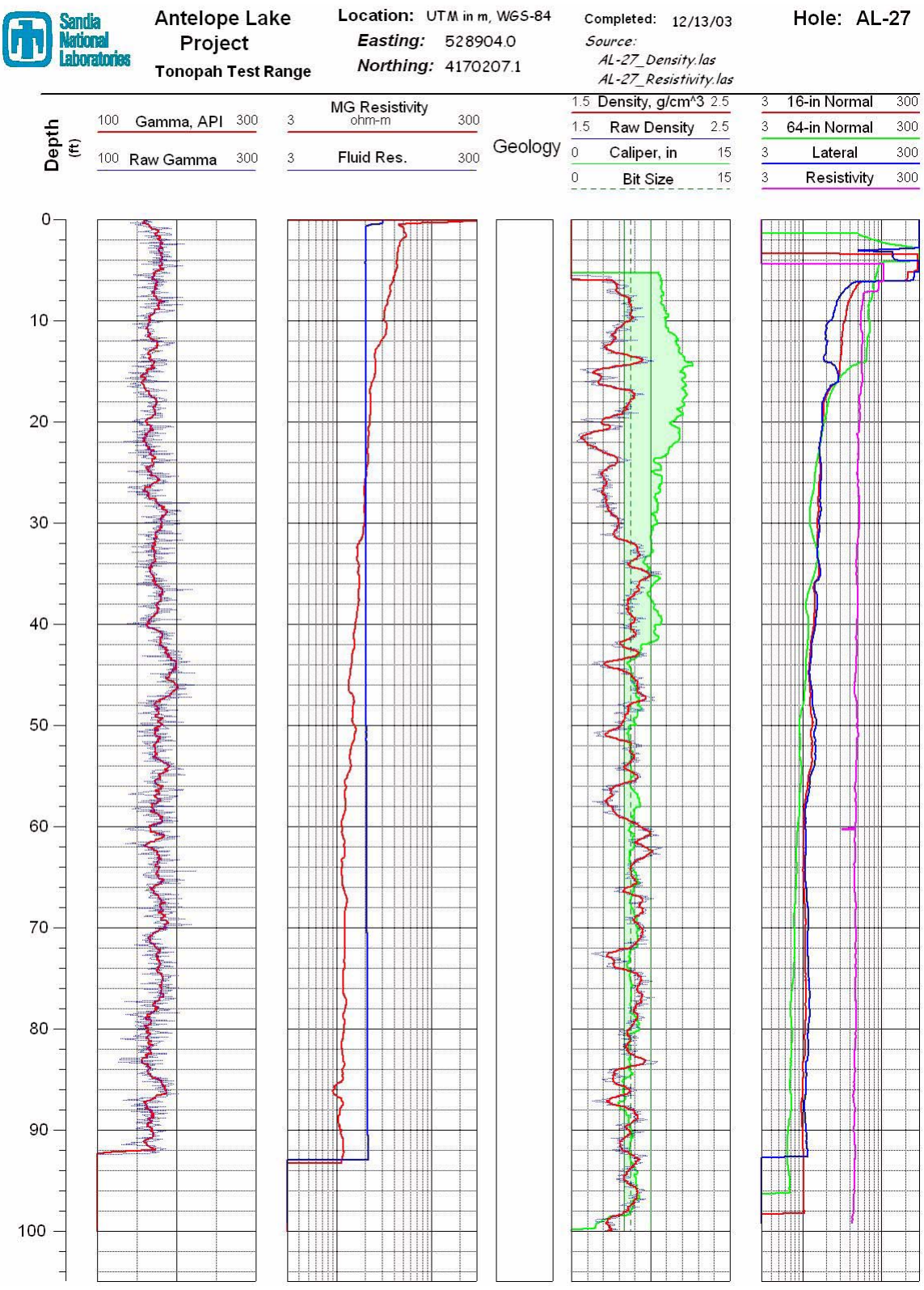

Figure G-26 Geophysical logs for drill hole AL-27.

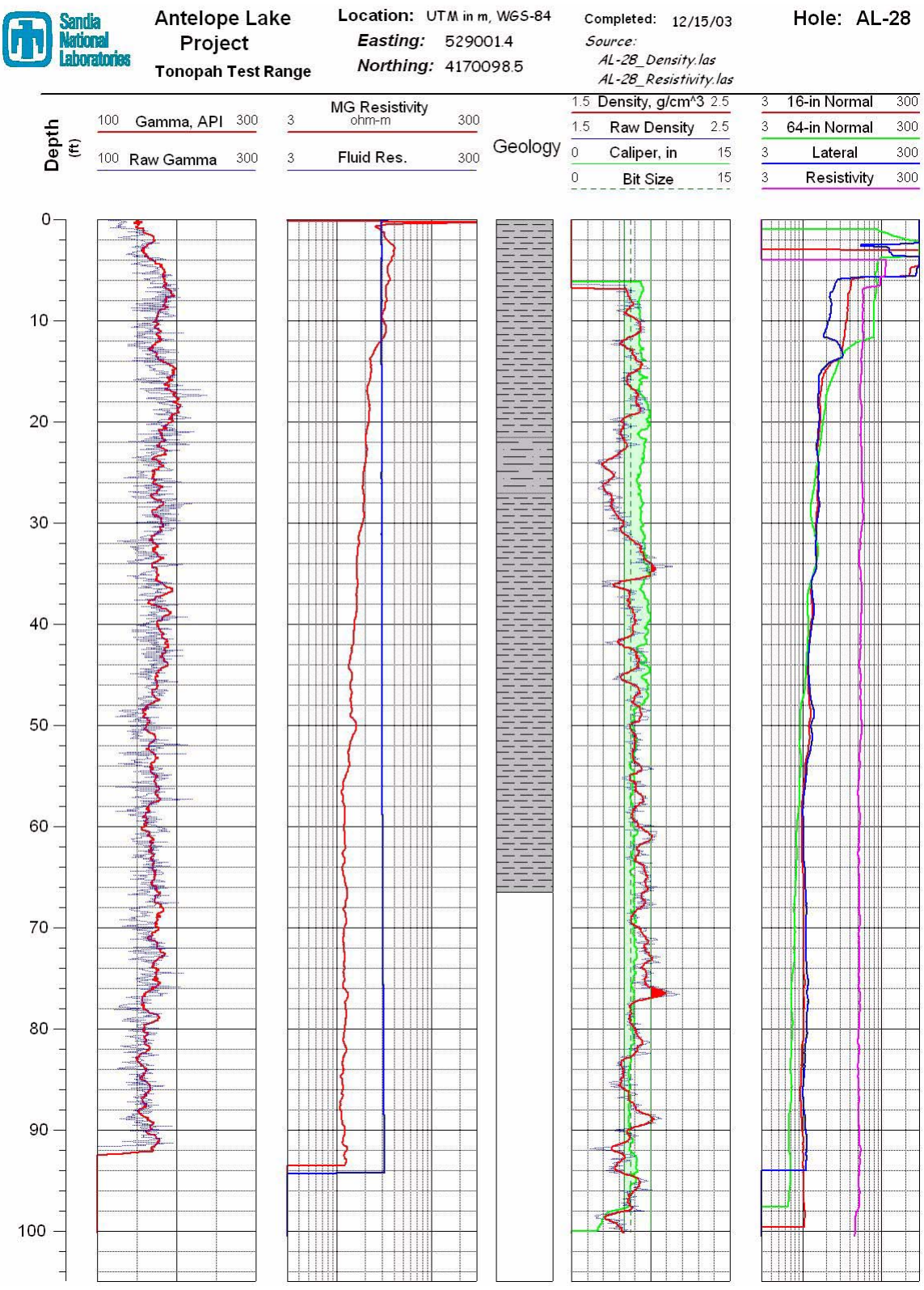

Figure G-27 Geophysical logs for drill hole AL-28.

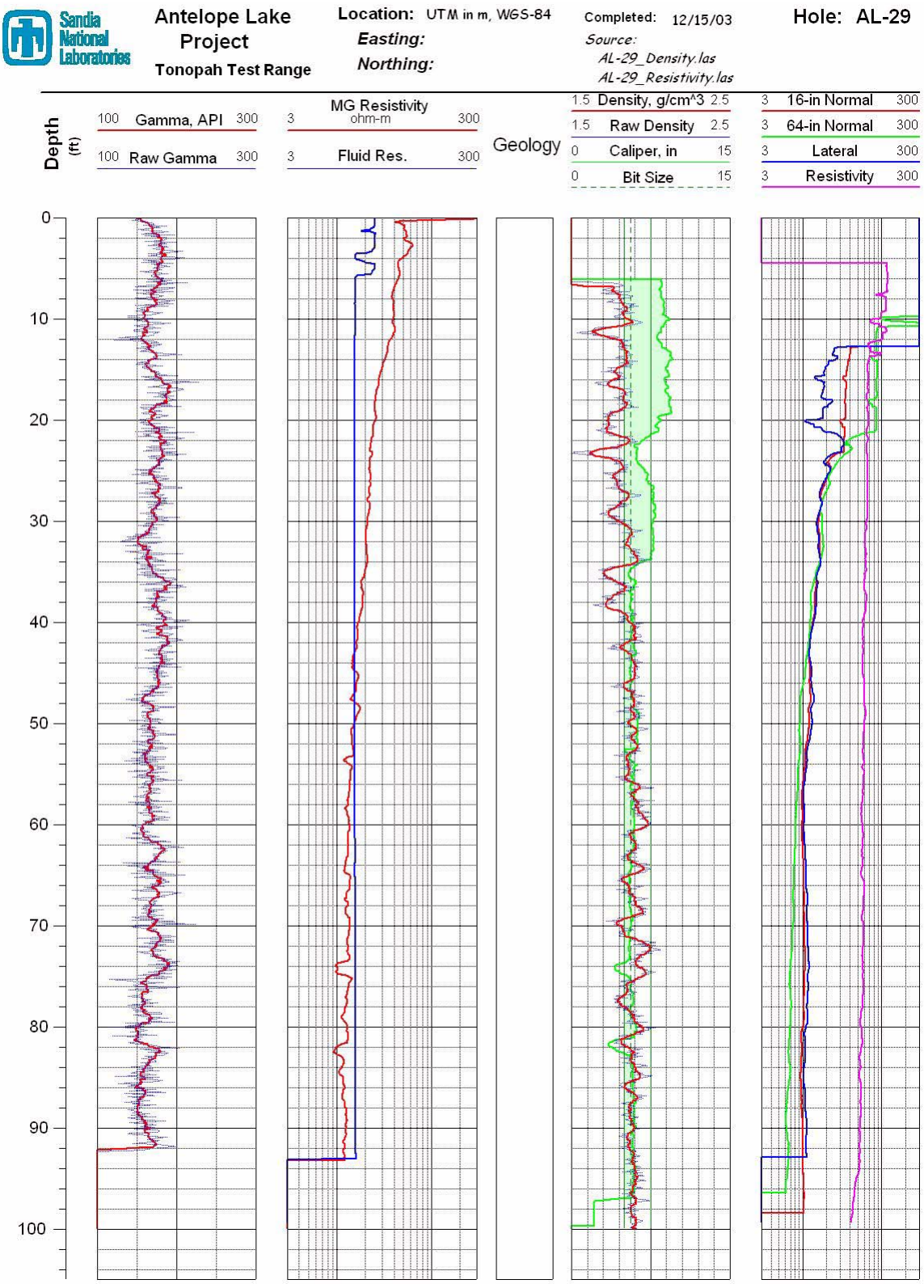

Figure G-28 Geophysical logs for drill hole AL-29.

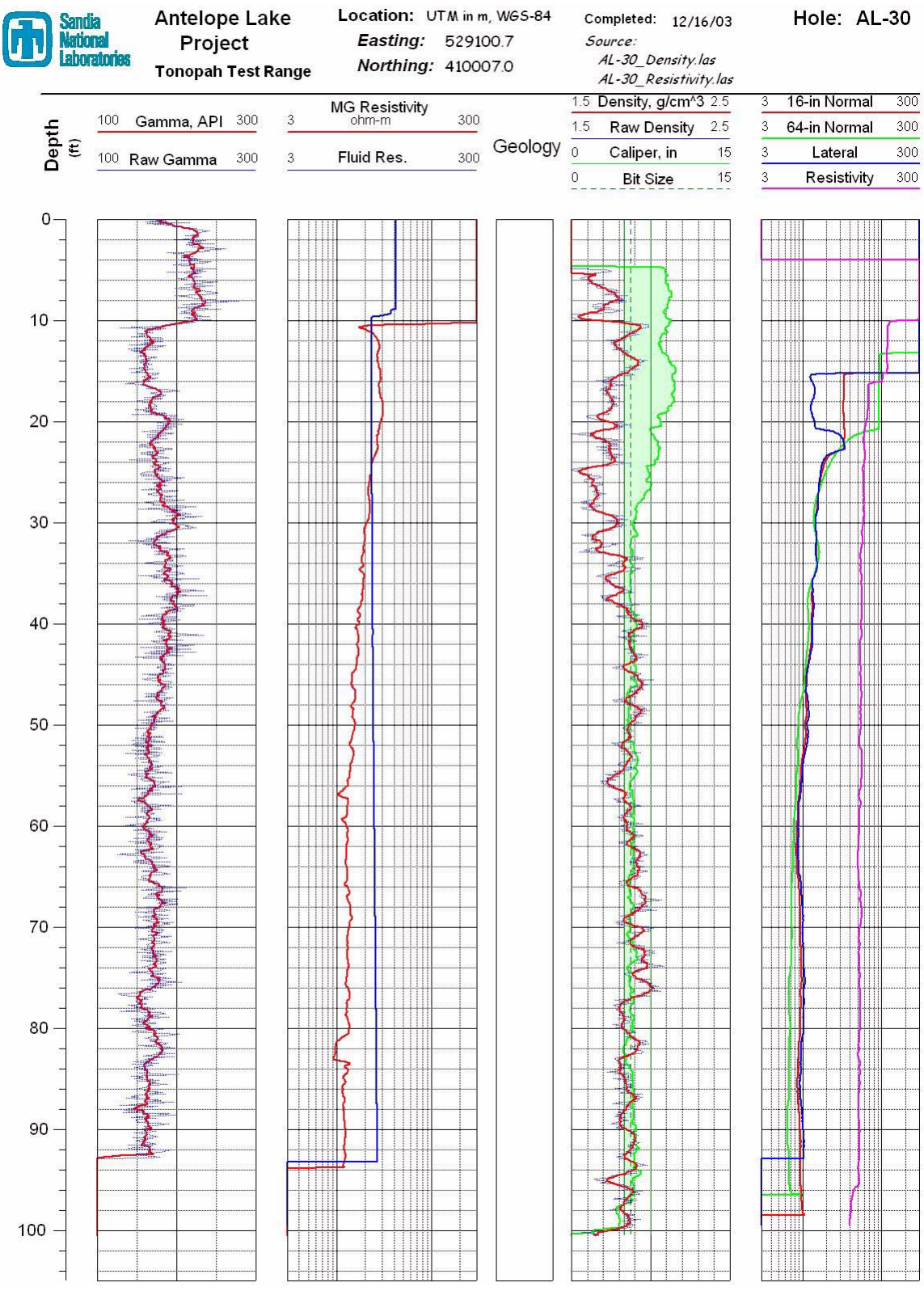

Figure G-29 Geophysical logs for drill hole AL-30.

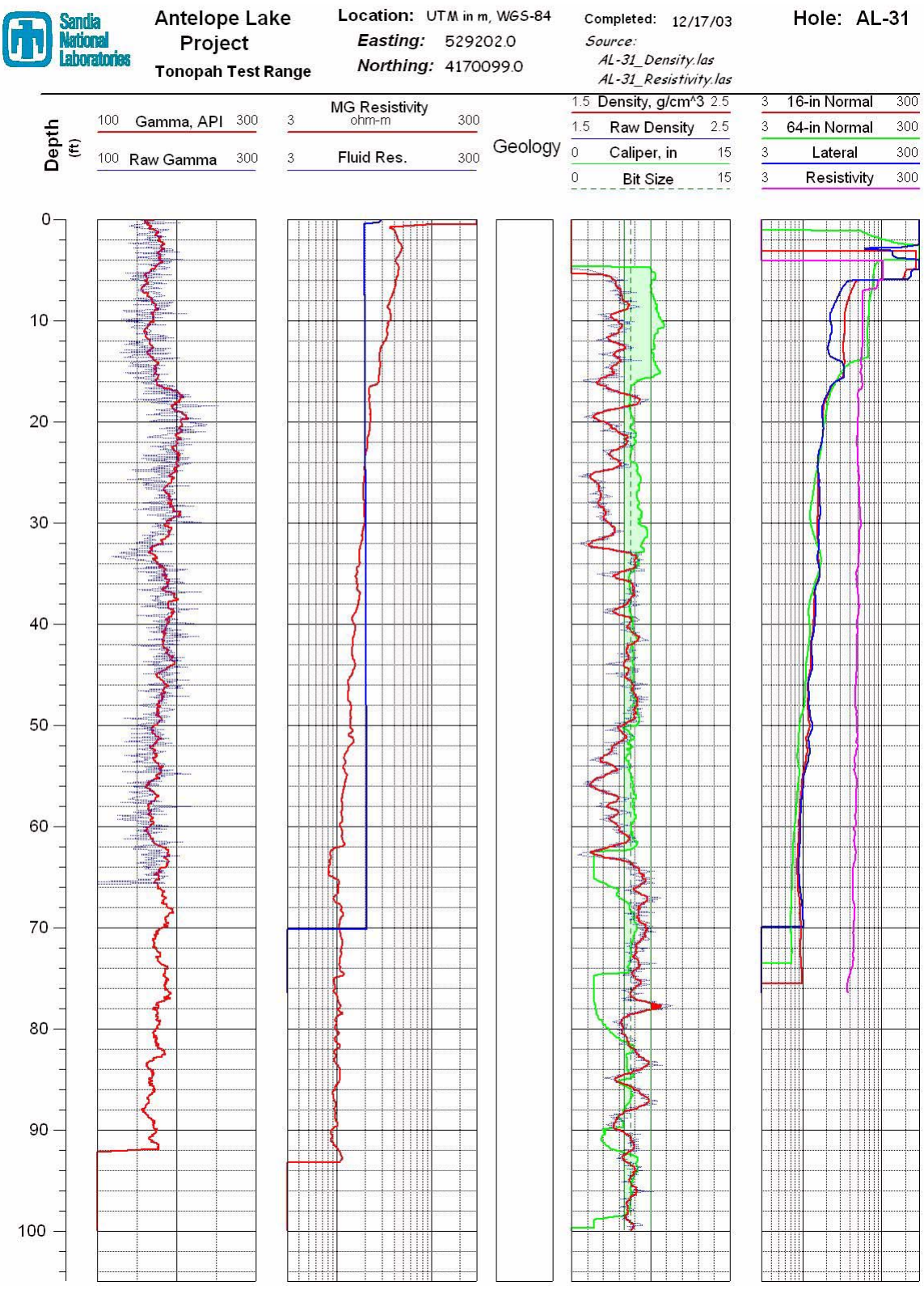

Figure G-30 Geophysical logs for drill hole AL-31.

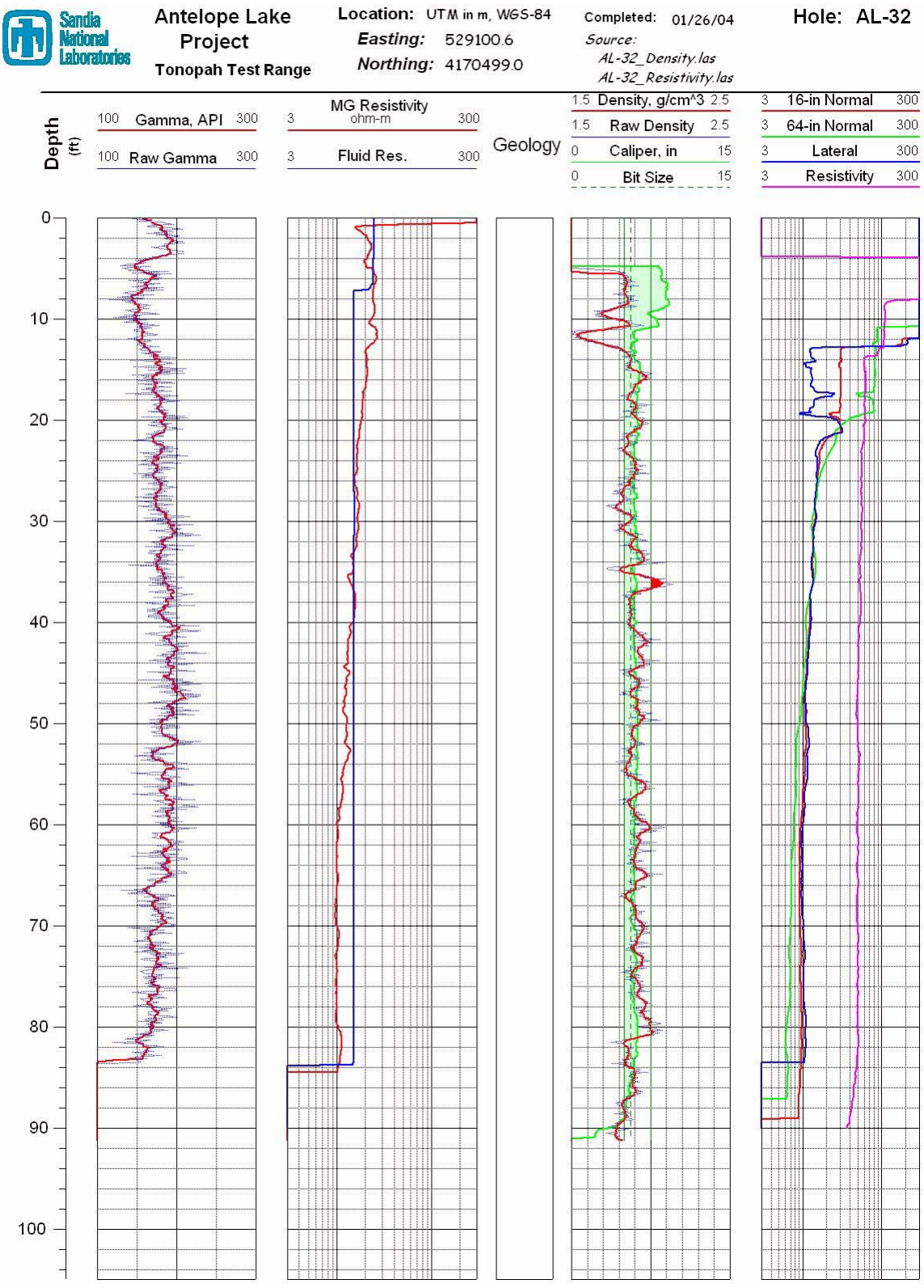

Figure G-31 Geophysical logs for drill hole AL-32.

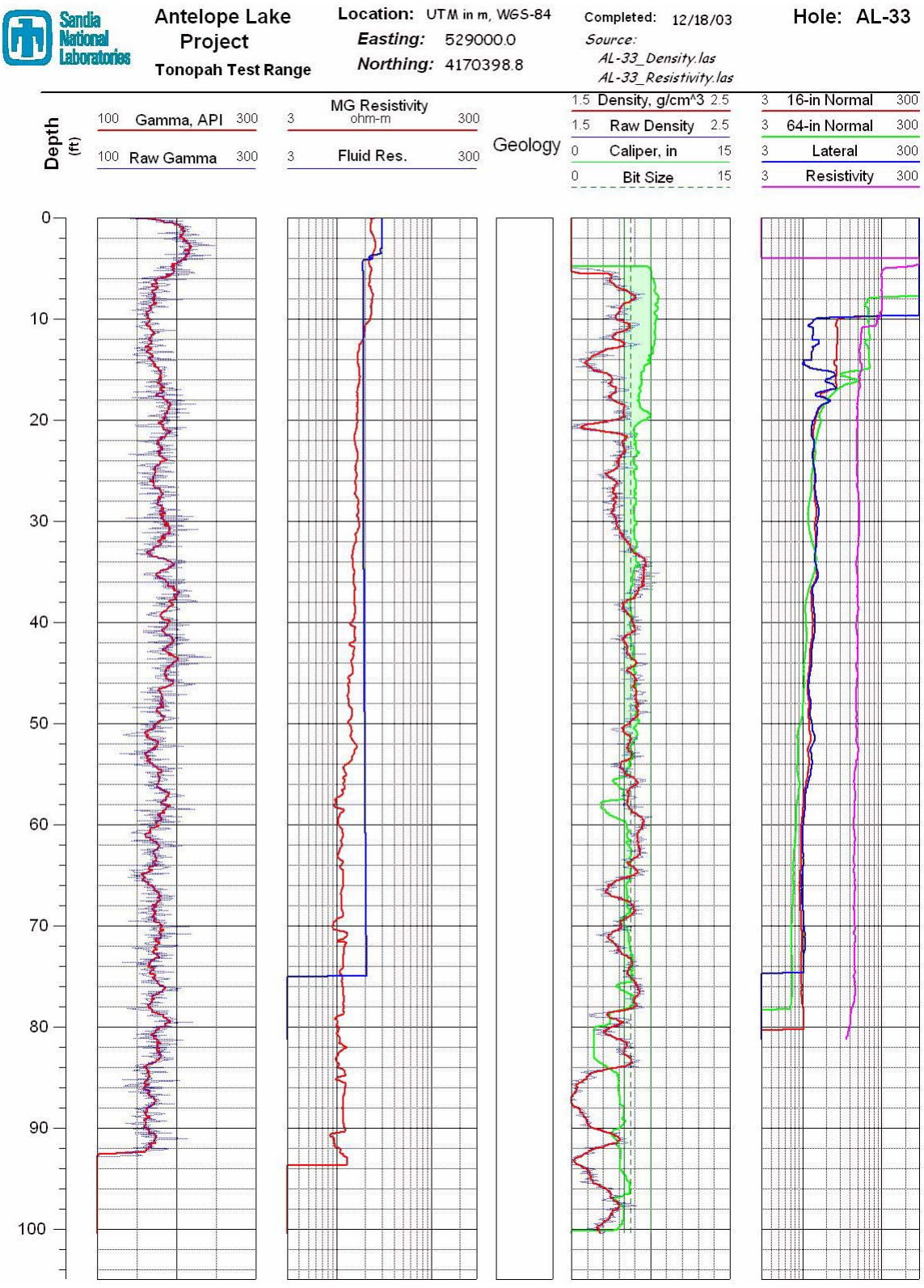

Figure G-32 Geophysical logs for drill hole AL-33.

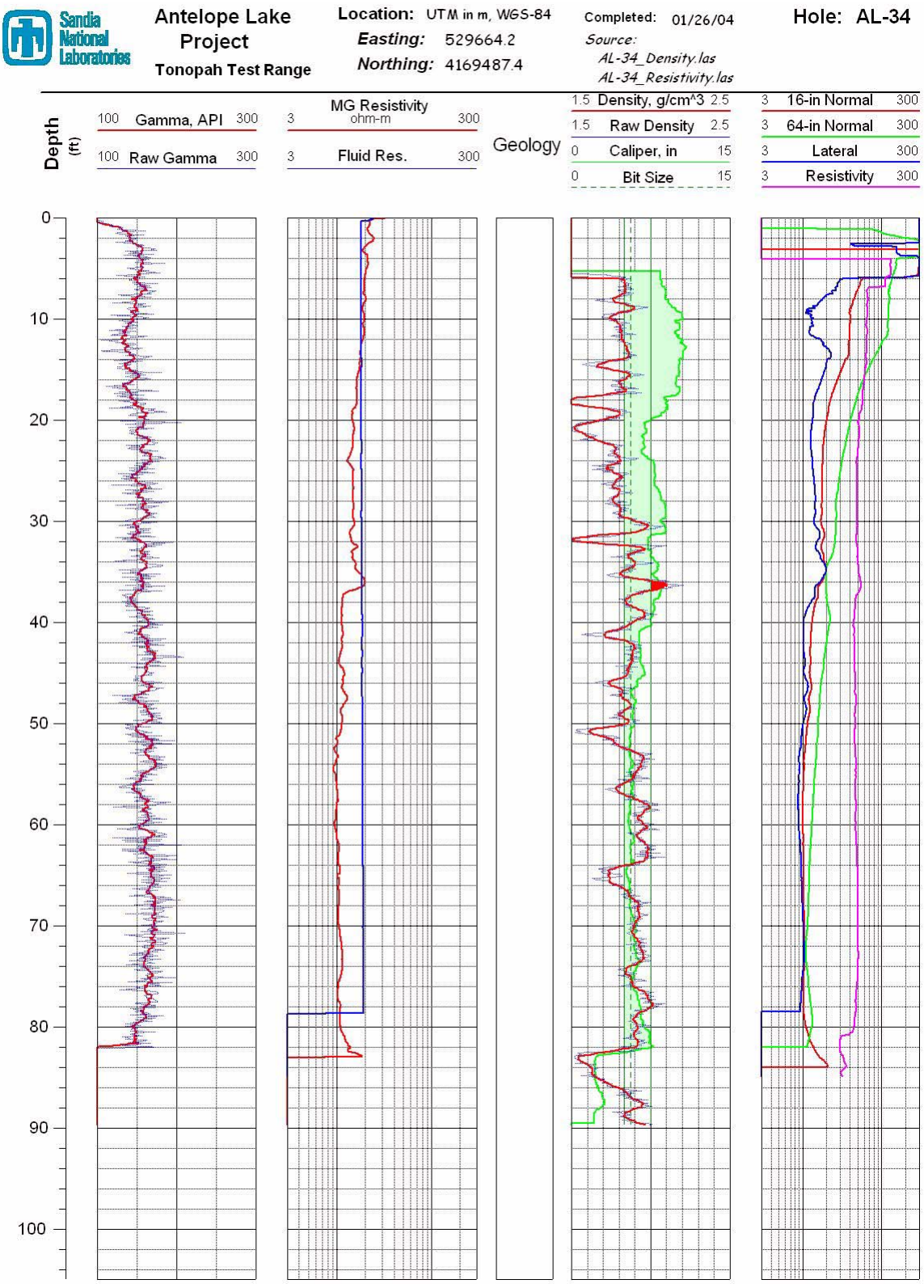

Figure G-33 Geophysical logs for drill hole AL-34.

This page intentionally left blank.

Appendix H: Logs for Cored Drill Holes on Antelope Lake

This page intentionally left blank.

INTRODUCTION

This appendix presents graphical geologic logs of the core that was obtained from drill holes AL-1 through ML-34 Emphasis is primarily on the geology — lithology, grain size, fractures (if any), and other visually observable features — of the core itself. Core recovery is also presented, as this value reflects the maximum possible "quality" of the core description. Lost core cannot be described, and thus descriptions from intervals of severe core loss are potentially suspect. A simplified version of the geophysical log suite from Appendix C is also presented for direct comparison with the lithologic descriptions. The core logging effort for the Antelope Lake drilling was identical to that employed at the Main Lake, as described in Appendix D, beginning on page 187. That descriptive material is not repeated here. Lithologic symbols used on the core logs are shown below.

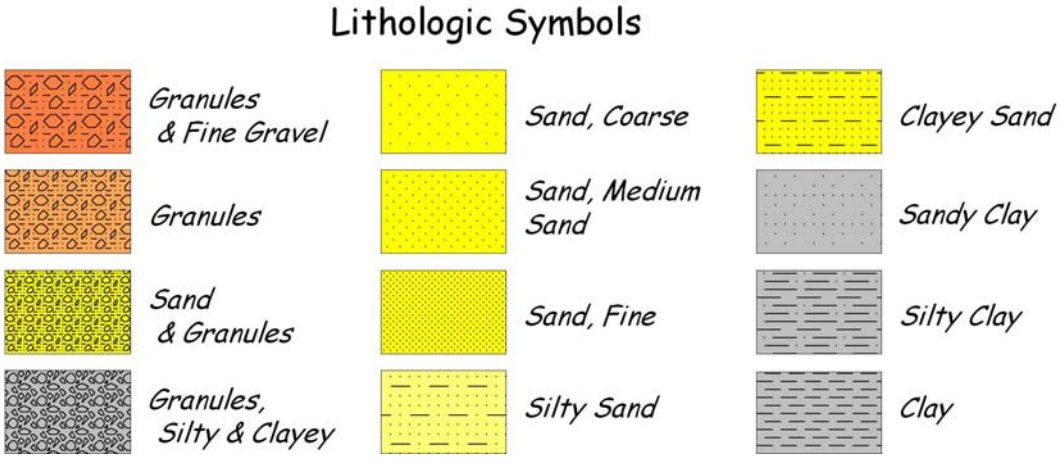

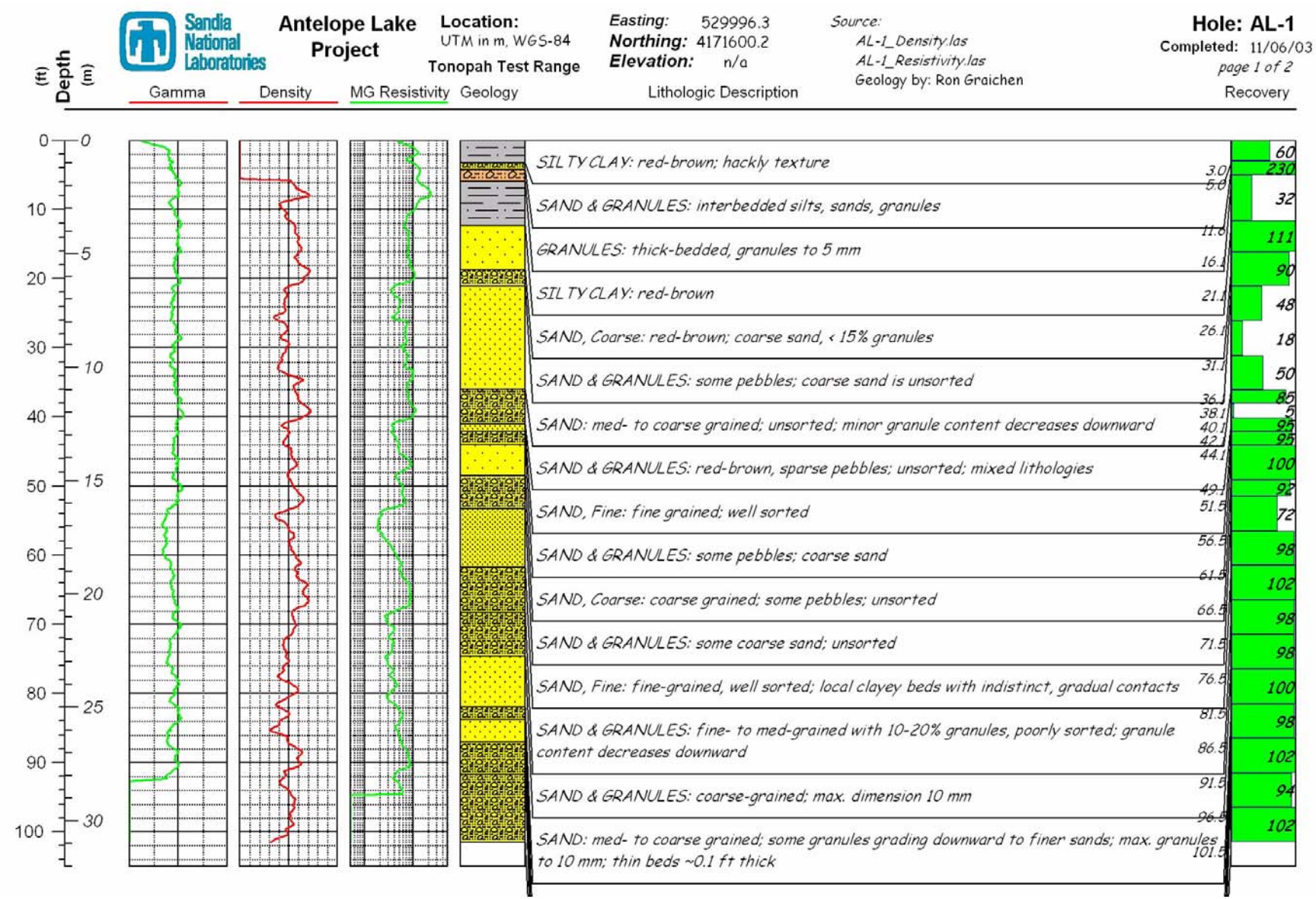

Figure H-1 Geologic core log and geophysical logs for drill hole AL-1.

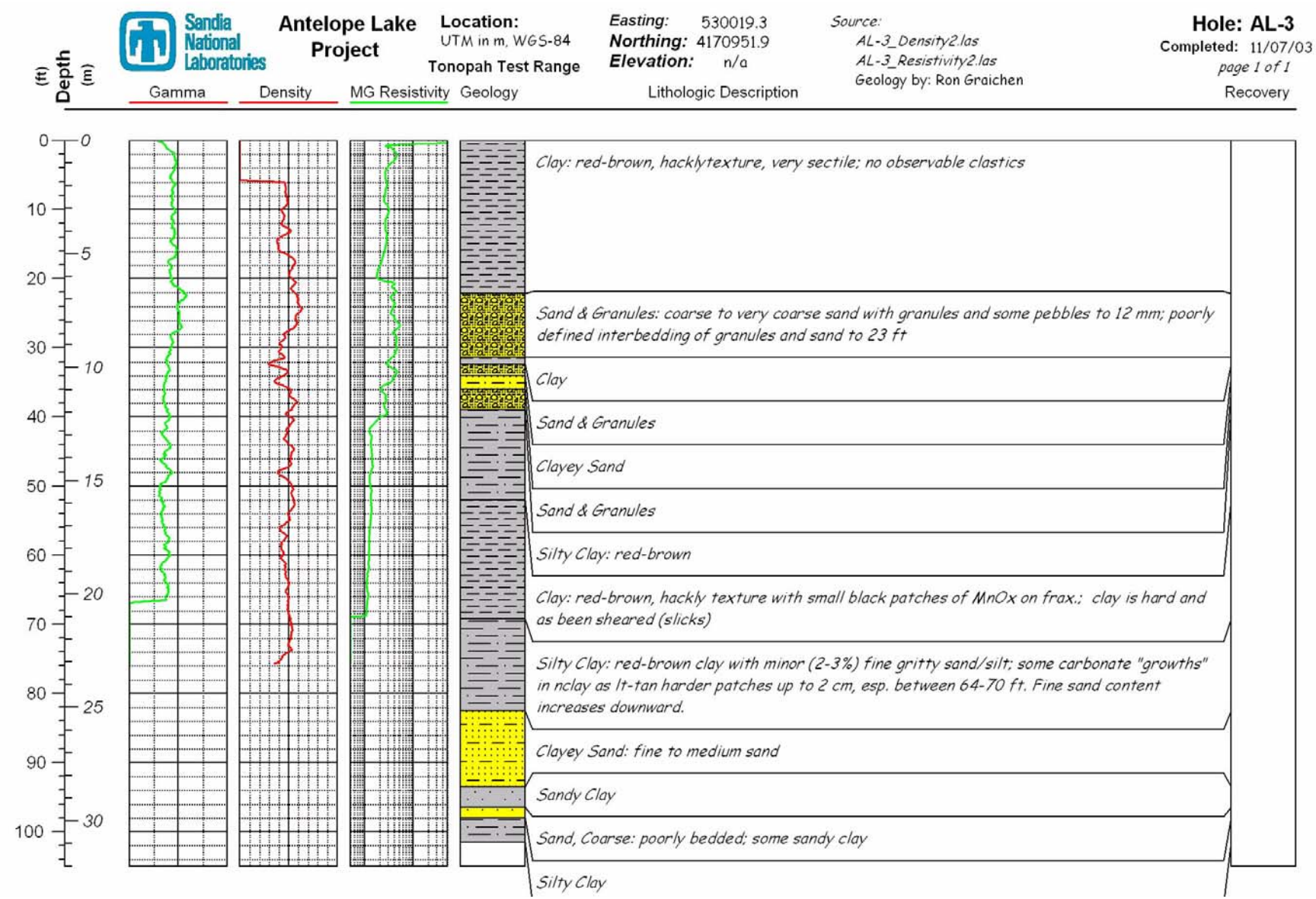

Figure H-2 Geologic core log and geophysical logs for drill hole AL-3.

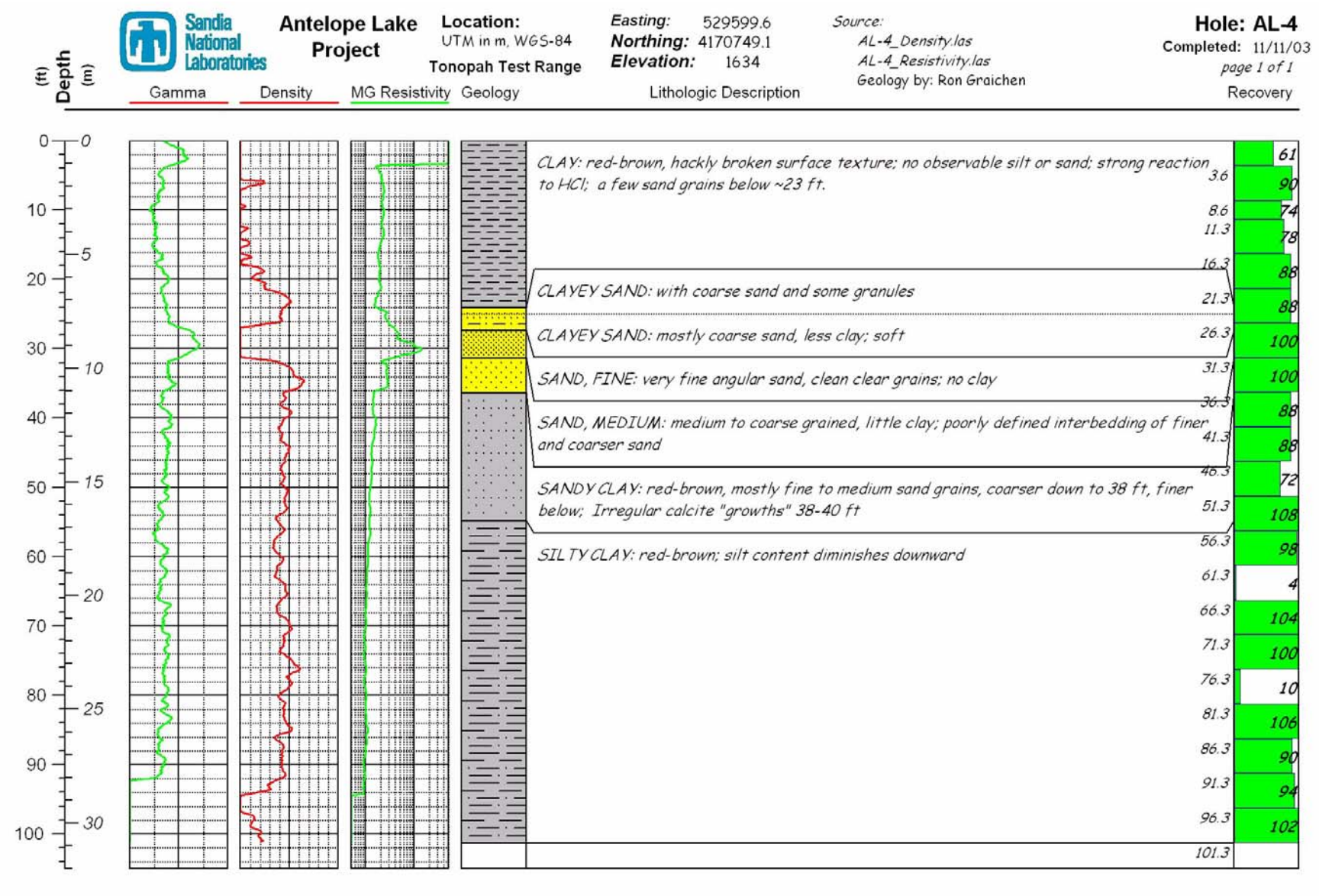

Figure H-3 Geologic core log and geophysical logs for drill hole AL-4.

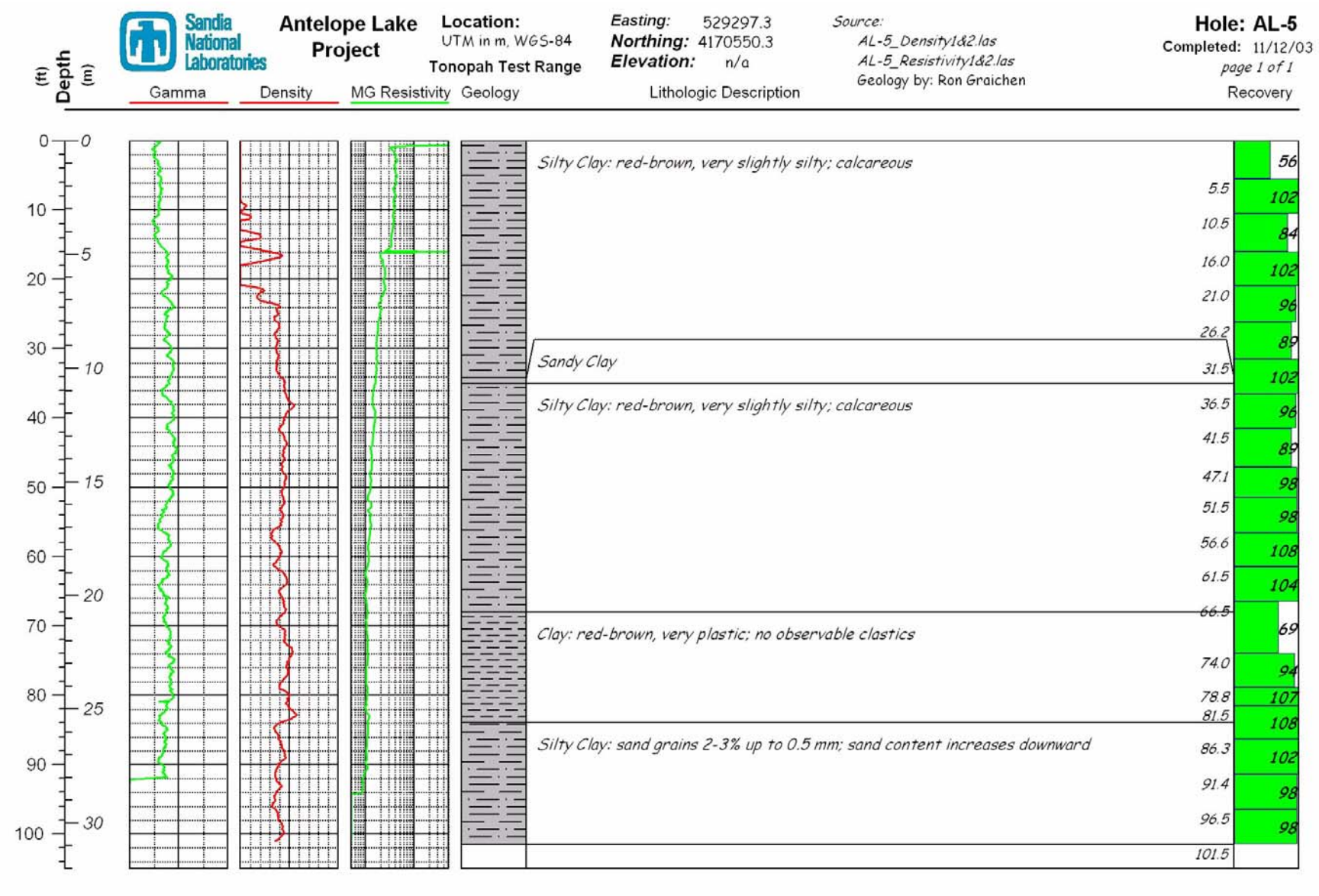

Figure H-4 Geologic core log and geophysical logs for drill hole AL-5.

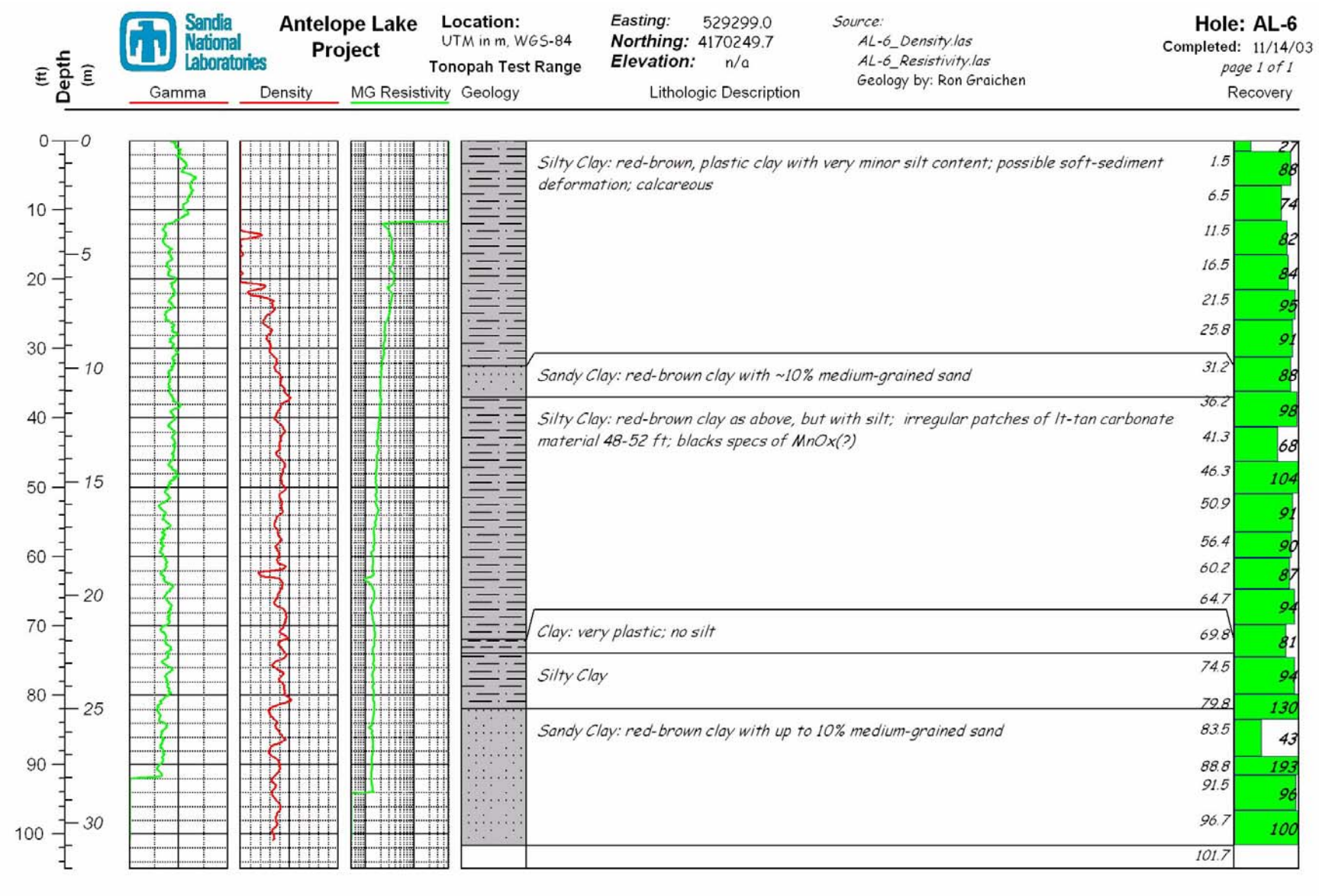

Figure H-5 Geologic core log and geophysical logs for drill hole AL-6.

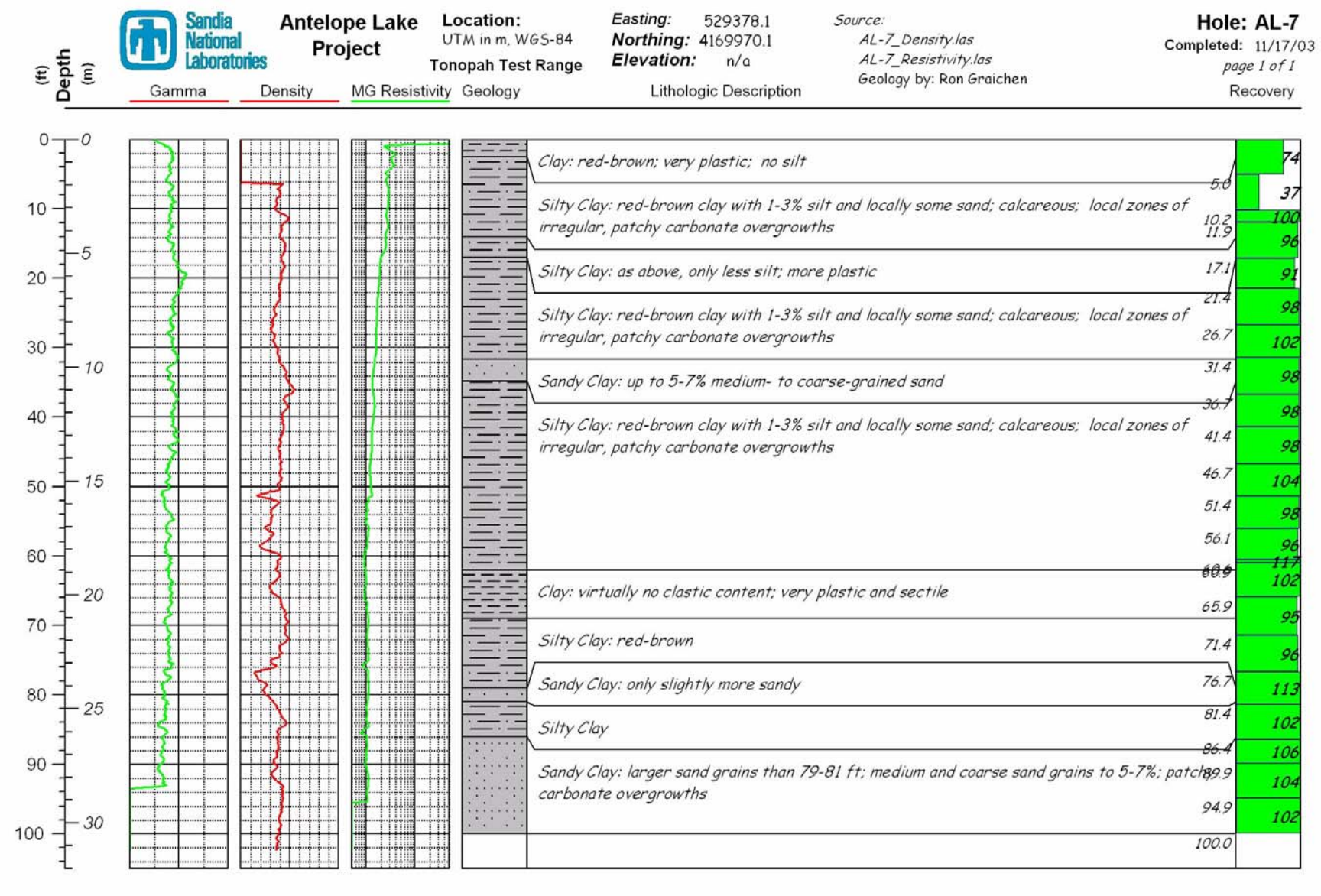

Figure H-6 Geologic core log and geophysical logs for drill hole AL-7.

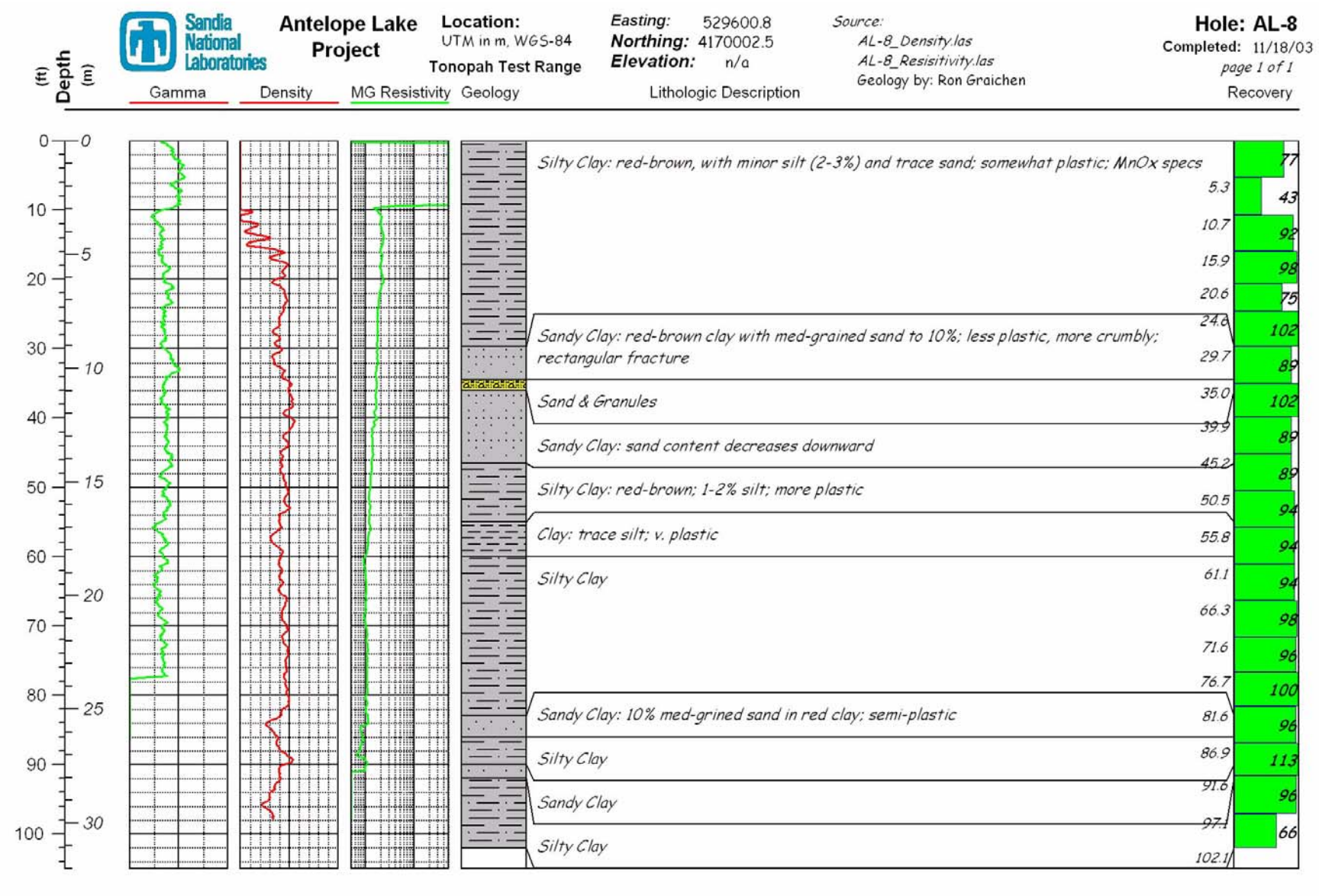

Figure H-7 Geologic core log and geophysical logs for drill hole AL-8.

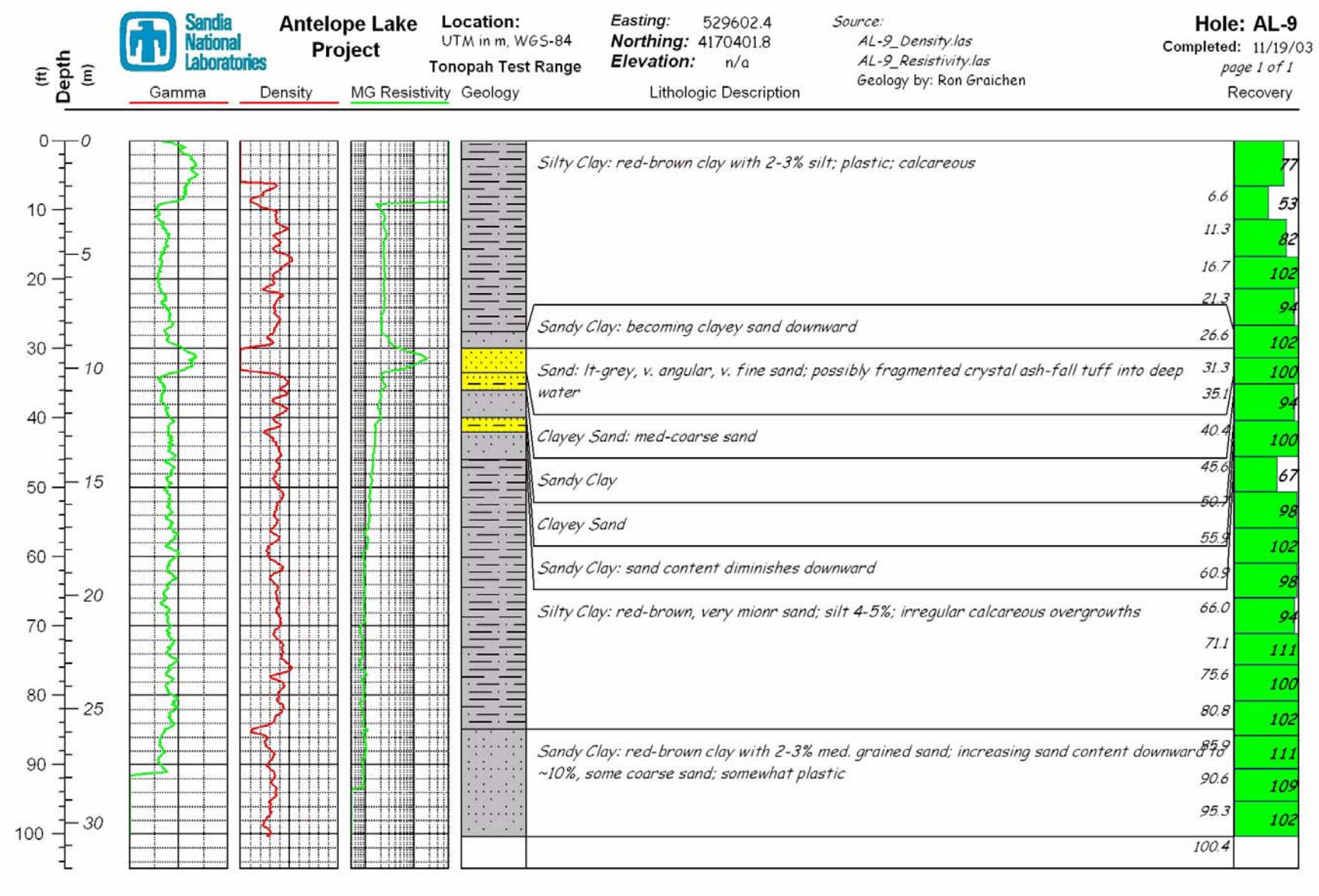

Figure H-8 Geologic core log and geophysical logs for drill hole AL-9.

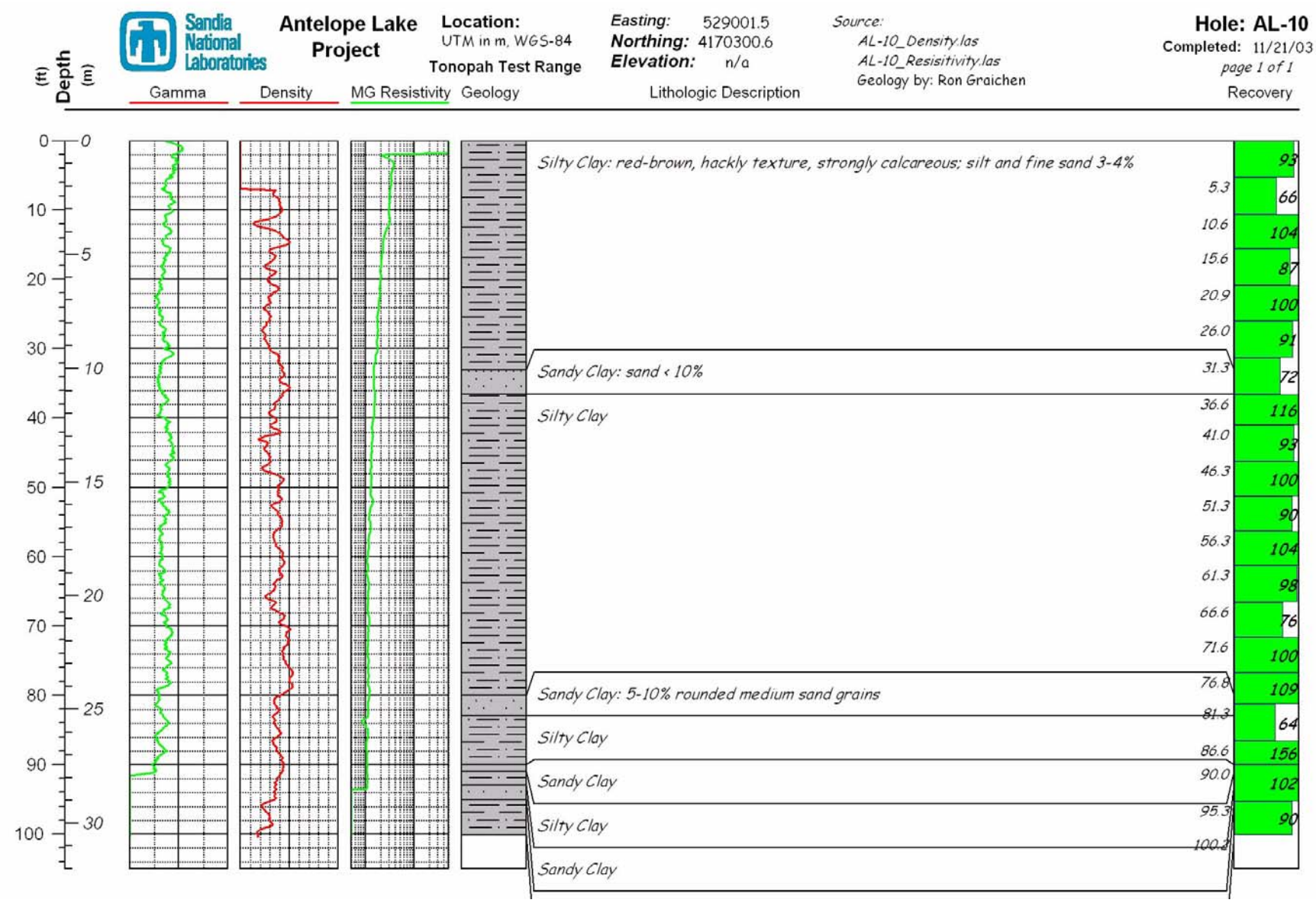

Figure H-9 Geologic core log and geophysical logs for drill hole AL-10.

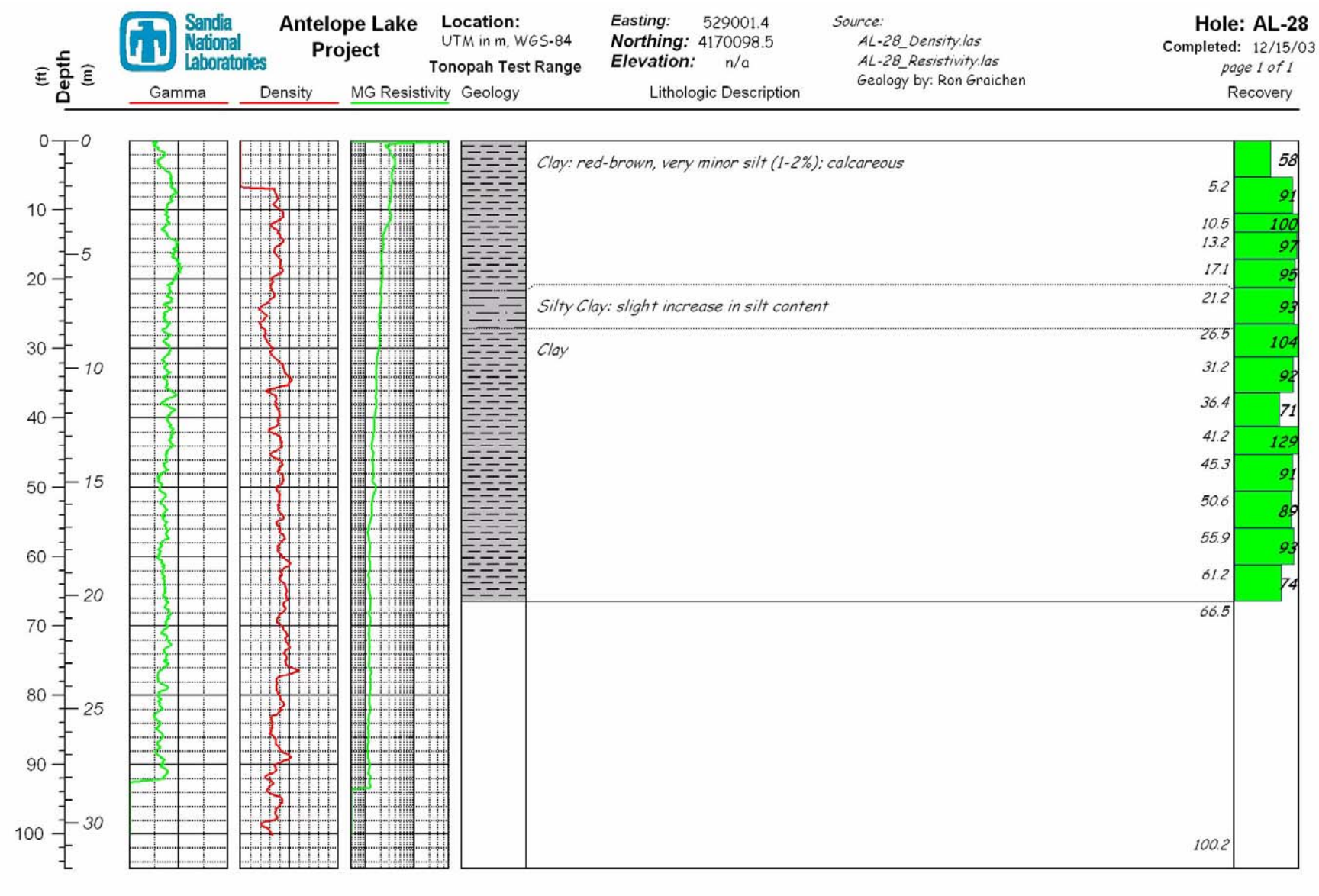

Figure H-10 Geologic core log and geophysical logs for drill hole AL-28.

This page intentionally left blank.

Appendix I: Material Properties Data from Antelope Lake Samples

This page intentionally left blank.

INTRODUCTION

This appendix contains the results of laboratory material-properties testing on specimens removed from the core drilled at Antelope Lake. Specimens were tested both in hydrostatic compression and in triaxial compression. The final laboratory values are given in table I-1. A full discussion of the laboratory testing procedure and the implications of the results is beyond the scope of this data report.

The use of rotary drilling for the majority of holes comprising the confirmatory grid limits the amount of core that is available for sampling and material-properties testing. However, the combination of confirmation of surface geophysics by the core and downhole geophysical logs and the confirmation of the downhole geophysics by the core across a broad spectrum of lithologies from very coarse to fine strongly suggested that the geophysical logs would be a sufficient indicator of suitable materials.

We sampled the available core with two objectives that were believed compatible with definition of a suitable test area and aim point. (1) We collected samples of the "hardest" material in each core hole within and adjacent to the 500-m-diameter test area. Typically, this was done using the most dense interval on the geophysical log, but physical hardness determined with a knife blade was also considered. (2) We also collected some samples of coarser-grained materials from holes farther away from the test region.

The object was to collect material that would both yield "worst-case" compressive strengths and provide a crude correlation between the geophysical-log signatures and lab-measured material properties. If the identifiably hardest/densest/coarsest materials from within the grid-defined test region do not pose a problem for penetration as determined by numerical calculations (e.g., cavity-expansion models), then presumably the softer materials inferred elsewhere in the section via downhole geophysics should not either. Laboratory test results for the selected core specimens are reported elsewhere. However, it should be noted that the "average" of the properties reported by the rock-mechanics laboratory *may overestimate* the overall strength of the bulk of the materials within the target region.

Table I-1: Laboratory test data for samples collected from Antelope Lake drill holes

Core samples tested by the rock mechanics laboratory at Sandia National Laboratories, M.Y. Lee and D.R. Bronowski. --: not applicable]

Test ID	Drill Hole	Depth Interval		Diameter (inch)	Length (inch)	Diameter (mm)	Length (mm)	Weight (g)	Density (g/cm^3)	Confining Pressure (MPa)	Peak Axial Stress (MPa)
		Top (ft)	Bottom (ft)								
Hydrostatic Compression Tests											
AL-HC01	AL-10	15.10	15.30	2.55	2.58	64.77	65.53	413.0	1.91	--	--
AL-HC02	AL-28	23.90	24.10	2.43	2.20	61.72	55.88	307.0	1.42	--	--
AL-HC03	AL-06	35.40	35.60	2.37	2.33	60.20	59.06	322.9	1.92	--	--
AL-HC04	AL-09	31.80	32.00	2.44	2.32	61.98	58.93	208.1	1.17	--	--
AL-HC05	AL-05	35.30	35.50	2.40	2.38	60.96	60.45	337.5	1.91	--	--
Triaxial Compression Tests											
AL-TC01	AL-10	14.50	14.95	2.44	4.98	61.98	126.49	748.9	1.96	20	7.49
AL-TC02	AL-06	34.10	34.55	2.35	4.86	59.69	123.44	635.0	1.84	10	12.41
AL-TC03	AL0-6	15.65	16.00	2.41	4.19	61.21	106.43	582.2	1.86	5	7.23
AL-TC04	AL-10	37.05	37.45	2.44	4.70	61.98	119.38	687.0	1.91	10	4.13
AL-TC05	AL-23	34.35	34.75	2.41	4.48	61.09	113.67	653.2	1.96	20	5.65
AL-TC06	AL-06	48.35	48.70	2.33	4.05	59.18	102.87	530.0	1.87	20	17.35
AL-TC07	AL-04	23.60	24.00	2.40	4.70	60.96	119.38	707.0	2.03	10	3.18
AL-TC08	AL-05	34.80	35.20	2.40	4.79	60.83	121.67	684.0	1.93	20	17.6
AL-TC09	AL-09	35.25	35.55	2.42	3.60	61.47	91.44	545.6	2.01	20	NA
AL-TC10	AL-09	31.50	31.80	2.42	3.50	61.47	88.90	345.0	1.31	10	26.31
AL-TC11	AL-05	14.30	14.60	2.38	3.21	60.45	81.53	440.8	1.88	10	13.27
AL-TC12	AL-04	29.40	29.70	2.36	3.58	59.94	90.93	347.0	1.35	20	12.45
AL-TC13	AL-03	26.05	26.40	2.44	4.19	61.98	106.43	678.0	2.11	20	NA
AL-TC14	AL-01	19.25	19.60	2.37	4.42	60.20	112.27	692.0	2.17	20	66.12

Appendix J: Contractor Report on Surface Geophysical Investigations

This page intentionally left blank.

INTRODUCTION

This appendix serves as a ***reference*** to the contractor report entitled *Antelope Lake Geophysical Investigations Report, Tonopah Test Range, Nevada*, prepared by Geophysical Solutions, of Albuquerque, New Mexico. The appendix is presented only in electronic format because of the size of the original report (the document is approximately 1-inch thick, printed single-sided. The electronic copy of this report is in Adobe Acrobat® *pdf* format and the file may be found on the CD-R in the pocket in the rear of this SAND report.

The report contains all of the TEM, Schlumberger sounding, and EM-31 survey locations and data in graphical form. Some illustrations are oversize (greater than 8-1/2 x 11 inches). However, if tabloid-size paper (11 x 17 inches) is available and the printer is set to use this size media, these maps will print as in the original document. "Fit to page" settings may also be used within Adobe Acrobat®.

ELECTRONIC DATA

The actual geophysical data and location information are also included on the CD-R in Microsoft Excel® format and in plain ASCII-text format as comma-separated values (.csv format). Any text editor, such as Microsoft Notepad, should be able to read (and print) the data values.

This page intentionally left blank.

DISTRIBUTION:
Sandia Internal:

MS 0634 T. Lee Post, 2951 (2)
MS 1392 R.C. Sherwood, 2915 (2), for TTR
MS 0706 C.A. Rautman, 6113 (2)
MS 9018 Central Tech. Files, 8945-1
MS 0899 Technical Library, 9616 (2)

via CD-R only
MS-0482 E.R. Hoover, 2131
MS-0482 T.C. Togami, 2131
MS-0482 J.C. Wirth, 2131
MS-0751 L.S. Costin, 6111
MS-0750 S.C. Cooper, 6116
MS-0751 K.N. Gaither, 6117
MS-0417 A.R. Lappin, 6117
MS-0316 D.R. Gardner, 9233
MS-1160 D.A. Dederman, 15412
MS-0750 G.J. Elbring, 6116